AVERTISSEMENT

Ce document est le fruit d'un long travail approuvé par le jury de soutenance et mis à disposition de l'ensemble de la communauté universitaire élargie.

Il est soumis à la propriété intellectuelle de l'auteur. Ceci implique une obligation de citation et de référencement lors de l'utilisation de ce document.

D'autre part, toute contrefaçon, plagiat, reproduction illicite encourt une poursuite pénale.

Contact : ddoc-theses-contact@univ-lorraine.fr

LIENS

Code de la Propriété Intellectuelle. articles L 122. 4
Code de la Propriété Intellectuelle. articles L 335.2- L 335.10
http://www.cfcopies.com/V2/leg/leg_droi.php
http://www.culture.gouv.fr/culture/infos-pratiques/droits/protection.htm

THÈSE

Présentée à l'Université de Lorraine
Ecole Doctorale SIMPPÉ : Science et Ingénierie des Molécules, des Produits, des Procédés et de l'Énergie
Laboratoire Réactions et Génie des Procédés (UMR 7274 CNRS)
pour l'obtention du grade de

Docteur de l'Université de Lorraine
Spécialité Génie des Procédés

par

Erika BARTOLOMEI

Biorefinery: lignin liquefaction to produce green aromatic chemicals

---

Thèse soutenue publiquement le 9 juillet 2021 à Nancy devant le jury composé de:

Rapporteurs:	Sylvette BRUNET – Université de Poitier-CNRS Dorothée LAURENTI – Université Lyon1-CNRS
Examinateurs:	Vanessa FIERRO – Université de Lorraine-CNRS Pascal FONGARLAND – Université Lyon1-CNRS Anthony DUFOUR – Université de Lorraine-CNRS (Directeur de thèse) Yann LE BRECH – Université de Lorraine-CNRS (Co-directeur de thèse)
Invités:	Frédérique BERTAUD – CTP Grenoble

Hunc igitur terrorem animi tenebrasque necessest

non radii solis neque lucida tela diei

discutiant, sed naturae species ratioque.

Titus Lucretius Carus, De rerum natura 1.146-148

Acknowledgements

I would like first to express my sincere gratitude to my advisors, Dr. Anthony Dufour and Dr. Yann Le Brech, for their guidance all along my journey. Their guidance has been irreplaceable for me and my work. During these years, I feel I improved a lot as a scientist, as a team-worker and as a communicator, and it was possible thanks to their critical feedback and challenges. I would also thank all my committee members, for accepting to evaluate and active participate to my dissertation.

A big thanks is owed to all the members of the GREENER group. You have been my second family here in France: always ready to support me in any work difficulty and to share life moments together. In particular, special thanks to some past and current members: Dr.Guillain Mauviel, Dr. Gabriel Wild, Dr. Mohammed Bettahar, Michel Mercy, Richard Lainé, Philippe Arnoux, Hélène Lichère, Maxime Hervy, Damien Remy, Felipe Buendia Kandia, Diego Peña Zapata, Miguel Ruiz Bailon, Rémi Demol, Pierre-Alann Cablé, and Nabil Hassibi. Thank you also to all the researchers, technicians and PhD fellows I worked and shared with during these years. In particular, to the entire mechanical workshop and different technical services, without whom there would be no possible to achieve all the experimental work done; to the *Bureau de Jeunes Chercheurs* for all the moments spent together; to all the friends I found at LRGP, with particular refer to Matteo Pietraccini. Thank you all to have made the time spent together unforgettable.

My gratitude goes also to all the partners of the ANR project *Phenoliq*, in particular Dr. Frédérique Bertaud, Dr. Laurent Djakovitch, Dr. Pascal Fongarland, Dr. Léa Vilcocq and Antonio Hernandez Mañas, for the great collaboration and exchanges occurred during this time.

I would like to thank also Dr. Manuel Garcia-Perez who welcomed me in his group at Washington State University. This opportunity really enriched me from scientific and human points of view. I had the chance to find amazing people over there, in particular my colleague and friend Evan Terrell.

A special thanks also to Dr. Blaž Likozar group at the National Institute of Chemistry in Ljubljana, Slovenia, for hosting me. It was a pleasure to collaborate with Dr. Miha Grilc, Dr. Edita Jasiukaitytė-Grojzdek and Tina Ročnik.

Many thanks also to all my friends all over the world; from my old friends in Rome to all the people I connected during this PhD time. I had the chance to find special people, I am grateful for that. Your support and presence made life's challenges easier. I will always remember all the good times we spent together.

Un ringraziamento veramente speciale per la mia famiglia. Se mi trovo qui oggi è solamente grazie a voi e per voi. Come ogni cosa finora nelle nostre vite, anche questo traguardo lo abbiamo raggiunto insieme. A voi, che siete sempre state e sempre sarete al mio fianco, dedico il frutto del mio lavoro.

Outline

INTRODUCTION **1**

1. - General Context 1

2. - Scope of the Thesis 1

3. - Thesis Layout 2

4. - List of Publications 3

5. - International Conferences 4

6. - References 5

A. LITERATURE REVIEW/ FEATURES AND PERSPECTIVES OF LIGNIN **7**

1. - Lignocellulosic Biomass 7

1.1. - General composition 7

1.2. - Extractives and inorganic matter 9

1.3. - Cellulose and Hemicellulose 9

1.4. - Lignin 10

2. - Biorefinery to high value bio-products 13

3. - Technical Lignins from Biorefinery 15

3.1. - Lignin types 15

3.2. - Kraft Process 18

4. - Thermochemical Conversion of Lignin 24

4.1. - Generalities 24

4.2. - Lignin Pyrolysis 25

4.3. - Lignin Liquefaction 27

5. - Conclusions 31

6. - References 32

B. MULTI-ANALYTIC CHARACTERIZATION OF TECHNICAL LIGNINS AND BLACK LIQUORS 45

1. - Introduction 45

2. - Materials and Methods 47

2.1. - Physico-chemical characterization of commercial/technical lignins 47

2.2. - Black Liquor and softwood Kraft Lignin from Black Liquor 50

3. - Results 51

3.1. - Technical Lignins 51

3.2. - Black Liquor and softwood Kraft Lignin from Black Liquor 64

4. - Conclusions 72

5. - References 76

6. - Supporting Information 78

6.1. - References 86

C. LIGNIN DEPOLYMERIZATION: A COMPARISON OF METHODS TO ANALYZE MONOMERS AND OLIGOMERS 90

1. - Introduction 90

2. - Materials and Methods 93

2.1. - Chemicals 93

2.2. - Catalytic liquefaction experiments 94

2.3. - Analysis of products 95

3. - Results 97

3.1. - Analysis of lignin liquefaction products by conventional methods 97

3.2. - Analysis of lignin products by UV spectroscopy 104

4. - Discussion on the complementarity between UV fluorescence and GC/MS, MALDI-TOFMS and GPC analysis 113

5. - Conclusions 119

6. - References 121

7. - Supporting Information 132

7.1. - References of chemicals 132
7.2. - NMR characterization of Soda lignin and oligomers extracted after lignin liquefaction 132
7.3. - Autoclave set-up 135
7.4. - Isolation of solid residue and oligomers at the end of liquefaction experiments 135
7.5. - GC/MS6FID analysis 136
7.6. - GPC analysis 139
7.7. - MALDI-TOFMS analysis 139
7.8. - UV spectroscopy analysis of model compounds and of lignin liquefaction liquids . 141
7.9. - References cited in supporting information 145
D. EFFECT OF TECHNICAL LIGNIN TYPE AND CATALYST (NI/C, RU/C, PT/C) ON DEPOLYMERIZATION PRODUCTS IN SUPERCRITICAL ETHANOL 147
1. - Introduction 147
2. - Material and Methods 150
2.1. - Characterization of the technical lignins 151
2.2. - Characterization of catalysts 151
2.3. - Catalytic depolymerization of the technical lignins 152
2.4. - Analysis of liquid products 153
3. - Results 153
3.1. - Characterization of lignins 153
3.2. - Characterization of the catalysts 154
3.3. - Effect of catalyst (Ni/C, Ru/C, Pt/C) on Kraft lignin liquefaction 159
3.4. - Effect of technical lignin types on their liquefaction with Ni/C 163
4. - Conclusions 167
5. - References 168
6. - Supporting Information 170
6.1. - Bibliography 170

6.2. - Characterization of lignins 171
6.3. - Results of catalyst characterization 176
6.4. - Analysis of liquids 184
6.5. - References 187
E. SELECTIVE CATALYTIC TEMPO-MEDIATED OXIDATION OF KRAFT LIGNIN TO VANILLIN 190
1. - Introduction 190
2. - Experimental Section 191
3. - Results 192
4. - Conclusions 193
5. - References 195
6. - Supporting Information 199
6.1. - Literature review 199
6.2. - Fractionation method 200
6.3. - GC-MS/FID 201
6.4. - FT-IR 203
6.5. - XRD of catalyst 204
6.6. - References cited in the supporting info 206
F. INTEGRATING LIGNIN DEPOLYMERIZATION IN KRAFT MILLS: EXPERIMENTS, PROCESS MODELLING AND TECHNO-ECONOMIC ASSESSMENT 210
1. - Introduction 210
2. - Methodology 212
2.1. - Experimental section 212
2.2. - Description of the AspenPlus® model 213
2.3. - Techno-economic assessment 215
3. - Results and discussion 215
3.1. - Experiments on lignin depolymerization 215

3.2. - Modelling 216
3.3. - Techno-economic analysis 219
4. - References 224
5. - Supporting Information 228
5.1. - Elemental and Proximate analysis of solids 228
5.2. - GC-MS/FID method and monomers yields 230
5.3. - Assumption and prices for the techno-economic assessment 231
G. CATALYTIC HYDROTREATMENT OF LIGNIN IN A TRICKLE BED REACTOR 233
1. - Introduction 233
2. - Theoretical reactor design 234
2.1. - Hydrodynamics 234
2.2. - Pre-sizing 235
2.3. - Pressure drops 236
2.4. - Set-up development 236
2.5. - Mass transfer 238
3. - Preliminary experimental results 239
3.1. - Catalyst 239
3.2. - Bio-oils analysis 240
4. - References 242
H. CONCLUSIONS AND PERSPECTIVES 243
I. APPENDICES 247
1. - Article in development: Catalytic depolymerization of lignins with Ru/C: effect of lignin structure and H_2 247
1.1. - Introduction 247
1.2. - Materials and Methods 249
1.3. - Results and Discussion 252

1.4. - References 264

2. - Article in development: Study on the extraction of phenolic compounds from bio-oils. 267

2.1. - Introduction 267

2.2. - Materials and methods 269

2.3. - Results and Discussions 272

2.4. - Conclusions 273

2.5. - References 274

3. - Article in development: Oxidation and Reduction for Kraft Lignin Depolymerization: Comparison and Coupling 277

3.1. - Development 277

3.2. - References 280

3.3. - Supporting Information 280

J. RÉSUMÉ **283**

1. - Introduction 283

2. - Revue de la littérature: caractéristiques et perspectives de la lignine 285

3. - Caractérisation multi-analytique des lignines techniques et des liqueurs noires 286

4. - Dépolymérisation de la lignine: une comparaison des méthodes d'analyse des monomères et des oligomers 288

5. - Effet du type de lignine technique et du catalyseur (Ni/C, Ru/C, Pt/C) sur les produits de dépolymérisation dans l'éthanol supercritique 291

6. - Oxydation catalytique sélective à médiation TEMPO de la lignine Kraft en vanilline ... 291

7. - Intégration de la dépolymérisation de la lignine dans les usines de pâte kraft: expériences, modélisation des procédés et évaluation technico-économique 292

8. - Conclusions 293

Figures List

INTRODUCTION **1**

Figure 1 Desired change of scenario for pulp and paper mills. 1

A. LITERATURE REVIEW/ FEATURES AND PERSPECTIVES OF LIGNIN **7**

Figure 1 Distribution of biomass carbon worldwide 7

Figure 2 Hierarchical scale of biomass from full plant to molecular level 8

Figure 3 (top) Cellulose structure; (bottom) Hemicellulose's monomeric units, adapted. 10

Figure 4 Lignin structure example (re-edited) 12

Figure 5 Bonding types connecting lignin's monomer units. 12

Figure 6 General biorefinery approach to biomass. 14

Figure 7 Main lignin extraction processes. 17

Figure 8 Pulp and paper mill process. 19

Figure 9 LignoBoost® scheme : Kraft black liquor and lignin extraction 23

Figure 10 Lignin thermochemical conversion pathways (adapted) 24

Figure 11 Lignin liquefaction categories. 28

B. MULTI-ANALYTIC CHARACTERIZATION OF TECHNICAL LIGNINS AND BLACK LIQUORS **45**

Figure 1 Lignin monomeric units and typical bonds. 46

Figure 2 Pulping of different biomass feedstock and their market.[8] 47

Figure 3 Scheme of the Kraft lignin preparation at semi-pilot scale (CTP):
the standard protocol (BL 40% dry matter, 70°C, pH 9 and acidic washings) 53

Figure 4 Mass balance from Klason and sugar residue analysis. 53

Figure 5 Thermogravimetric analysis. 55

Figure 6: DTG analysis lignin thermal stabilities 55

Figure 7 Kraft 1 SEM analysis and granulometry 56

Figure 8 Kraft 2 SEM analysis and granulometry 56

Figure 9 Soda SEM analysis and granulometry 57

Figure 10 Organosolv SEM analysis and granulometry 57

Figure 11 FT-IR spectra. 63

Figure 12 PCA analysis based on FT-IR characterization. 63

Figure 13 : Chromatograms of aqueous GPC (NaOH / UV 254nm) 68

Figure 14 ^{13}C NMR spectrum of precipitated lignin KL.Re.I and KL.Re.II 69
Figure 15 %molC repartition in lignins KL.Re-I and KL.Re-II determined by ^{13}C NMR. 70
Figure 16 ATG analysis of KL.Re-I (K3) and KL.Re-II (K4),
comparison with LN20.Re.II (LN20) and with LN45.Re.II (LN45) 71
Figure 17: Derivative thermogravimetry analysis of KL.Re-I (K3) and KL.Re-II (K4), comparison with LN20.Re.II (LN20) and with LN45.Re.II (LN45) 72
Figure S1 TGA proximate analysis of LN45.Re-II 81
Figure S2 TGA proximate analysis of LN20.Re-II 82
Figure S3 Functional group analysis of Soda lignin by quantitative 31P NMR after phosphitylation 83
Figure S4 Functional group analysis of Kraft1 lignin by quantitative 31P NMR after phosphitylation 84
Figure S5 Functional group analysis of Kraft2 lignin by quantitative 31P NMR after phosphitylation 85
Figure S6 Functional group analysis of Kraft3 lignin by quantitative 31P NMR after phosphitylation 85
Figure S7 Functional group analysis of Organosolv lignin by quantitative 31P NMR after phosphitylation 86

C. LIGNIN DEPOLYMERIZATION: A COMPARISON OF METHODS TO ANALYZE MONOMERS AND OLIGOMERS 90

Figure 1 Yield (wt. lignin based) for the principal products after 4 hours of reaction, with and without catalyst. 98
Figure 2 Monomers mass yields (based on lignin mass) by GC/MS-FID as a function of the time of reaction. 99
Figure 3 Mw and Mn of lignin oils from GPC analysis, with and without catalyst, as a function of reaction time. 101
Figure 4 MALDI-TOF spectra of lignin oils, at initial time (0h at 250°C) and 4 hours for both catalytic and non-catalytic reactions (* is at m/z 273, the peak of DHB matrix). 102
Figure 5 Integration of the signal of ions detected by MALDI-TOFMS in lignin oils from 0 to 240Da and 240 to 1800Da as a function of reaction time, without and with catalyst. 103
Figure 6 Molecular weight distribution (Mw and Mn) of lignin oils obtained by MALDI-TOFMS as a function of time on stream (at 250°C), with and without catalyst (Pt/C). 104

Figure 7. Synchronous UV fluorescence with 20 nm offset of model compounds, lignin and oligomers (diluted in ethanol) 107
Figure 8. Emission peak maxima in synchronous excitation fluorescence (20 nm offset) for model compounds, oligomers and lignin, diluted in ethanol. 109
Figure 9. Synchronous Fluorescence (offset 20nm) for different reaction time: a) without catalyst b) synchronous fluorescence with catalyst. 110
Figure 10. Depolymerization index (DI) and monomeric products index (MPI) obtained by UV fluorescence analysis as a function of liquefaction time (at 250°C), without and with catalyst (Pt/C). 112
Figure 11 Simplified representation of lignin products in solution and of the analytical methods assessed in this work. 113
Figure 12 Comparison between the MALDI analysis (integration of all detected ions from m/z 0 to 1800) and the depolymerization index (DI) derived from UV fluorescence for the 8 lignin oils (without and with catalyst, 4 samples upon liquefaction time). 114
Figure 13 Comparison between low MW species detected by MALDI (m/z 0-240), products quantified by GC/MS (up to 240Da) and the monomers index (MPI) derived from UV fluorescence. 116
Figure 14. Simplified representation of lignin depolymerization in ethanol based on the complementary methods employed in this work. 118
Figure S1 HSQC spectra of Soda Protobind lignin 133
Figure S2 HSQC spectra of precipitated oligomers after reaction (4h, without catalyst) 134
Figure S3 HSQC spectra of precipitated oligomers after reaction (4h, with catalyst) 134
Figure S4 13C NMR comparison between lignin (before liquefaction) and oligomers (after 4h liquefaction, no catalyst) 135
Figure S5 Scheme of the autoclave setup (Parr Instrument, 300mL) 135
Figure S6 HSQC spectra of Soda Protobind lignin GC/MS chromatograms without catalyst and with catalyst (Pt/C) after 4 hours of isothermal liquefaction (250°C) (internal standard, hexadecane at 50.79min) 137
Figure S7 Mass yields of total and main monomeric products of two different experiments performed at same conditions (4 hours sampling time, with 1%wt Pt/lignin) 137
Figure S8 GPC curves of liquefaction products with catalyst at different sampling times ... 139
Figure S9 MALDI-TOF spectra of raw lignin, matrix and a mix of the two 140
Figure S10 MALDI-TOFMS mass spectra of lignin and bio-oils with 51% of laser power . 140

Figure S11 MALDI-TOF mass spectra with and without catalyst at 30 minutes and 2 hours 60% laser power (optimized conditions) 141
Figure S12 UV absorption spectra of model compounds, lignin and isolated oligomers (also characterized by NMR) 142
Figure S13 UV fluorescence spectra for model compounds excited at 275 nm. The area of each curve is function of the quantum yield of each compound. 143
Figure S14 Example of deconvolution on UV fluorescence spectra (20nm offset) with the 3 characteristic peaks (306, 350 and 375nm), a) Pt/C catalytic liquefaction, 2 hours at 250°C, b) Pt/C catalytic liquefaction, 4 hours at 250°C 144
Figure S15 Effect of spiking guaiacol (1.1mg/L and 6.7mg/L of guaiacol in the final solution of ethanol) on the fluorescence spectra of naphthol (at 3.3mg/L in ethanol), 20nm offset. .. 145
D. EFFECT OF TECHNICAL LIGNIN TYPE AND CATALYST (NI/C, RU/C, PT/C) ON DEPOLYMERIZATION PRODUCTS IN SUPERCRITICAL ETHANOL 147
Figure 1 Analytical methods used in this section of the PhD thesis 150
Figure 2 SEM analysis of the catalyst before and after K3 lignin depolymerization 154
Figure 3 TEM analysis before and after K3 lignin depolymerization..... 155
Figure 4 XRD analysis of the catalyst before and after K3 lignin depolymerisation. 157
Figure 5 Evolution of the UV fluorescence spectra as a function of time for all studied conditions. 160
Figure 6 Alkyl, alkene & not substituted phenols yields (wt.%) for the 4 conditions after 4h.. 161
Figure 7 Mass yields of major molecules for 4 conditions after 4hours of K3 lignin depolymerization.. 161
Figure 8 Main monomers as a function of time of stream (lignin K3 conversion at 250°C, ethanol, H2).. 162
Figure 9 Alkyl, alkene & not substituted phenols yields (wt.%) for the 4 conditions after 4h. 165
Figure 10 Mass yields of major molecules for the 4 lignins with Ni/C catalyst after 4hours of conversion. 165
Figure 11 Main monomers as a function of time of stream (different lignins, Ni/C, conversion at 250°C, ethanol, H2).. 166
Figure S1 Functional group analysis of Soda lignin by quantitative 31P NMR after phosphitylation. 174

Figure S2 Kraft1 (Southern Pine) 31P NMR 174
Figure S3 Kraft3 lignin 31P NMR 175
Figure S4 Kraft2 (Eucalyptus) from 31P NMR 175
Figure S5 SEM pictures for the three catalysts before and after reaction. 176
Figure S6 EDX mapping of Ni/C before reaction. 177
Figure S7 EDX mapping of Ni/C after reaction. 177
Figure S8 EDX mapping of Pt/C before reaction. 178
Figure S9 EDX mapping of Pt/C after reaction. 178
Figure S10 EDX mapping of Ru/C before reaction. 179
Figure S11 EDX mapping of Ru/C after reaction. 179
Figure S12 Particle size distributions (based on TEM) for the three catalysts before and after reaction. 180
Figure S13 Sorption of N2 in the pristine and spent catalysts. 182
Figure S14 Distribution of pores size by NL-DFT: 183
E. SELECTIVE CATALYTIC TEMPO-MEDIATED OXIDATION OF KRAFT LIGNIN TO VANILLIN 190
Figure 1 Proposed mechanism of TEMPO-mediated oxidation of lignin 193
Figure S1 Fractionation method 201
Figure S2 Example of GC-MS/FID chromatogram of one oxidized bio-oil 202
Figure S3 Vanillin calibration curve. 202
Figure S4 FT-IR spectra of solid residue (precipitated at pH=1) for different reaction conditions 203
Figure S5 XRD spectrum of CuO/TiO2 catalyst before reaction. 205
Figure S6 XRD spectrum of CuO/TiO2 after oxidation with only copper-based catalyst 205
Figure S7 XRD spectrum of CuO/TiO2 after oxidation with 2-TEMPO. 206
F. INTEGRATING LIGNIN DEPOLYMERIZATION IN KRAFT MILLS: EXPERIMENTS, PROCESS MODELLING AND TECHNO-ECONOMIC ASSESSMENT 210
Figure 1 Scheme of the process with all the scenarios. 212
Figure 2 Mass and heat main streams for the four scenarios. 217
Figure 3 Fixed capital investment required for the fours scenarios and contribution of each sub process area. 219
Figure 4 Main operating costs for the four scenarios. 219

Figure 5 Revenues sources for the four scenarios. 220
Figure 6 Net Present Value for the four scenarios. 221
Figure 7 Impact of the investment on pulp production cost [€/kg of pulp] for the four scenarios. 222
Figure 8 Sensitivity analysis for scenario 3. 223
G. CATALYTIC HYDROTREATMENT OF LIGNIN IN A TRICKLE BED REACTOR 233
Figure 1 Co-current downflow regimes.[7] 234
Figure 2 Set-up scheme. 237
Figure 3 Cylindrical pellets and trilobes of SiC. 239
Figure 4 XRD of SiC and Ni/SiC before and after reaction. 239
I. APPENDICES 247
1
Figure 1 Yield of the products at the different reaction conditions 253
Figure 2 Van Krevelen diagram for precipitated oligomers 254
Figure 3 ^{1}H NMR spectrum of Soda lignin and its precipitated oligomers obtained after reaction 255
Figure 4 ^{13}C NMR spectrum of Soda lignin and its precipitated oligomers obtained after reaction 255
Figure 5 FTIR spectra of soda lignin, kraft lignin and oligomeric fragments produced after the catalytic and non-catalytic hydrogenation 256
Figure 6 UV-Vis synchronous fluorescence spectra of soda lignin samples withdrawn at different time intervals of catalytic hydrogenation (H2_catalyst) 258
Figure 7 UV-Vis synchronous fluorescence spectra after 4h at different reaction conditions 259
Figure 8 The yield of the most relevant monomers with time under the different reaction conditions 261
Figure 9 The yield of monomers obtained after soda lignin depolymerisation as a function of time. 262
Figure 10 The yield of monomers obtained after kraft lignin depolymerization as a function of time. 263
2

Figure 1 Scheme process of extracting phenols experiment. 271
Figure 2 The recovery yields of batch experiments
(a) Phenol recovery yield; (b) Organics recovery yield of batch experiments..... 278
3

Figure 1 Organic carbon content in the liquid phase..... 279
Figure 2 Monomers yields from GC-MS/FID..... 283
Figure 3. Synchronous (20nm offset) UV fluorescence spectra of the four conditions..... 288

Tables List

A. LITERATURE REVIEW/ FEATURES AND PERSPECTIVES OF LIGNIN 7

Table 1 Cellulose, hemicellulose and lignin composition (dry, ash-free basis) for different biomasses 8

Table 2 Lignin types and their characteristics, adapted 16

B. MULTI-ANALYTIC CHARACTERIZATION OF TECHNICAL LIGNINS AND BLACK LIQUORS 45

Table 1 Suppliers' data of commercial lignins studied 47

Table 2 Analysis forecasted by FJV to characterize the commercial lignins. 49

Table 3 Physico-chemical characteristics of commercial lignins. 52

Table 4 : Inorganic content quantification 54

Table 5 Lignins granulometry 56

Table 6 : Lignin GPC-UV characterizations 58

Table 7: Acetylated lignin GPC-UV characterizations 58

Table 8 : Lignin GPC-MALS 59

Table 9 Comparison between different GPC methods. 60

Table 10 : ^{13}C NMR quantification for main lignin moieties (mmol/g lignin) 61

Table 11 : ^{1}H-^{13}C HSQC Quantification of side chains present in lignins 61

Table 12 : Hydroxyl function assignments and quantification for ^{31}P NMR 62

Table 13 : Description of sampled black liquors (BL). 64

Table 14 Main characteristics measured of the sampled black liquors 65

Table 15 : Carbon Organic (TOC) analysis compared to Elemental analysis (CHNS) 65

Table 16 : Description of 2nd campaign-sampled black liquors (BL). 66

Table 17 : Main characteristics measured of 2nd campaign-sampled black liquors (BL). 66

Table 18 : Total Organic Carbon (TOC) of 2nd campaign-sampled black liquors (BL). 67

Table 19 Proximate analysis of black liquors. 67

Table 20 Physico-chemical characteristics of the softwood Kraft lignin produced 69

Table 21 ^{1}H-^{13}C HSQC Quantification of side chains present in lignins. 70

Table S1 Reproducibility of Soda 31P NMR results 83

Table S2 Comparison of Soda ^{31}P NMR results with literature 84

C. LIGNIN DEPOLYMERIZATION: A COMPARISON OF METHODS TO ANALYZE MONOMERS AND OLIGOMERS 90

Table S1 Quantification of ether bonds in Soda lignin by HSQC NMR 133
Table S2 Mass yields of char and oligomers for the 2 conditions (after 4h at 250°C) 136
Table S3 Retention times and quantification of monomers (wt. % lignin mass basis) by GC/MS-FID for the 8 sampled solutions 138
Table S4 Main UV absorption and fluorescence characteristics of model compounds (diluted in ethanol) 144

D. EFFECT OF TECHNICAL LIGNIN TYPE AND CATALYST (NI/C, RU/C, PT/C) ON DEPOLYMERIZATION PRODUCTS IN SUPERCRITICAL ETHANOL 147

Table 1 Code and suppliers of the technical ligninss 153
Table 2 Main chemical properties of the 4 technical lignins 153
Table 3 Total pore volume (Vp), BET surface area (SBET), micropore volume (VN_2) and ultramicropore volume (VCO2) for pristine and spent catalysts after K3 lignin depolymerization 158
Table 4 Yield char, yield monomer (GC/MS) after 4 hours of reaction at 250°C 159
Table 5 Yields of char and monomers 159
Table S1 Overview of technical lignins (Kraft or Soda) catalytic conversion in alcohols 170
Table S2 Molecular weights of the four lignins. 172
Table S3 Hydroxyl function assignments for 31P NMR 173
Table S4 Detailed monomers yields from GC-MS/FID. 186
Table S5 Molecular weights of bio-oils.. 187

E. SELECTIVE CATALYTIC TEMPO-MEDIATED OXIDATION OF KRAFT LIGNIN TO VANILLIN 190

Table 1 Experimental results for catalytic air oxidation of kraft lignin. 192
Table S1 Summary of recent relevant research for applications of TEMPO in catalytic reaction systems and production of vanillin from model and kraft lignin 199
Table S2 Peaks assignment for FT-IR spectra 204

F. INTEGRATING LIGNIN DEPOLYMERIZATION IN KRAFT MILLS: EXPERIMENTS, PROCESS MODELLING AND TECHNO-ECONOMIC ASSESSMENT 210

Table 1 Experimental conditions 212

Table S1 Proximate analysis of Kraft lignin and chars for different scenarios. 228
Table S2 Elemental analysis of Kraft lignin and chars for different scenarios. 228
Table S3 Proximate analysis of oligomers for different scenarios. 228
Table S4 Elemental analysis of oligomers for different scenarios. 228
Table S5 Atomic balances for each solids and all the scenarios. 229
Table S6 Detailed monomers yields from GC-MS/FID analysis. 230
Table S7 Cost information 231
G. CATALYTIC HYDROTREATMENT OF LIGNIN IN A TRICKLE BED REACTOR 233
Table 1 Correlations for diphasic pressure drops. 236
Table 2 Kinetics and diffusivity parameters. 238
Table 3 Internal and external mass transfer criteria for lignin. 238
Table 4 Bio-oils analysis by HPLC and GC-MS/FID. 240
I. APPENDICES 247
1
Table 1 GPC molecular weight of bio-oil and in THF-soluble oligomer fragments.. 257
Table 2 Lignin depolymerization index (DI) based on from UV-Vis measurements at the different reaction conditions 259
2
Table 1 The structural and molecular formulas of all reagents used The summary of the structural and molecular formulas of all reagents.. 270
3
Table 1 Experiments list. 277

Introduction

1. - General Context

Over the last centuries global energy demand has risen exponentially, and it is intended to rise even more because of the combined increase in world population and the development of emerging countries. Fossil fuels, such as coal, oil and natural gas, account for more than 80% of the world's energy mix.[1] The harsh exploitation of these non-renewable resources leads to a global warming. The growing concerns about climate changes and the related environmental and economic effects favor the advancement of research on renewable and sustainable resources.[2] Among those alternatives, the production of fuels and chemicals through an effective utilization of lignocellulosic biomass is one of the most challenging and interesting.[3,4] Between the main components of biomass, lignin is the most under valorized and recalcitrant because of its complex chemical structure: it is in fact a biopolymer made of aromatic units (mainly *p*-coumaryl, coniferyl and sinapyl alcohols) bonded through different linkages (ether and C-C bonds).[5,6] Even though many researches on this subject, its high potential for producing biofuels and/or platform chemicals is still not sufficiently exploited.

2. - Scope of the Thesis

Based on these premises, the aim of this study is to valorize lignin to produce platform chemicals for more sustainable biorefineries. In particular, we are interested in the valorization of the lignin stream in pulp and paper mills. In this specific context, our purpose is to integrate, in already existent paper industries, a lignin valorization unit, producing green aromatic chemical through liquefaction.

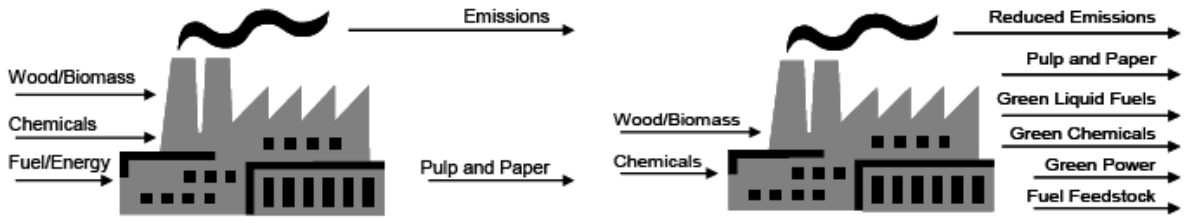

Figure 1 Desired change of scenario for pulp and paper mills.[7]

This research is funded by ANR (*Agence Nationale de la Recherche*). In this national project are involved different laboratories: FJV (*Fédération Jacques Villermaux*) in Nancy for its expertise in chemical engineering and analytical platforms, CTP (*Centre Technique du Papier*)

in Grenoble because of its knowledge in pulping processes, IRCELyon (*Institut de Recherches sur la Catalysee et l'Environnement*) and LGPC (*Laboratoire de Génie des Procédés Catalytique*) in Lyon for a better understanding in catalyst mechanisms. Moreover, this work is the result of very synergetic collaborations, including also other international partners: Washington State University (USA) and National institute of Chemistry in Ljubljana (Slovenia). Sharing results and knowledge between all these research centers made possible to advance faster in the right way.

3. - Thesis Layout

In the following chapters the most relevant results of this study will be presented.

First of all, a literature review is given in Chapter A to understand what lignin is, in which context we are placed and which are currently the valorization technologies to upgrade lignin. Particular emphasis is put on pulp and paper mills as biorefineries that produce cellulose and separate lignin. This chapter describes the state of art and the environment in which this research has been conceived.

In Chapter B, a detailed characterization of the technical lignins and industrial black liquors used in this work is presented. Before converting lignin or black liquors, it is fundamental to understand as much as possible the structure, characteristics, thermal behaviors and compositions of the starting materials.

In the following chapter, Chapter C, is presented a work already published in ChemSusChem (2020 Sep 7;13(17):4633-4648) titled "*Lignin Depolymerization: A Comparison of Methods to Analyze Monomers and Oligomers*". The scope of this study is to find a fast and effective way to analyze lignin liquefaction products. We have compared different analytical techniques to highlight which could be the limitations and the advantages of each.

Chapter D contains the article submitted to Energy & Fuels about the "Effect of technical lignin type and catalyst (Ni/C, Ru/C, Pt/C) on depolymerization products in supercritical ethanol". In this paper are highlighted the differences in yields and products of lignin liquefactions, varying catalysts and lignin kinds.

Chapter E is dedicated to the products of an international collaboration between France and United States of America, on lignin oxidation using TEMPO as catalyst. This work has been submitted as a full paper to Industrial Crops and Product journal.

Chapter F shows and compares different possible scenarios in pulp and paper mills to include a lignin valorization unit. Techno-economic analysis is also given.

To conclude, Chapter G presents some preliminary results on lignin continuous liquefaction in trickle bed. Theoretical design of the set-up and few experimental results are given. This work is still undergoing.

General conclusions are then given to summarize all these studies and make perspectives.

In Appendices are presented many supplementary materials and works related to the subject of this thesis and conducted meanwhile.

4. - List of Publications

I. Bartolomei E, Le Brech Y, Dufour A, Carre V, Aubriet F, Terrell E, Garcia-Perez M, Arnoux P. Lignin depolymerization: A comparison of methods to analyze monomers and oligomers. *ChemSusChem* **2020**. https://doi.org/10.1002/cssc.202001126

II. Terrell E, Dellon LD, Dufour A, Bartolomei E, Broadbelt LJ, Garcia-Perez M. A review on lignin liquefaction: Advanced characterization of structure and microkinetic modeling. *Industrial & Engineering Chemistry Research* **2020**, 59(2), 526-555. https://doi.org/10.1021/acs.iecr.9b05744

III. Bartolomei E, Hernandez A, Terrell E, Garcia-Perez M, LeBrech Y, Djakovitch L. Selective catalytic TEMPO-mediated oxidation of kraft lignin to vanillin. *Industrial Crops and Products* **2020**, To be submitted.

IV. Bartolomei E, Le Brech Y, Vidal L, Le Meins JM, Gadiou R, Dufour A. Effect of technical lignin type and catalyst (Ni/C, Ru/C, Pt/C) on depolymerization products in supercritical ethanol. *Energy & Fuels* **2021**, To be submitted.

V. Bartolomei E, Demol R, Buendia-Kandia F, Le Brech Y, Dufour A. Evaluating aromatics production from lignin depolymerisation: experiments, process modelling and tech-eco assessment. *ACS Sustainable* **2021**, To be submitted.

Other articles are under development and they have not been submitted yet. The most relevant are described in the Appendices.

5. - International Conferences

I. *Lignin Depolymerization: Analysis of Monomers and Oligomers by UV fluorescence, MALDI-TOFMS and GPC*, Bartolomei E., Le Brech Y., Dufour A., Jasiukaityte Grojzdek E., Ročnik T. , Grilc M. , Terrell E., Garcia-Perez M., Carré V., Aubriet F., Arnoux P., ePYRO2020, Ghent Belgium, April 2021

II. *Lignin Depolymerization: Analysis of Monomers and Oligomers by UV fluorescence, MALDI-TOFMS and GPC*, Bartolomei E., Le Brech Y., Dufour A., Jasiukaityte Grojzdek E., Ročnik T. , Grilc M. , Terrell E., Garcia-Perez M., Carré V., Aubriet F., Arnoux P., TCS, Richland, WA, October 2020

III. *Technical lignin conversion via TEMPO-mediated oxidation*, Bartolomei E., Terrell E., Hernandez A., Djakovitch L., Garcia-Perez M., Le Brech Y., Dufour A., NWBC Stockholm, October 2020

IV. *Characterization of lignin depolymerization products by UV fluorescence spectroscopy*, Bartolomei E, Le Brech Y, Dufour A, Terrell E, Garcia Perez M, Aubriet F, Carre V, Arnoux P, Fall 2019 ACS National Meeting, San Diego, CA, August 2019

V. *Comparisons among technical and milled wood lignins through principal component analysis of FTIR spectra*, Evan Terrell, Erika Bartolomei, Yann Le Brech, Manuel Garcia-Perez, Anthony Dufour, PyroLiq 2019, Cork Ireland, 16-20 June 2019

VI. *Analyzing the degree of branching in lignins*, Evan Terrell, Erika Bartolomei, Yann Le Brech, Anthony Dufour, Manuel Garcia-Perez, Fall 2019 ACS National Meeting, San Diego, CA, August 2019

VII. *Analysis of liquids from lignin depolymerisation: UV synchronous fluorescence spectroscopy as a fast screening method*, Erika Bartolomei, Yann Le Brech, Anthony Dufour, Evan Terrell, Manuel Garcia-Perez, Frederic Aubriet, Vincent Carre, Philippe Arnoux, GDR Thermobio, November 2019

VIII. *Pyrolysis Activation Energy for Carbonaceous Materials: from Biomass to Low Rank Coal*, Terrel E., Bartolomei E., Garcia-Perez M., International Mechanical Engineering Congress & Exposition, Salt Lake City, UT, November 2019

IX. *Multi-analysis characterization of lignins*, Bartolomei E, Le Brech Y, Lichère H, Dufour A, Zelcor Summer School, Wageningen, September 2018

6. - References

1. Data & Statistics - IEA. https://www.iea.org/data-and-statistics?country=WORLD&fuel=Energy%20supply&indicator=TPESbySource.

2. Davidson, D. J. Exnovating for a renewable energy transition. *Nature Energy* **4**, 254–256 (2019).

3. Chundawat, S., Beckham, G., Himmel, M. & Dale, B. Deconstruction of Lignocellulosic Biomass to Fuels and Chemicals. *Annual Review of Chemical and Biomolecular Engineering* 2, 121–145 (2011).

4. Brandt, C. C. et al. 2016 Billion-Ton Report: Advancing Domestic Resources for a Thriving Bioeconomy, Volume 1: Economic Availability of Feedstocks. https://www.osti.gov/biblio/1435342-billion-ton-report-advancing-domestic-resources-thriving-bioeconomy-volume-economic-availability-feedstocks (2016) doi:10.2172/1435342.

5. Saraeian, A. *et al.* Evaluating lignin valorization via pyrolysis and vapor-phase hydrodeoxygenation for production of aromatics and alkenes. *Green Chem.* **22**, 2513–2525 (2020).

6. Schutyser, W. *et al.* Chemicals from lignin: an interplay of lignocellulose fractionation, depolymerisation, and upgrading. *Chemical Society Reviews* **47**, 852–908 (2018).

7. Wising, U. & Stuart, P. Identifying the Canadian forest biorefinery. *PATAC Annual Meeting* (2006).

A. Literature Review: Features and perspectives of lignin

1. - Lignocellulosic Biomass

1.1. - General composition

A necessary component for the advancement of green chemistry and engineering is effective utilization of biomass. There is approximately 550 Gt of carbon on earth in the form of biomass, which includes microorganisms, animals and plants[1], distributed worldwide (Figure 1). Plants alone account for 80% of all biomass carbon (an estimated 450 Gt C)[1]. Although there is an energy decarbonization necessity by reducing energy consumption, the sustainable production of carbonaceous fuels is a promising option to reduce climate changing effects. A promising feedstock for this purpose is lignocellulosic biomass, which includes trees, grasses and agriculture residues[2]. The conversion of these materials into high value compounds and materials is among the most significant challenges for their effective utilization[3].

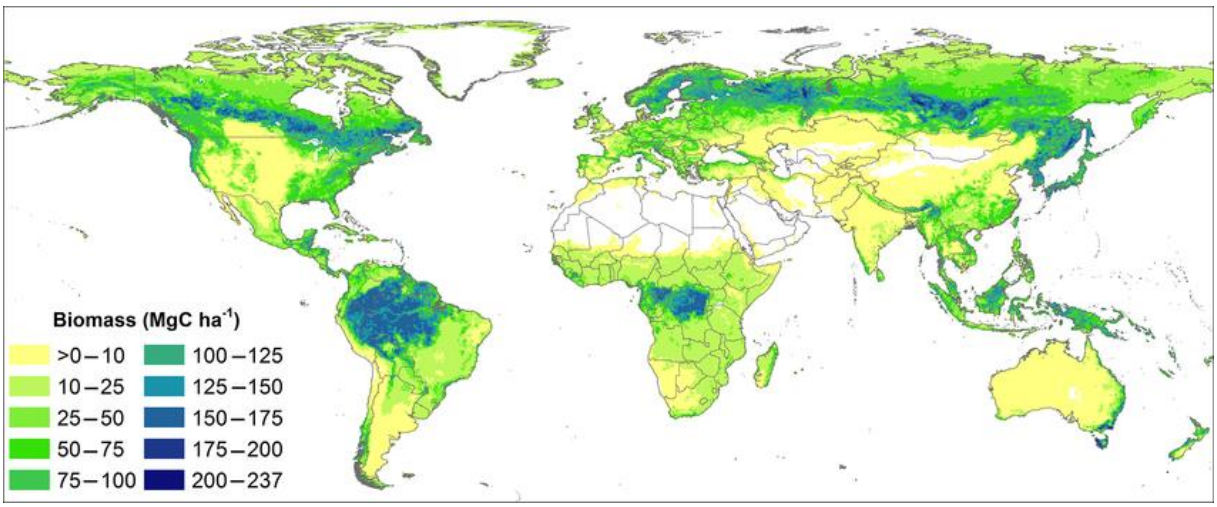

Figure 1 Distribution of biomass carbon worldwide[4]

Lignocellulosic biomass is primarily made up of three carbon-based polymers: cellulose, hemicellulose, and lignin[3]. A relative variable quantity of inorganic ash and organic extractives (e.g., proteins, lipids, soluble sugars) are also present[2,5].

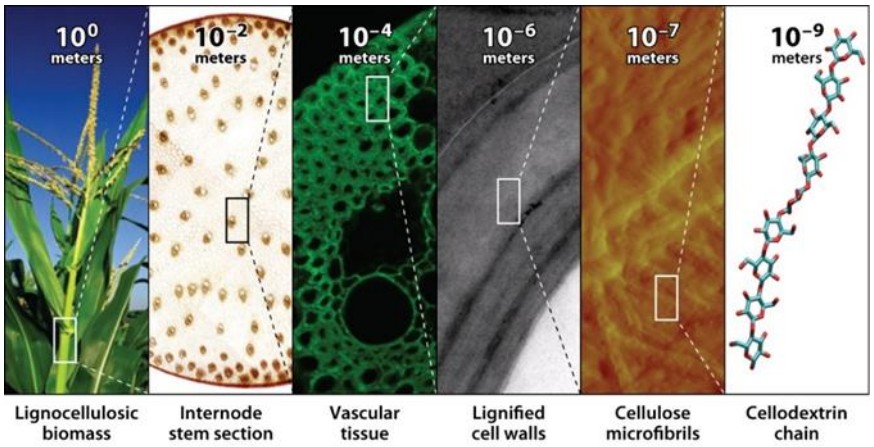

Figure 2 Hierarchical scale of biomass from full plant to molecular level[2]

Figure 2 shows lignocellulosic biomass from natural to 10^{-9} scale. Cellulose and hemicellulose structures are primarily polymers made up of sugar/carbohydrate monomers with glycosidic linkages. Lignin structure is also polymeric, its base monomer is a variety of methoxylated phenylpropane structures[6]. The inorganic components of biomass are metals and/or metal oxides (typically known as ash)[7]. Although the inorganic content of biomass is small in comparison to the organic fraction, its presence still can have a great impact on its conversion for both inert atmosphere liquefaction technologies as well as oxidative technologies like combustion and gasification.[8,9] A more detailed breakdown of the cellulose/hemicellulose/lignin composition of several biomasses is given in Table 1.

Table 1 Cellulose, hemicellulose and lignin composition (dry, ash-free basis) for different biomasses[5]

BIOMASS	CELLULOSE (%)	HEMICELLULOSE (%)	LIGNIN (%)
Beech	45.2	32.7	22.1
Birch	50.2	32.8	17.0
Eucalyptus	52.7	15.4	31.9
Oak	58.4	31.4	23.5
Pine	48.1	23.5	28.4
Spruce	43.6	27.4	29.0
Pine cones	34.3	39.5	26.2
Bamboo	43.9	26.5	29.6
Sugar cane	45.8	31.3	22.9
Switchgrass	48.7	38.4	12.9
Wheat straw	44.5	33.2	22.3
Olive husk	25.0	24.6	50.4
Corn cob	48.1	37.2	14.7
Cattle manure	32.7	24.5	42.8

1.2. - Extractives and inorganic matter

Two minor components of biomass are organic extractives and inorganic matter. Extractive compounds are so-named because they can be extracted directly from biomass with organic solvents and/or water. The extractive content of biomass is usually less than 10%, although higher quantities can be found in woody bark and leaf samples[10]. Common classes of extractives that can be found in woody biomass samples include terpenes, fatty acids, triglycerides, flavonoids, and tannins[10].

Inorganics ash within biomass are made up of mineral content that is typically characterized as the residue left after combustion (ash content)[7]. The primary composition of characterized biomass ashes include oxides of aluminium, calcium, iron, magnesium, potassium, silica, sodium, and titanium. The ash content of woody biomasses is typically low (approximately <5%), but the ash content of grasses and agriculture residues can be significantly higher (up to 20%)[7]. Inorganic matter may have strong impacts during thermochemical processing (e.g., pyrolysis, gasification, combustion) of feedstock[11–13]. Several studies have highlighted the catalytic effect of inorganics on the conversion of biomass during pyrolysis.[14,15] The residual inorganic content of the resulting solid product after slow pyrolysis also has important contributions to the biochar's properties[16]. In gasification and combustion, inorganic content can also have a catalytic role[17,18]. The management of ash after gasification and combustion is also an important technical challenge, especially for larger-scale operations.

1.3. - Cellulose and Hemicellulose

Cellulose is the most abundant component of lignocellulosic biomass and is made up of repeating glucose units with a degree of polymerization between 1000 and 5000[19]. β-D-glucopyranose units within cellulose are linked via glycosidic bonds (β 1,4) with interlayer hydrogen-bonding networks[17,20].

Cellulose exists within plants in the form of long fibrils embedded in a matrix of hemicellulose and lignin. The conversion of cellulose into renewable fuels and chemicals can be achieved through a variety of methods, including thermochemical and biochemical processes.[21–23] Thermochemical routes rely on depolymerization of cellulose using elevated temperatures, while biochemical routes rely on microbial fermentation of the glucose units within cellulose to produce small molecules like alcohols, alkanes or terpenes[17].

Hemicellulose is similar to cellulose in that it is a polymer composed of repeating carbohydrate units (see Figure 3). However, hemicellulose also features a wider variety of monomer types (especially pentoses), including mannose, glucose, galactose, arabinose, xylose, rhamnose, fucose and uronic acids[18]. Hemicelluloses are also frequently found in lignin-carbohydrate complexes within biomass. Like cellulose, hemicellulose can also be converted through biochemical and thermochemical processes. The most important conversion product from pentose-abundant hemicellulose is furfural, a five-member ring platform molecule that can be upgraded into a wide variety of chemicals and fuels[24].

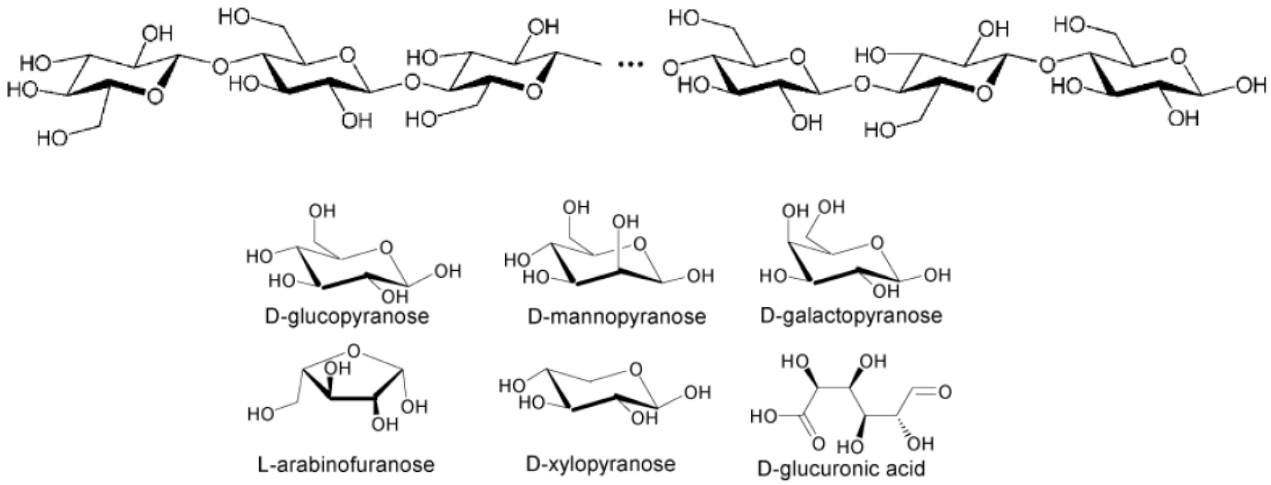

Figure 3 (top) Cellulose structure[23]; (bottom) Hemicellulose's monomeric units, adapted[16].

1.4. - Lignin

Lignin is the third primary component of lignocellulosic biomass and is made up of aromatic methoxylated phenylpropane subunits (monolignols). Lignin is the first source of renewable aromatic carbons, making it especially attractive for conversion into high value products[26]. The three primary monolignols that make up a lignin polymer are p-hydroxyphenyl, guaiacyl, and syringyl units[27] (Figure 4). In lignocellulosic biomass, the biosynthesis of these monomers occurs via enzymatic pathway transformations from phenylalanine.[28,29] In addition to the three primary monolignols, recent work has identified a greater diversity of monomers that can exist in lignin. To date, the identification and characterization of lignin monomers and structure remains an ongoing challenge. Some of the "new" monomers that have been proposed are coniferyl/sinapyl acetates, benzoates, p-hydroxybenzoates, p-coumarates, and ferulates; caffeyl alcohol, 5-hydroxy-coniferyl alcohol, coniferyl/sinapyl aldehyde, dihydroconiferyl alcohol, and ferulate esters; tricin, resveratrol, isorhapontigenin, piceatannol, piceid, isorhapontin,

astringin, feruloyltyramine, and diferuloylputrescine.[30] These monomers are connected in a variety of ways, of which the majority of bond types include β-O-4, β-5, β-β, 4-O-5, 5-5 and β-1 bonds (Figure 5).

The most abundant of these is the β-O-4 aryl ether linkage, accounting for 50-80% of the total in native lignin[26]. In addition to more labile ether bond types, native lignin can also feature more recalcitrant carbon-carbon bond types. The analysis of different bond types in lignin is important due to the nature of the cleavage of these bonds during both lignin extraction and lignin conversion in liquefaction, pyrolysis and/or oxidation technologies. Because of the remarkable diversity present in the native structure of lignin, due to a wide variety of monomers and bond types, analytical characterization is a significant and ongoing challenge. Many methods exist to study different facets of lignin structure, including wet chemistry, chromatography, thermochemical, and spectroscopy methods.[31]

Finally, another critical component in the characterization of lignin structure is measurement or estimation of its molecular weight. Lignin molecular weight is a fundamental property that influences the recalcitrance of biomass and lignin valorization.[32] Molecular weight determination is performed on extracted lignin, thereby presenting a difficulty to estimate molecular weight of native lignin. Indeed, the result of extraction processes modifies the lignin structure. Furthermore, measuring the frequency of branching in lignin structure faces a similar problem, and there is still no clear consensus on whether or not native lignin features branching.[33] Depending on how the lignin was extracted, many different molecular weights may be measured.[32] A wide variety of extraction methods exist for removing lignin from biomass, each yielding different purity/quality among final lignin products[34].

To date, effective and economically viable valorization of lignin has remained elusive, despite the fact that it is produced in large quantities in industry as a major byproduct[26]. The primary focus of this manuscript is on developing further research outcomes that emphasize lignin conversion through thermochemical liquefaction technologies.

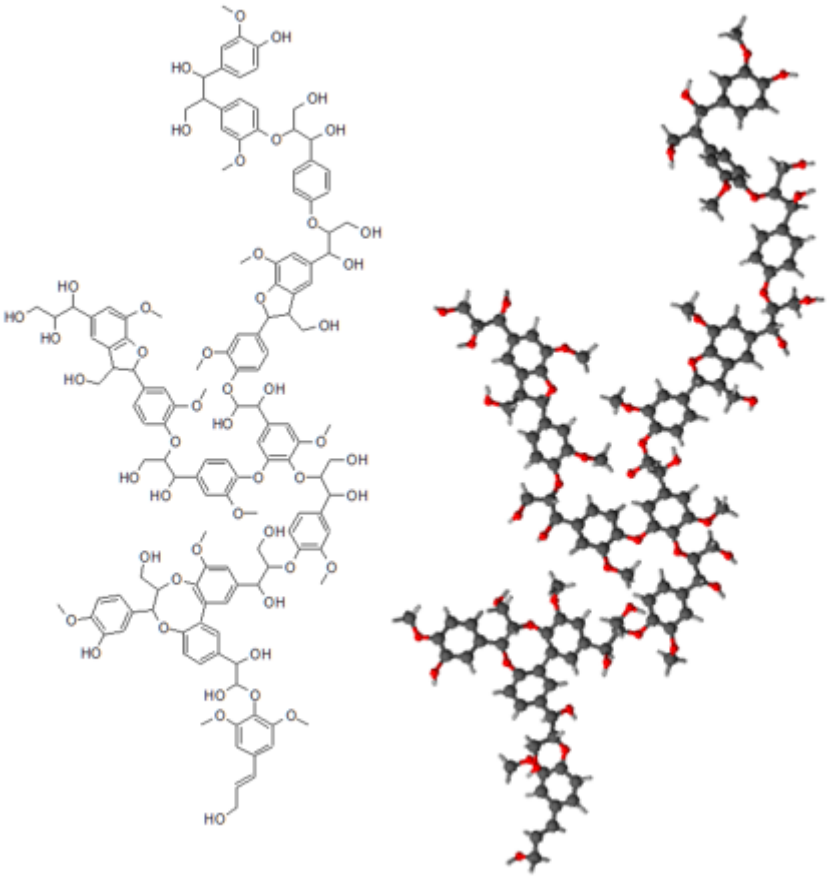

Figure 4 Lignin structure example (re-edited)[33,34].

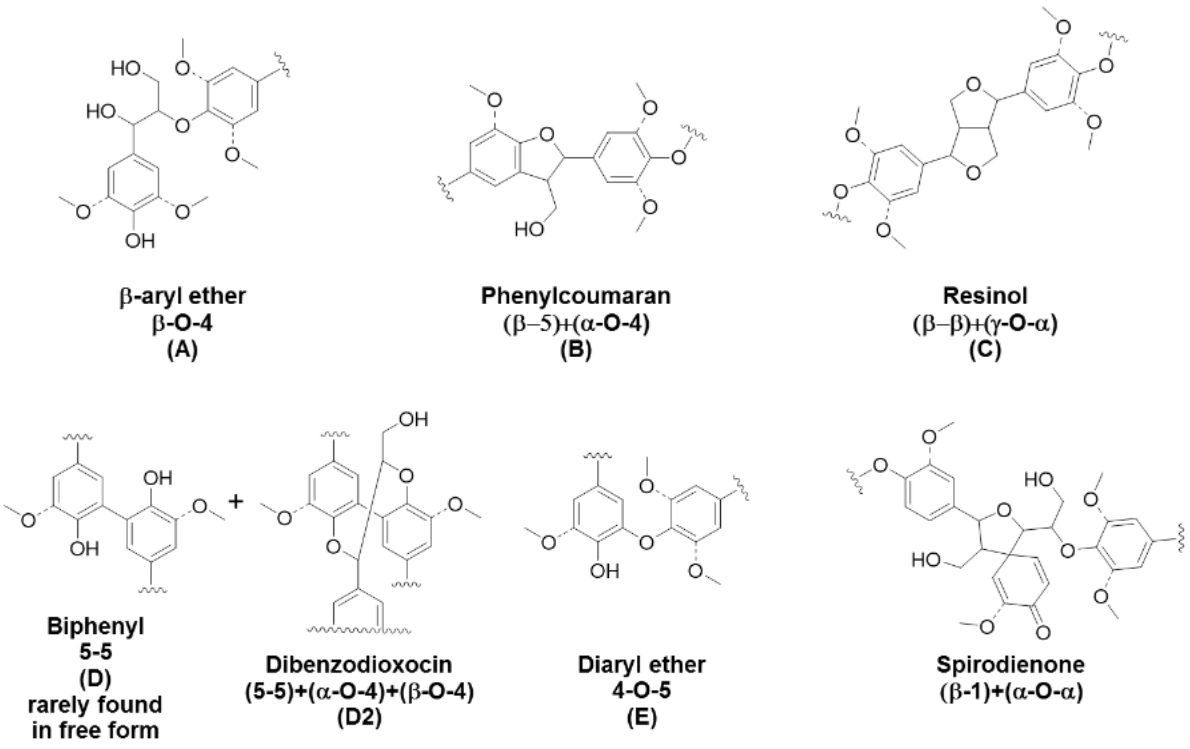

Figure 5 Bonding types connecting lignin's monomer units.[3]

2. - Biorefinery to high value bio-products

From the Industrial Revolution in the end of XVIII century, the world demand of energy and fuels and products continues increasing every year[38]. Primary energy consumption is based mainly on fossil fuels (gas, oil, coal), around 80% in 2018[39]. Therefore, massive impacts on environment are felt, ending in many dramatic phenomena such as global warming, climate change and deforestation all around the world. The great majority of these effects are the direct result of increasing carbon dioxide concentration in the atmosphere[40,41]. The Intergovernmental Panel on Climate Change (IPCC) estimates an increase of global mean temperature change of 2 °C by 2050, with the greatest impact being felt in arctic regions. IPCC also identifies 2-3 °C of additional warming as high risk for extensive biodiversity loss, decreases in crop yields and water availability, and irreversible sea level rise.

However, significant researches have been started in order to develop alternatives to fossil energy sources. Among alternative energy technologies, biomass is one of the most promising. The aim is to replace fossil fuels, a non-renewable material (taking millions of years to regenerate itself), with biomass, which has much greater potential availability and capability for fast regeneration in the biosphere, to produce a wide variety of chemicals, fuels and energy.[42]

An emerging perspective for biomass utilization in biorefineries first relies on biomass fractionation, followed by targeted conversions of different biomass components (i.e., cellulose, hemicellulose and lignin)[43]. These conversion technologies can be thermochemical, biological or a sequence of them. For example, in a recent study, Yamaguchi et al.[44] present a system in which the cellulose and hemicellulose fractions from biomass are converted into sugar alcohols and the recovered lignin is converted into high-value aromatics. This so-called “cascade utilization” strategy is conceptually similar to the more mature pulp and paper industry, in which delignified biomass is used to produce paper products, and the remaining lignin-rich fraction is burned for process heat. A very large variety of products can come from biomass, such as biochemicals, biochar, biofuels and different kinds of sugars (see Figure 6).

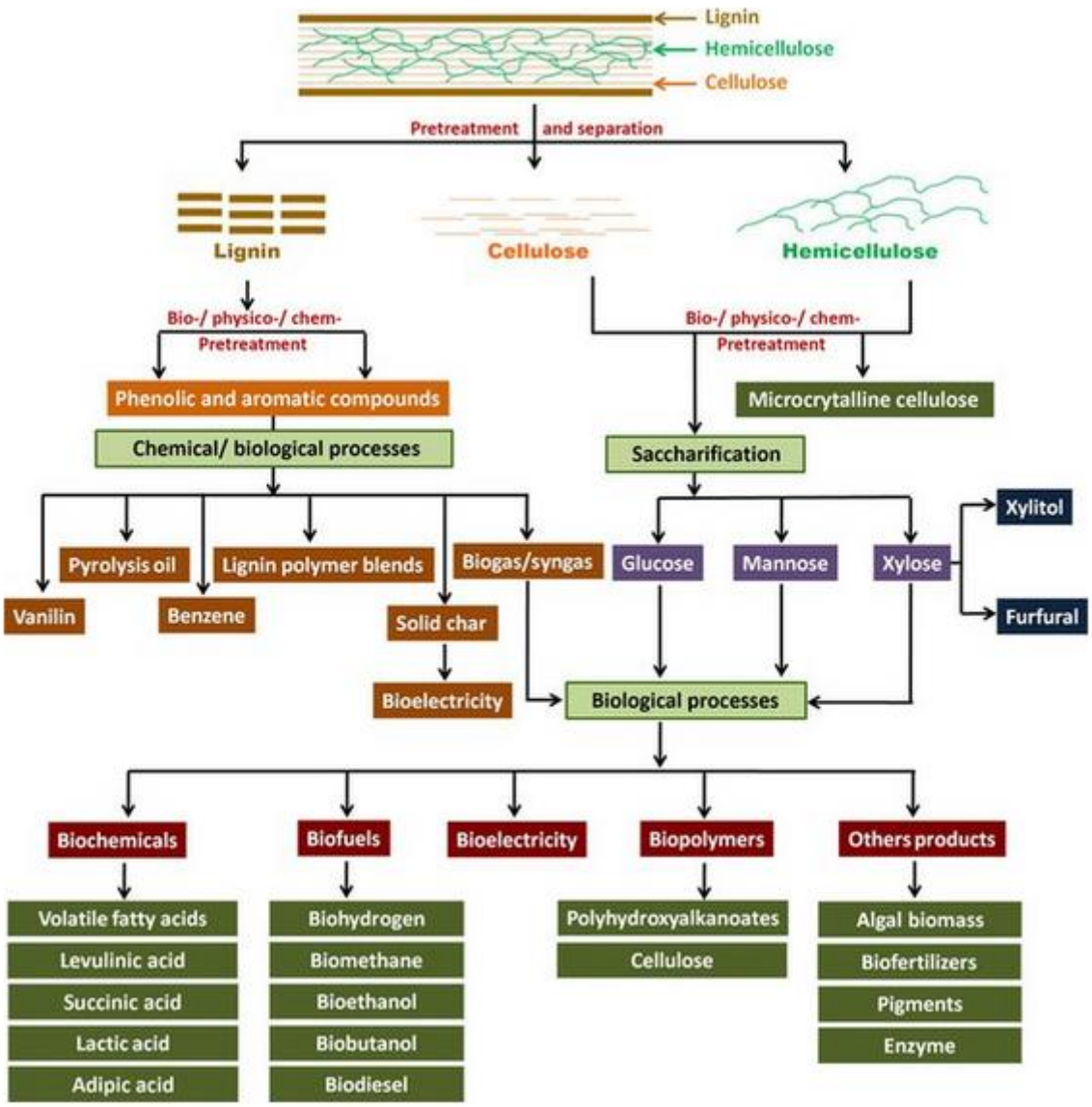

Figure 6 General biorefinery approach to biomass.[43]

3. - Technical Lignins from Biorefinery

3.1. - Lignin types

During the past several centuries, different kinds of biorefinery have been proposed and developed. Each one is oriented to different final products and each one has still limitations to be improved upon. The biggest industries that can be classified as a biorefinery (based on a modern interpretation) are pulp and paper mills. They are one of the first and the most diffused lignocellulosic biorefineries, aimed at producing high quality pulps for the paper and packaging industry.[46] Another kind of emerging biorefinery is bio-ethanol production through lignocellulosic carbohydrates fermentation. In a recent review, Karagoz et al. highlight 10 operational cellulosic ethanol plants in Europe, with outputs between approximately 10 to 10^4 tons per year[47]. For both these examples, the main valorized products come from the carbohydrate fraction of the biomass (i.e. cellulose and hemicellulose). Lignin is mostly considered as low-value residual fraction, commonly used as an energy source for the plant through burning it to recover electricity. However, in order to integrate economic viability of biorefineries, a better valorization of lignin has to be made. Since it is the largest renewable source of aromatics, lignin can be used to produce important aromatic molecules as bio-based chemical building blocks.[48,49]

In terms of numbers, about 100 million Tons of industrial lignin is produced every year[50]. A consistent part of this amount comes from pulp and paper mills, that alone can produce 50-70 million Tons/year.[37,51,52] Only the 2% of lignin from paper industry is commercially employed, and the rest is burnt as a low-value fuel[53]. Overall, the lignin business today represents roughly 300 million dollars[53]. Thanks to the success of emerging biorefinery, at present about 2.11 million Ton of chemicals are bio-based[54].

Such an important and considerable feedstock like lignin cannot be ignored, although its complete integration in paper industry and in our markets is still challenging. There are some intrinsic limitations about lignin. One major consideration is that there is no fixed, explicit structure and associated properties for lignin. Indeed, lignin structure and properties heavily depend on the kind of original biomass, its growth, and the extractions and pretreatment methods applied. It is important to highlight that any kind of lignin available is not representative of the native lignin in a plant wall cell. In the end, the “technical lignins”

produced should be the protagonists of the research for added-value products. Table 2 presents a general view on the main available technical lignins, their characteristics and potentials.

Table 2 Lignin types and their characteristics, adapted from [35,50]

Lignin Type	Production Scale	Separation Method	Pretreatment Chemistry	Lignin Purity	Sulphur Content	Potential Products
Kraft	Industrial	Precipitation or ultrafiltration	Alkaline	Moderate	Moderate	Fertilizer and pesticide carrier, carbon fibers, addition to thermoplastic polymers, binders, resins, activated carbon. Chemical - vanillin, hydroxylated aromatics, quinine, aldehydes and fatty acids
Soda	Industrial	Precipitation or ultrafiltration	Alkaline	Moderate -Low	Free	Production of phenolic resins, animal nutrition, dispersants, polymer synthesis
Lignosulfo_ nate	Industrial	Ultrafiltratio n	Acid	Low	High	Colloidal suspensions, stabilizers, dispersants, binders, detergents, adhesives and components of feed, particle board, surfactants, adhesives and additives for cements
Organosolv	Pilot-Demo	Dissolved air flotation, precipitation	Acid	High	Free	Additives for paints, varnishes, paints and create new substances
Hydrolysis	Industrial-Pilot		Acid	Moderate -Low	Low-Free	Preparation of polymeric materials, dispersants, deflocculating agents
Steam Explosion	Pilot-Demo		Acid	Moderate -Low	Low-Free	Chemicals such as phenols or biodiesel

A summary of four of the most prominent lignins is given below and shown in Figure 7. As it can be noticed from the figure, lignin extraction processes can be divided into sulfur and sulfur-

free ones. Between the sulfur processes, we find the sulfite and the Kraft ones. The main difference between their conditions is the pH necessary for the extraction. In fact, Kraft process is conducted at very alkaline condition, while the sulfite one takes place in acid environment. A similar distinction can be remarked between the sulfur-free entraction processes, solvent and Soda pulping. If the solvent pulping occurs in precence of acids, Soda pulping is conducted at high alkaline conditions.

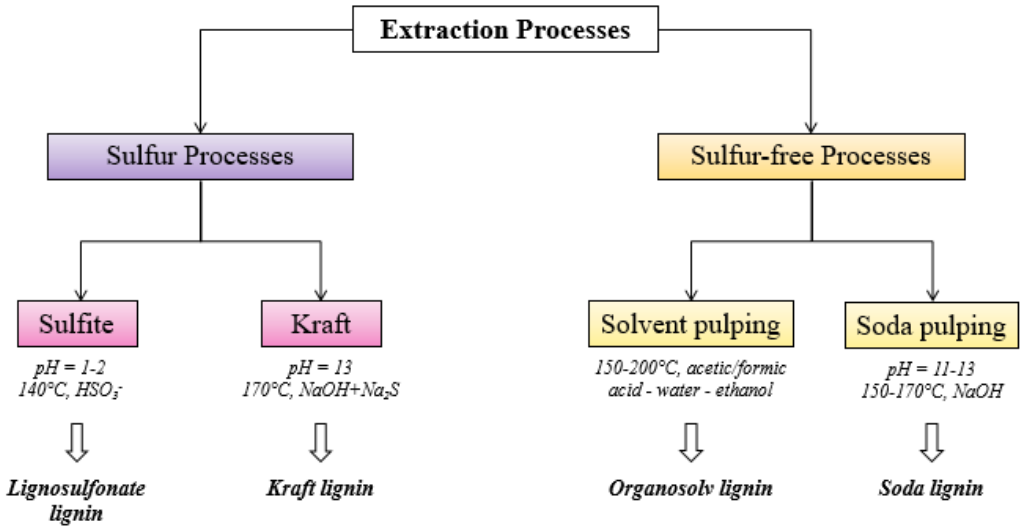

Figure 7 Main lignin extraction processes.

***Lignosulfonates**:* The acidic (pH=1-2, HSO_3^-) sulfite processes produces lignin that is sulfonated on the propyl side chain, thereby giving lignosulfonates. Sulfonation yields lignin material with polar groups and is and therefore water-soluble, unlike other technical lignin varieties. A greater prevalence of functional groups makes lignosulfonates useful in colloidal applications as stabilizers, dispersants, surfactants and adhesives. Lignosulfonates tend also to be of relatively low purity with high remaining carbohydrate content and high molecular weight.

***Kraft lignin**:* Kraft lignin is produced from the kraft pulping process, which relies on a cooking liquor containing NaOH and Na_2S to remove lignin from biomass (pH=13). Consequently, kraft lignin is high in thiol S content, is highly condensed and has relatively few remaining cleavable ether bonds. Compared to other lignins, Kraft lignin typically has a large quantity of phenolic OH and is high in recalcitrant C-C bonds.[37] Kraft lignin is the most widely produced type of industrial lignin.[55]

***Soda lignin**:* The soda pulping process, unlike sulfonation and kraft pulping, does not rely on any sulfur-containing species and therefore yields S-free lignin. However, the harsh pulping

conditions (pH=11-13, 150-170°C) yield a recalcitrant, condensed lignin material as a product. Vinyl ethers may also be present in soda lignin due to the non-acidic nature of the pulping[37].

***Organosolv lignin**:* Organosolv processes rely on applications of organic solvents (generally acetic/formic acid, water, ethanol) to solubilize lignin directly from biomass under less harsh conditions than other pulping techniques. This gives a lignin product that is more similar to the native lignin found in biomass, with lower molecular weight and higher remaining ether bond content. Organosolv lignins are also S-free. Harsher conditions utilized in organosolv extraction, however, can still yield lignins that are as recalcitrant as kraft or soda lignins. Organosolv processes, compared to other technical lignin extraction methods, are relatively newer and not nearly as widespread in industrial applications.

3.2. - Kraft Process

Being the most used process in paper industry and the most promising lignin to be integrated into a biorefinery vision, a special importance will give to Kraft process used in pulp and paper mills. In particular, the possible development and modification coupling the LignoBoost® lignin precipitation process to the existing mill will be highlighted.

3.2.1. - Basic Papermaking Process

The pulp and paper industry plays an important role in the economy. On the other hand, it is the fourth largest consumer of primary energy in the industrial sector[56]. However, as an energy and pollution intensive industry, the green development of paper mills has received widespread attention.

The first step in the paper industry is the fractionation of wood. Two typologies of separation can be identified: a mechanical one and a chemical one. In the first one, wood is weakened by mechanical means only and thus the lignin is separated from the rest. In the chemical paper mill instead, the wood is treated with various chemical products (salts in particular) in controlled temperature and pH conditions. It is precisely this type of plant that is of greatest interest for energy and economic optimization. For that reason only this kind of process will be taken in count in this study.

The paper industry is a technology- and capital-intensive industry, and it is also subject to resource constraints[57]. Several pulp and paper companies have already accepted the challenge to improve their energy efficiency and have started reaping the rewards of energy efficiency investments[58]. Energy efficiency is doing more work with the same amount of energy or doing

the same amount of work using less energy. After years of development, a mature set of technologies for black liquor burning for power generation and useful product recovery have been developed.

The Kraft process is the most diffused process to separate lignin from cellulose in paper industry. It has different stages and all of them are well interconnected[59,60] (see Figure 8). Three sequential steps can be individuated: impregnation, digestion and recuperation. The main target product is pulp for which black liquor is a byproduct/waste. For 1 Ton of dry pulp, 7 Tons of black liquor (15%wt solids content) are produced[61]. Lignin is the main organic component of black liquor, along with some sodium salts and water.[62]

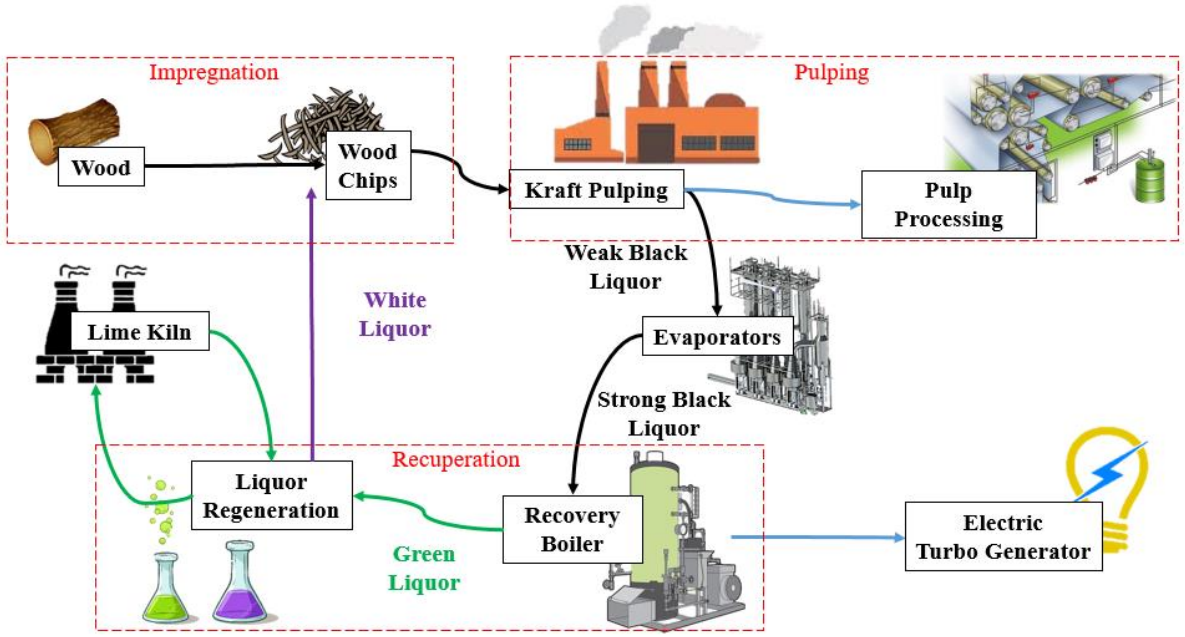

Figure 8 Pulp and paper mill process.

Impregnation. Raw wood is first peeled, debrided and cut into pieces. Wood chips are introduced in the pre-steaming zone, where they are moisturized and preheated (<100°C) with steam. This operation allow the air, naturally present in wood cavities, to be replaced by steam water. Wood chips are soaked with a mix of recycled white liquor, basically a solution of sodium hydroxide (NaOH 1 mol/L) and sodium sulfide (Na_2S 0,2 mol/L) at pH 13,5-14.

Pulping. Impregnated wood is conducted into the digester. The cooking temperature is about 160-180°C for about 2-4 hours. It mainly depends on the OH^-, SH^- concentrations in the cooking solution to break some of the bonds between the lignin macromolecules in order to dissolve the

lignin and remove it from the fiber cell wall and intercellular layer. This degradation process produces fragments of lignin (Na org., S org.), which are soluble in that high alkaline solution. The following reaction occurs[63,64]:

$$NaOH + NaS_2 + wood \rightarrow Na\ org. + S\ org. + NaHS$$

Na and S org. are lignin-derived macromolecules separated in the pulping and linked to sodium and sulfur species.

Since the carbon-carbon bond is stable under alkaline conditions, the cleavage of the oxygen-carbon bonds is the main reaction in the cooking process. This reaction will take place and produce phenolic hydroxyl groups from the cleavage of aryl-alkyl-ether bonds. Most of the alkalis are consumed in the cooking process by the saccharin acids ($C_7H_5NO_3S$) formed during the degradation of hemicelluloses. In the cooking reaction many of the resins forms sodium salts of fatty and harts resins this are occurring a soap. And are usually skimmed of from the black liquor in the evaporation area. They are also processed to produce *tall oil*.[63,64]

The obtained coarse pulp is suspended in black liquor, so a liquid-solid phase separation (filtration and washing technologies) is applied to wash the pulp with water. Black liquor washing and extraction equipment is a series (usually 3 to 4) of vacuum or pressure drum washing in countercurrent mode.

Recuperation. The content of dry solids in black liquor extracted from the washing process is generally below 15%wt. After a first evaporation stage, it increases up to 30%wt, it is called weak black liquor. Concentration process continues till concentration of 65-80%wt, strong black liquor. Then it can be finally burned in the recovery boiler (1200°C) to recycle the inorganic chemical products in the pulp process. The flue gas generated by combustion rises in the furnace and the heat carried by it is absorbed through the boiler to produce steam. Then, the flue gas is further used by the evaporator to extract the waste heat, or it is discharged after the electrostatic precipitator or other devices to recover alkali dust.

During black liquor combustion, many reactions take place. The predominant products are Na_2S and Na_2CO_3.[64]

The organic compounds of sodium (Na org.) in black liquor are burned and the reaction yields prevalently Na_2SO_4, which is then carbothermal reduced into Na_2S thanks to the presence of organic compounds (C org.).

$$Na_2SO_4 + 2C\ org. \rightarrow Na_2S + CO_2$$

$$Na_2\,SO_4 + 4CO \rightarrow Na_2S + 4CO_2$$

The inorganic compounds are collected at the bottom of the boiler; they are in a melted form so some water is added to recuperate them. The resulting solution is called green liquor and it is mainly made by Na_2S and Na_2CO_3. Sodium carbonate is then causticized by lime to make a sodium hydroxide solution, or a mixed solution of sodium hydroxide and sodium sulfide (known as white liquor), and recycled in the impregnation step. Then, it is regenerated by the following caustic reaction:

$$Na_2CO_3 + Ca(OH)_2 \rightarrow 2NaOH + CaCO_3$$

Once the solid $CaCO_3$ (lime) is separated from white liquor, the lime is burned:

$$CaCO_3 \rightarrow CaO + CO_2$$

Then, the burned lime is used to produce $Ca(OH)_2$ adding water:

$$CaO + H_2O \rightarrow Ca(OH)_2$$

Kraft process has the following advantages: (1) The chemical and thermal energy recovery system in the cooking waste liquid, namely the alkali recovery technology, is very efficient, so that the environmental pollutants generated during the process can be effectively treated and the consumption of materials and energy is reduced; (2) The pulp has excellent mechanical strength; (3) It is suitable for almost all kinds of plant fiber raw materials, so it has been most widely used in industry. However, it produces stronger fibers that are coarser and dull, making bleaching more complicated.

3.2.2. - Process Improvement

With the expansion of production scale, paper mills need to continuously improve their productivity. Therefore, the black liquor processing capacity also needs to be increased accordingly, but it is difficult to upgrade the recovery boiler, and the replacement cost is very high, which has become a restricting factor for continuous development.

A common problem which occurs during the traditional precipitation and separation process of lignin from Kraft pulp black liquor, is the clogging of the filter medium in whole or in part. A full or near-full blockage will result in a decrease in the flow rate of the washing liquid through the filter cake (which is initially zero). Partial clogging of the filter cake results in low purity of the lignin. The negative effects of these filtrations are due to changes in the solubility of the lignin, which in turn is caused by changes in the filter cake pH ionic strength gradient during

the washing process. These changes can cause particles to restructure, such as peptization (returning to a colloidal state) or lignin dissolution.

LignoBoost® overcomes conventional filtering and sodium separation problems by redissolving the lignin in spent wash water and acid (H_2SO_4). In this process, a part of the concentrated black liquor (from the evaporation step) is firstly precipitated using CO_2. Since lignin is insoluble in water and acid, CO_2 (flue gas), SO_2 or inorganic acid is added directly into the black liquor to lower the pH, so that the alkali lignin can precipitate. At pH~10, almost no H_2S gas is released, but all other gases are collected and recycled to the sulfate pulping process. Generally the CO_2 used in this step is a purchased pure one. However, due to the high cost of CO_2, researchers have focused on the use of high CO_2 content flue gas from a lime kiln, which is then concentrated using standard techniques and then reused. The precipitated lignin is dewatered with a filter press, and then the resulting slurry is once again dewatered and washed, with acidified wash water, to produce virtually pure lignin cakes. The lignin lean liquor is returned to the liquor cycle. LignoBoost® works in conjunction with evaporation (see Figure 9). The two-step process yields a very pure lignin with low ash content[65].

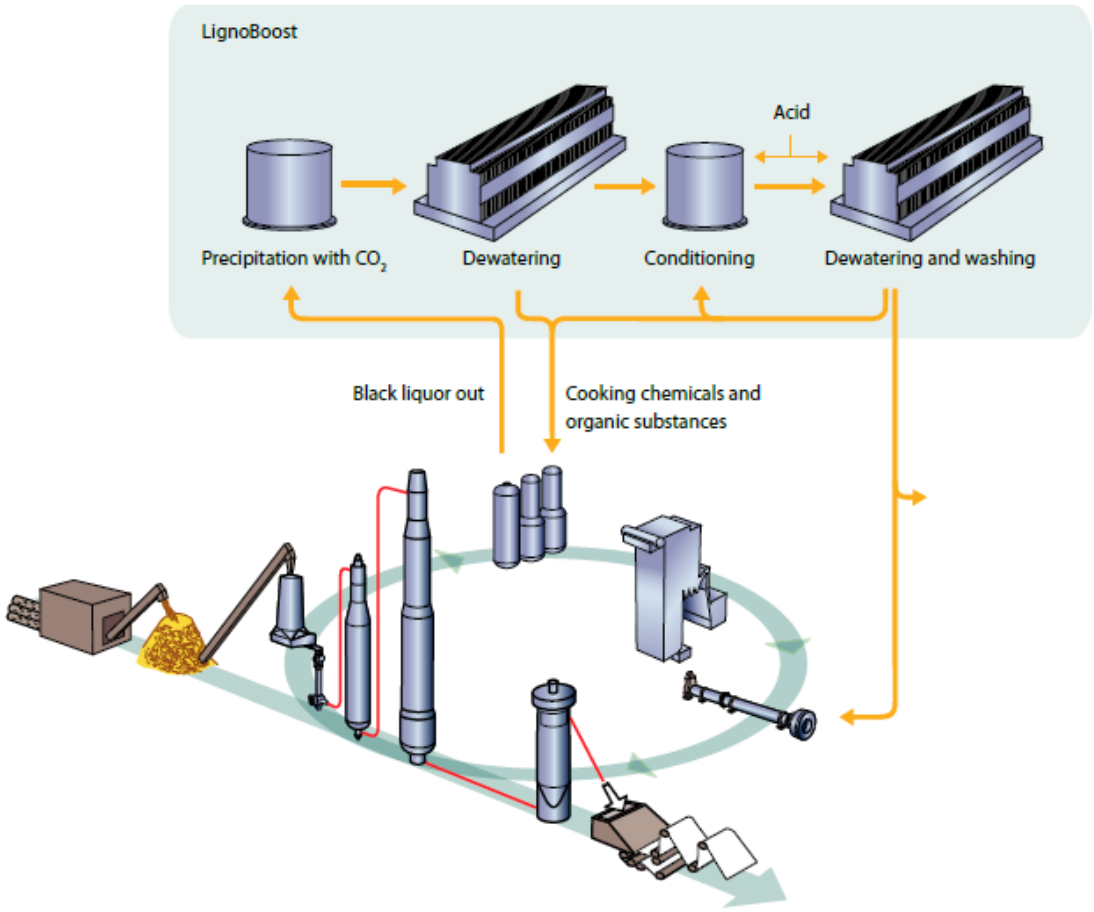

Figure 9 LignoBoost® scheme : Kraft black liquor and lignin extraction[64]

The precipitated lignin can be used and upgraded for producing bioplastics, adhesives and chemicals such as phenol or BTX or replacing fossil based fuel. Another interesting area is that it can be utilized in carbon fiber production (low cost carbon fiber) and precursor to "green carbon" products such as reinforcement filler or activated carbon.

The LignoBoost® technology has the following advantages: enhances the pulp production by reducing the thermal load of the recovery boiler; reduces the mill's dependence on fossil fuel and its fluctuating price; adds revenue to the mills by selling Kraft lignin for further processing as specialty chemicals (carbon fiber, binder, activated carbon, dispersants, asphalt emulsions etc.) energy sources and other uses.[46,67] The first two commercial LignoBoost® installations are at the Domtar - Plymouth plant in North America (25.000 Tons/year of lignin)[68], and more recently the Stora Enso - Sunila plant in Finland (370.000 Tons/year of lignin)[69], both of them are held by Valmet company.

4. - Thermochemical Conversion of Lignin

4.1. - Generalities

In general, there are four broad methods by which lignin can undergo thermochemical conversion. These include 1) pyrolysis, in which the feedstock is processed in an inert gas atmosphere; 2) liquefaction, in which lignin is dissolved in a solvent to yield bio-oil which can be then upgraded into biochemicals and biofuels; 3) gasification, in which the feedstock is partially oxidized to produce syngas, primarily a mixture of CO and H_2; and 4) combustion, in which the feedstock is completely oxidized (i.e., burned) to produce heat. Among these three possible processes, only pyrolysis and liquefaction can directly yield interesting products in the resulting bio-oil, in particular there are many applications of these aromatic molecules for polyurethane foams, phenol-formaldehydes resins and also as dispersants or as additives for concrete and rubber.[50] An overview of lignin thermochemical conversion technologies is given in Figure 10.

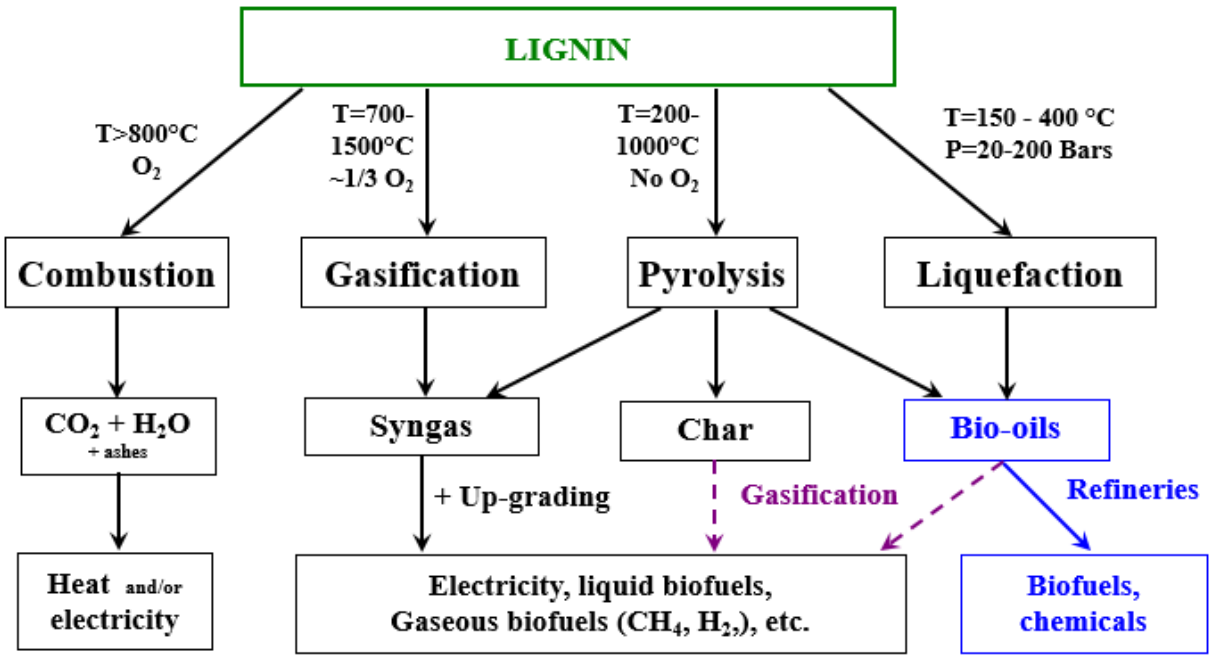

Figure 10 Lignin thermochemical conversion pathways (adapted[70])

However, among these three technologies, the depolymerization of lignin into liquid products is relatively the most challenging. In a pulp and paper mill setting, lignin is present as a by-product in black liquors, which also contain inorganic chemicals used for delignification. Heat

from the boiler is used to produce steam/power. Although this technology is very mature, electricity generation efficiency is low and sulfur-gas emissions can be high. If heat and/or power production remains a target, a viable alternative for black liquor processing is gasification.[71] Integrated gasification technologies have potential for higher electricity production efficiency, reduced emissions, and greater opportunities for alternative products from syngas (e.g., renewable fuels and chemicals).

4.2. - Lignin Pyrolysis

The thermochemical conversion of lignin under an inert atmosphere (typically nitrogen) is known as pyrolysis. The goal of pyrolysis technologies is to valorize the feedstock by depolymerization, which can then be followed by targeted upgrading. During fast pyrolysis with high heating rates (≥50-100 °C/s), lignin is converted into non-condensable gas (i.e. CO, H_2, CH_4, CO_2), vapor phase (monomers and oligomers), and solid-phase (biochar).[35] Slow pyrolysis is primarily focused on the production of biochar only. In a multitechnique characterization of lignin softening and pyrolysis, Shrestha et al.[72] highlight the series of transformations Kraft lignin goes through in a pyrolysis process, with emphasis on viscoelastic behavior. Initially upon heating, lignin begins swelling and softening, with a glass transition temperature and fluidity onset of approximately 140 °C. At 200 °C, lignin begins to lose side chains through pyrolytic reactions, with significant mass loss occurring at temperatures of 250 °C and greater, where the carbon content increases and oxygen content decreases.[72] At higher temperatures (>350 °C) lignin begins to undergo solidification reactions, crosslinking, and polyaromatic condensation to for char compounds.[72–75] With respect to the production of liquid/vapor-phase products, Windt et al.[76] report that approximately 10-15% of technical lignin pyrolysate can be quantified by gas chromatography (GC) for fast pyrolysis in a temperature range of 500-800 °C. GC-detectable compounds tend to be low molecular weight monomers and volatile organic small molecules; however, the total liquid yield (including higher molecular weight liquid-phase oligomers) can be roughly 40-60%wt. The majority of these monomeric compounds are made up of guaiacols and phenols, with measurable influences of heating rate and pyrolysis temperature.[76]

For the production of fuels and chemicals, upgrading of lignin pyrolysis bio-oils (condensates) is often necessary. Several approaches exist, largely focused on hydrotreating the lignin pyrolysis products to remove its significant oxygen content. Hydrodeoxygenation (HDO) can

take place either on downstream, condensed pyrolysis liquids or through online vapor HDO. In a study of catalytic HDO of guaiacol as a lignin pyrolysis model compound, Olcese et al.[77] report the production of phenol, benzene and toluene during HDO through a series of 8 different reactions. The primary guaiacol HDO reactions feature the cleavage of bonds between oxygen and aromatic carbon, to yield aromatic hydrocarbons, water and methane.[77] Common catalysts used in HDO processing include those that are Ni-based, Co-Mo, and noble metals (e.g., Ru, Rh, Pt).[78,79] In particular, Badawi et al.[80] report the high efficiency of $CoMo/Al_2O_3$ in the hydrodeoxygenation of phenolic compounds. Many studies propose mechanisms for phenolic compounds HDO reaction in presence of CoMo based catalyst: it has been assessed that Co promotes the direct deoxygenation, while Mo favors hydrogenation leading to non-aromatic products.[80–82] The major monomeric HDO products are alkylphenols from lignin pyrolysis oils initially made up of cresols and methoxylated phenols.[83]

Similar results are obtained for direct HDO of vapor-phase pyrolysis products, which is a potentially more efficient process that does not require prior condensation of lignin pyrolysis liquids. Saraeian et al.[84] report significant yields of aromatic hydrocarbons and alkenes from vapor-phase HDO, and Olcese et al.[85] report yields of phenol, alkyl phenols and aromatic hydrocarbons, with near-complete conversion of higher oxygen content aromatics (like guaiacol, catechol and vanillin). A major challenge in online vapor HDO is managing coke formation, which occurs both as "catalytic coke" from gas and small molecule conversion within the catalyst and "thermal coke" resulting from deposition of heavy vapor phase lignin oligomers.[84,85]

An alternative to HDO is catalytic hydropyrolysis of lignin, in which pyrolysis occurs under reactive hydrogen atmosphere rather than an inert atmosphere (like nitrogen), sharing the goal of HDO to produce deoxygenated aromatics from lignin.[86–88] This technology has also been shown to be successful in yielding phenols and alkylphenols.[87,88] In fact, it has been shown that using Mo/SiO_2-Al_2O_3 and Cr_2O_3/Al_2O_3 catalysts, the pyrolytic oil yield increases and the methoxyphenols products are replaced by phenol, cresols and xylenols.[89] In a study on catalytic hydropyrolysis of organocell lignin, Meier, et al.[90] report yields of ~20% phenol and ~75% alkyl phenols among GC/MS-detectable compounds (with MoO_3-NiO/aluminosilica catalyst). Jan et al. have reported the production of cycloalkanes in addition to aromatics from recent hydropyrolysis work that utilizes Pd catalysis.[91]

4.3. - Lignin Liquefaction

4.3.1. - Generalities

Liquefaction can be defined as a hybrid process between pyrolysis, because it is based on the same thermal chemistry, and hydrolysis, occuring in liquid media.[92] The temperature range also is between the two conversion processes mentioned above, with most lignin liquefaction technologies utilizing temperatures between 200-400°C. At this temperature range with suitable residence time, liquefaction can achieve an inexpensive bio-crude, which can be then upgraded into final specialties.

Liquefaction can boast some advantages compared to pyrolysis. One of the major inconveniences during lignin depolymerization is that undesired reactions, such as recondensation and repolymerization of intermediates, are very prominent.[93,94] Operating in a liquid phase can prevent those reactions.[95] Besides, the use of a solvent for the reaction can promote the solubility of gas reagents and in some cases bring additional effects to the reaction (e.g. ethanol can act as a hydrogen donor itself).[96–99]

Since the peculiarity of liquefaction is the use of a solvent, its choice is particularly relevant. In general it has to be chosen to be effective in delivering high bio-crude yield, easily recoverable from the bio-crude product, low solvent cost and low impact on reactor cost[95].

Another important consideration is the chemistry of the reaction but also the stability of the desired products. According to the solvent, the atmosphere and the catalyst used during the reaction, different categories of liquefaction can be distinguished: reductive; oxidative; acid/base catalyzed; and solvolytic liquefaction (see Figure 11). Catalytic liquefaction is particularly interesting because based on the catalyst used the selectivity for different products an vary.[100]

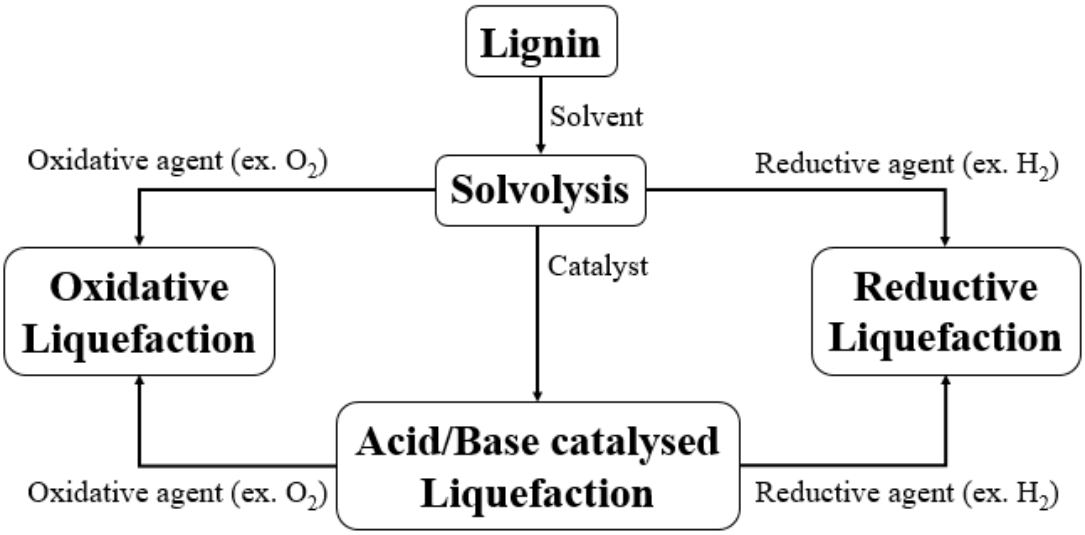

Figure 11 Lignin liquefaction categories.

4.3.2. - Solvolysis

Among the most simple and apparently inexpensive method to convert lignin via liquefaction is solvolysis. It consists in the solvolytic and thermal depolymerization of lignin in a liquid medium, at mild or harsh temperature and pressure.[101] Most of the time the solvents are water, alcohols or a mixture of them. One of the most popular combination of solvent is ethanol in water (60-70 %vol.).[102] This concentration is the result of lignin solubility studies.[103] Being hydrophobic, lignin is not soluble in neutral pH water, so ethanol can increase its solubilization in the reaction medium. With this kind of solvent mixture lignin can be converted in liquid products up to ~65%wt (lignin basis), of which about 30% are value-added phenolic compounds.[104] Generally solvolysis is always the first approach for lignin liquefaction, even if the final target is to push further lignin conversion using for example some catalysts.[105] In many works results of comparative solvolysis can be found, varying reaction conditions, such as pressure and temperature. Increasing these two parameters, the reaction condition become harsher and the conversion into monomers increases, while heavier compounds are the main products at lower temperature and pressure.[98,105,106]

4.3.3. - Acid/Base catalysed Liquefaction

This process is the conversion of lignin using thermal, solvolytic and catalytic means. It differs from solvolysis just by the addition of a catalyst. Generally it makes the lignin depolymerization more efficient.[92]

Regarding base-catalysed depolymerization, different kinds of soluble or solid bases can be used, like NaOH, KOH, LiOH, K_2CO_3 or $Ca(OH)_2$. Indeed, the most largely used is NaOH because it seems to be the most effective in the oil yield compared to the others.[107] Even if the monomeric yield is not so high, the selectivity is. In some studies it has been noticed catechol and substitued catechols as predominant products.[107–109]

Concerning acid-catalysed depolymerization, many acids can be used with water and/or other organic solvents (Lewis and Bronsted acids). It can be noticed that the choice on the solvent can play a role in the monomeric products selectivity. In fact, when water is used phenols and catechols are prevalent, while ethanol or similar alcohols are used phenols and guaiacols are favoured. Moreover, under these reaction media, methoxyphenols with oxygenated side-chains (vanillin, homovanillic acid and guaiacylacetone) can be the main low molecular weight products.[110]

4.3.4. - Oxidative Liquefaction

Oxidative liquefaction differs from solvolysis for the presence of an oxidizing agent, which can be O_2, H_2O_2 and less often CuO. Generally temperature and pressure are not very elevated (<200°C, 20 bar).[92] This lignin conversion method can be either catalytic or not. The main purpose of oxidative liquefaction is the cleavage of side-chains, yielding phenolic compounds, and sometimes also aromatic rings cleavage to target aliphatic carboxylic and dicarboxylic acids.[92] The main target product of this process is vanillin through alkaline lignin oxidation.[111] For vanillin and other phenolic aldehydes production a high pH (generally alkaline water) is required to favor the reaction (according to mechanisms proposed[112,113]) and also to stabilize the products in the reaction media. Since H_2O_2 can be quite dangerous at large scale, oxygen is the most common oxidant agent. It could be pure molecular oxygen or air.[111] Even if alkaline water is the most common solvent used in oxidative lignin liquefaction, studies involving alcohols or other peculiar solvents (acidic or ionic liquids for example) can be found in literature.[114,115] Many studies have been conducted on model compounds, not lignin, and their conversion can reach the 15%wt.[92,116,117]

4.3.5. - Reductive Liquefaction

Under this name go all those hydrocracking reactions which occurred in the presence or not of a redox catalyst and a reducing agent, commonly molecular hydrogen (*hydroprocessing*) or a hydrogen donor (*liquid-phase reforming*)[92]. Thanks to the presence of hydrogen, during reductive liquefaction lignin is not only depolymerized but it starts to be deoxygenated as well

(through *hydrodeoxygenation*, HDO). The temperature range is large, between 150 and 450°C, and so is the hydrogen pressure, between 10 and 100 bar. Therefore, two categories of conditions can be identified: mild when temperature is above 300°C and harsh till 450°C. Independently from the reaction conditions severity, reductive depolymerization results more selective than pyrolysis[87], but the nature of the main compounds depends on many factors: lignin nature, solvent, catalyst and reaction severity. It has been demonstrated that there is a correlation between the lignin conversion and the β-O-4 content initially present in lignin.[118,119] Many studies have been conducted on lignin reductive liquefaction, using many kinds of catalyst (base or noble metallic ones such as Ni, CoMo, Cr, Pd, Pt, Ru…) and many different solvents (water, alcohols, THF…). The most common solvents are alcohols, which can be in sub- or super-critical phase.[6,97,120,121] As mentioned before, the selectivity normally converges in phenols and guaiacols, up to 40%wt.[92]

4.3.6. - Characterization of Lignin Products from Liquefaction

To well achieve lignin depolymerization, it is important to deep understand its structure and features. After decades of studies and achievements in lignin upgrading, there is still a lack in analytical methods to analyze lignin and its products.[122] One of the main reasons is the absence of proper model compounds to compare its structure. This problem involves lignin itself but also all the oligomeric products which are normally produced during liquefaction. In fact, liquefaction bio-oil is generally composed by a low percentage of monomers, easy to characterize by many techniques, but also a large amount of oligomers. Those molecules are too heavy to be detected by chromatography for example, and there is still a lack in methods to analyze them. The most emblematic example of analytical issues related to lignin characterization is gel permeation chromatography to determine the molecular weight of lignin and its liquefaction products. This technique is suitable, for the most part, for polymers, but very limited for lignin because of the lack of pertinent calibration standards. Generally polystyrenes are used as standard even if their structure does not match lignin to a great extent.[123,124] Lignin rigidity also has steric effects in GPC results.[125,126] Moreover, other issues have been highlighted, like the possible interaction between phenolic polymers and the columns and the different responses to the detectors of the different functional groups.[127–129] Anyway, GPC is under continuous development and it is still used for lignin because is the most accessible technique to evaluate its molecular weight and compare it. A good insight of GPC analysis and not only is given from Constant et al.[130] They compared different GPC methods showing that the choice of the eluent and the columns can drastically change the results. They

also characterized lignin with other analytical tools pointing out their advantages and shortcomings.

5. - Conclusions

As mentioned before, today is clear the need to encourage an energy transition towards renewables sources. Biomass can be one of the solutions to avoid the overexploitation of fossil fuels, especially because of its availability worldwide. In this chapter an overview on biomass and more in details on lignin has been given. Particular attention has been put on technical lignins, since those are waste/co-products already existent in biorefineries and paper industries. Depending on the lignin extraction method, it takes peculiar characteristics, structures and possible applications. One of the most abundant in the world is Kraft lignin, a co-product of the paper industry which largely uses Kraft delignification process to separate cellulose pulp to make paper from biomass. This Kraft lignin today is mostly combusted in the paper mill itself to generate energy for the plant, but this resource could and should be better valorized to produce interesting high-valued molecules (for biofuels and biomaterials). Lignin composition, rich in phenols, makes it a valuable bio-resource which deserves to be exploited to the fullest and not just burned.

Many conversion pathways already exist for lignin, but there is still a lot of research in this field. In this chapter, all the thermochemical conversion processes have been described and particular emphasis has been given to lignin liquefaction, since it is the most promising process to yield green aromatic molecules from lignin. On this subject hundreds of studies can be found in literature, but actually many of these researches have been conducted on model compounds and just at lab scale nowadays. So it is evident that research on lignin valorization in general is still not exhaustive and more attention should be given on technical and commercial lignins. Finally, an emphasis should be given to scaling up those studies to pilot and industrial scales.

6. - References

1. Bar-On, Y. M., Phillips, R. & Milo, R. The biomass distribution on Earth. *PNAS* **115**, 6506–6511 (2018).

2. Chundawat, S., Beckham, G., Himmel, M. & Dale, B. Deconstruction of Lignocellulosic Biomass to Fuels and Chemicals. *Annual Review of Chemical and Biomolecular Engineering* 2, 121–145 (2011).

3. Sanderson, K. Lignocellulose: A chewy problem. *Nature* **474**, S12–S14 (2011).

4. Pettinari, M. L. & Chuvieco, E. Generation of a global fuel data set using the Fuel Characteristic Classification System. *Biogeosciences* **13**, 2061–2076 (2016).

5. Vassilev, S. V., Baxter, D., Andersen, L. K., Vassileva, C. G. & Morgan, T. J. An overview of the organic and inorganic phase composition of biomass. *Fuel* **94**, 1–33 (2012).

6. Zakzeski, J., Jongerius, A. L., Bruijnincx, P. C. A. & Weckhuysen, B. M. Catalytic Lignin Valorization Process for the Production of Aromatic Chemicals and Hydrogen. *ChemSusChem* **5**, 1602–1609 (2012).

7. Cai, J. *et al.* Review of physicochemical properties and analytical characterization of lignocellulosic biomass. *Renewable and Sustainable Energy Reviews* **76**, 309–322 (2017).

8. Seehar, T. H. *et al.* Influence of process conditions on hydrothermal liquefaction of eucalyptus biomass for biocrude production and investigation of the inorganics distribution. *Sustainable Energy Fuels* **5**, 1477–1487 (2021).

9. Tian, C. *et al.* Hydrothermal liquefaction of harvested high-ash low-lipid algal biomass from Dianchi Lake: Effects of operational parameters and relations of products. *Bioresource Technology* **184**, 336–343 (2015).

10. Debiagi, P. E. A. *et al.* Extractives Extend the Applicability of Multistep Kinetic Scheme of Biomass Pyrolysis. *Energy Fuels* **29**, 6544–6555 (2015).

11. Yildiz, G. *et al.* Effect of biomass ash in catalytic fast pyrolysis of pine wood. *Applied Catalysis B: Environmental* **168–169**, 203–211 (2015).

12. Yao, X. *et al.* A comprehensive study on influence of operating parameters on agglomeration of ashes during biomass gasification in a laboratory-scale gasification system. *Fuel* **276**, 118083 (2020).

13. Wang, L., Hustad, J. E., Skreiberg, Ø., Skjevrak, G. & Grønli, M. A Critical Review on Additives to Reduce Ash Related Operation Problems in Biomass Combustion Applications. *Energy Procedia* **20**, 20–29 (2012).

14. Safar, M. *et al.* Catalytic effects of potassium on biomass pyrolysis, combustion and torrefaction. *Applied Energy* **235**, 346–355 (2019).

15. Wang, J. *et al.* Catalytic effects of six inorganic compounds on pyrolysis of three kinds of biomass. *Thermochimica Acta* 110 (2006).

16. Allen, Jessica. A. & Downie, Adriana. E. Predicting Slow Pyrolysis Process Outcomes with Simplified Empirical Correlations for a Consistent Higher Heating Temperature: Biochar Yield and Ash Content. *Energy Fuels* **34**, 14223–14231 (2020).

17. Carroll, A. & Somerville, C. Cellulosic Biofuels. *Annual Review of Plant Biology* **60**, 165–182 (2009).

18. Zhou, X., Li, W., Mabon, R. & Broadbelt, L. J. A Critical Review on Hemicellulose Pyrolysis. *Energy Technology* **5**, 52–79 (2017).

19. Hallac, B. B. & Ragauskas, A. J. Analyzing cellulose degree of polymerization and its relevancy to cellulosic ethanol. *Biofuels, Bioproducts and Biorefining* **5**, 215–225 (2011).

20. Mukarakate, C. *et al.* Influence of Crystal Allomorph and Crystallinity on the Products and Behavior of Cellulose during Fast Pyrolysis. *ACS Sustainable Chem. Eng.* **4**, 4662–4674 (2016).

21. Mosier, N. *et al.* Features of promising technologies for pretreatment of lignocellulosic biomass. *Bioresource Technology* **96**, 673–686 (2005).

22. Dalluge, D. L. *et al.* Continuous production of sugars from pyrolysis of acid-infused lignocellulosic biomass. *Green Chem.* **16**, 4144–4155 (2014).

23. Jarboe, L. R., Wen, Z., Choi, D. & Brown, R. C. Hybrid thermochemical processing: fermentation of pyrolysis-derived bio-oil. *Appl Microbiol Biotechnol* **91**, 1519–1523 (2011).

24. Luo, Y. *et al.* The production of furfural directly from hemicellulose in lignocellulosic biomass: A review. *Catalysis Today* **319**, 14–24 (2019).

25. Hosoya, T. & Sakaki, S. Levoglucosan Formation from Crystalline Cellulose: Importance of a Hydrogen Bonding Network in the Reaction. *ChemSusChem* **6**, 2356–2368 (2013).

26. Xu, C. C., Dessbesell, L., Zhang, Y. & Yuan, Z. Lignin valorization beyond energy use: has lignin's time finally come? *Biofuels, Bioproducts and Biorefining* **15**, 32–36 (2021).

27. Sun, R.-C. Lignin Source and Structural Characterization. *ChemSusChem* **13**, 4385–4393 (2020).

28. Vanholme, R., Demedts, B., Morreel, K., Ralph, J. & Boerjan, W. Lignin Biosynthesis and Structure. *PLANT PHYSIOLOGY* **153**, 895–905 (2010).

29. Rinaldi, R. *et al.* Paving the Way for Lignin Valorisation: Recent Advances in Bioengineering, Biorefining and Catalysis. *Angewandte Chemie International Edition* **55**, 8164–8215 (2016).

30. del Río, J. C. *et al.* Lignin Monomers from beyond the Canonical Monolignol Biosynthetic Pathway: Another Brick in the Wall. *ACS Sustainable Chem. Eng.* **8**, 4997–5012 (2020).

31. Lupoi, J. S., Singh, S., Parthasarathi, R., Simmons, B. A. & Henry, R. J. Recent innovations in analytical methods for the qualitative and quantitative assessment of lignin. *Renewable and Sustainable Energy Reviews* **49**, 871–906 (2015).

32. Tolbert, A., Akinosho, H., Khunsupat, R., Naskar, A. K. & Ragauskas, A. J. Characterization and analysis of the molecular weight of lignin for biorefining studies. *Biofuels, Bioproducts and Biorefining* **8**, 836–856 (2014).

33. Balakshin, M. *et al.* Spruce milled wood lignin: linear, branched or cross-linked? *Green Chem.* **22**, 3985–4001 (2020).

34. Obst, J. R. & Kirk, T. K. Isolation of lignin. in *Methods in Enzymology* vol. 161 3–12 (Academic Press, 1988).

35. Terrell, E. *et al.* A Review on Lignin Liquefaction: Advanced Characterization of Structure and Microkinetic Modeling. *Industrial & Engineering Chemistry Research* **59**, 526–555 (2020).

36. Dellon, L. D., Yanez, A. J., Li, W., Mabon, R. & Broadbelt, L. J. Computational Generation of Lignin Libraries from Diverse Biomass Sources. *Energy & Fuels* **31**, 8263–8274 (2017).

37. Bruijnincx, P., Weckhuysen, B., Gruter, G.-J. & Engelen-Smeets, E. *Lignin valorisation: the importance of a full value chain approach*. (2016).

38. Global direct primary energy consumption. *Our World in Data* https://ourworldindata.org/grapher/global-primary-energy.

39. World Energy Balances – Analysis. *IEA* https://www.iea.org/reports/world-energy-balances-overview.

40. Solomon, S., Plattner, G.-K., Knutti, R. & Friedlingstein, P. Irreversible climate change due to carbon dioxide emissions. *PNAS* **106**, 1704–1709 (2009).

41. AR5 Climate Change 2014: Impacts, Adaptation, and Vulnerability — IPCC. https://www.ipcc.ch/report/ar5/wg2/.

42. Bauer, F., Coenen, L., Hansen, T., McCormick, K. & Palgan, Y. V. Technological innovation systems for biorefineries: a review of the literature. *Biofuels, Bioproducts and Biorefining* **11**, 534–548 (2017).

43. Liu, Y. *et al.* Cascade utilization of lignocellulosic biomass to high-value products. *Green Chem.* **21**, 3499–3535 (2019).

44. Yamaguchi, A., Mimura, N., Shirai, M. & Sato, O. Cascade Utilization of Biomass: Strategy for Conversion of Cellulose, Hemicellulose, and Lignin into Useful Chemicals. *ACS Sustainable Chem. Eng.* **7**, 10445–10451 (2019).

45. Chakraborty, D., Dahiya, S., Kotamraju, A., Srivastav, K. & Venkata Mohan, S. Valorization of paper and pulp waste: Opportunities and prospects of biorefinery. in 623–656 (2019). doi:10.1016/B978-0-12-815907-1.00027-1.

46. Ragnar, M. *et al.* Pulp. in *Ullmann's Encyclopedia of Industrial Chemistry* 1–92 (American Cancer Society, 2014). doi:10.1002/14356007.a18_545.pub4.

47. Karagoz, P., Bill, R. M. & Ozkan, M. Lignocellulosic ethanol production: Evaluation of new approaches, cell immobilization and reactor configurations. *Renewable Energy* **143**, 741–752 (2019).

48. M. Abu-Omar, M. *et al.* Guidelines for performing lignin-first biorefining. *Energy & Environmental Science* **14**, 262–292 (2021).

49. Dessbesell, L., Paleologou, M., Leitch, M., Pulkki, R. & Xu, C. (Charles). Global lignin supply overview and kraft lignin potential as an alternative for petroleum-based polymers. *Renewable and Sustainable Energy Reviews* **123**, 109768 (2020).

50. Bajwa, D. S., Pourhashem, G., Ullah, A. H. & Bajwa, S. G. A concise review of current lignin production, applications, products and their environmental impact. *Industrial Crops and Products* **139**, 111526 (2019).

51. Tribot, A. *et al.* Wood-lignin: Supply, extraction processes and use as bio-based material. *European Polymer Journal* **112**, 228–240 (2019).

52. Ľudmila, H., Michal, J., Andrea, Š. & Aleš, H. LIGNIN, POTENTIAL PRODUCTS AND THEIR MARKET VALUE. *WOOD RESEARCH* 15.

53. Smolarski, N. High value Opportunities for Lignin Unlocking its Potential Market Insights. *Frost & Sullivan* 15 pp.

54. Stichnothe, H., Bell, G. & Jørgensen, H. Ed de Jong, Avantium (The Netherlands). 79.

55. Chen, H. 3 - Lignocellulose biorefinery feedstock engineering. in *Lignocellulose Biorefinery Engineering* (ed. Chen, H.) 37–86 (Woodhead Publishing, 2015). doi:10.1016/B978-0-08-100135-6.00003-X.

56. Dessbesell, L. *et al.* Bio-based polymers production in a kraft lignin biorefinery: techno-economic assessment. *Biofuels, Bioproducts and Biorefining* **12**, 239–250 (2018).

57. Ubando, A. T., Felix, C. B. & Chen, W.-H. Biorefineries in circular bioeconomy: A comprehensive review. *Bioresource Technology* **299**, 122585 (2020).

58. Lundberg, V. *et al.* Converting a kraft pulp mill into a multi-product biorefinery: techno-economic analysis of a case mill. *Clean Techn Environ Policy* **16**, 1411–1422 (2014).

59. Chakar, F. S. & Ragauskas, A. J. Review of current and future softwood kraft lignin process chemistry. *Industrial Crops and Products* **20**, 131–141 (2004).

60. Kangas, P., Kaijaluoto, S. & Määttänen, M. Evaluation of future pulp mill concepts – Reference model of a modern Nordic kraft pulp mill. *Nordic Pulp & Paper Research Journal* **29**, 620–634 (2014).

61. Bajpai, P. Chapter 12 - Pulping Fundamentals. in *Biermann's Handbook of Pulp and Paper (Third Edition)* (ed. Bajpai, P.) 295–351 (Elsevier, 2018). doi:10.1016/B978-0-12-814240-0.00012-4.

62. Lappalainen, J. *et al.* Sub- and Supercritical Water Liquefaction of Kraft Lignin and Black Liquor Derived Lignin. *Energies* **13**, 3309 (2020).

63. The chemical reactions in Kraft pulping process | pulp paper mill. (2015).

64. Chemical Reactions in Kraft Pulping. 6.

65. Tomani, P. THE LIGNOBOOST PROCESS. 6.

66. Metso global website. *Metso* https://www.metso.com/.

67. Vakkilainen, E. & Välimäki, E. Effect of Lignin Separation to Black Liquor and Recovery Boiler Operation. 17.

68. LignoBoost plant at Domtar's Plymouth mill in North Carolina. https://www.valmet.com/about-us/references/pulping-and-fiber/lignoboost-plant-at-domtars-plymouth-mill-in-north-carolina/.

69. Sunila makes the most out of lignin. https://www.valmet.com/media/articles/pulping-and-fiber/chemical-pulping/sunila-makes-the-most-out-of-lignin2/.

70. Brosse, N., Dufour, A., Meng, X., Sun, Q. & Ragauskas, A. Miscanthus: a fast-growing crop for biofuels and chemicals production. *Biofuels, Bioproducts and Biorefining* **6**, 580–598 (2012).

71. Naqvi, M., Yan, J. & Dahlquist, E. Black liquor gasification integrated in pulp and paper mills: A critical review. *Bioresource Technology* **101**, 8001–8015 (2010).

72. Shrestha, B. *et al.* A Multitechnique Characterization of Lignin Softening and Pyrolysis. *ACS Sustainable Chemistry & Engineering* **5**, 6940–6949 (2017).

73. Collard, F.-X. & Blin, J. A review on pyrolysis of biomass constituents: Mechanisms and composition of the products obtained from the conversion of cellulose, hemicelluloses and lignin. *Renewable and Sustainable Energy Reviews* **38**, 594–608 (2014).

74. Kawamoto, H. Lignin pyrolysis reactions. *Journal of Wood Science* **63**, 117–132 (2017).

75. Sharma, R. K. *et al.* Characterization of chars from pyrolysis of lignin. *Fuel* **83**, 1469–1482 (2004).

76. Windt, M., Meier, D., Marsman, J. H., Heeres, H. J. & Koning, S. de. Micro-pyrolysis of technical lignins in a new modular rig and product analysis by GC-MS/FID and GC × GC-TOFMS/FID. *Journal of Analytical and Applied Pyrolysis* **85**, 38–46 (2009).

77. Olcese, R. N., Francois, J., Bettahar, M. M., Petitjean, D. & Dufour, A. Hydrodeoxygenation of Guaiacol, A Surrogate of Lignin Pyrolysis Vapors, Over Iron Based Catalysts: Kinetics and Modeling of the Lignin to Aromatics Integrated Process. *Energy Fuels* **27**, 975–984 (2013).

78. Bu, Q. *et al.* A review of catalytic hydrodeoxygenation of lignin-derived phenols from biomass pyrolysis. *Bioresource Technology* **124**, 470–477 (2012).

79. Ambursa, M. M. *et al.* A review on catalytic hydrodeoxygenation of lignin to transportation fuels by using nickel-based catalysts. *Renewable and Sustainable Energy Reviews* **138**, (2021).

80. Badawi, M. *et al.* Hydrodeoxygenation of Phenolic Compounds by Sulfided (Co)Mo/Al2O3 Catalysts, a Combined Experimental and Theoretical Study. *Oil Gas Sci. Technol. – Rev. IFP Energies nouvelles* **68**, 829–840 (2013).

81. Gonçalves, V. O. O., Brunet, S. & Richard, F. Hydrodeoxygenation of Cresols Over Mo/Al2O3 and CoMo/Al2O3 Sulfided Catalysts. *Catal Lett* **146**, 1562–1573 (2016).

82. Bui, V. N., Laurenti, D., Afanasiev, P. & Geantet, C. Hydrodeoxygenation of guaiacol with CoMo catalysts. Part I: Promoting effect of cobalt on HDO selectivity and activity. *Applied Catalysis B: Environmental* **101**, 239–245 (2011).

83. de Wild, P. J., Huijgen, W. J. J., Kloekhorst, A., Chowdari, R. K. & Heeres, H. J. Biobased alkylphenols from lignins via a two-step pyrolysis - Hydrodeoxygenation approach. *Bioresour Technol* **229**, 160–168 (2017).

84. Saraeian, A. *et al.* Evaluating lignin valorization via pyrolysis and vapor-phase hydrodeoxygenation for production of aromatics and alkenes. *Green Chem.* **22**, 2513–2525 (2020).

85. Olcese, R. N. *et al.* Aromatic Chemicals by Iron-Catalyzed Hydrotreatment of Lignin Pyrolysis Vapor. *ChemSusChem* **6**, 1490–1499 (2013).

86. Resende, F. L. P. Recent advances on fast hydropyrolysis of biomass. *Catalysis Today* **269**, 148–155 (2016).

87. Meier, D., Ante, R. & Faix, O. Catalytic hydropyrolysis of lignin: Influence of reaction conditions on the formation and composition of liquid products. *Bioresource Technology* **40**, 171–177 (1992).

88. Meier, D., Berns, J., Faix, O., Balfanz, U. & Baldauf, W. Hydrocracking of organocell lignin for phenol production. *Biomass and Bioenergy* **7**, 99–105 (1994).

89. Joffres, B. *et al.* Thermochemical Conversion of Lignin for Fuels and Chemicals: A Review. *Oil Gas Sci. Technol. – Rev. IFP Energies nouvelles* **68**, 753–763 (2013).

90. Meier, D., Berns, J., Grünwald, C. & Faix, O. Analytical pyrolysis and semicontinuous catalytic hydropyrolysis of Organocell lignin. *undefined* (1993).

91. Jan, O. *et al.* Hydropyrolysis of Lignin Using Pd/HZSM-5. *Energy Fuels* **29**, 1793–1800 (2015).

92. Schutyser, W. *et al.* Chemicals from lignin: an interplay of lignocellulose fractionation, depolymerisation, and upgrading. *Chemical Society Reviews* **47**, 852–908 (2018).

93. Huang, X., Korányi, T. I., Boot, M. D. & Hensen, E. J. M. Catalytic Depolymerization of Lignin in Supercritical Ethanol. *ChemSusChem* **7**, 2276–2288 (2014).

94. Limarta, S. O., Kim, H., Ha, J.-M., Park, Y.-K. & Jae, J. High-quality and phenolic monomer-rich bio-oil production from lignin in supercritical ethanol over synergistic Ru and Mg-Zr-oxide catalysts. *Chemical Engineering Journal* **396**, 125175 (2020).

95. Lange, J.-P. Lignocellulose Liquefaction to Biocrude: A Tutorial Review. *ChemSusChem* **11**, 997–1014 (2018).

96. Huang, X., Korányi, T. I., Boot, M. D. & Hensen, E. J. M. Ethanol as capping agent and formaldehyde scavenger for efficient depolymerization of lignin to aromatics. *Green Chemistry* **17**, 4941–4950 (2015).

97. Jeong, S., Yang, S. & Kim, D. H. Depolymerization of Protobind lignin to produce monoaromatic compounds over Cu/ZSM-5 catalyst in supercritical ethanol. *Molecular Catalysis* **442**, 140–146 (2017).

98. Cheng, S., D'cruz, I., Wang, M., Leitch, M. & Xu, C. (Charles). Highly Efficient Liquefaction of Woody Biomass in Hot-Compressed Alcohol−Water Co-solvents †. *Energy & Fuels* **24**, 4659–4667 (2010).

99. Agarwal, A., Park, S.-J. & Park, J.-H. Catalytic upgrading of Kraft lignin derived bio-oil in supercritical ethanol over different crystal size hierarchical nano-HZSM5. *Fuel* **271**, 117630 (2020).

100. Bourbiaux, D. *et al.* Reductive or oxidative catalytic lignin depolymerization: An overview of recent advances. *Catalysis Today* **373**, 24–37 (2021).

101. Nielsen, J. B., Jensen, A., Schandel, C. B., Felby, C. & Jensen, A. D. Solvent consumption in non-catalytic alcohol solvolysis of biorefinery lignin. *Sustainable Energy Fuels* **1**, 2006–2015 (2017).

102. Feng, S., Wei, R., Leitch, M. & Xu, C. C. Comparative study on lignocellulose liquefaction in water, ethanol, and water/ethanol mixture: Roles of ethanol and water. *Energy* **155**, 234–241 (2018).

103. Ni, Y. & Hu, Q. Alcell® lignin solubility in ethanol–water mixtures. *Journal of Applied Polymer Science* **57**, 1441–1446 (1995).

104. Ye, Y., Zhang, Y., Fan, J. & Chang, J. Novel Method for Production of Phenolics by Combining Lignin Extraction with Lignin Depolymerization in Aqueous Ethanol. *Ind. Eng. Chem. Res.* **51**, 103–110 (2012).

105. Huang, X. *et al.* Catalytic Depolymerization of Lignin and Woody Biomass in Supercritical Ethanol: Influence of Reaction Temperature and Feedstock. *ACS Sustainable Chemistry & Engineering* **5**, 10864–10874 (2017).

106. Hu, L. *et al.* The degradation of the lignin in Phyllostachys heterocycla cv. pubescens in an ethanol solvothermal system. *Green Chem.* **16**, 3107–3116 (2014).

107. Toledano, A., Serrano, L. & Labidi, J. Organosolv lignin depolymerization with different base catalysts. *Journal of Chemical Technology & Biotechnology* **87**, 1593–1599 (2012).

108. Du, L., Wang, Z., Li, S., Song, W. & Lin, W. A Comparison of Monomeric Phenols Produced from Lignin by Fast Pyrolysis and Hydrothermal Conversions. *International Journal of Chemical Reactor Engineering* **11**, 135–145 (2013).

109. Beauchet, R., Monteil-Rivera, F. & Lavoie, J. M. Conversion of lignin to aromatic-based chemicals (L-chems) and biofuels (L-fuels). *Bioresource Technology* **121**, 328–334 (2012).

110. Deepa, A. K. & Dhepe, P. L. Lignin Depolymerization into Aromatic Monomers over Solid Acid Catalysts. *ACS Catal.* **5**, 365–379 (2015).

111. Sales, F. G., Abreu, C. a. M. & Pereira, J. a. F. R. Catalytic wet-air oxidation of lignin in a three-phase reactor with aromatic aldehyde production. *Brazilian Journal of Chemical Engineering* **21**, 211–218 (2004).

112. Tarabanko, V. E., Fomova, N. A., Kuznetsov, B. N., Ivanchenko, N. M. & Kudryashev, A. V. On the mechanism of vanillin formation in the catalytic oxidation of lignin with oxygen. *React Kinet Catal Lett* **55**, 161–170 (1995).

113. Tarabanko, V. E. & Petukhov, D. V. Study of Mechanism and Improvement of the Process of Oxidative Cleavage of Lignins into the Aromatic Aldehydes. 13.

114. Hafezisefat, P., K. Lindstrom, J., C. Brown, R. & Qi, L. Non-catalytic oxidative depolymerization of lignin in perfluorodecalin to produce phenolic monomers. *Green Chemistry* **22**, 6567–6578 (2020).

115. Voitl, T. & Rudolf von Rohr, P. Oxidation of Lignin Using Aqueous Polyoxometalates in the Presence of Alcohols. *ChemSusChem* **1**, 763–769 (2008).

116. Santos, S. G., Marques, A. P., Lima, D. L. D., Evtuguin, D. V. & Esteves, V. I. Kinetics of Eucalypt Lignosulfonate Oxidation to Aromatic Aldehydes by Oxygen in Alkaline Medium. *Ind. Eng. Chem. Res.* **50**, 291–298 (2011).

117. Xiang, Q. & Lee, Y. Y. Production of Oxychemicals from Precipitated Hardwood Lignin. in *Twenty-Second Symposium on Biotechnology for Fuels and Chemicals* (eds. Davison, B. H., McMillan, J. & Finkelstein, M.) 71–80 (Humana Press, 2001). doi:10.1007/978-1-4612-0217-2_6.

118. Bouxin, F. P. *et al.* Catalytic depolymerisation of isolated lignins to fine chemicals using a Pt/alumina catalyst: part 1—impact of the lignin structure. *Green Chemistry* **17**, 1235–1242 (2015).

119. Lancefield, C. S. *et al.* Investigation of the Chemocatalytic and Biocatalytic Valorization of a Range of Different Lignin Preparations: The Importance of β-O-4 Content. *ACS Sustainable Chem. Eng.* **4**, 6921–6930 (2016).

120. Patil, P. T., Armbruster, U., Richter, M. & Martin, A. Heterogeneously Catalyzed Hydroprocessing of Organosolv Lignin in Sub- and Supercritical Solvents. *Energy Fuels* **25**, 4713–4722 (2011).

121. Barta, K., R. Warner, G., S. Beach, E. & T. Anastas, P. Depolymerization of organosolv lignin to aromatic compounds over Cu-doped porous metal oxides. *Green Chemistry* **16**, 191–196 (2014).

122. Bartolomei, E. *et al.* Lignin Depolymerization: A Comparison of Methods to Analyze Monomers and Oligomers. *ChemSusChem* **13**, (2020).

123. Mahmood, N., Yuan, Z., Schmidt, J., Tymchyshyn, M. & Xu, C. (Charles). Hydrolytic liquefaction of hydrolysis lignin for the preparation of bio-based rigid polyurethane foam. *Green Chem.* **18**, 2385–2398 (2016).

124. McClelland, D. J. *et al.* Functionality and molecular weight distribution of red oak lignin before and after pyrolysis and hydrogenation. *Green Chemistry* **19**, 1378–1389 (2017).

125. Lange, H., Rulli, F. & Crestini, C. Gel Permeation Chromatography in Determining Molecular Weights of Lignins: Critical Aspects Revisited for Improved Utility in the Development of Novel Materials. *ACS Sustainable Chemistry & Engineering* **4**, 5167–5180 (2016).

126. Andrianova, A. A. *et al.* Electrospray Ionization with High-Resolution Mass Spectrometry as a Tool for Lignomics: Lignin Mass Spectrum Deconvolution. *Journal of The American Society for Mass Spectrometry* **29**, 1044–1059 (2018).

127. Andrianova, A. A. *et al.* Size exclusion chromatography of lignin: The mechanistic aspects and elimination of undesired secondary interactions. *J Chromatogr A* **1534**, 101–110 (2018).

128. Harman-Ware, A. E. & Ferrell, J. R. Methods and Challenges in the Determination of Molecular Weight Metrics of Bio-oils. *Energy & Fuels* **32**, 8905–8920 (2018).

129. Hoekstra, E., Kersten, S. R. A., Tudos, A., Meier, D. & Hogendoorn, K. J. A. Possibilities and pitfalls in analyzing (upgraded) pyrolysis oil by size exclusion chromatography (SEC). *Journal of Analytical and Applied Pyrolysis* **91**, 76–88 (2011).

130. Constant, S. *et al.* New insights into the structure and composition of technical lignins: a comparative characterisation study. *Green Chemistry* **18**, 2651–2665 (2016).

B. Multi-analytic Characterization of Technical Lignins and Black Liquors

Erika Bartolomei[a], Frédérique Bertaud[b], Isabelle Ziegler-Devin[c], Sebastien Leclerc[d], Yann Le Brech[a]*

[a] LRGP, CNRS, Université de Lorraine, 1 rue Grandville, 54000 Nancy, France

[b] Centre Technique du Papier, 341 Rue de la Papeterie, 38400 Saint-Martin-d'Hères, France

[c] LERMAB, CNRS, Université de Lorraine, 4370 boulevard des Aiguillettes, 54506 Vandoeuvre-les-Nancy, France

[d] LEMTA, CNRS, Université de Lorraine, 4370 boulevard des Aiguillettes, 54506 Vandoeuvre-les-Nancy, France

* corresponding authors: yann.le-brech@univ-lorraine.fr

1. - Introduction

In paper industry, lignin is the most under estimated and under valorized product. Every year 50-70 Tons of lignin are produced besides paper and burned in the boiler to supply electricity to the plant itself[1–3]. Lignin, as it is the most abundant natural source of aromatic molecules, can be used as a raw feedstock of fundamental aromatic chemicals, necessary to produce various kinds of plastics, in addition to biofuels and chemicals.

Lignin presents a very complex structure, which has been reconstructed after decades of analysis. In fact, once lignin is extracted from wood, it loses its original structure (called native lignin). Therefore, specific features come from different extraction methods also the kind of original biomass.

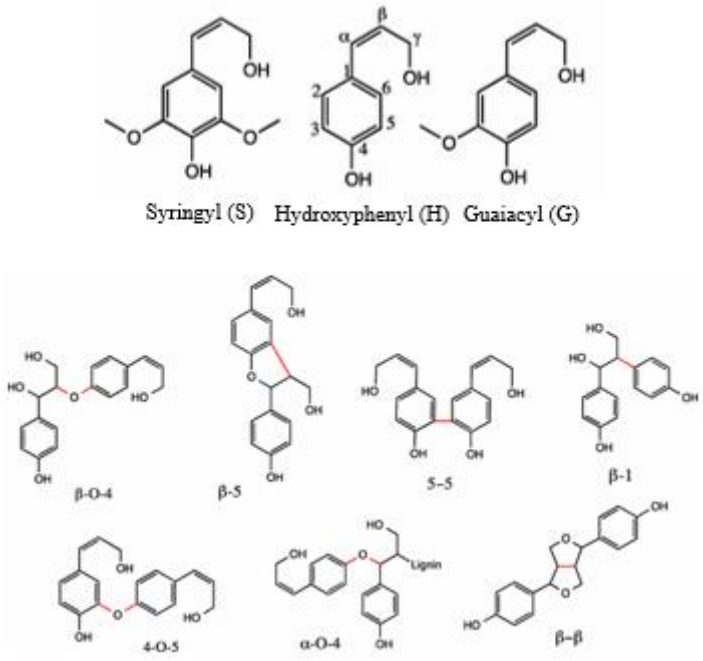

Figure 1 Lignin monomeric units and typical bonds.[4]

Indeed, depending on the feedstock, different ratios of the three monomeric alcohols units (Figure 1) can be found in lignin structure: in softwood the main one is guaiacyl (G) unit; hardwood is a mix of guaiacyl (G) and syringyl (S) ones; and in non-wood/herbaceous biomass we can find the three units and also a high presence of carboxylic groups (COOH) [4]. The lignin separation process then influences mostly the bonds in its structure. For example, β-O-4 bonds are the most abundant in lignin (between 45 and 84% occurrence depending on the biomass type)[5,6] but they decrease significantly after pulping processes (till ~6% occurrence), especially the Kraft one, in favor of more condensed structures (tertiary and quaternary C-C bond-based linkages).[7]

Figure 2 presents the main pulping processes used for each kind of biomass and their market (already at industrial scale or potentially emerging).[8]

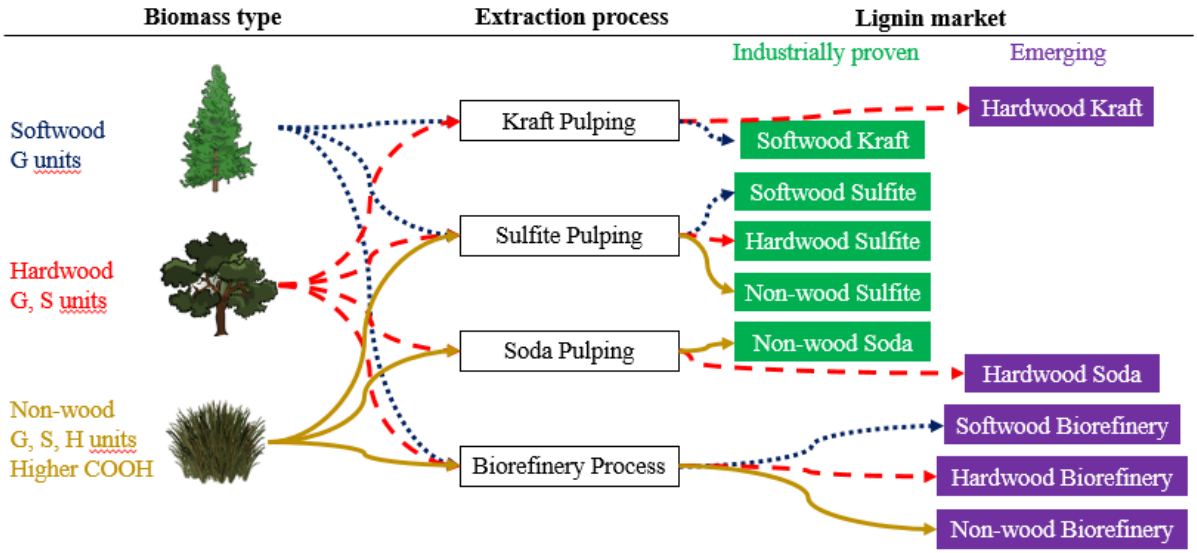

Figure 2 Pulping of different biomass feedstock and their market.[8]

Among all the lignin extraction methods, Kraft process is the most common worldwide, from pulp and paper industry (see Chapter 1). Therefore, Kraft lignin presents significant interest to investigation and valorization. The purpose of this study is to deeply characterize different commercial lignins from different biomasses.

2. - Materials and Methods

2.1. - Physico-chemical characterization of commercial/technical lignins

Four different samples of commercial lignins were purchased (after a deep investigation made by the CTP, project partner). Lignins were characterized, in order to better understand their common or different features. In the following table (Table 1) names, suppliers and main characteristics from the origin company are given. The goal is to get the main technical lignin types, such as Kraft, Soda and Organosolv, from different kinds of biomass.

Table 1 Suppliers' data of commercial lignins studied

Name	Type / Ref.	Physico-chemical data
Kraft1	Softwood Kraft lignin BioPiva™ 100 (CAS 8068-05-01)	Purity : 80 % - 98 % Impurity ($Na2SO_4$) : 0.5 % - 3 % pH (10% solution) : 2.5 – 4.5 Min Ignition temperature (layer): > 440°C Mini Ignition temperature (cloud) : 400°C Lower Explosivity Limits : 30 g/m^3

		Decomposition temperature ≥ 220°C Solid content : 65% (Dryness) Molecular weight (MW): 5 000 g/mol Ash contents < 3% Sulphur content < 3% Storage stability (20°C) : 3 months Low Heating value : 5.97 MWh / t
Kraft2	Hardwood Kraft lignin (Eucalyptus) (CAS 8068-05-01)	Purity : 50 - 100 % Impurity ($Sulfur_4$) : 0 - 3 % pH : 3-7
Soda	Soda Lignin Protobind 1000 (Wheat straw) (CAS 9005-53-2)	Purity : > 88 % Impurity : xylose < 4 % Na_2SO_4 < 3 % Water < 10 % pH (10% solution) : 3-4 Melting point : 200°C Density: 1.3 g/cm^3 Bulk density : 0.3 – 0.4 g:cm^3 Acute toxicity : LD50 oral-rat : > 5 000 mg/kg Solid content : > 95% (Dryness) Molecular weight (Mw): 4 000 – 6 000 g/mol Number average Molecular Weight (Mn) : 1 000 – 2 000 g/mol Particle size: < 210µm
Organosolv	Oragnosolv lignin BioLignine™ (CAS 8068-05-01)	Solid content : 95.6 % (Dryness) Impurity: Acetic acid < 0.7% Formic acid < 0.7% Water < 4% Ash content : 1.3% Pentosan content : 2.7 % Purity : Klason Lignin = 81.7% ASL = 2.6% Proteins = 11.7% Molecular weight : Mn =900 - 1 100 g/mol Mw =1 900 - 2 300 g/mol Ip = 2.0 – 2.2

		OH phenolic : 1.9 mmol/g OH aliphatic : 1.9 mmol/g COOH : 0.7 mmol/g Elementar analysis : CHN : 60.8% / 5.4% / 2.2% Min Ignition temperature (layer) : 340°C Min Ignition temperature(cloud) : 520°C

The four lignins have been extensively analysed by different technics and methods (mainly at FJV, IRCELyon, LGPC and CTP). In this chapter, only the analysis conducted at FJV there will be presented. They are briefly presented below in Table 2 and more extensively in the supporting information at the end of the chapter. All the tests have been conducted on different samples of the same batch of lignin. The purchased lignins have been delivered in 3-5 kg bin. In order to verify the homogeneity of the batches, three samplings at different locations of the bins have been done. Analysis performed on those samples (elemental analysis, Klason, ashes, LHV/HHV) have shown no significant variations due to sampling location.

Table 2 Analysis forecasted by FJV to characterize the commercial lignins.

Characteristic measured	**Technique – Method**
Dry matter content (dryness)	ISO 638
Particles size	Malvern Laser and SEM
Purity (KLASON + ASL)	Protocol NREL-42618
LHV / HHV	Bomb Calorimeter
Ash content	ISO 1762 à 525°C (furnace)
Minerals	ICP-OES Thermo ICAP 6000 Series ICP Spectrometer
Elemental Analysis CHNS-O	Thermo Fischer EA 111
Molecular Mass	SEC – THF, HPLC Shimadzu Prominence
Sugars	HPLC Dionex ICS-3000, Carbo pac PA20
TG/DSC	Mettler Toledo
Functional groups	Liquid state NMR ^{13}C/ ^{1}H-^{13}C / ^{31}P (300MHz Bruker) FT-IR

2.2. - Black Liquor and softwood Kraft Lignin from Black Liquor

Kraft lignin was prepared at semi-pilot scale from industrial black liquors from the industrial partner's mill. Fresh black liquors were sampled and delivered upon two sampling campaigns by CTP: first campaign on July 2018 and second campaign on September 2019. Several physico-chemical characteristics of black liquors have been measured, as reported for commercial lignins. After that, two precipitations of Kraft lignin have been carried out following a standard production protocol, developed in the framework of InTechFibres platform, allowing for the production of ~2-4 kg dry basis lignin. The procedure comprises 4 sequential steps described below and in Figure 3.

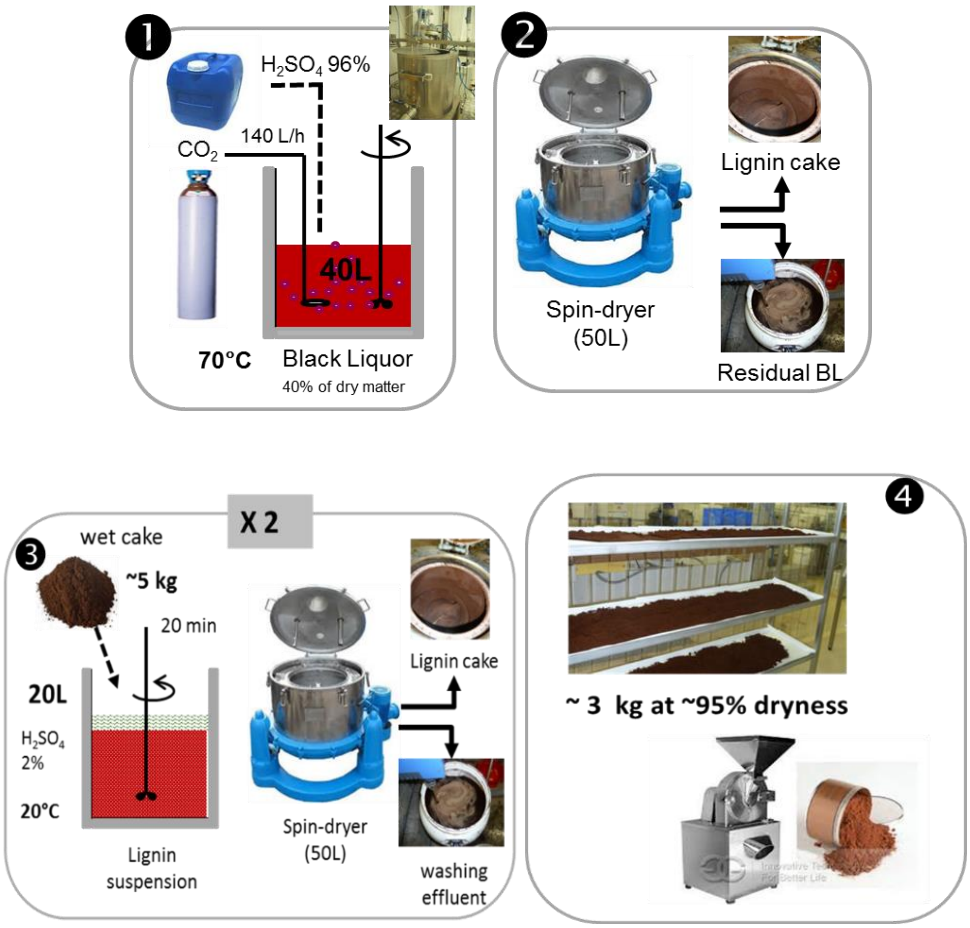

Figure 3 : Scheme of the Kraft lignin preparation at semi-pilot scale (CTP): the standard protocol (BL 40% dry matter, 70°C, pH 9 and acidic washings)

1) Neutralization of the black liquor (BL) until pH 9 Lignin by CO_2 bubbling, which leads to a lignin suspension (dilution of the BL at 40% dry matter if necessary, neutralisation at 70°C/

Patm under continuous stirring). In some cases, sulphuric acid addition could be needed to reach pH 9 faster.

2) Lignin separation by filtration of the obtained suspension, using a spin dryer, which leads to a crude lignin cake and the residual black liquors (RBL)

3) Lignin purification by successive acidic washings of the lignin cake (two times in the standard protocol), which leads to a purified lignin cake,

4) Lignin cake drying by laying the crumbled lignin cake on rack at ambient conditions during 3-5 days, and re-powdering

The final kraft lignin powder sample was characterised according to the same analytical methods as applied on commercial lignins (see Table 2).

3. - Results

3.1. - Technical Lignins

3.1.1. - Global analysis

Elemental and proximate analysis have been conducted on the four technical lignins, the results are summarized in Table 3. Elemental analysis provides the C, H, S, N and O weight contents (dry basis), while proximate analysis gives the moisture content, volatiles matter, and fixed carbon. From the analysis of the moisture content, we can deduct that most of the industrial lignins are commercialized in dry form (dryness ~ 94-96%). Only Kraft softwood lignin (BioPiva^{TM} 1000) is sold raw without additional drying with a residual water content of 35%, as indicated by the supplier. In terms of elemental analysis, the lignins all have 62-65% carbon, ~ 5.5% hydrogen, 25-28% oxygen. Kraft lignins contain significant sulfur amounts (2%wt db), mainly due to the thiol group of Kraft lignin (-SH). The sulfur content is much lower in Soda lignin and would be rather mineral sulfur (sulfate). Sulfur is non significant in Organosolv lignin (0.2%wt db). Due to their feedstock (wheat straw), Soda and Organosolv lignins both contain significant amounts of organic nitrogen.

They are relatively pure with a lignin content (KL + ASL) varying from 87% to 96%, minerals (ash) from 1% to 2%, and residual sugars from 2% to 5%. Organosolv lignin is the most contaminated with a residual sugar level of 5%, a protein level up to almost 11% (i.e. Supplier's

data), resulting in a rate of 2.2% nitrogen (N_2). The mineral contaminants of Kraft lignins (Lignins 1 and 2) are mainly sodium carbonate (0.2% Na).

In the end, also the lower and higher heating values (LHV and HHV) have been evaluated and all the four lignins results similar.

Table 3 Physico-chemical characteristics of commercial lignins.

	1_ Kraft1	2_ Kraft2	3_Soda	4_Organosolv
				
Moisture content (%wt)	32	3.5	4.4	5.8
Purity (KL+ASL) (%wt)	91.5/4.8	73.4/10	83.4/7	82.7/3.3
Ashes (575°C) (%)	1.02	1.92	1.73	1.59
Residual sugars (%wt)				
C_6-Galactose	1.79 (±0,17)	0.39 (±0,05)	0.93 (±0,02)	0.25 (±0,01)
C_6-Glucose	0.41 (±0,05)	<0.1	0.60 (±0,02)	0.15 (±0,01)
C_5-Arabinose	0.33 (±0,05)	<0.1	0.46 (±0,08)	0.23 (±0,01)
C_5-Xylose	1.45 (±0,27)	0.52 (±0,12)	2.41 (±0,48)	0.28 (±0,01)
C_6-Mannose	0.11 (±0,01)	<0.1	<0.1	0.15 (±0,01)
Total	4.1 ± 0.5	0.9 ± 0.2	4.4 ± 0.6	1.1 ± 0.05
Na (%wt (dry basis)	0.26	0.21	0.17	0.09
K (%wt (dry basis)	n.d	0.05	n.d	0.02
CHONS = tot (%wt dry basis)	64.1/5.8/21.1/0.1/ 2.3 = 93.5	61.6/5.6/26.4/0.1/ 2.6 = 96.3	62.9/5.8/25.5/0.4/ 0.7 = 95.3	59.4/5.9/32.6/2.2/ 0.1 = 100.2
LHV / HHV (MJ / kg dry sample)	26,56 (±1) / 28,01 (±1)	25,54 (±1,14) / 26,98(±1,14)	25,01 (±0,39) / 26,48 (±0,39)	22,95(±0,06) / 24,46(±0,06)

Figure 4 shows the mass balance achieved for the four lignins based on Klason and sugar residues analysis.

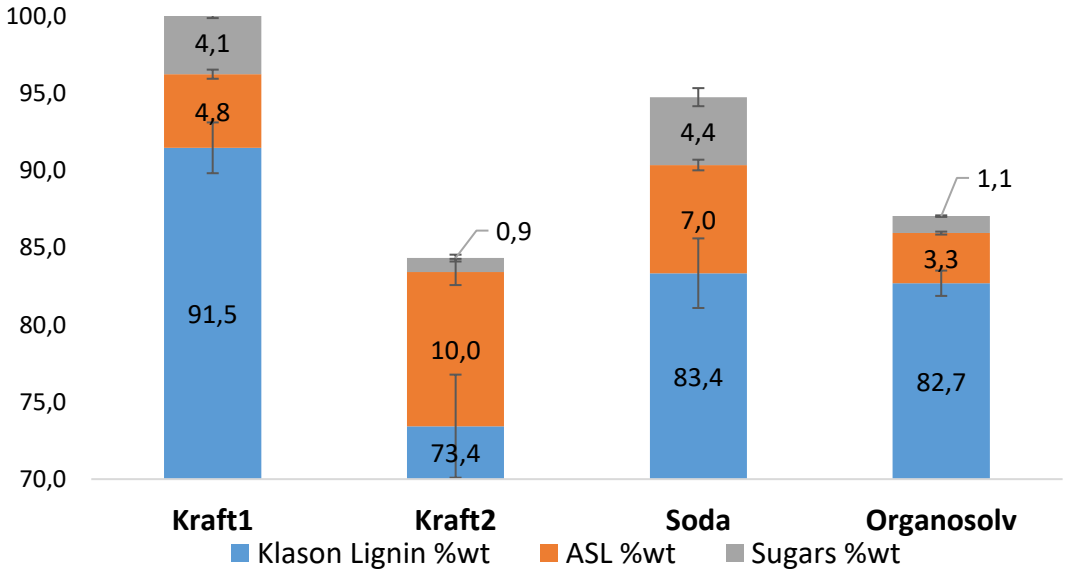

Figure 4 Mass balance from Klason and sugar residue analysis.

3.1.2. - Inductively Coupled Plasma (ICP) and Optical Emission Spectroscopy.

Lignins' mineral content has been evaluated by inductively coupled plasma optical emission spectroscopy (ICP-OES). The results are resumed in Table 4 below.

The main elements present in these four studied lignin are Na, S and Ca, due to their utilization during lignin fractionation from biomass. In particular, it can be noticed that the amount of those two elements are higher in Kraft lignins. Contrary to Soda and Organosolv processes, this fractionation process is sulfur-based. The sulfur content in the four lignins can be compared to the elemental analysis previously presented. It can be noticed that there is a very good correlation between the results of these two techniques: in terms of %wt elemental analysis gives 2.3, 2.6, 0.7, and 0.1 for the four lignins and ICP-OEs respectively 1.7, 2.4, 0.6, and 0.2.

Table 4 Inorganic content quantification

	Inorganic content ppm, mg/kg starting lignin (d.b)			
Element	Kraft 1	Kraft 2	Soda	Organosolv
Al	62	70	150	440
Ca	40	2260	4150	2900
Co	0.1	0.02	0.15	0.4
Na	2630	2110	1650	860
Cr	0.01	0.3	1	145
Mn	27	20	6	6.5
Ni	0,14	2	3	40
Cu	1	3	9	28
Zn	8	2	4	8
Cd	0.14	0.01	0.1	0.07
S	16645	24680	6340	2220
Mg	90	35	130	90
Fe	50	75	110	1540
B	25	85	15	7
K	n.d	530	n.d	165
Si	215	255	530	615

3.1.3. - TGA/DSC

The four commercial lignins have been analysed by thermogravimetric analysis (Figure 5). The analysis was carried out in a Mettler Toledo TC/DSC, according the following method: 10 °C/min, N_2 5 Nml/min, 25 °C to 700 °C. Because of its high moisture content, Kraft1 has been previously dried.

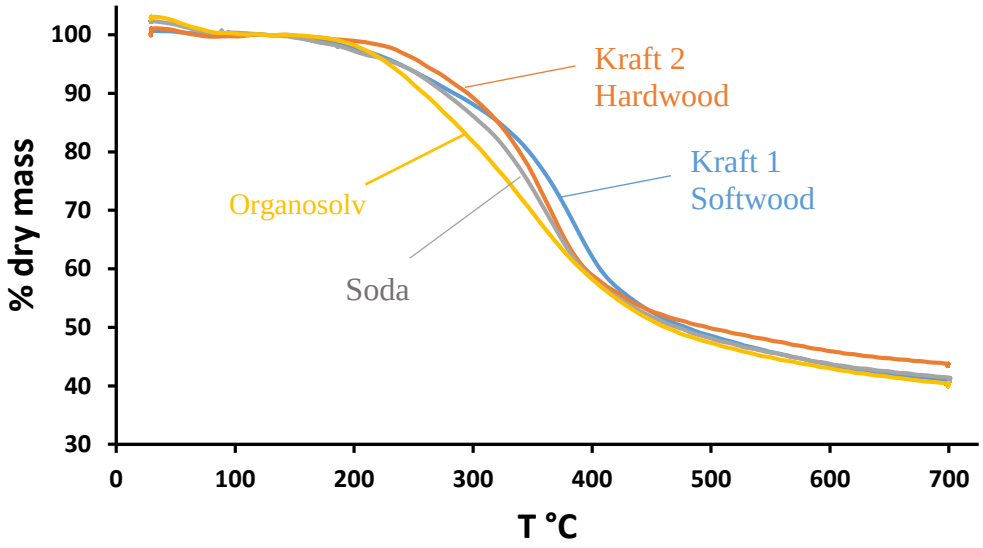

Figure 5 Thermogravimetric analysis

Lignins present different chemical stabilities as function of temperature. Indeed Organosolv, Kraft1 and Soda start to lose mass first (approx. 175°C), whereas Kraft 2 starts at 200°C.

Derivatives curves from ATG results show the different thermal stabilities related to lignin origins (see Figure 6). Organosolv lignin has the wider range of temperature volatilisation (150 to 500°C). Whereas Soda and Kraft2 have similar volatilization temperature ranges (225 to 450°C). Kraft1, on the other hand, has a smaller range of volatilization temperature (300-450 °C).

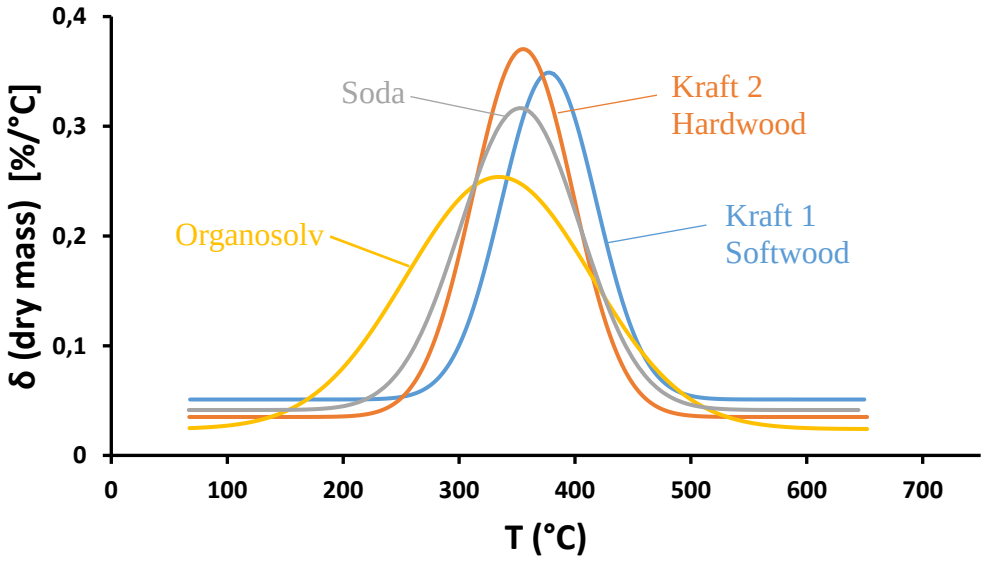

Figure 6: DTG analysis lignin thermal stabilities

3.1.4. - Scanning Electron Microscopy (SEM) analysis and Laser Granulometry

Lignin particles then have been analysed by Scanning Electron Microscopy. Photos and particle size distributions are given in Figures 7-10. The result obtained for Soda lignin agrees with the data given by the supplier (particle size < 210 µm). No details were available from suppliers for the other lignins. Table 5 presents the average surface and volume given from granulometry. The particle size distribution of lignin particles is rather dispersed except in the case of Kraft lignin from eucalyptus (Kraft 2).

Table 5 Lignins granulometry

	Surface Weighted Mean (µm)	Volume Weighted Mean (µm)
Kraft 1	33.8 (±2.3)	222.6 (±5.5)
Kraft 2	11.4 (±0.4)	123.2 (±7.8)
Soda	13.0 (±0.1)	30.2 (±0.9)
Organosolv	42.4 (±2.0)	177.8 (±8.2)

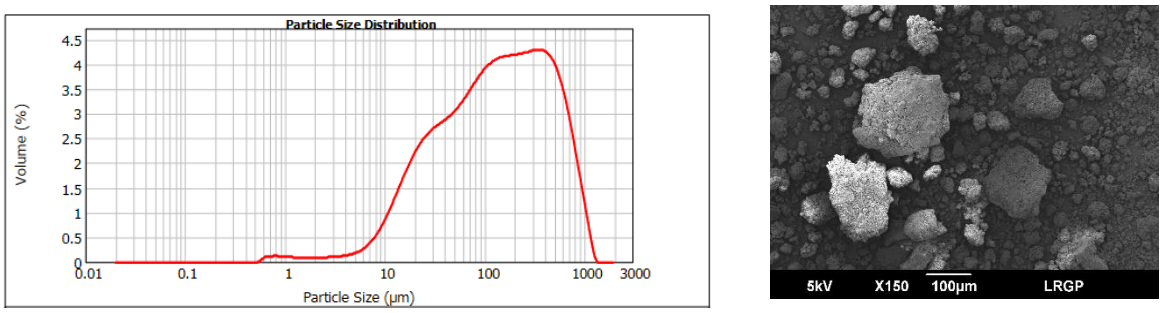

Figure 7 Kraft 1 SEM analysis and granulometry

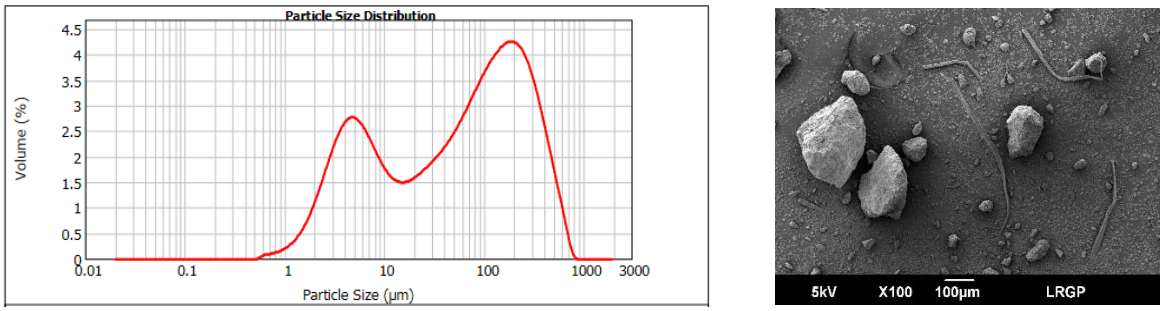

Figure 8 Kraft 2 SEM analysis and granulometry

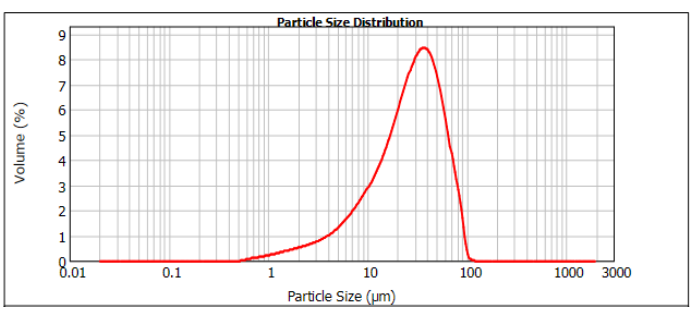

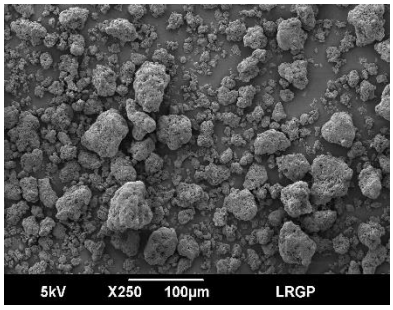

Figure 9 Soda SEM analysis and granulometry

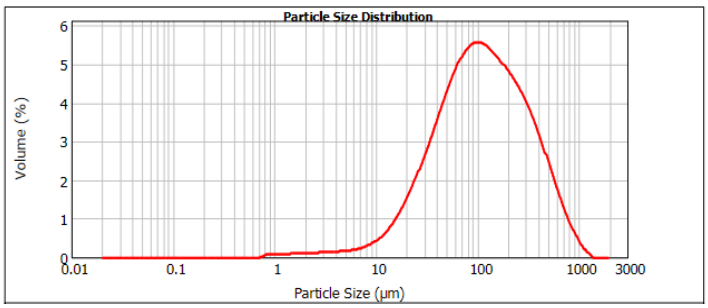

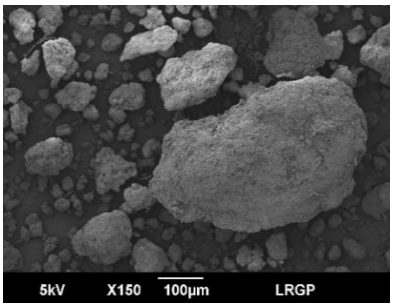

Figure 10 Organosolv SEM analysis and granulometry

3.1.5. - Lignin Molecular Weight measurement by GPC (Gel Permeation Chromatography)

The molecular weight is a critical parameter for lignin. GPC is a very useful and largely used technique for linear polymers, but the geometry of lignin structure (highly branched) makes GPC characterization very complex and relative. Indeed, generally GPC is applied to polymers with a simpler structure. The calibration standards are generally linear molecules, like polystyrenes. The lack of ramified (branched) standards for lignin is an issue in order to estimate its real molecular weight.[9,10] Moreover, during the analysis there can be interactions between the products, the mobile phase and the column.[11–13] Anyway, it is common to use GPC analysis to follow the depolymerization reaction or for comparison of different lignins. Many studies in literature can be found about gel permeation chromatography (or size exclusion chromatography).[4,7,14] In our study, we analyzed lignins by GPC-UV after solubilization in THF (Table 6). Since lignins were not totally soluble in this solvent, we tried also acetylation to make them more soluble. The acetylation procedure and the analytical methods are extensively described in the supporting information at the end of this chapter. Table 7 and 6 present GPC results for both acetylated and non-acetylated lignins. We can notice that the effect of the acetylation is not correlated to the molar mass weight value. For the non-acetylated analysis, the M_w are very similar for the four lignins, but once acetylated they differ a lot. This

phenomenon could be explained by the different degree of acetylation for each lignin.[7] They contain different amounts of –OH groups (see paragraph 3.1.8 for more details from NMR ^{31}P) which are involved in the acetylation process. The results have been also compared with literature and they are coherent with the value proposed in other studies.[7] Moreover, the acetylated samples show closer results to the values given from suppliers (see Table 1).

GPC analysis (Table 6-8) present two specific average molecular weight :1) Number average molecular weight (Mn) 2) Weight average molecular weight (Mw). The ratio Mw/Mn (polydispersity index) is also presented.

$$\text{Mn} = \frac{\sum NiMi}{\sum Ni} \quad \text{and} \quad Mw = \frac{\sum NiMi^2}{\sum NiMi}$$

with Ni: the number of moles with a molar mass of Mi.

Table 6 : Lignin GPC-UV characterizations

Mol. Weight (g/mol)	Kraft1	Kraft2	Soda	Organosolv
Mn	400	500	450	460
Mw	700	740	600	780
Mw/Mn	1.77	1.49	1.34	1.70

Table 7 Acetylated lignin GPC-UV characterizations

Mol. Weight (g/mol)	Kraft1	Kraft2	Soda	Organosolv
Mn	2200	1600	1525	1550
Mw	6270	3640	3650	4040
Mw/Mn	2.85	2.27	2.39	2.60

To investigate the molar mass distribution of the lignins, a multi angle light scattering gel permeation chromatography has been performed. Multi-Angle Light Scattering Detection (MALS) results in the measurement of absolute molecular weight which is independent from the column calibration. The amount of light scattered (measured by MALS) is proportional to the molar mass of the polymer, the concentration of the polymer, and the

square of specific refractive index increment (dn/dC).[15] It was chosen an average dn/dC of 0,179 after some test in refractometer with our four lignins in THF.

Table 8 Lignin GPC-MALS

Mol. Weight (g/mol)	Kraft1	Kraft2	Soda	Organosolv
Mn	2,7E+04	4,4E+04	1,7E+05	7,6E+04
Mw	3,1E+04	6,2E+04	1,9E+05	9,6E+04
Mw/Mn	1,2	1,4	1,1	1,2

Even if the GPC-MALS is in principle an absolute method for molecular weight distribution, some errors can occur during the analysis, once again the resulting M_w value could not be taken as realistic. In fact, this technique can be influenced by fluorescence phenomena, which can overestimated the molecular weights.[16] Fluorescence can be avoid with specific filters, where it is possible to insert them in the set-up, but it was not possible in our case.

GPC analysis shows different results as function of the method. Indeed, lignin molecular weight measurement is challenging because many factors can influence results significantly (lignin acetylation, detection method, solvent polarity, columns and so on). For that reason, GPC can be considered just for a qualitative comparison.

In order to estimate the influence of GPC analytic method (cf Constant et al.[7]) we made a comparison with different analytical technics: the three presented above, plus two other methods performed in other laboratories (LGPC Lyon and CTP Grenoble). It is clear that GPC-MALS tends to overestimate the molecular weights for all the lignins. All the values strictly depend on the method used (see Table 9).

Table 9 Comparison between different GPC methods.

		GPC-UV (Acetylation)	GPC-UV	GPC-MALS	GPC-visco	GPC-UV -DMA
	Calib.Standards	PS	P.S	dn/dc	PS + Univ. Cal	PS
	Method	A (FJV)	A (FJV)	B (FJV)	D (LGPC)	C (CTP)
	Solvent	THF	THF	THF	THF	DMAc/LiCl
	Name	A.1	A.2	B.1	C.1	D.1
Kraft 1 (Softwood Biopiva)	Mn	2198	396	27000	1262	4 600
	Mw	6270	701	31000	2925	6 000
	Mw/Mn (PD)	2.85	1.77	1.15	2.32	1.30
Kraft 2 (eucalyp. Fibria)	Mn	1606	496	44000	609	2 950
	Mw	3642	737	62000	1456	3 550
	Mw/Mn (PD)	2.27	1.49	1.41	2.392	1.20
Soda Protobind	Mn	1525	450	170000	1262	2 790
	Mw	3650	603	190000	2925	4 170
	Mw/Mn (PD)	2.39	1.34	1.12	2.317	1.49
Organosolv CIMV	Mn	1554	461	76000	_	3 840
	Mw	4040	784	96000	_	6 400
	Mw/Mn (PD)	2.6	1.70	1.26		1.67

3.1.6. - Carbon Nuclear Magnetic Resonance (^{13}C NMR) Analysis

Solution state NMR is one of the main spectroscopic methods which have been extensively used to elucidate the lignin structures[17]. Indeed, solution state NMR is an accurate method to analyse the carbon skeleton and proton moieties but also to characterize inter-unit linkages and their relative abundances in lignin (also in plant biomass). For these reasons, in this project, technical lignins were analysed by ^{13}C, ^{1}H-^{13}C HSQC (heteronuclear single quantum coherence) and ^{31}P NMR methods to characterize their carbon structures. Results are presented in Table 10-12.

Table 10 ^{13}C NMR quantification for main lignin moieties (mmol/g lignin)

Assignements	Kraft1	Kraft2	Soda	Organosolv
C aliphatics 36-10 ppm	1.2	2.1	5.0	4.9
CH_3-O 58-54 ppm	6.2	7.3	6.6	9.0
C aliphatique-O (without CH_3O) 58-100 ppm	1.5	5.1	8.6	16.3
Caromatics (C-C; C-H) 100-140 ppm	27.7	22.1	21.5	7.3
Caromatics-O 140-155ppm	16.6	13.5	9.4	2.9
COOR 168-180 ppm	0.2	1.2	1.4	9.0
Total C	53.4	51.3	52.4	49.5

^{13}C NMR quantifications were performed by integration of the total ^{13}C signal. The atomic % abundances are presented in Table 10.

3.1.7. - ^{1}H-^{13}C HSQC Analysis

HSQC semi-quantification of the main lignin linkages (*β-O-4*, *β-β*, *β-5*) were performed using the correlation peak according to aromatic carbons. $S_{2,6}$ (104.2/6.7) and G_2 (110.2/6.9) have been used as internal standard and linkages concentration are expressed as a number per 100 aromatic units (S+G). The integral value for each linkage were divided by the integral value for $S_{2,6}/2$ + integral value for G_2.

The analysis was not performed for Organosolv lignin because it was insoluble in DMSO-d6.

Table 11 ^{1}H-^{13}C HSQC Quantification of side chains present in lignins

	Kraft 1	Kraft 2	Soda	Organosolv
% β-O-4	7.4	10.0	5.65	n.d
% β-β	3.6	0.8	4.25	n.d
% β-5	4.6	6.5	1.25	n.d

3.1.8. - Free Hydroxyl functions analysis by NMR ^{31}P

The quantification of OH groups has been done based on the internal standard (cyclohexanol 144.4ppm). The signal assignments were realised as follow.

Table 12 Hydroxyl function assignments and quantification for ^{31}P NMR

	mmol/g lignin				
Lignin sample	Al-OH (150-145 ppm)	Syringyl OH/ Condensed structure (144-140ppm)	Guaiacyl OH / p-hydroxy phenyl OH (140 - 136 ppm)	Carboxylic acid (136-132 ppm)	Total OH
Kraft 1	1.68	1.86	2.66	0.51	6.71
Kraft 2	1.39	3.45	1.38	0.48	6.70
Soda	1.33	2.27	1.64	0.88	6.12
Organosolv	1.21	0.61	0.82	0.62	3.26

3.1.9. - FT-IR

Lignins have been analyzed by Fourier-transform infrared spectroscopy (FTIR-ATR) with the aim to demonstrate clear divisions and comparisons can be made among a variety of lignins based on their FTIR spectra quantitatively assessed through principal component analysis (PCA). To validate this technique, four lignins have been added to this study to demonstrate that the PCA can identify and group different lignins according to their biomass feedstock and their extraction or isolation method. In the figures below are presented our four lignins' spectra (Figure 11) and the PCA analysis with the other lignins also (Figure 12). Principal component analysis revealed that among the eight lignins, they can be qualitatively grouped based on both their feedstock variety (e.g., hardwood, softwood) and isolation method (i.e., kraft, MWL, soda, organosolv).

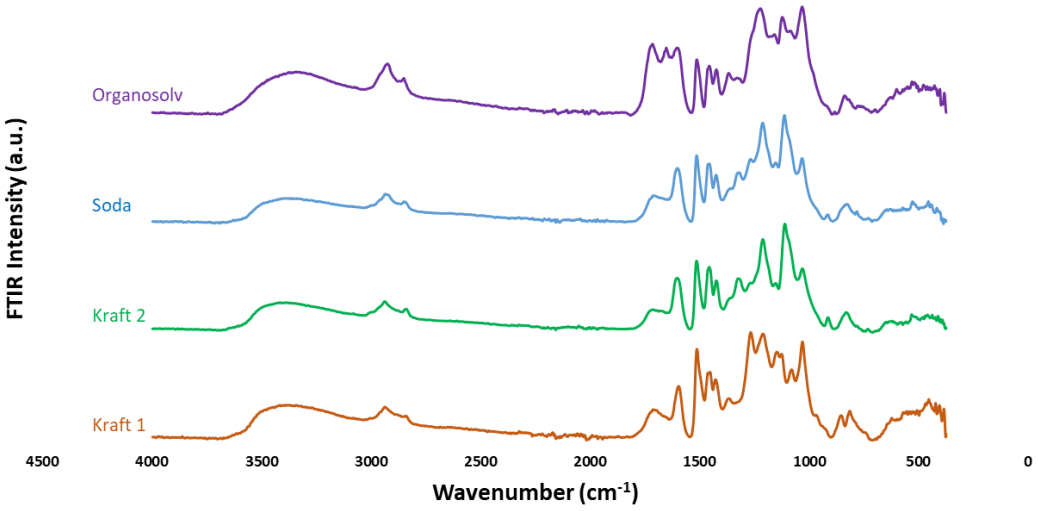

Figure 11 FT-IR spectra.

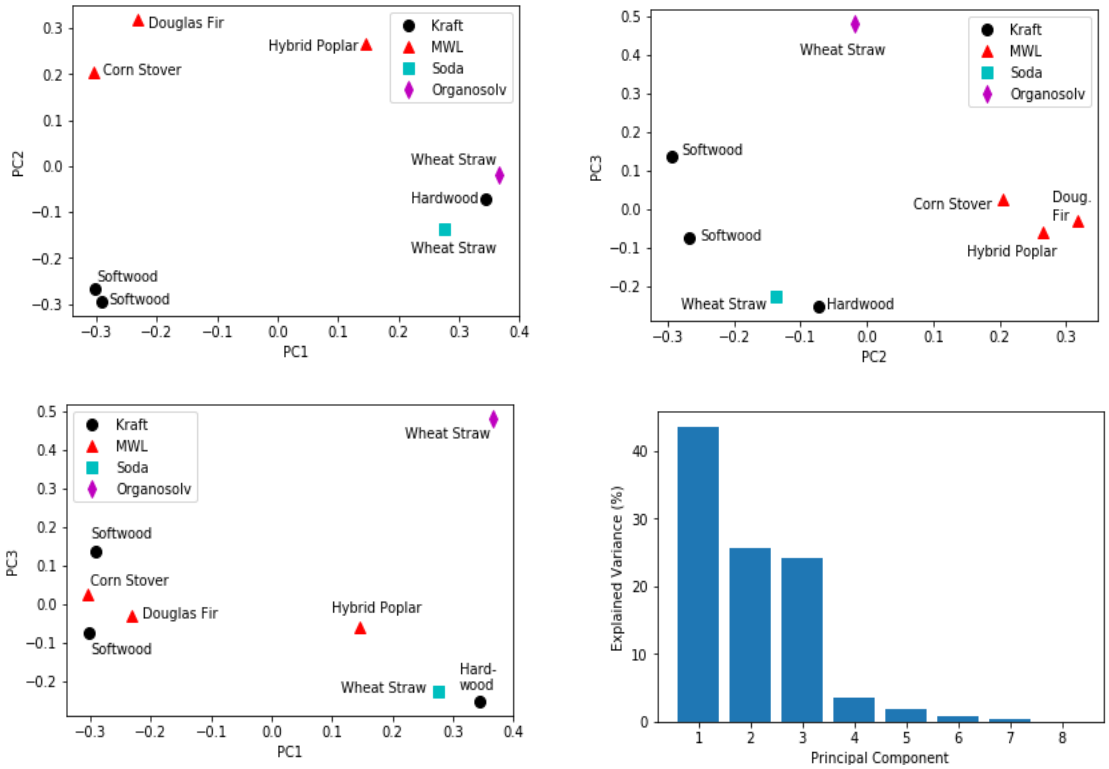

Figure 12 PCA analysis based on FT-IR characterization.

Quantification of the explained variances for each principal component (PC) suggests that three PC's are necessary to capture over 90% of the variation among the samples (Figure). The principal component plots show that softwood kraft lignins are clustered, corn stover and Douglas fir MWLs are clustered, and hardwood kraft and wheat straw soda are clustered. The

two wheat straw and two hardwood samples tend to have positive values for PC1, while the softwoods and corn stover are negative. The MWLs are closely grouped along PC2, and the organosolv wheat straw is uniquely large along PC3. Depending on which of the three PC plots are assessed, other possible groupings can be reasonably drawn.

3.2. - Black Liquor and softwood Kraft Lignin from Black Liquor

3.2.1. - Campaign N°1 : Liquors analysis

In July 2018, a first sampling campaign has been carried out by CTP, in order to collect sufficient black liquors (BL) for the preparation of lignin, characterization and assays.

Three types of BL were studied (Table 13):

1) LN.Re-I: the BL entering in the last concentration steps at ~50-55% of dry matter is suitable for lignin preparation (sufficiently concentrated and not too viscous for handling),
2) LN.ReS.-I: the BL outgoing from the digester (before soap recovering) with low dry matter content and which could be suitable for direct liquefaction,
3) LN.Re.SF-I: The same BL but without soap to avoid foam during the liquefaction assays.

Table 13 Description of sampled black liquors (BL).

	BL.LN.Re-I 26/07/2018	**BL.LN.ReSF-I 26/07/2018**	**BL.LN.ReS-I 26/07/2018**
Description	BL entering in the sur-concentrator (50 - 55% DM*)	BL after soap recovering and before concentration steps (28% DM*)	BL before soap recovering, coming out from digester (18% DM*)
Sampled volume	**200 L** 100 L for Lignin preparation ➔ 10 kg of lignin powder + 100 L in extra if need	**20 L**	**20 L**

*DM: Dry matter content (%, g/100g of crude sample)

The main characteristic from elemental and proximate analysis of the black liquors are reported in Table 14.

Table 14 Main characteristics measured of the sampled black liquors

BLACK LIQUORS	LN.Re-I 26/07/2018	LN.ReSF-I 26/07/2018	LN.ReS-I 26/07/2018
pH $_{20°C}$	14.0	13.5	13.6
Dry matter content (%, g/100g of crude sample)	43.6	10.5	22.6
Density $_{20°C}$ (g/cm^3)	1.21	1.02	1.08
CHNS(%, g/100g dry sample)	33.69 / 3.85 / 0.10 / 1.21	20.34 / 3.50 / 0.12 / 4.39	30.44 / 3.73 / 0.10 / 1.20

Carbon quantification by TOCmeter were compared to carbon quantification made by the elemental analysis (CHNS) on the dried liquor residues. Results are similar (ratio presented in Table 15). It means that almost all the carbon determined by TOC, which is dissolved in the solution, is quantified by CHNS after drying. Concerning LN.ReS and LN.ReSF, the %C is higher by COT quantification whereas for LN.Re is very similar. Each analysis was repeated three times to estimate standard deviation. Analysis on LN.ReS-I (001 and 002) were performed on two different sample of the initial batch (2 different sample with 3 repeats each). We concluded that batches could be considered homogenous for these characterizations.

Table 15 Carbon Organic (TOC) analysis compared to Elemental analysis (CHNS)

	C (TOC) (g/g liq)	Std deviation	% MS BL	%C MS (TOC)	%C (CHNS)	ratio TOC/CHNS
LN.Re-I	0.14	0.005	43.6	32.42	33.69	0.96
LN.ReS-I 001	0.08	0.002	22.6	36.75	30.44	1.21
LN.ReS-I 002	0.08	0.001	22.6	35.94	30.44	1.18
LN.ReSF-I	0.02	0.001	10.5	23.52	20.34	1.16

3.2.2. - Campaign N°2 – Liquor analysis

In September 2019, a second sampling campaign has been carried out,(always from CTP) especially to collect additional data for the pulp mill line simulation. This second sampling campaign was also an opportunity to collect fresh black liquors for lignin preparation.

For this time, only two types of BL were studied (Table 16):

4) LN.Re-II: the BL entering in the last concentration steps at ~50-55% of dry matter is suitable for lignin preparation (sufficiently concentrated and not too viscous for handling), and for liquefaction assays;
5) LN.Re.SF-II: The same BL but without soap for additional liquefaction assays.

Table 16 Description of 2nd campaign-sampled black liquors (BL).

	LN.Re-II 26/09/2019	**LN.ReSF-II 26/09/2019**
Description	BL entering in the sur-concentrator (50 - 55% DM*)	BL after soap recovering and before concentration steps (28% DM*)
Sampled volume	**150 L** 2 x 50 L for Lignin preparation ➔ 10 kg of lignin powder and 100 L in extra if need	**25 L**

*DM: Dry matter content (%, g/100g of crude sample)

For the second campaign the main characteristics of the black liquor have been determined by elemental, proximate and total organic carbon analysis (Tables 17-19). The results are very similar to the ones of the first campaign.

Table 17 Main characteristics measured of 2nd campaign-sampled black liquors (BL).

BLACK LIQUORS	**LN(45).Re-II 26/07/2018**	**LN(20).ReSF-II 26/07/2018**
pH $_{20°C}$	14	14
Dry matter content (%, g/100g of crude sample)	44.0	24.7
Density $_{20°C}$ **(g/cm^3)**	1.22	1.045

Table 18 Total Organic Carbon (TOC) of 2nd campaign-sampled black liquors (BL).

	aver C(g/g)	Std dev.	% MS	%C MS	%C CHNS	ratio TOC/CHNS
LN45-I	0.14	0.005	44.0	32.12	33.20	0.97
LN20-I	0.08	0.002	24.7	33.63	-	-

Table 19 Proximate analysis of black liquors.

	%dried liquors (dry basis)			%liquors			
	Volatile Matter	Fixed Carbon	Ashes	DM liquor	Volatile Matter	Fixed Carbon	Ashes
LN45.Re-II	59.28	22.87	17.85	44	26.1	10.1	7.9
LN20.Re.SF-II	60.19	16.76	23.04	24.7	14.9	4.1	5.7

Volatile matters was similar between the two samples. Whereas fixed carbon and ashes contents are different. Mass loss profiles are presented in supporting information at the end of the chapter. For both samples, volatilisation starts around 175°C until 900°C. Two main phases were detected. First an important degradation between 175°C and 700°C (which is consistent with ATG analysis of precipitated lignins). The char yield was about 65%wt at 700°C (for both samples). Second volatilisation between 700 to 900°C. At 900°C char yield is about 25%wt (for both samples). According to Proximate analysis, we obtained 17.85 and 23.04%wt for ashes, that are oxygenated minerals (i.e NaO).

Qualitative results of molecular mass distribution are presented in Figure 13. The purpose of this analysis is to qualitatively compare the black liquors and not evaluate their molecular mass, because as mentioned before GPC is not a suitable quantitative analysis for lignin, but it can be considered relative.

In the figure are reported the four spectra for black liquor at 20% and 45% solid content directly analyzed (LN20 and LN45) and also the dried (105 °C) solid content of the same two black liquor solubilized (2 mg/mL) in alkaline water (NaOH pH=12). See supporting information for more details on the method.

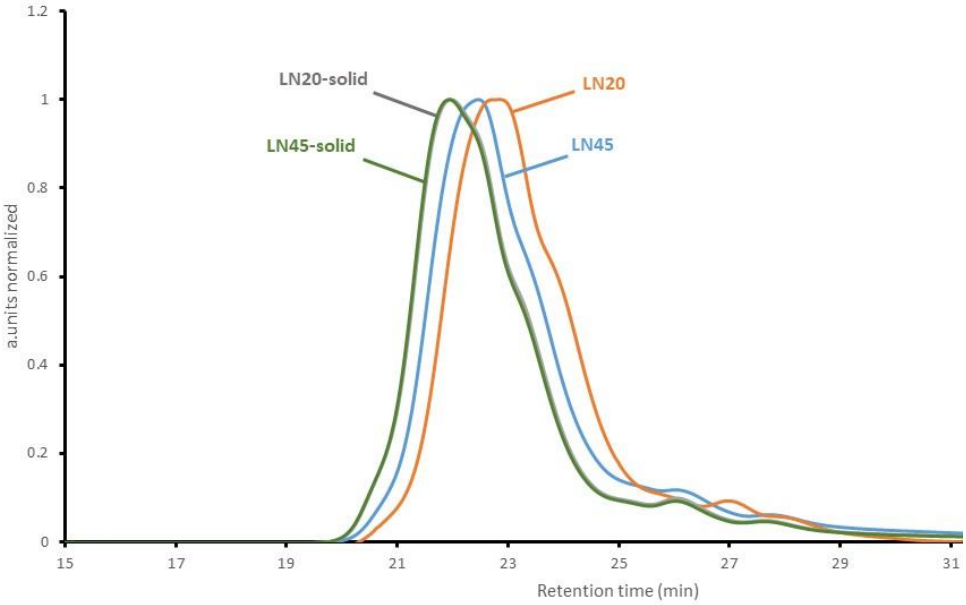

Figure 13 Chromatograms of aqueous GPC (NaOH / UV 254nm)

LN20-Re-II liquors and LN45-Re-II do not present the same mass distribution. Indeed LN20-Re-II seems to be "lighter" than LN45-Re-II. Mass distribution profiles were similar for both samples oven dried (LN20-solid and LN45 solid).

3.2.3. - Tailored Kraft lignin characterization

The precipitation of lignin from the collected black liquor have been performed by CTP.

7 kg o.d. eq. Kraft lignin powder were produced according to two successive batches: 1st using 50 L and 2^{d} using 30L. The global yield was of 22.1 % (g of dry lignin powder / 100g of o.d matter initially).

9.5 kg o.d. eq. Kraft lignin powder were produced according to two successive batches using 50 L of concentrated BL (LN.Re.II). The global yield was of 21.5 % (g of dry lignin powder / 100g of o.d matter initially), comparable to the previous one (ie. 22.1%). In Table 20 are presented the dry matter and the elemental analysis of the two tailored lignins.

Table 20 Physico-chemical characteristics of the softwood Kraft lignin produced

	Softwood Kraft Lignin – 1st Campaign Ref. KL.Re.I (yield : 22.1%)	Softwood Kraft Lignin – 2d Campaign Ref. KL.Re.II (yield : 21.5%)
		
Dry matter	95.0 %	84.9 %
CHN (dry basis)	64.0 / 5.2 / 0.2	64.9 / 4.7 / 0.1

Lignins were then analyzed by ^{13}C NMR method to characterize their carbon structures.

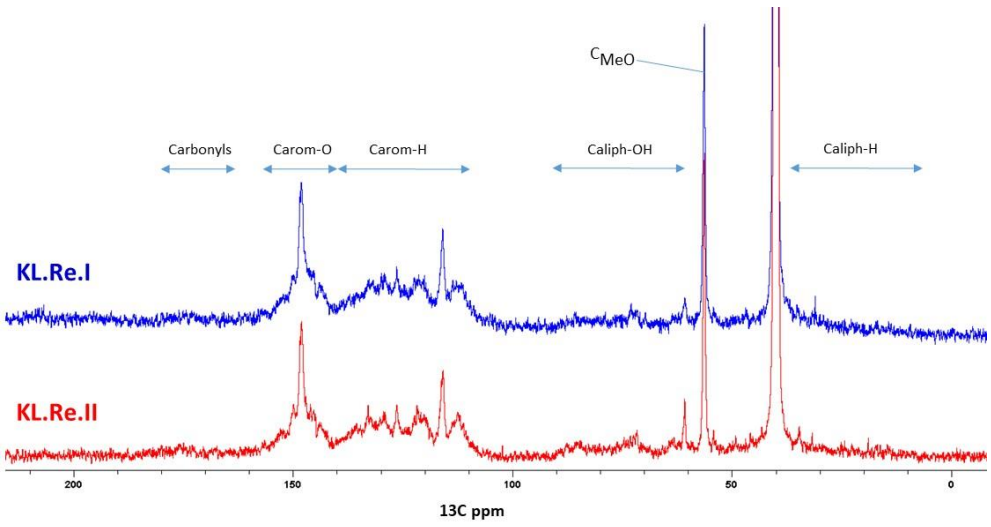

Figure 14 ^{13}C NMR spectrum of precipitated lignin KL.Re.I and KL.Re.II

Figure 15 presents the repartition of carbon moieties in the two tailored Kraft lignins.

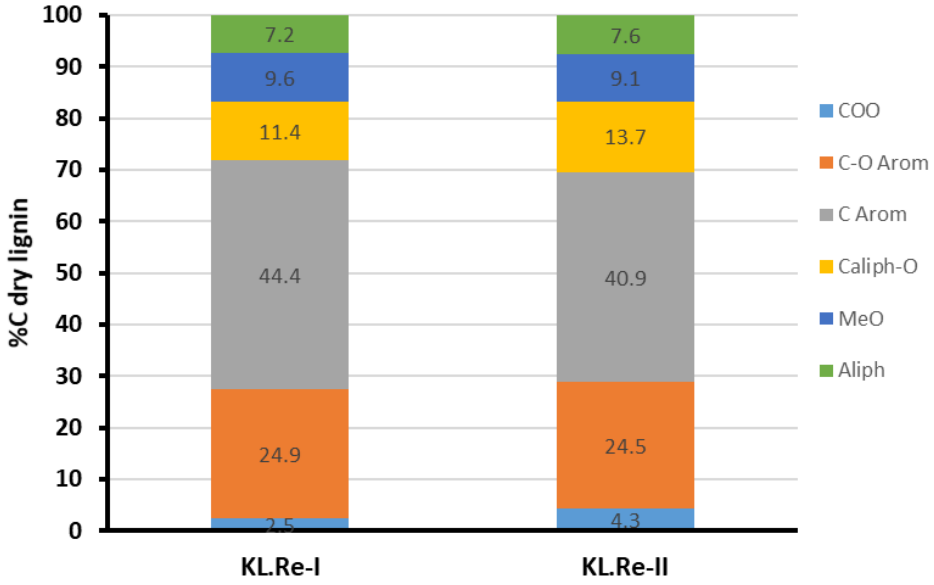

Figure 15 %molC repartition in lignins KL.Re-I and KL.Re-II determined by ^{13}C NMR.

Carbon moieties composition is almost the same between the two samples. Methoxyl carbons, aromatic carbons and aromatic oxygenated carbons content were in agreement with contents expected in G-units lignin structure. Indeed, in C10 G-units: 40% C are aromatic non-oxygenated, 20%C aromatic oxygenated and 10%C are methoxyls.

HSQC semi-quantification (Table 21) of the main lignin linkages (*β-O-4*, *β-β*, *β-5*) were performed using the correlation peak according to aromatic carbons. $S_{2,6}$ (104.2/6.7) and G_2 (110.2/6.9) have been used as internal standard and linkages concentration are expressed as a number per 100 aromatic units (S+G). The integral value for each linkage were divided by the integral value for $S_{2,6}/2$ + integral value for G_2.

Table 21 ^{1}H-^{13}C HSQC Quantification of side chains present in lignins.

		KL.Re-I		KL.Re-II	
	corr. Assig.	Average %	Std dev.	Average %	Std dev.
% β-O-4	72.1/4.88	4.60	0.47	12.69	0.50
% β-β	86/4.69	5.44	1.07	5.34	0.56
% β-5	87.3/5.53	2.50	0.33	3.17	0.24

HSQC quantification on the main lignin linkages (*β-O-4, β-β, β-5*) show that KL.Re-II has more ether linkages than KL.Re-I.

KL.Re-I and KL.Re-II have been analysed by thermogravimetric analysis following the same method of the commercial lignins. Results are presented in Figure 16. In the figure LN20 and LN45 refer to the solids from black liquors' evaporation, while K3 and K4 are respectively the precipitated lignins from the first and second campaigns.

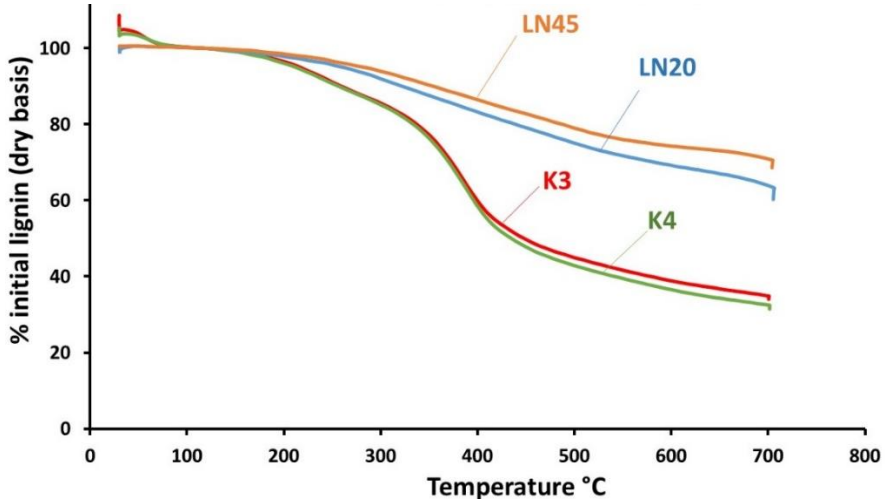

Figure 16 ATG analysis of KL.Re-I (K3) and KL.Re-II (K4), comparison with LN20.Re.II (LN20) and with LN45.Re.II (LN45)

ATG profiles are similar for KL.Re-I and KL.Re-II. Volatilization starts around 175°C to 700°C. Maximum rate volatilization is reached at 370°C. Volatilization starts at approx. 175°C for LN45.Re-II and LN20.Re-II but the degradation rate (%wt/°C) is slower. Probably this huge difference between the precipitated lignins and the residues from black liquor evaporation is due to the high mineral content in the latter.

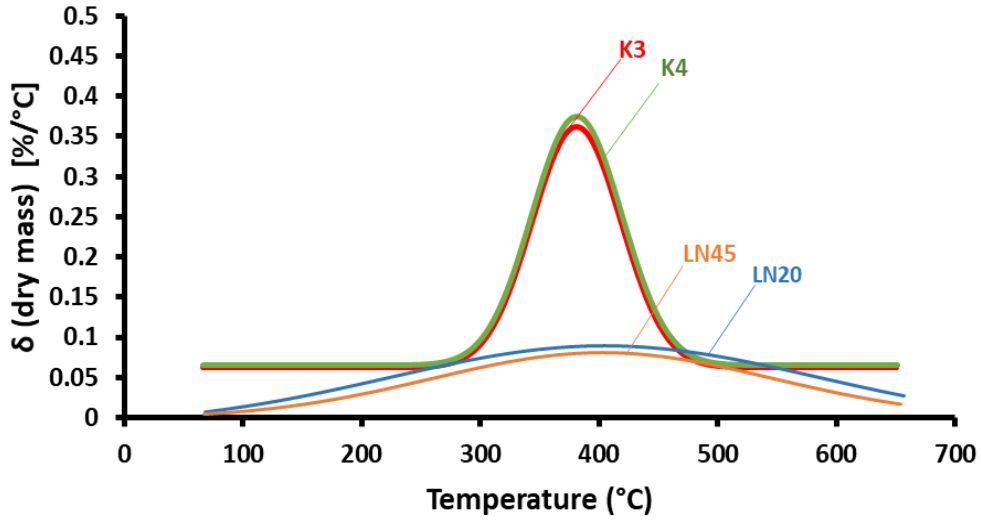

Figure 17 Derivative thermogravimetry analysis of KL.Re-I (K3) and KL.Re-II (K4), comparison with LN20.Re.II (LN20) and with LN45.Re.II (LN45)

4. - Conclusions

This study has the aim of deeply analysing and understanding the composition, structure and features of technical lignins. Many different analytical techniques have been employed for this scope.

In summary, from the characterisation of the 4 commercial lignins we deduced the following results. Industrial lignins were commercialized in dry form (dryness ~ 94-96%), only Kraft softwood lignin (BioPivaTM 1000) was sold raw without additional drying with a residual water content of 35%, as indicated by the supplier. They were relatively pure with a lignin content (KL + ASL) varying from 87% to 96%, minerals (ash) from 1% to 2%, and residual sugars from 2% to 5%. Organosolv lignin was the most contaminated with a residual sugar level of 5%, a protein level up to almost 11% (ie Supplier's data), resulting in 2.2% nitrogen (N).

The mineral contaminants of kraft lignins were mainly sodium carbonate (0.2% Na), while soda and organosolv lignin were rather rich in silica given the raw material used (wheat straw).

The phenolic contents and especially $–OH_{Ar}$ groups were ranging from 2.0 mmol/g until 3.0 mmol/g by potentiometric dosage, whereas ^{31}P NMR showed higher level (from 1.4 to 4.8 mmol/g), with the highest phenolic contents in Kraft lignins (both softwood and hardwood).

HSQC-NMR analyses showed slightly higher β-O-4 links in Eucalyptus Kraft lignin, than in softwood Kraft lignin and even higher than in soda lignin.

TG/DSC analyses showed that lignins presented different chemical stabilities as function of temperature. Indeed Organosolv, softwood Kraft and Soda lignins started to lose mass first (approx. 175°C) whereas Eucalyptus Kraft lignin started at 200°C. Organosolv presented also the wider range of temperature volatilisation (150°C – 500°C), whereas soda and Eucalyptus had similar volatilisation temperature ranges (225°C – 450°C). Therefore, Eucalyptus Kraft lignin would be slightly more thermostable than the others.

Molecular Mass – GPC analyses showed that softwood Kraft lignin presented the highest MM. The Mw of softwood Kraft lignin was of 2 900 g/mol with a DP of 16 using SEC-THF and of 6 270 g/mol and DP of 2.8 using SEC-THF after acetylation. Organosolv lignin analysed by SEC-THF after acetylation led to a Mw of 4 000 g/mol. Eucalyptus Kraft lignin and Soda lignin presented similar MM profiles with Mw of 3 600 by THF after acetylation and 1 500 by SEC-THF.

NMR analyses showed slightly higher β-O-4 links in Eucalyptus Kraft lignin, than in softwood Kraft lignin and even higher than in soda lignin.

Beside the commercial lignins, some black liquors with different concentration of organic content and sampled from different streams of a partner paper mill (Smurfit Kappa) have been included in this study.

Industrial black liquors (BL) were sampled and analysed in the frame of two distinctive campaigns (07/2018 and 09/2019), followed by lignin preparation. About the features of black liquors, we can affirm as follows. The quality of the 45% BL was rather stable, and contained ~75% of organic matter with remaining residual cooking reagents (residual alkali and sulphurous compounds). The organic composition was partly identified with ~ 33% of lignin, ~1 % of sugars, and ~ 0.5-1% of wood extractives. Other small organics, as hydroxyl acids derive from carbohydrate, represented ~8% with mainly acetic acid, formic acid, lactic acid, and glycolic acid. The physico-chemical characteristics of the 20% BL were more variable. For the second campaign, MW and TG/DSC analyses were performed and showed that both BL presented similar Molecular Mass distribution profiles, and that for both samples, volatilisation starts around 175°C until 900°C. Two main phases were detected. First an important degradation between 175°C and 700°C (which is consistent with TGA analysis of precipitated lignins). The char yield was about 65%wt at 700°C (for both samples). Second volatilisation between 700 to 900°C. At 900°C char yield is about 25%wt (for both samples).

Lignin preparation led to a similar lignin yield from both campaign (22% and 21.5%), and both prepared lignins are highly similar, containing a low amount of impurities, with ~2.3 % of residual sugars (mainly galactose, xylose and arabinose), and 2 % of minerals (mainly sodium sulfate and sodium carbonate). The residual sodium (Na) and potassium (K) were of 0.3% and 0.15%, respectively. The purity was then of 93%. The final sulfur content is of 2%wt, which is due to the organic sulfur linked to lignin as thiol group. All these characteristics were then very similar to those of the commercial softwood kraft lignin.

The lignin powder was constituted of fine particles of 16.5 µm of average diameter, with a narrow distribution around this diameter. These particles sizes were slightly higher than those of commercial lignin particles (i.e. ~9.5 µm).

The polymeric size and distribution of the lignin, analysed by GPC, were very similar to the commercial lignins previously studied. Nevertheless, this prepared lignin showed the highest Mw, compared to the 4 commercial samples. The prepared lignin contained significant reactive phenol groups (i.e. 2.9 mmol/g) and only low amount of carboxyl groups (i.e. 1.1 mmol/g). The TGA profiles were similar for both lignin samples, with a volatilization starting around 175°C to 700°C. Maximum rate volatilization was reached at 370°C.

Nevertheless, the second prepared lignin contained slightly lower ashes amounts (-0.6%), slightly lower potassium but slightly higher sodium (+0.11%). It contained lower residual sugars (-0.6%), and lower size polymers. The CHONS analysis showed slightly more oxidized lignin, with less carbon quantity.

HSQC quantification on the main lignin linkages (β-O-4, β-β, β-5) show that the second lignin sample has more ether linkages than the first one.

All those results were necessary to understand lignin's features and behaviour, both if it is a commercial one and if it is from an industrial black liquor. In fact, knowing better the raw material, it will be easier figure out the mechanisms to convert it through thermochemical processes into high value products.

The following main conclusions can be highlighted:

- GPC to evaluate lignin molar weight cannot be used as a quantitative analysis, but it can be considered relative. It strongly depends on the methods, the solvents and the columns used to perform the characterization;

- FT-IR coupled with a PCA analysis can be a useful and fast tool to characterize and separate families of lignins according their original biomass or their extraction method;
- NMR analysis is indispensable to investigate lignin structure.

5. - References

1. Bruijnincx, P., Weckhuysen, B., Gruter, G.-J. & Engelen-Smeets, E. *Lignin valorisation: the importance of a full value chain approach*. (2016).

2. Tribot, A. *et al.* Wood-lignin: Supply, extraction processes and use as bio-based material. *Eur. Polym. J.* **112**, 228–240 (2019).

3. Ľudmila, H., Michal, J., Andrea, Š. & Aleš, H. LIGNIN, POTENTIAL PRODUCTS AND THEIR MARKET VALUE. *WOOD Res.* 15.

4. Dellon, L. D., Yanez, A. J., Li, W., Mabon, R. & Broadbelt, L. J. Computational Generation of Lignin Libraries from Diverse Biomass Sources. *Energy Fuels* **31**, 8263–8274 (2017).

5. Rinaldi, R. *et al.* Paving the Way for Lignin Valorisation: Recent Advances in Bioengineering, Biorefining and Catalysis. *Angew. Chem. Int. Ed.* **55**, 8164–8215 (2016).

6. Zakzeski, J., Jongerius, A. L., Bruijnincx, P. C. A. & Weckhuysen, B. M. Catalytic Lignin Valorization Process for the Production of Aromatic Chemicals and Hydrogen. *ChemSusChem* **5**, 1602–1609 (2012).

7. Constant, S. *et al.* New insights into the structure and composition of technical lignins: a comparative characterisation study. *Green Chem.* **18**, 2651–2665 (2016).

8. Lora, J. H. Lignin: A Platform for Renewable Aromatic Polymeric Materials. in *Quality Living Through Chemurgy and Green Chemistry* (ed. C.K. Lau, P.) 221–261 (Springer, 2016). doi:10.1007/978-3-662-53704-6_9.

9. Mahmood, N., Yuan, Z., Schmidt, J., Tymchyshyn, M. & Xu, C. (Charles). Hydrolytic liquefaction of hydrolysis lignin for the preparation of bio-based rigid polyurethane foam. *Green Chem.* **18**, 2385–2398 (2016).

10. McClelland, D. J. *et al.* Functionality and molecular weight distribution of red oak lignin before and after pyrolysis and hydrogenation. *Green Chem.* **19**, 1378–1389 (2017).

11. Andrianova, A. A. *et al.* Size exclusion chromatography of lignin: The mechanistic aspects and elimination of undesired secondary interactions. *J. Chromatogr. A* **1534**, 101–110 (2018).

12. Harman-Ware, A. E. & Ferrell, J. R. Methods and Challenges in the Determination of Molecular Weight Metrics of Bio-oils. *Energy Fuels* **32**, 8905–8920 (2018).

13. Hoekstra, E., Kersten, S. R. A., Tudos, A., Meier, D. & Hogendoorn, K. J. A. Possibilities and pitfalls in analyzing (upgraded) pyrolysis oil by size exclusion chromatography (SEC). *J. Anal. Appl. Pyrolysis* **91**, 76–88 (2011).

14. Lancefield, C. S. *et al.* Investigation of the Chemocatalytic and Biocatalytic Valorization of a Range of Different Lignin Preparations: The Importance of β-O-4 Content. *ACS Sustain. Chem. Eng.* **4**, 6921–6930 (2016).

15. GPC - MALS | Materials Research Laboratory at UCSB: an NSF MRSEC. https://www.mrl.ucsb.edu/polymer-characterization-facility/instruments/gpc-mals.

16. Fredheim, G. E., Braaten, S. M. & Christensen, B. E. Molecular weight determination of lignosulfonates by size-exclusion chromatography and multi-angle laser light scattering. *J. Chromatogr. A* **942**, 191–199 (2002).

17. Ralph, J. & Landucci, L. NMR of lignins. *Lignin Lignans Adv. Chem.* (2010) doi:10.1201/EBK1574444865-c5.

18. Gómez, D. *et al.* Chapter 2: Stationary Combustion. in 2.1-2.47 (2006).

19. *Methods in Lignin Chemistry*. (Springer-Verlag, 1992).

20. Joffres, B. *et al.* Thermochemical Conversion of Lignin for Fuels and Chemicals: A Review. *Oil Gas Sci. Technol. – Rev. D'IFP Energ. Nouv.* **68**, 753–763 (2013).

21. Serrano, L. *et al.* Fast, Easy, and Economical Quantification of Lignin Phenolic Hydroxyl Groups: Comparison with Classical Techniques. *Energy Fuels* **32**, 5969–5977 (2018).

22. Strassberger, Z. *et al.* Lignin solubilisation and gentle fractionation in liquid ammonia. *Green Chem.* **17**, 325–334 (2014).

6. - Supporting Information

The analytical methods and standards followed for the characterization of lignin and black liquor mentioned in chapter 2 will be described below.

Elemental and Proximate Analysis. The dry matter was evaluated following the standard NF EN ISO 18134-3: the samples were heated up to 105°C till the mass was constant. The elemental composition was measured according to the standard NF EN 15407. The ash content was measured at 550°C (2°C/min; >2 hours) according to the standard NF EN 15403. The Higher Heating Value (HHV) was measured with a calorimetric bomb (NF EN 15400) and the Lower Heating Value (LHV) by difference, according the following equation:

$$LHV = HHV - 0.212*(\%H) - 0.0245*(\%Moisture) - 0.008*(\%O)$$ [1]

Klason Lignin. The determination of acid-soluble and acid-insoluble (Klason) lignin were made following the book "Methods in Lignin Chemistry"[2]. Sugar content was achieved through ionic chromatography equipped with an amperometric pulsed detector: sodium acetate 1M + NaOH 10mM and NaOH 250mM as eluents; Carbo pac PA20 as column; 35°C.

ICP-OES. To quantify low-concentrated chemical elements in lignin, the Inductively Coupled Plasma – Optical Emission Spectrometry (ICP-OES) was used. Lignin samples were previously mineralized under micro-waves thanks to the utilization HNO_3. Then, the sample were opportunely diluted and filtrated before injection. Solid samples (0.15 g) were digested with 5 mL of HNO_3 in a microwave oven Milestone Start D Microwave Digestion. Samples were analysed by plasma emission spectroscopy (ICP-OES) (Thermo ICAP 6000 Series ICP Spectrometer). Quality controls were performed with standard solutions prepared from a multi-element certified solution (1000 mg L−1 SCP sciences).

TGA/DSC. The thermogravimetric analysis was carried out according the following method: 10°C/min, N_2 5Nml/min, 25°C to 700°C. Because of its high moisture content, Kraft1 has been previously dried.

SEM. Particle size analyses were carried out by image analysis (FPIA-Flow Particles Image Analysis) on Malvern-Sysmex 3000 device, fitted with two filters ('lens') which makes it possible to analyse the size of particles with diameters between 1.5 µm and 40 µm (High Power Field mode [1.5 µm - 40 µm] and between 6 µm and 150 µm (Low Power Field mode [6 -160

µm]. Data processing was carried out in surface mode, and led to different dimensions such as the average diameter and the median diameter (D50), and provides the particle size distribution.

GPC. Samples were dried in an oven overnight. 2ml of acetic anhydride/pyridine (1:1) mixture were added to 20 mg of lignins extractive free. The mixture was kept at room temperature with stirring for 24 hrs. 25 ml of Ethanol were added to the reaction mixture and kept for 30 min. Then ethanol was evaporated. This step was repeated until the acetic anhydride and pyridine were evaporated. Acetylated lignin is dissolved in 2 ml of Chloroform and added solution drop wise to 100 ml magnetically stirred diethyl ether. Precipitated acetylated lignin was collected after centrifugation. Then dissolved in 25 ml THF for GPC investigations.

GPC analyses have been performed on a HPLC Shimadzu Prominence. The stationary phases are a Phenomenex Phenogel 5 µm (7.8 x 50 mm) guard column, and the analytical columns a 10 µm (8.0 x 300 mm) Shodex GPC KF-806L and a Phenomenex Phenogel 5 µm 100 Å (7.8 x 300 mm). The mobile phase is unstabilized THF. The samples are separated at 35°C with a flow rate of 1 ml/min and the detection is carried out by UV detectors (at 280 and 254 nm, Shimadzu SPD-20A) and RID (Refractive Index Detector, Shimadzu RID-20A). The standards used for calibration are polystyrene.

For GPC-MALS measurements, lignins were dissolved in THF (1 mg/mL), filtered in a 0.22 µm PTFE before injection. The sample is then injected with a 1 mL/min flowrate in a miniDAWN TREOS (WYATT) instrument. This instrument features a fused silica cell, a laser operating at 657 nm and three angles of detection (46.6° ; 90.0° ; 133.40°). The detector is an Optilab rEX RI set at 685 nm.

NMR. To analyse the structure and functionalities of the lignins, different kind of nuclear magnetic resonance have been performed.

^{13}C NMR spectra were acquired on a Bruker Avance III HD 300 MHz spectrometer (75.46 MHz for ^{13}C) equipped with a BBO probe at 50°C in order to reduce viscosity. An inverse-gated decoupling pulse sequence (zgig pulse program) was used to avoid NOE effects. 10, 000 scans were collected with a pulse delay of 12s. The lignins were dissolved in DMSO-d6 after overnight stirring (200 mg/750 µL) and chemical shifts were referenced to the solvent signal (39.5ppm). The spectra were processed on Topspin 4.0.6 software. Integration areas were used to calculate carbon concentration (mmol/glignin) based on the weight percentage of carbon given by elemental analysis.

For ^{1}H-^{13}C HSQC analysis lignins were dissolved in DMSO-d6 after overnight stirring (200 mg/750 µL) and chemical shifts were referenced to the solvent signal (39.5ppm). The spectra were processed on Topspin 4.0.6 software. The 2D HSQC NMR spectra were acquired on a Bruker Avance III HD 300 MHz spectrometer equipped with a BBO probe at 50°C using the hsqcetgp pulse program. Matrices of 1024 data points for the 1H-dimension and 256 data points for the 13C-dimension were collected with a relaxation delay of 1.5s and spectral widths from 9.5 to -0.5ppm and from 180 to 0ppm for the 1H and 13C dimensions, respectively. Number of scans NS=128.

For ^{31}P analysis, lignin samples were dried at 105°C overnight. Approximately 25 mg were used for each analysis. Lignin samples were weighed in to a 5ml volumetric flasks. A solvent mixture of pyridine(99.9%)/$CDCl_3$ (1.6/1 v/v) was prepared in a 20ml volumetric flask. We introduced 8ml of pyridine (w.ap: 7.88g for density of 0.978) and 5ml of $CDCl_3$ (7.5g for density of 1.5). This mixture was use for further preparation/dissolution. A solution of chromium (III) acetylacetonate and cyclohexanol were prepared in a solvent mixture of pyridine(99.9%)/$CDCl_3$ (1.6/1 v/v). Approximately 36mg of Chromium (II) and 40mg of cyclohexanol were weighed into a 10ml volumetric flask and 10ml of Pyridine/$CDCl_3$ mixture was added. This mixture was stirred in order to dissolve the Chromium. Cyclohexanol must be introduced with extremel precaution because any error could extensively change quantification. 400µL of Pyridine/$CDCl_3$ were added to the solid lignin. The solvent mixture was introduced carefully into the 5ml flask and flask was stirred by hand until complete dissolution. 150µL of chromium/cyclohexanol solution was introduced into the 5ml flask. The lignin solution was then mixed. Minutes before the NMR experiments, 50µL of TMDP (2-chloro-4,4,5,5-tetramethyl-1,3,2-dioxaphospholane) was added to the 5ml flask. The flask was shaken (slowly) by hand for 1-2 minutes. The solution was transferred into a 5mm NMR tube. Each sample was prepared before analysis to avoid chemical evolution during storage. NMR measurements were performed on a Bruker 300MHz (^{31}P resonance of 121.5MHz). The following acquisition parameters were used: 200 scans, 25s relaxation delay, 62ppm spectral width.

FT-IR. FT-IR images were acquired using a FTIR ATR BRUCKER ALPHA P spectrometer (Ettlingen, Germany). ATR spectra were collected with 4 cm-1 resolution. Spectra are the result of averaged 32 scans manually baseline corrected and normalized.

Black Liquor proximate and elemental analysis. Dried masses have been determined by the mass loss after drying at 105°C for 24h of approx. 0.6g of liquors. Density have been performed by measuring the mass of 20ml of each liquors. Each dried liquors samples have been analyzed

by ThermoScientific Analyseur CHONS FLASH EA1112 to determine the % in C, H, N and S. pH value for each liquor is high (approx. 14). This points out the high concentration in sodium hydroxide in liquors from pulping process. Dry matter content are close to the expected values. Carbon content (dry matter basis) is between 20 and 30%wt. It seems that carbon content is not very important in liquors. In order to analyze the dissolved carbon content, it was measured by Shimadzu TOC-meter Vcsh. Approximatively 0.5g of liquors for LN.ReSF-I and LN.ReS-I ; 0.1g of liquors for LN.Re-I were diluted into 20ml of deionized water. Proximate analysis was performed on TGA/DSC METTLER TOLEDO. A protocol including five steps was used: 1) 30-105°C 15°C/min, 2) 105°C during 20 minutes, 3) 105-900°C at 15°C/min 4) 900°C during 20 minutes. Steps 1 to 4 were performed under Nitrogen (50Nml/min). 5) 900°C during 20 minutes under Air (50Nml/min).

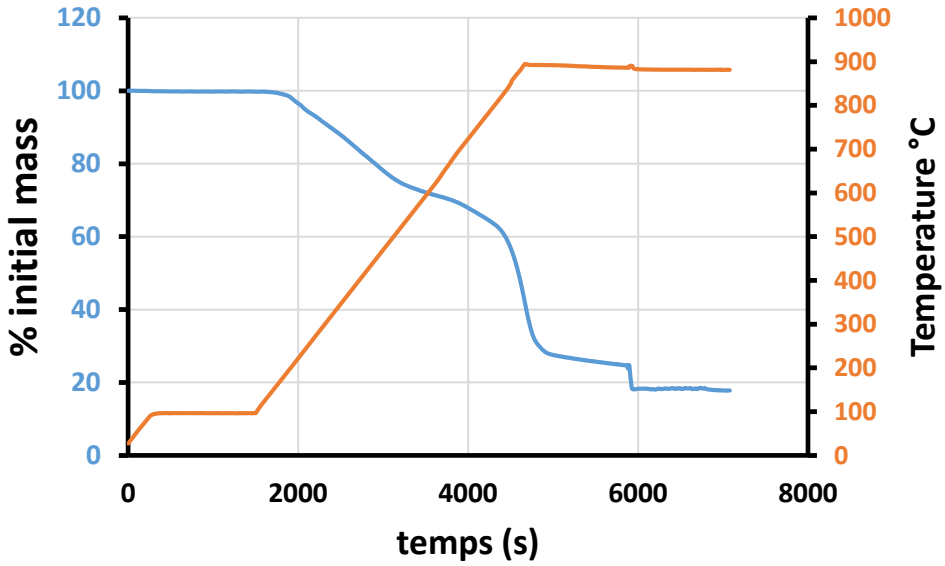

Figure S1 ATG proximate analysis of LN45.Re-II

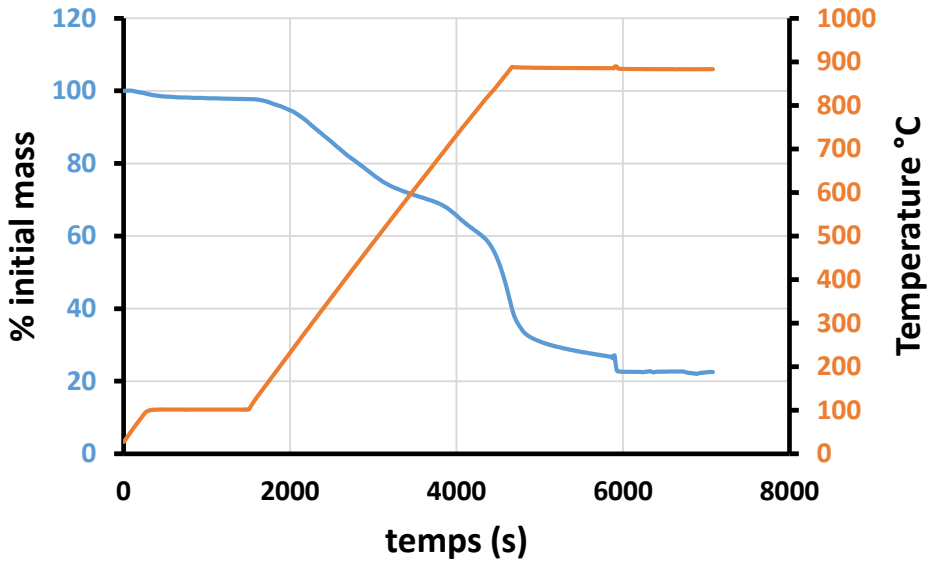

Figure S2 ATG proximate analysis of LN20.Re-II

SEC for Black Liquor. The molar mass distribution of the black liquors was determined using an aqueous SEC method on a Prominent Shimadzu HPLC equipped with a guard column Phenomenex Polysep GFC-P (7.8 × 35 mm) and two analytical columns Phenomenex Polysep P2000 (7.8 × 300 mm) and P3000 (7.8 × 300 mm). A solution of sodium hydroxide (NaOH) at 10 mM was used as the mobile phase. Liquors were diluted by approx. 1/100 w/w ratio with deionized water and filtered through 0.45 µm PTFE membrane filters. Twenty µL of sample solutions were injected. The separation was performed at 30 °C and 0.35 mL·min−1 NaOH flow rate. An ultraviolet spectroscopy detector (UV) at 254 nm (Shimadzu SPD-20A). Calibration was not performed because no standard were available to calibrate lignin in basic aqueous phase.

NMR for Black Liquor. To analyse the structure and functionalities of black liquors, different kind of nuclear magnetic resonance have been performed.

^{13}C NMR spectra were acquired on a Bruker Avance III HD 400 MHz spectrometer (100 MHz for ^{13}C) equipped with a BBO probe at 50°C in order to reduce viscosity. An inverse-gated decoupling pulse sequence (zgig30 pulse program) was used to avoid NOE effects. 10,000 scans were collected with a pulse delay of 12s. The lignins were dissolved in DMSO-d6 after overnight stirring (200 mg/750 µL) and chemical shifts were referenced to the solvent signal (39.5ppm). The spectra was processed on Topspin 4.0.6 software. Integration areas were used

to calculate carbon concentration (mmol/glignin) based on the weight percentage of carbon given by elemental analysis. Below are given the spectra and the reproducibility tests done on Soda lignin.

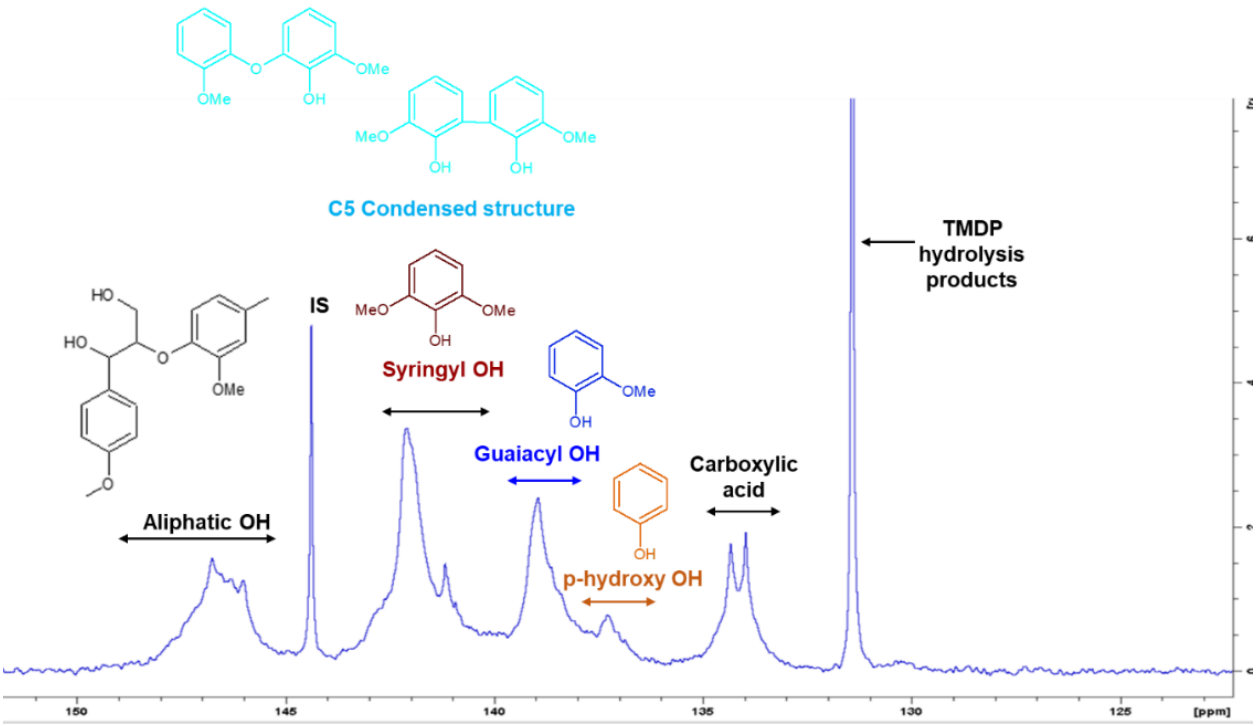

Figure S3 Functional group analysis of Soda lignin by quantitative 31P NMR after phosphitylation

Observation: Soda lignin is composed by S/G/H free hydroxyl units. S signal overlapped signal for C5 substitued functions. So we did not attempt the estimation of S units. Peak at 141.15 ppm could be lignins 5-5 condensation.

Table S1 Reproducibility of Soda ^{31}P NMR results.

	mmol/g lignin			
	Al-OH (150-145 ppm)	**Syringyl OH/ Condensed structure (144-140ppm)**	**Guaiacyl OH / p-hydroxy phenyl OH (140 - 136 ppm)**	**Carboxylic acid (136-132 ppm)**
Soda_31P_01	1.32	2.30	1.64	0.90
Soda_31P_02	1.34	2.24	1.64	0.87

Results were compared to literature as Soda lignin has been extensively characterized. It appears that the composition change as function of the study.

Table S2 Comparison of Soda ^{31}P NMR results with literature.

	Origin	Al-OH	S + C5 units	G+ hydroxy	Carboxylic
Soda	GreenValue Indian wheat straw	1.34	2.24	1.64	0.87
Joffres_2014[3]	P1000 GreenValue Wheat Straw	1.6	1.1	1.2	0.9
Constant_2016[4]	P1000 GreenValue Wheat Straw/Sarkanda grass	1.26	1.73	1.13	0.8
Serrano_2018[5]	GreenValue P1000 Wheat Straw	1.5	1.53	1.17	n.a
Strassberger_2015[6]	P1000 Wheat Straw/Sarkanda	1.59	2.3	1.45	1.16
Boerius_2014	P1000 Wheat Straw/Sarkanda	1.76	1.37	1.26	1.11
Boerius_2014	Soda Wheat Straw	2.01	1.76	1.39	1.04

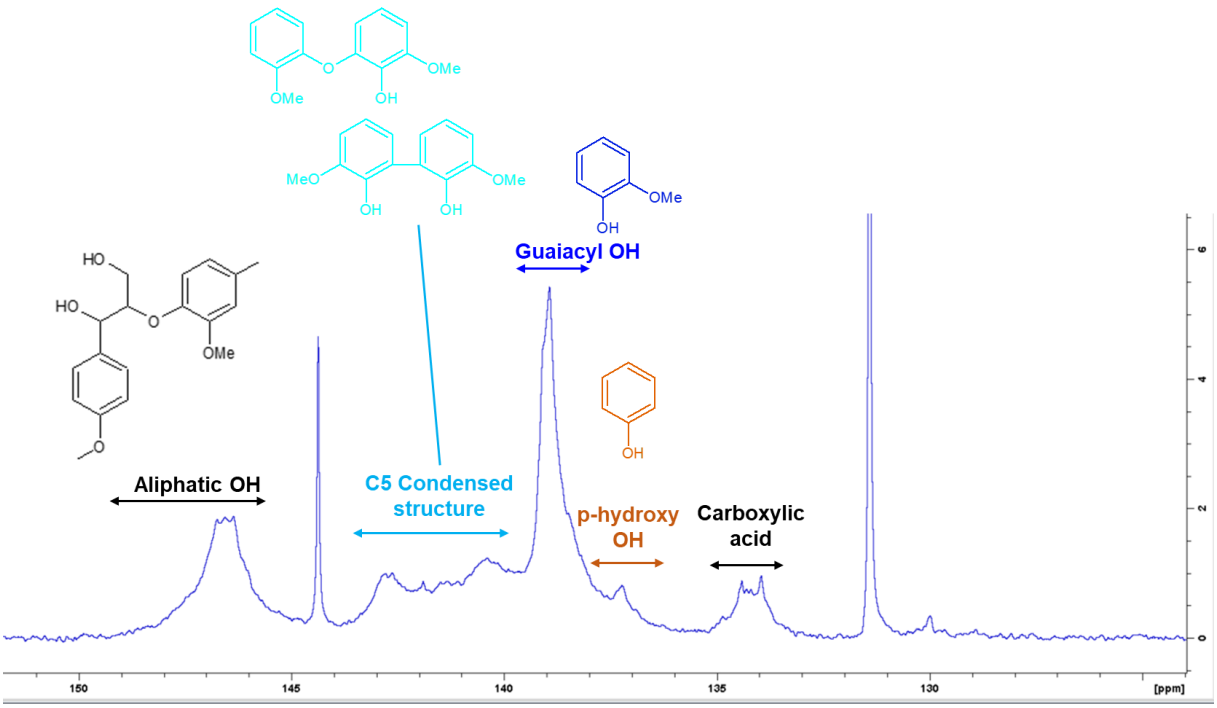

Figure S4 Functional group analysis of Kraft1 lignin by quantitative 31P NMR after phosphitylation

Observation: No S units seems to detected (normal from Pine lignin).

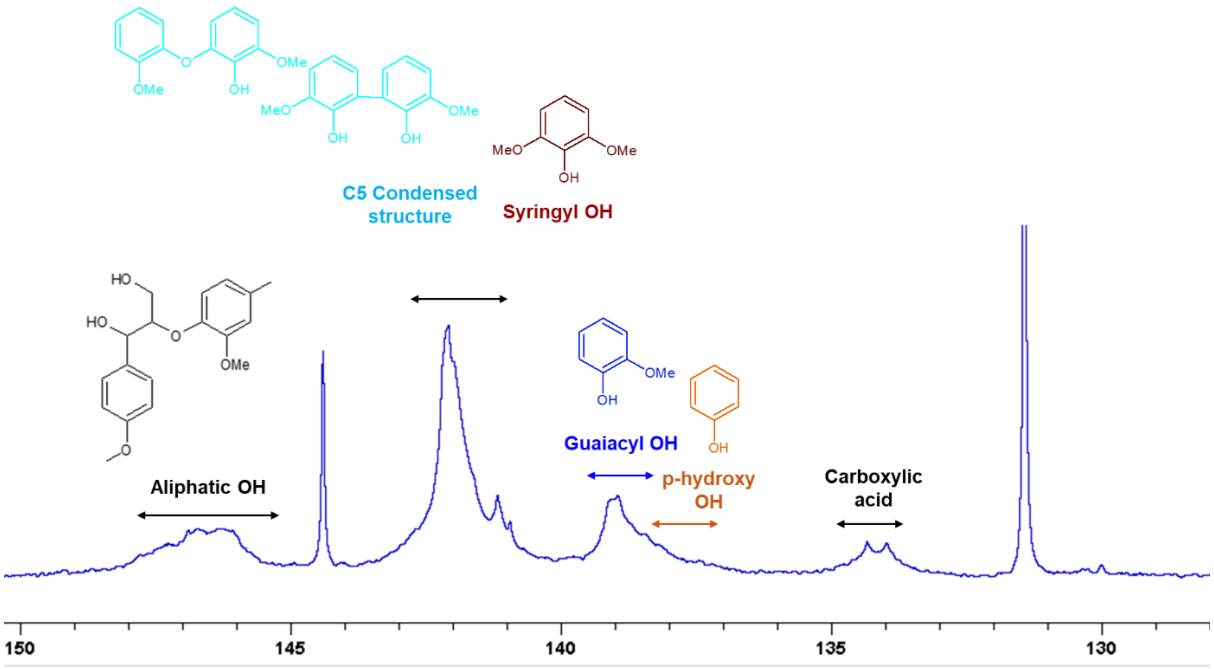

Figure S5 Functional group analysis of Kraft2 lignin by quantitative 31P NMR after phosphitylation.

Observations: G and H free OH units content is lower than other Kraft. The S free units seems to be the most important unit for this lignin.

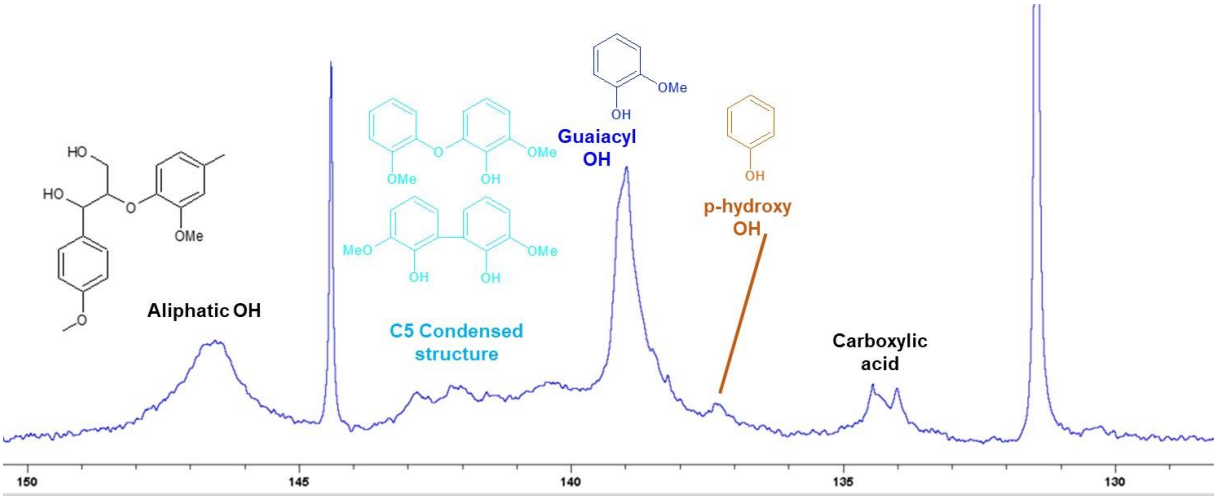

Figure S6 Functional group analysis of Kraft3 lignin by quantitative 31P NMR after phosphitylation.

Observations : G units seems to be the more important units. C5 condensed units are observed and small amount of S units seems to be detected. However the solubility of Kraft3 into

Pyridine/Chloroform-d appears to be limited. So we should be sure that the sample is totally soluble.

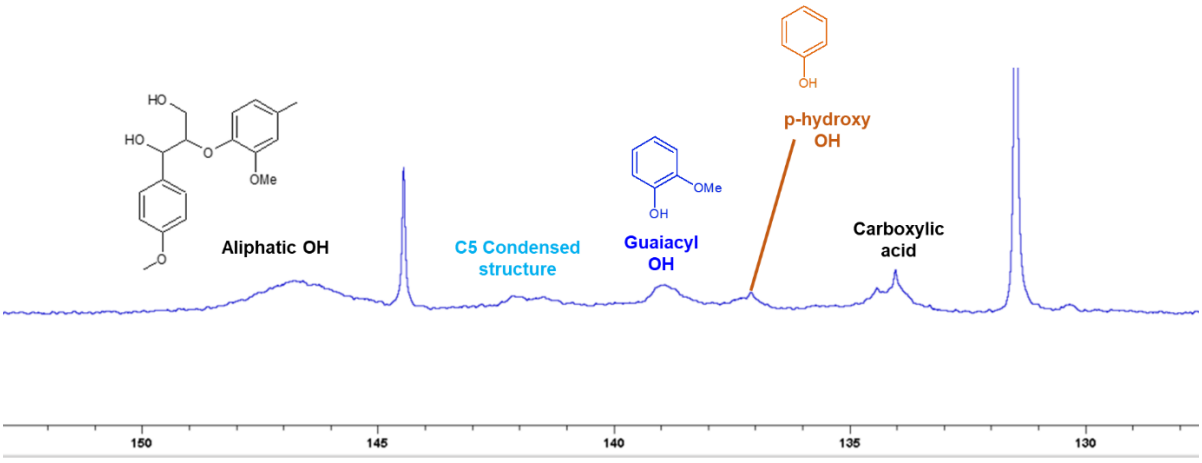

Figure S7 Functional group analysis of Organosolv lignin by quantitative 31P NMR after phosphitylation.

Observation: Lignin is not soluble into Pyridine/Chloroform-d.

For 2D HSQC NMR, the lignins were dissolved in DMSO-d6 after overnight stirring (200 mg/750 µL) and chemical shifts were referenced to the solvent signal (39.5ppm). The spectra were processed on Topspin 4.0.6 software. The 2D HSQC NMR spectra were acquired on a Bruker Avance III HD 400 MHz spectrometer equipped with a BBO probe at 50°C using the hsqcetgp pulse program. Matrices of 1024 data points for the ^{1}H-dimension and 256 data points for the ^{13}C-dimension were collected with a relaxation delay of 1.9s and spectral widths from 8 to 0ppm and from 180 to 0ppm for the ^{1}H and ^{13}C dimensions, respectively. Number of scans NS=128.

6.1. - References

1. Gómez, D. *et al.* Chapter 2: Stationary Combustion. in 2.1-2.47 (2006).

2. *Methods in Lignin Chemistry*. (Springer-Verlag, 1992).

3. Joffres, B. *et al.* Thermochemical Conversion of Lignin for Fuels and Chemicals: A Review. *Oil Gas Sci. Technol. – Rev. D'IFP Energ. Nouv.* **68**, 753–763 (2013).

4. Constant, S. *et al.* New insights into the structure and composition of technical lignins: a comparative characterisation study. *Green Chem.* **18**, 2651–2665 (2016).

5. Serrano, L. *et al.* Fast, Easy, and Economical Quantification of Lignin Phenolic Hydroxyl Groups: Comparison with Classical Techniques. *Energy Fuels* **32**, 5969–5977 (2018).

6. Strassberger, Z. *et al.* Lignin solubilisation and gentle fractionation in liquid ammonia. *Green Chem.* **17**, 325–334 (2014).

C. Lignin Depolymerization: A Comparison of Methods to Analyze Monomers and Oligomers

ChemSusChem 2020, 13, 1 – 17, 4633-4648

Erika Bartolomei[a], Yann Le Brech[a], Anthony Dufour[a]*, Vincent Carre[b], Frederic Aubriet[b], Evan Terrell[c], Manuel Garcia-Perez[c], Philippe Arnoux[a]*

[a] LRGP, CNRS, Université de Lorraine, 1 rue Grandville, 54000 Nancy, France

[b] LCP-A2MC,Université de Lorraine, 1 Boulevard Arago, F-57078, Metz, France

[c] Department of Biological Systems Engineering, Washington State University, Pullman, WA 99164, USA

* corresponding authors: anthony.dufour@univ-lorraine.fr, philippe.arnoux@univ-lorraine.fr

Abstract

Catalytic liquefaction of lignin is an attractive process for the production of fuels and chemicals, but it forms a wide range of liquid products from monomers to oligomers. Oligomers represent an important fraction of the products and their analysis is complex. Therefore, rapid characterization methods are needed in order to screen liquefaction conditions based on the distribution in monomers and oligomers. For this purpose, we propose UV spectroscopy as a fast and simple method to assess the composition of lignin-derived liquids. UV absorption and fluorescence were studied on various model compounds and liquefaction products. Liquefaction of Soda lignin was conducted in an autoclave, in ethanol and with Pt/C catalyst (H2, 250°C, 110 bar). Liquids were sampled at isothermal conditions every 30 minutes for 4 hours. UV fluorescence spectroscopy is related to GC/MS, GPC, MALDI-TOFMS and NMR characterizations. A depolymerization index is proposed from UV spectroscopy in order to rapidly assess the relative distribution of monomers and oligomers.

1. - Introduction

Lignin is the main renewable resource of aromatic compounds.[1] The native lignin present in biomass is a three-dimensional amorphous macromolecule made up principally by the combination of three different phenylpropane monomer units: p-coumaryl alcohol (H), guaiacyl alcohol (G) and syringyl alcohol (S), linked mainly by aryl ether bonds (β-O-4) in a randomized way.[2–9] Lignin is an abundant aromatic feedstock, but it is still largely considered as a source for heat and power for bio-refinery or pulping processes.[1,3,10–12] The lack of well-established processes that add value to lignin can be largely attributed to its structural complexity and associated chemical recalcitrance.[8,13–15]

The use of lignin as a feedstock for the production of bio-based chemicals has received increasing interest[16–21]. The development of efficient processes for lignin valorization presents an important potential to improve the economic feasibility and overall sustainability of both pulp and paper processing and cellulosic-based ethanol biorefineries.[1,22,23]

Lignin conversion to value-added products is chiefly governed by an interplay of three technological biorefinery aspects: (i) lignocellulosic biomass fractionation, (ii) lignin depolymerization, and (iii) upgrading towards targeted (intermediate or final) chemicals, such as through hydrotreatment.[24]

Efficient lignin depolymerization could produce a wide range of fuels and chemicals (and/or their precursors).[1,2,17,24,25] Numerous studies have been carried out on lignin depolymerization to obtain phenolic compounds in an oil fraction (lignin-oil).[16,24–28] These molecules (especially alkylated phenol like guaiacol) could be used to produce chemicals and materials (polymers, antioxidants, resins, medicines, or pesticides) in substitution to fossil fuel resources.[24,29]

Lignin reductive depolymerization is often performed in the presence of a reduced metallic catalyst on various supports (e.g., Ru/Al2O3, Ru/C, Ru/TiO2, Pd/C, Pt/C)[30–35], a reducing agent (which is mainly hydrogen) and a solvent. The mechanisms of lignin depolymerization have been reviewed recently.[36,37]

Molecular hydrogen can be brought directly as a gas (H2), solubilized in the solvent, and/or it can be derived from organic H-donors, such as alcohols (like ethanol) or even from the lignin matrix itself. Hydrogen transfer from organic H-donors is an attractive alternative to using high-pressure H2, which presents important safety and handling issues.[38]

For this reason, reductive depolymerization of lignin with alcohol is a promising process to produce phenolic compounds.[30–34] Supercritical alcohols are effective for lignin depolymerization because of their unique physical-chemical properties, namely: (i) high heat transfer, (ii) high solubilisation capability, and (iii) hydrogen donor behaviour.[30–33,33,34] Ethanol is an interesting solvent for lignin liquefaction because it is a cheap solvent which could be produced in the biorefinery from cellulose. Furthermore, ethanol is considered as formaldehyde scavenger to prevent the repolymerization of lignin decomposition products.[32] Ethanol can react with lignin side-chains to prevent the condensation reaction between lignin fragments.[39]

Among all tested catalysts, Pt/C has been shown as one of the most effective catalysts for lignin depolymerization processes, producing large yields of lignin-oil (77.4 wt%) with a small amount of char (3.7 wt%); there is also high selectivity for monomeric phenols.[30] For all these reasons, we have selected Pt/C and ethanol as liquefaction conditions for the present study.

Reductive liquefaction is generally operated at about 300°C and 100 bar. It forms various monomers that are mainly p-substituted methoxyphenols.[27,30,40–43] Lignin catalytic depolymerization in supercritical ethanol can lead to a yield between 5 and 20%wt of monomers from initial lignin.[30,33,34,44]

Nevertheless, there is still an important yield of non-monomeric compounds remaining after treatment (i.e. oligomers, condensed insoluble fractions, solid char). For instance, high molecular-weight phenolic compound ("oligomers") yields have been obtained in the range of 35 to 65% (wt.) with methanol, ethanol and propanol used as solvent in the presence of different catalysts.[30] Therefore, it is of tremendous importance to develop analytical approaches in order to assess the mass yield and composition in oligomers as a function of operating conditions.

Various methods have been reported in literature in order to analyze oligomers from lignin depolymerization. Acid precipitation followed by solvent extraction and evaporation has been proposed[33] to isolate oligomers from the solvent. It is a valuable method to quantify the mass yield of oligomers; however, it is time consuming and requires a significant amount of toxic solvent (like THF).

Gel permeation chromatography (GPC) is a common method for analyzing the molecular weight of macromolecules. It has been extensively studied on lignin and liquefaction products.[45–48] But a careful calibration must be achieved due to potential chemical interactions between lignin molecules and the column.[49] The different structure (hydrodynamic volume)

between lignin products and calibration standards also impairs the quality of the molar masses determined by GPC.[50]

Laser desorption ionization mass spectrometry (LDI-MS) as well as other ionization techniques has been used on lignin and its products [51–55] for "lignomic" studies.[56,57] Computational and graphical methods are currently used to elucidate the composition of oligomers.[57,58] LDI has been combined with high resolution mass spectrometry (HRMS) to analyze lignin and wood bio-oil[59,60], biochar[61] and on lignin pyrolysis intermediates.[47] Matrix assisted LDI (MALDI) combined with time of flight mass spectrometry (TOFMS) has been used on lignin liquefaction products.[21,62,63] This method gives the distribution of main m/z values from monomeric and oligomeric species present in the bio-oil. A tentative description of oligomeric structure is derived from MALDI MS analysis, but other HRMS techniques (i.e., FT-ICR MS) are more recommended, in comparison to TOFMS, for elucidating the chemical composition of lignin oligomers.[57,58]

UV-visible (UV-Vis) spectroscopy has been used to quantify soluble lignin[64,65]. Chen et al. have monitored lignin electrochemical depolymerization using UV spectroscopy[66]. UV-Vis is sensitive to aromatic species, and the solubilized lignin can be characterized by the evolution of specific electronic transitions[67]. UV fluorescence spectroscopy (UV-FS) can also be used to study aromatic molecules [68]. Both UV-Vis and UV-FS are non-destructive, fast and do not require large sample amounts[69].

Among UV fluorescence methods, synchronous fluorescence spectroscopy has been extensively used to study complex aromatic mixtures from coal[68–72], asphaltenes[73,74] and biomass pyrolysis[67,75–78]. In synchronous fluorescence, excitation and emission wavelengths vary simultaneously separated by a constant offset. The obtained spectrum depends on both fluorophore absorption and emission. Synchronous fluorescence spectroscopy has been demonstrated as a powerful method to analyze the molecular size of the conjugated compounds present in a complex mixture.[69,70,74,79,80] Despite numerous studies on lignin UV spectroscopy, synchronous UV fluorescence has not yet been proposed for lignin liquefaction products.

To date, this approach has not yet been rationalized and compared with other techniques for lignin liquid analysis.

It is of tremendous importance to combine analytical methods in order to obtain a more complete assessment of the complex liquids produced from lignin.

UV-FS has been compared to HPLC on coal liquids by Katoh et al. [70] This early work has demonstrated the usefulness of synchronous fluorescence spectroscopy on coal-derived liquids, despite the limitation of the method in which some molecules give only weak peaks. GPC, HPLC and UV-fluorescence have been compared in detail by Delpuech et al.[79] on coal hydroliquefaction and pyrolysis liquids. SEC, LDI-MS and fluorescence have been compared on coal tar pitch.[69] Some inconsistency may occur with LDI-MS notably due mass discrimination effects.[81] These studies on coal liquids are an important source of information which can be extended and adapted for lignin liquids.

SEC, MALDI-TOFMS and LDI-MS (among other methods) have been compared by Meier et al.[82] on different pyrolytic lignins produced from wood pyrolysis. SEC was the only method that allowed a mathematical calculation of molar mass characteristics. LDI-MS gave the molar mass of oligomer subunits.

All these studies highlight potential inconsistencies between methods used to analyse heavy liquid products. For this reason, the goal of this study is to compare the methods for analyzing the liquids from lignin liquefaction. To the best of our knowledge, we propose for the first time the use of synchronous UV fluorescence spectroscopy as a fast screening method to assess oligomers/monomers relative distribution from lignin liquefaction. A lignin "depolymerization index" is proposed based on UV spectroscopy. The UV results are discussed with complementary analysis, namely NMR, GPC, MALDI-TOF-MS and GC/FID-MS. The pitfalls and benefits associated to each method for analyzing lignin-derived liquids are discussed.

2. - Materials and Methods

2.1. - Chemicals

The lignin used for liquefaction experiments was a Protobind 1000, produced by soda pulping of wheat straw and marketed by GreenValue®.

Elemental analysis showed the following composition (wt. %): C, 62.9 (±0.09); H, 5.8 (±0.01); O, 29.5 (±0.01); N 0.4 (±0); S, 0.7 (±0.1); ash content 1.73 (±0.37); dry mass 95.6 (±0.6). Relative Mn (number average molecular weight) and Mw (weight average molecular weight) were respectively 1525 and 3650 g/mol (similar as Constant[8], based on PS standards, THF GPC method after acetylation). This GPC method may under-estimate lignin molecular weight.[50]

The catalyst used was Platinum on carbon (5% wt., Pt/C) from Sigma Aldrich (ref.205931). The references of model compounds are given in supplementary material.

2.2. - Catalytic liquefaction experiments

Lignin liquefaction was carried out in a 300 mL autoclave purchased from Parr Instruments (4890 series, see Supplementary Material). The reactor was loaded with 9.56 g of lignin (dry basis), 200 mL of pure ethanol as solvent and Pt/C solid catalyst to reach 1% wt. Pt on lignin, mass basis (2.0 g of Pt/C catalyst, 5% wt. of Pt loading on catalyst mass basis).

An internal standard (100 µl, hexadecane, Sigma Aldrich ref 52209) was injected in the autoclave (with 200mL ethanol, lignin and catalyst) before the start of the reaction. Hexadecane has been checked to be not reactive under the reaction conditions. This internal calibration allows a more accurate quantification of monomers present in the sampled solutions by GC/MS-FID.

After loading and sealing, the reactor was purged 5 times with N_2 in order to remove the air and charged with H_2 (10 bar, MESSER H_2>99.9%) to set a reductive atmosphere. The autoclave was heated by the following temperature program: start temperature = 20°C, heating rate=5 K min^{-1}, final temperature=250°C, 4h at 250°C, cooling time of about 35 min to room temperature (cooling by a high flow rate of compressed air flushing the outer the surface of the reactor). In this work, time "0" is defined once the temperature reached 250°C (first sampling). The magnetic stirrer was maintained at 400 rpm during the reaction.

The liquid was sampled under isothermal condition (at 250°C) by a sampling device including high pressure valves and a fixed sampling volume (of 3 mL). The sampling line was purged 2 times before the sample was collected in order to avoid contaminations between different samples. The sampled volume is small compared to the initial 200mL of solution and it does not impact the overall reaction conditions (checked by experiments without sampling).

All the samples were analyzed by different analytical techniques without any further manipulation (such as solvent extraction). Oligomers and solid residue obtained at the end of the reaction (after cooling of the autoclave) were also isolated (see supplementary material).

2.3. - Analysis of products

2.3.1. - GC-MS analysis

The samples were analyzed by an Agilent 7890 gas chromatograph combined to an Agilent 5975C MS (operated by electron impact at 70eV) and an FID placed in parallel to the mass spectrometer. The samples were filtered (0.45 µm glass filters) and no additional dilution was applied. The sample was injected (1 µL) with a split ratio of 10 into an Agilent HP-5MS (5% phenyl 95% methyl siloxane) column. The oven was maintained at 50°C for 10 min; then the temperature was increased with a first ramp of 5°C/min to 120°C, maintained for 10 min and then with a second ramp of 5°C/min to 250°C and maintained for 18 min. By comparison between the mass spectra and the NIST database, more than 40 compounds have been identified. The quantification was achieved by the FID detector based on the de Saint Laumer[83] method as previously described in detail[59]. This method is able to predict the relative response factor of a compound on a FID based on its combustion enthalpy.

2.3.2. - GPC-UV analysis

The molecular weight distribution of lignin liquefaction products was determined by GPC using a Shimadzu Prominence HPLC system.

Acetylation was used on Soda lignin but not on the liquefaction products because it was complex to control the acetylation in the presence of ethanol. The samples, in ethanol from the reaction, were filtered (0.45 µm glass filters) and then diluted in THF (by 1:4 v/v), the same solvent of the mobile phase. 20 µL was injected. The stationary phase was composed of: 1) a Phenomenex Phenogel 5 µm (7.8 x 50 mm) guard column, 2) a Shodex GPC KF-806L 10 µm (8.0 x 300 mm) analytical column and 3) a Phenomenex Phenogel 5 µm 100 Å (7.8 x 300 mm). The samples were separated at 35 ° C with a flow rate of 1 mL/min. The standards used for calibration were polystyrenes. We are aware that polystyrenes and lignin products present different hydrodynamic volumes for a same molecular weight but PS standards were used for sake of comparison with the available literature on lignin liquefaction[31,34,82,84]. The absorbance of the eluted products is presented at 254 nm (Shimadzu SPD-20A). Data were collected and analyzed with LabSolutions software.

2.3.3. - MALDI-TOF MS

Lignin and liquefaction products (in ethanol) were analyzed by matrix-assisted laser desorption/ionization (MALDI) time of flight (TOF) mass spectrometry (MS) (Bruker Ultraflex

II, 355 nm Nd:YAG laser, ~60µm spot diameter, ~ 107 W cm-2 at 50% power). The method was established according to previously published protocols[85]. For calibration of the mass spectrometer, the polyethylene glycol (PEG 600) mixed with 2,5-dihydroxy benzoic acid (2,5 DHB) matrix was used. A saturated 2,5 DHB solution (30 mg mL^{-1} in methanol/water 50/50) was added to the different lignin-derived solutions (sampled directly from the autoclave, in ethanol, see supplementary materials for more details).

After homogenization of the solution, it was deposited dropwise (~10 µL) onto the instrument sample holder in distinct spots. Deposit of collected samples but without DHB matrix were also analyzed for comparison. 2,5 DHB was shown to be needed in order to reduce fragmentation and aggregation[56,58,82,85]. Only the MALDI results are presented in this paper. The reported mass spectra were obtained in positive ion detection mode and are the sum of 1000 individual mass spectra (200 shots on 5 different locations on the same spot).

The effect of laser energy has been studied as well as the effect of lignin concentration in DHB. Only ions in the 0 to 1800 m/z range were detected.

2.3.4. - UV spectroscopy

UV-visible absorption spectra were recorded on a UV-3600 double beam spectrophotometer (Shimadzu, Marne la Vallée, France). A spectral range from 200 nm to 500 nm and scan speed of 100 nm min^{-1} were selected with lamp change at 340 nm. The fluorescence spectra were recorded on a Fluorolog FL3-222 spectrofluorometer (HORIBA Jobin Yvon, Longjumeau, France) equipped with a 450 W Xenon lamp, and a UV-Visible photomultiplier R928 (HAMAMATSU Japan). All spectra were measured in a four-faced quartz cell. Fluorescence spectra were obtained with right angle detector position for both emission and synchronous acquisitions. Emission acquisition was performed with excitation wavelength of 275nm and a slit of 2nm for a spectral range of 280nm to 530nm. Synchronous acquisition was performed with a constant wavelength offset of 20nm in the spectral range from 250nm to 500nm. The 20nm offset has been selected based on previous work.[69,79]

The samples were diluted in ethanol until the absorption wavelength at 275nm was approximately 0.2, in order to avoid self-absorption effects.[69,86] For this purpose, the solutions sampled from lignin liquefaction (10g of lignin in 200mL ethanol, 50g lignin equivalent/L) were diluted 1000 or 2000 times in ethanol. Therefore, the concentration of analyzed solutions is in the range of 25-50mg lignin equivalent/L ethanol for UV analysis.

All the synchronous fluorescence spectra are presented at the same absorbance.

The whole procedure (including dilution, scan acquisition and treatment of data) lasts only about 15 minutes.

3. - Results

3.1. - Analysis of lignin liquefaction products by conventional methods

3.1.1. - Analysis of oligomers by NMR

Oligomers were isolated after the 4 hours liquefaction of lignin and characterized by NMR (presented in supplementary Material). The method of oligomers fractionation from the ethanol solution is also presented in supplementary material.

NMR characterization of the oligomers demonstrates that conjugated ether bonds are even lower (not detected) than in Soda lignin. Similar findings were shown for pyrolytic lignin from wood pyrolysis.[87] The "chemical severity" of 1) lignin extraction from biomass (by the Soda process) and 2) lignin liquefaction induces a complete conversion of ether bonds. Indeed, it is well known that lignin depolymerization induces a significant reduction in the number of the main ether linkages between lignin units: resinol structure (β-β/α-O-γ), phenylcoumaran (β-5/α-O-4) and β-O-4 structure.[37,88,89] The rupture of ether bonds leads to the formation of very reactive free phenolic hydroxyl groups (through radical or charged species) [33,37] and chains, unsaturated side chains, which both participate in condensation reactions[37,90]. The condensation reactions are favored by the proximities of fragments/moieties within the rigid lignin frame. This repolymerization leads to a more condensed structure, described as a char-like structure with fused aromatic rings[37,91], by different chemical mechanisms: vinylcondensation, quinone methide, radical coupling[91,92]. The mass of char has been analyzed (see supplementary material). Pt/C catalyst considerably reduces char formation compared to the experiment without catalyst in agreement with Kim et al.[30]. Pt/C also reduces the mass yield in precipitated oligomers. Therefore, Pt/C seems to inhibit some condensation reactions.

3.1.2. - Monomers quantification by GC/MS-FID

Chromatograms, reproducibility and a complete list of the monomeric products quantified by GC/MS-FID are presented in supplemental material. Figure 1 displays the total mass yield in monomers and the yield of some major selected species for liquefaction with and without catalyst (at the end of the liquefaction, after 4h at 250°C).

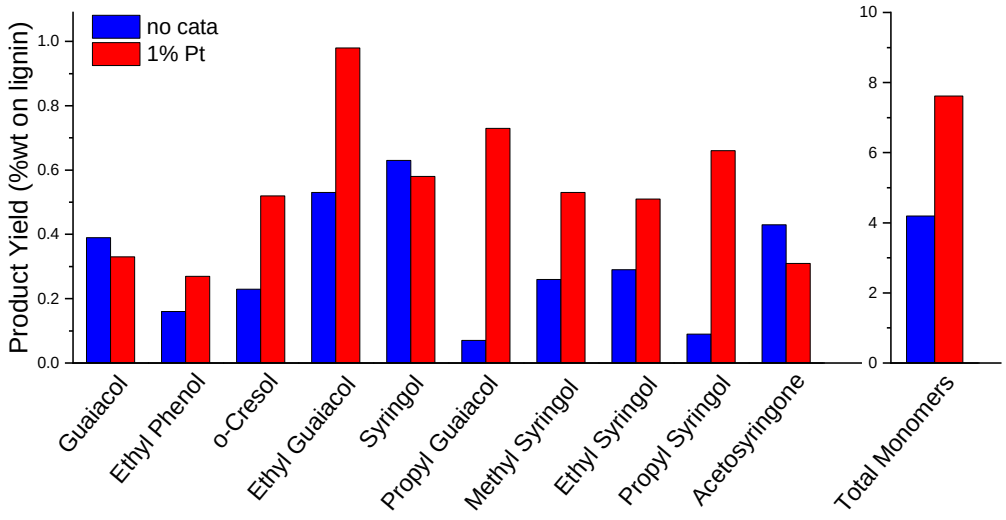

Figure 1 Yield (wt. lignin based) for the principal products after 4 hours of reaction, with and without catalyst.

The catalyst has a clear influence on the monomeric production. It doubles the total monomers (from 4 to 7.8wt%). To the best of our knowledge, Kim et al. has presented the closest conditions to ours (same lignin, ethanol, same catalyst, same load 20wt.%).[30] Their monomer mass yield (8.1wt.%) is very similar to our analysis despite a higher temperature and shorter residence time (350°C-40min, 250°C-4h, in our case). Monomer yields could be further increased by a decrease in catalyst load and by optimization of liquefaction conditions (reduction secondary reactions). This is due to excessive catalyst load inducing unwanted side reactions.[30]

The major monomers are alkyl methoxy-phenols, in close agreement with Kim et al.[30]. Pt/C promotes considerably the formation of ethyl- and propyl- guaiacol, and methyl-, ethyl- and propyl- syringol. Kim et al. also noticed the same remarkable increase of alkylphenols with the catalyst (under their Pt-20% condition).

Figure 2 presents the evolution of some selected monomers as a function of time for both catalyzed and not catalyzed conditions.

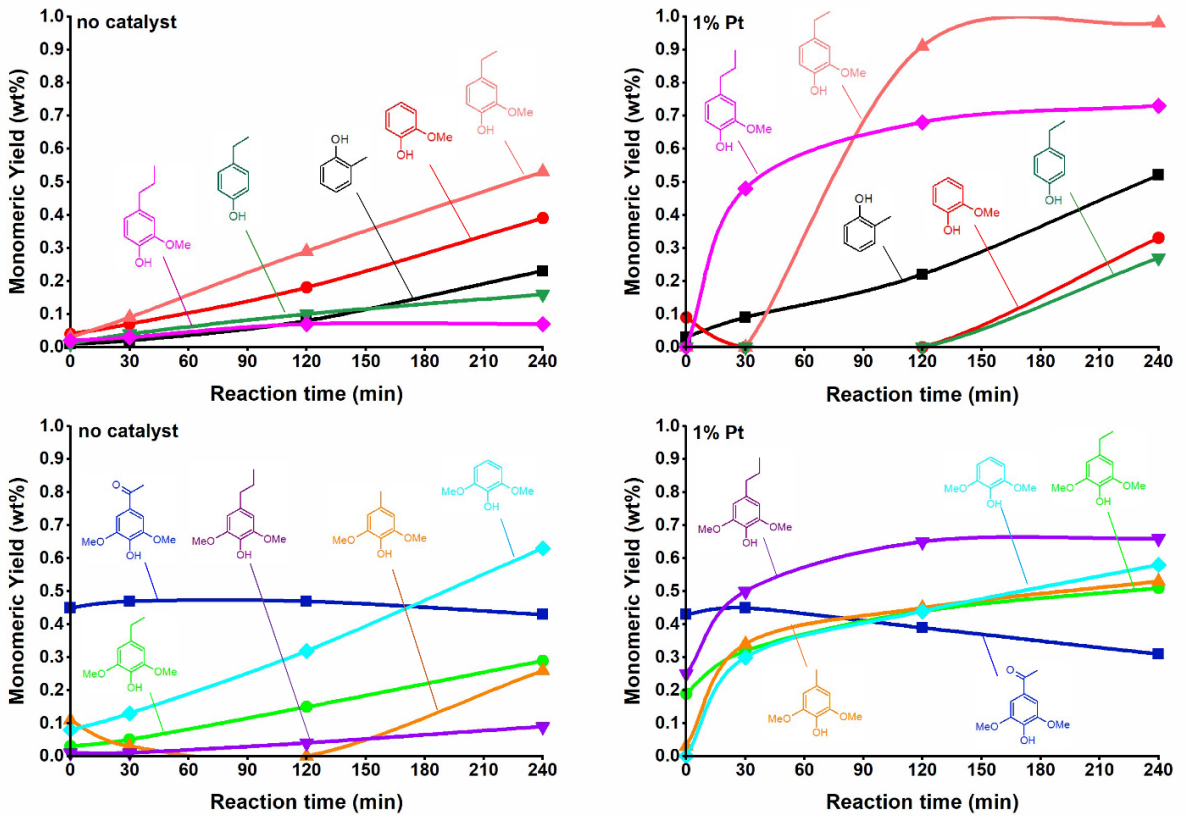

Figure 2 Monomers mass yields (based on lignin mass) by GC/MS-FID as a function of the time of reaction.

Without catalyst, the main monomers are progressively formed up to 4hours time on stream, except acetosyringone which is formed in the earlier step.

Pt/C significantly promotes the yields and the formation rates of alkyl phenols, such as ethyl- and propyl- guaiacol and of methyl-, ethyl- and propyl- syringol. These compounds are formed much earlier in the first 30 minutes' time on stream (except ethyl guaiacol) compared to results without catalyst.

The NMR analysis of the isolated oligomers demonstrates a complete rupture of ether bonds in oligomers even without catalyst (only with ethanol). The oligomers may be formed from homogeneous conversion in supercritical ethanol with a poor participation of the heterogeneous catalyst. Indeed, the Pt/C catalyst exhibits a high surface area of about 1100m^2/g (Pt/activated carbon) mainly due to micropores (<2nm).[30] Lignin macromolecules are unlikely to be converted within these pores due to mass transfer limitations. The important yield in alkylphenols with the catalyst may be explained by a promotion of C-C bond conversion in oligomers. Furthermore, Pt/C exhibits a high surface area which promotes the

adsorption/desorption of hydrogen atoms.[30] Therefore, Pt/C may also promote the transfer of H atoms to stabilize the broken C-C bonds and form more stabilized monomers. This mechanism is consistent with a lower char and oligomer yields with Pt/C (see supplementary material).

It is interesting to note that acetosyringone presents the same yield in the first 30min, with and without the catalyst. It may be formed by the early conversion of the few ether bonds present in Soda lignin. This finding is in excellent agreement with a study on model compounds under similar conditions.[93] It has been shown that the cleavage of the β-O-4 linkage is fast (< 15 min) and leads to the formation of acetophenone species (like acetosyringone in our case) through H-transfer hydrogenolysis of an intermediate pentacyclic ether bond.[93]

This similar feature of early acetosyringone formation with and without catalyst consolidates our discussion on the conversion of ether bonds without an important action of the catalyst (as supported by oligomers NMR analysis). Then, the conversion of acetosyringone is slightly promoted by the catalyst after 30min time on stream.

Cresol, guaiacol and ethyl-phenol are mainly formed after 2 hours time on stream. They may be formed by secondary reactions (like partial dealkylation) of primary monomers. The presence of cresol exemplifies an interesting feature of this catalytic system (ethanol and Pt/C): the methylation of the aromatic ring. This reaction is of high interest in increasing the carbon balance in monomers.

Some carbohydrate-derived compounds were detected in small yields (see supporting material), possibly formed by the conversion of lignin-carbohydrate linkages or residual carbohydrates (as evidenced by our NMR analysis of lignin). At low reaction time some ethanol-derived products are detected (1-Butanol; 1,4-Dioxin,2,3-dihydro; 1,1-diethoxy-Ethane; Butanoic acid, ethyl ester; 1,1-diethoxy-Butane; 2,4,6-Cyclopentanone,2-ethyl; 2-ethyl-Cyclopentanone; see supporting material for more details). In addition to monomeric phenols, low yields in esters and acids (like butanedioic acid, diethyl ester) are observed. They are probably the result of recondensation reactions between low molecular compounds with C-C or C-O bonds in lignin–oil, as shown in previous studies [84,94,95].

3.1.3. - Analysis by GPC-UV

The mass-average molecular weight (Mw) of pristine lignin was 3600Da and the isolated oligomer fraction was 800Da. We are aware that our GPC method may under-estimate the real molecular weight[50] but it allows a more direct comparison with other works using the same

GPC method.[30,82] Lignin oils (compounds soluble in ethanol) were sampled at specified reaction times, then diluted in THF and analyzed by GPC (Figure 3).

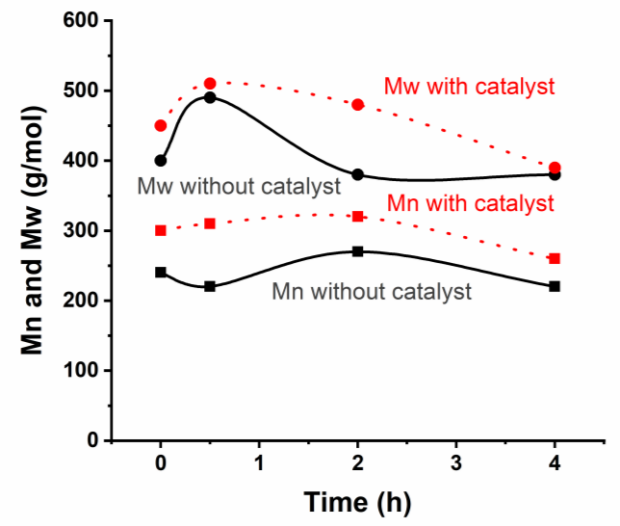

Figure 3 Mw and Mn of lignin oils from GPC analysis, with and without catalyst, as a function of reaction time.

All GPC curves exhibit only one major peak with a unimodal distribution (see Supplementary Material). Our columns and calibration method were not tailored for a separation between monomers, dimers, tetramers, etc. The catalyzed and uncatalyzed experiments presents a similar evolution on Mw and Mn (figure 3) with relatively stable Mw and Mn. Mw and Mn are slightly higher for catalytic liquefaction. The Mw and polydispersity index (PDI, Mw/Mn) of lignin oil found by Kim et al.[30] were 595Da and 1.3 (with 20% wt. Pt/C). In our case (with catalyst), Mw is between 400 and 500Da, with a constant PDI of 1.5. The oligomers (Mw ~800Da) extracted by acid precipitation represent a heavy part of the GPC curve of lignin-oil.

Although Mw of lignin-oil is relatively stable across reaction sampling times, the monomer yields increase as analysed by GC/MS. This finding displays the concurrent depolymerization of the oligomeric pool (formation of monomers) and recondensation (formation of oligomers and char), as previously proposed by several authors.[30,33]

3.1.4. - MALDI-TOF MS analysis

Figure 4 presents the MALDI-TOF mass spectra of two samples (without catalyst and with Pt/C catalyst) at two reaction times (0 and 4 hours) for the same liquid samples (species soluble in ethanol) as the ones analyzed by GC/MS and GPC. MALDI ionization conditions have been optimized (see supporting material).

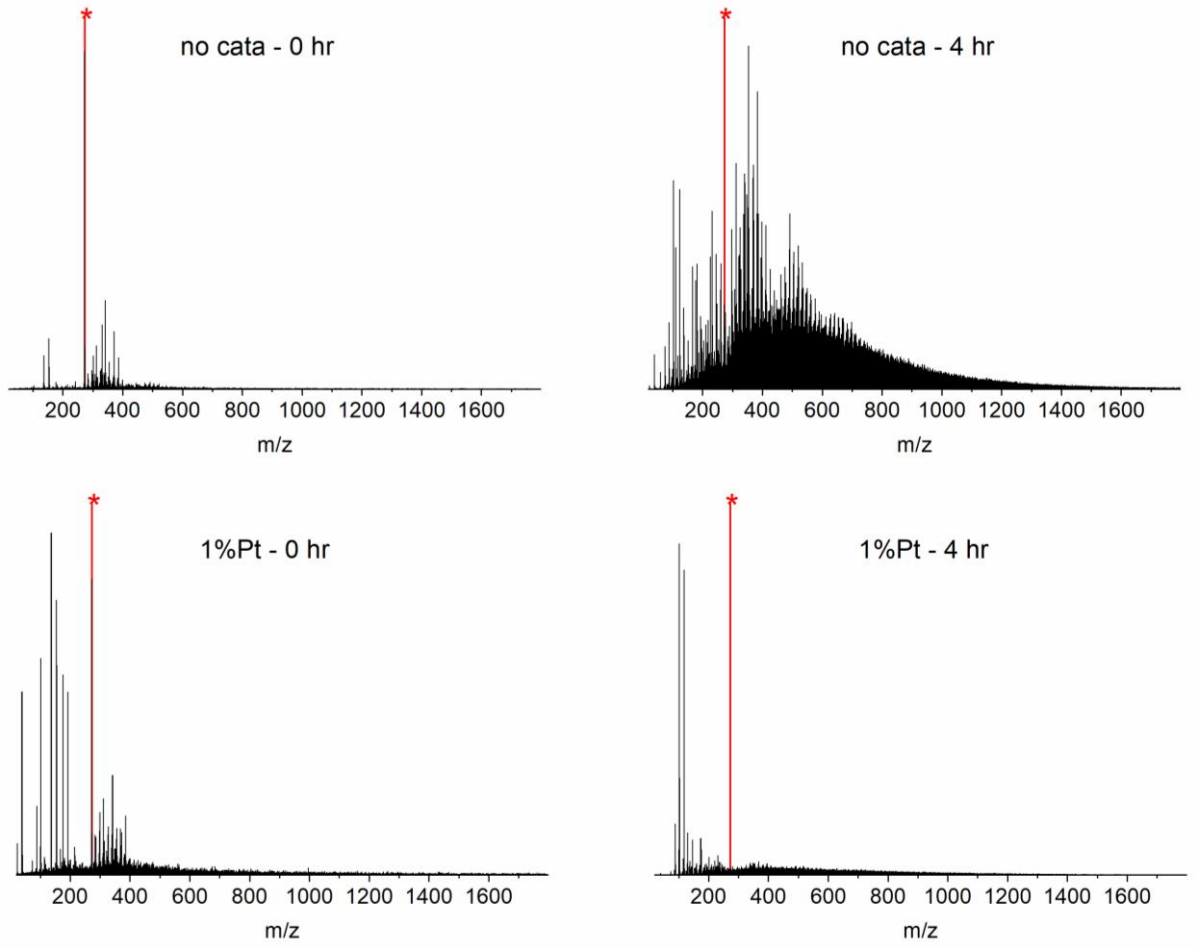

Figure 4 MALDI-TOF spectra of lignin oils, at initial time (0h at 250°C) and 4 hours for both catalytic and non-catalytic reactions (is at m/z 273, the peak of DHB matrix).*

The MALDI-TOFMS spectra for the other reaction time and for the raw lignin are presented in Supplementary Material.

Soda lignin presents only a weak ionization and featuring mainly peaks of about 400 Da, regardless of ionization optimization attempts (supplementary material). It was not possible under our conditions to analyze the molecular weight of lignin by MALDI-TOF MS. This finding is consistent with previous work.[55] Indeed, m/z higher than 2000 are poorly resolved in previous work on MALDI-TOF analysis of lignin. MALDI is rather used for lignomic analysis of oligomers[57,58] with higher resolution mass spectrometers (resolution in the range of 200000) than for TOFMS.

DHB has been shown as a good matrix for the detection of oxygen moieties in lignin oligomers.[56] For this reason, we have selected this matrix and optimized ionization conditions on lignin-oil analysis.

Figure 4 shows that a weak signal was detected between m/z 300 and 400 for the uncatalyzed experiment on the initial sampling (0h at 250°C). After 2h, a bimodal distribution is detected, composed of a primary ion pool from m/z 100-250 and secondary pool of 250+. The signal reveals ions up to 1200Da. The catalyzed experiments present a very different behavior. First (at 0h) a bimodal distribution is observed with ions detected between 100 to 200 Da (monomers) and 300 to 400Da (dimers). From 2 hours time on stream, the MALDI signal exhibits mainly a unimodal distribution centered on monomers (100-200 Da).

In order to better compare MALDI-TOFMS analysis with other methods, the sum of ion intensities was determined for 2 groups: 1) from 0 to 240Da (the biggest molecule quantified by GC/MS) and 2) for ions bigger than 240 (up to 1800 Da). Figure 5 displays the total ion current (TIC) for these 2 groups.

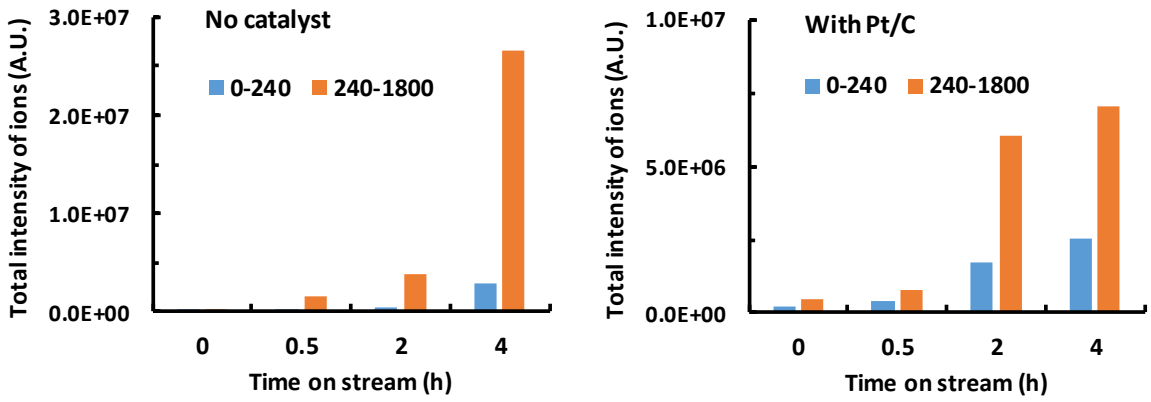

Figure 5 Integration of the signal of ions detected by MALDI-TOFMS in lignin oils from 0 to 240Da and 240 to 1800Da as a function of reaction time, without and with catalyst.

Figure 5 shows that more low molecular weight ions (< 240) are detected with Pt/C catalyst. An important signal in the range of 240-1800Da appears from 2 hours time on stream for both conditions (with and without catalyst). This signal may result from the concurrent depolymerization of lignin forming monomers and oligomers in competition with condensation reactions. This integration of all m/z peaks does not depict the high intensities of some major peaks for Pt/C experiments (with m/z lower than 200), which is overwritten by the sum of numerous ions with a small individual intensity.

Mw and Mn were also derived from MALDI-MS signals (figure 6).[55]

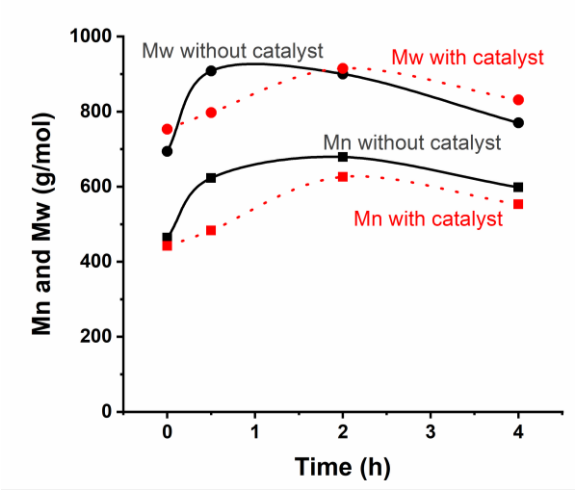

Figure 6 Molecular weight distribution (Mw and Mn) of lignin oils obtained by MALDI-TOFMS as a function of time on stream (at 250°C), with and without catalyst (Pt/C).

Mw and Mn of lignin oils obtained by MALDI are relatively stable across reaction sampling times and similar for both conditions (with and without catalysts, see figure 6). This relative stability is consistent with GPC analysis. However, the Mw determined by MALDI are higher (800-900 Da) than those determined by GPC (400-500 Da). The PDI is similar to GPC analysis (~1.5 for Pt/C experiment). It is possible to notice a slight increase in Mw after 30min of liquefaction followed by a small decrease until 4h. This feature may be assigned to secondary condensation reactions followed by a slow conversion of condensed oligomers.

3.2. - Analysis of lignin products by UV spectroscopy

3.2.1. - UV spectroscopy of model compounds, lignin and isolated oligomers

UV spectroscopy was initially carried out on nine complementary model compounds: phenol, guaiacol, syringol, catechol, iso-eugenol, 1-naphthol, sinapyl alcohol, coniferyl alcohol and guaiacyglycerol-β-guaiacyl ether, miming a β-O-4 dimer. They were chosen for their various side chains as good surrogates of lignin moieties.

First, the UV absorption of these model compounds was studied as well as the absorption of lignin and isolated oligomers. The results are presented in supplementary material.

Lignin, its monomers and oligomers present specific absorption spectra due to the presence of different chromophores as aromatic rings, alkenes and oxygenated chemical groups (ether,

carbonyl or hydroxyl)[75,86,96], which may be conjugated. These chromophores are also fluorophores according to the high electronic density of conjugated systems including aromatic rings.

The UV absorption spectra present mainly two absorption bands (for all analyzed compounds): 1) a first one at ~210 nm corresponding to a $\pi \rightarrow \pi^*$ transition in the aromatic ring and 2) a second one at ~275 nm associated to free and etherified hydroxyl groups, involving a lone pair of one of the oxygen atoms[67].

In lignin and model compounds the 210-220 nm absorption wavelength can be attributed to the methoxylated phenol ring. It was also shown that free and etherified hydroxyl groups contribute significantly to the characteristic absorption maximum around 280 nm.[67,97] Lignin and oligomer absorption present a broader absorption peak than model compounds due to the higher complexity in different chemical moieties. For this reason, UV absorption does not show high selectivity for discrimination of the chemical composition of lignin products, and therefore, UV fluorescence has been studied.[67]

All the studied compounds absorb at 275nm, so they were excited at 275nm to record the fluorescence spectra (see supplementary material).

UV fluorescence shows important different peak maxima and intensity depending on the functional groups present in the model compounds. This is in agreement with previous reports that indicate considerable sensitivity of UV fluorescence spectroscopy to the degree of substitution at adjacent positions on the ring, especially when such substitution involves a series of electronegative groups.[75,98]

Quantum yields were determined based on these fluorescence spectra excited at 275nm following the recommendations of IUPAC with quinine sulfate as reference[99]. Quantum yields are presented in the supporting material. They are higher than 20% for some monomers (such as phenol, guaiacol, eugenol) demonstrating the very high sensitivity of UV fluorescence for our compounds. The quantum yield depends on functional groups present on the aromatic ring. For instance, it decreases significantly for syringol (compared to phenol and guaiacol). Substitutions with electron donating groups like –OH or –OR induces a red shift in both absorption and fluorescence spectra. Nevertheless, the presence of lone pairs of electrons on the oxygen atoms does not change the nature of the π-π^* transitions of the aromatic system because these lone pairs are directly involved in π bonding in the molecule.[100] If methoxy groups are twisted out of the plane of the aromatic ring, for steric hindrance reasons, the degree

of conjugation of the system is decreased. Hydroxyl groups are nearly coplanar.[100] The distortions in coplanarity increase as the number of methoxy groups increases from zero (phenol, H) to one (guaiacol, G) to two (syringol, S). This mechanism explains the decreased fluorescence quantum yield of S compared to H and G.[98]

The low quantum yield of vanillin can be explained by the aldehyde group which leads to a n $\rightarrow \pi^*$ transition of low energy.[75]

Eugenol and naphthol exhibit a high quantum yield due to the high number of C=C bonds in the side chain and/or of the aromatic ring. The model dimer (guaiacylglycerol-beta-guaiacyl ether-GGGE) also presents a high quantum yield due to its 2 aromatic rings.

After 1) absorption, and 2) fluorescence at a constant excitation (275nm), we have studied 3) the synchronous fluorescence of our molecules. In synchronous fluorescence spectrometry (SFL), excitation and emission wavelengths vary simultaneously separated by a constant offset. Compared to conventional fluorescence at fixed wavelength, SFL shows much higher spectral resolution for complex mixtures by selecting the appropriate excitation/emission offset according to the molecular structure of the analytes.[68,70,79,80]

Figure 7 presents the synchronous spectra for the model compounds, lignin and isolated oligomers.

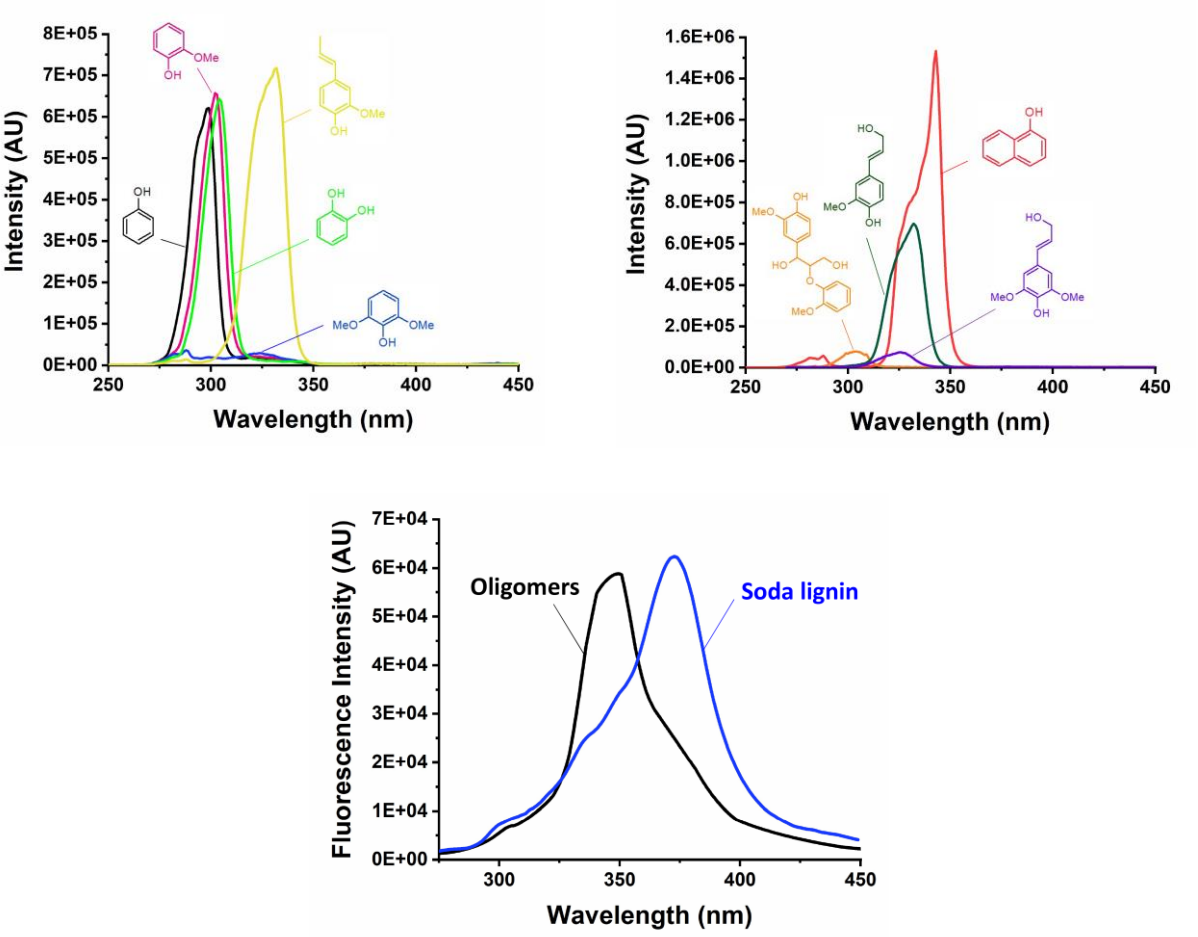

Figure 7 Synchronous UV fluorescence with 20 nm offset of model compounds, lignin and oligomers (diluted in ethanol)

It is well known that the emission peak in SFL is related to the number of undisrupted conjugated bonds in molecules. For instance, for aromatic hydrocarbons (like PAH), SFL peaks are related to the molecular weight of the molecules.[70,79,80] To the best our knowledge, we present here the first rationale on the synchronous emission on lignin surrogates.

The offset between excitation and fluorescence analysis (20nm) has been selected based on previous work.[69,79] This offset has shown an excellent selectivity to discriminate aromatic molecules in complex liquids.

Figure 7 shows that aromatic monomers with hydroxyl and methoxyl groups emit at about 305nm (phenol, guaiacol, catechol). Aromatic monomers with propyl side chains (like iso-eugenol, coniferyl alcohol, sinapyl alcohol) emit at about 330nm. This finding is consistent with the known fundamentals of fluorescence. Conjugated molecules present an alternation of

simple and double bonds where the π electron cloud is delocalized. The presence of two free pairs of electrons on the oxygen atom contributes to this π electron cloud delocalization. The increase in the number of conjugated bonds leads to a decrease of the energy between π and π*. Consequently a red shift (bathochromic) is observed in absorption and emission spectra[101–103]. On the contrary, smaller and less conjugated structures lead to a blue shift (hypsochromic) of absorption and emission spectra[101].

Naphthol is more conjugated molecule than phenol and therefore it emits at 343nm (vs. 300nm for phenol). GGGE emits at 305nm, in a similar range as aromatic monomers (like guaiacol). This fact can easily be explained: the two aromatic rings in GGGE are connected with a β-O-4 bond which interrupts the conjugation of the molecule. If the conjugation is interrupted and the electron π cloud is not in resonance, then the spectra are not redshifted as expected for conjugated molecules (as example for naphthol). Instead, the absorption and fluorescence spectra appear as the ones of a monomeric compound. However, an oxygen linkage between two conjugated moieties does not interrupt the fluorescence due to the 2 lone pairs of electron of the oxygen.[100] Consequently, bonds like 4-O-5 or C_{arom}-O-C_{arom} in lignin do not interrupt the conjugation of the aromatic rings.

The synchronous fluorescence of lignin is presented on figure 7. To the best of our knowledge, we present for the first time a UV synchronous analysis of lignin with a 20nm offset. Lignin can present conjugated ether bonds (like 4-O-5, C_{arom}-O-C_{arom}), unconjugated ether bonds (like β-O-4) and conjugated bonds (C_{arom}-C_{arom}, C=C). Fluorescent emission of lignins is attributed to conjugated carbonyl, biphenyl, phenylcoumarone and stilbene groups.[75,97] The broad nature of the fluorescence spectra is due to the presence of many different fluorophoric species present in the lignin macromolecule.[75,97]

In the raw Soda lignin used in this work, the unconjugated bonds (like β-O-4) are very low (see NMR analysis in Supplementary Material). Up to 90% of aromatic rings are linked by C-C bonds (and not by ether bonds). This feature explains the red shifted signal of lignin at about 375nm (see figure 7). Based on our GPC analysis of this lignin (Mw ~3500 Da), this peak at 375nm may correspond to the fluorescence of about 20 aromatic units which are connected without important disruption of the conjugation.

The oligomers isolated from the ethanol solution after lignin liquefaction (after 4h at 250°C) were also analysed by UV fluorescence (see figure 7). NMR analysis has revealed a complete conversion of the few ether bonds initially present in lignin. Oligomers exhibit a peak maximum

at 350nm, which are blue shifted compared to lignin (375nm) due to their lower molecular weight. The high conjugation nature of oligomers and lignin as analyzed by NMR is consistent with our UV fluorescence analysis. Indeed, peaks at 350nm and 375nm present a bathochromic (red) shift compared to the monomers (at about 300-320nm). GPC analysis of oligomers showed a Mw of about 800Da. The oligomers (fluorescence peak at about 350nm) may correspond to aromatic clusters in a range of 4-6 aromatic rings.

Figure 8 summarizes the emission peak maxima for model lignin compounds, lignin and oligomers for a synchronous excitation with 20 nm offset.

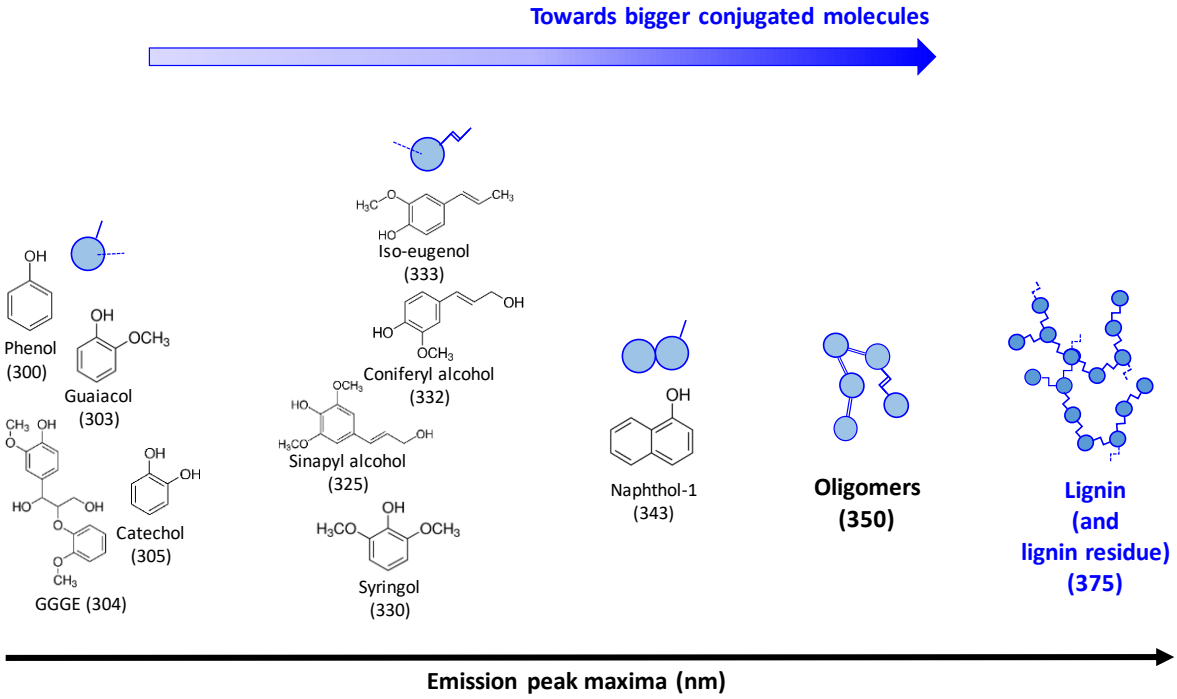

Figure 8 Emission peak maxima in synchronous excitation fluorescence (20 nm offset) for model compounds, oligomers and lignin, diluted in ethanol.

3.2.2. - UV fluorescence of lignin liquefaction products

Based on analysis of model compounds and lignin, we have studied the UV fluorescence of liquefaction products. The goal was to depict important differences between catalytic and non-catalytic experiments based on UV fluorescence. The results of the synchronous fluorescence spectra (20nm offset) are plotted for the different reaction times in figure 9.

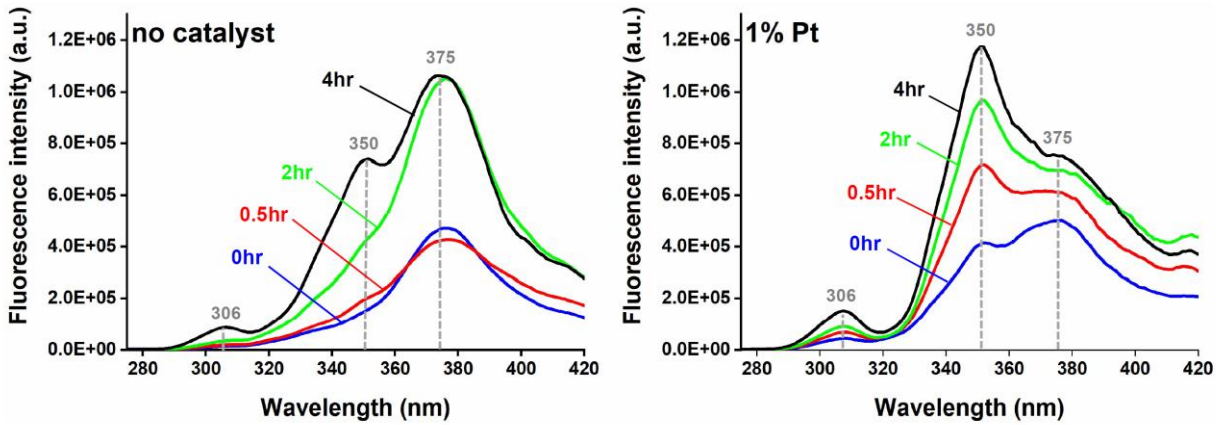

Figure 9 Synchronous Fluorescence (offset 20nm) for different reaction time: a) without catalyst b) synchronous fluorescence with catalyst.

All the spectra from liquefaction products display three main peaks (or shoulder) at 306, 350 and 375 nm, with and without catalyst. These 3 peaks are consistent with the previous section. The first peak can be assigned to monomers, mainly to (alkyl) phenols and guaiacols in agreement with the UV signals of model compounds and with the GC/MS analysis. The following peak (or shoulder) at 350nm can be assigned to oligomers and the last peak at 375 nm to the heavy "lignin residue". This last peak at 375nm accounts for big conjugated clusters derived from lignin conversion ("lignin residues") which are still soluble in ethanol.

The monomers (306nm), oligomers (350nm) and lignin-residues (375nm) peaks increase as function of time for both conditions displaying the depolymerization of lignin. The intensity of monomer and oligomer peaks is higher for catalytic conditions (figure 9). The spectra from non-catalytic conditions remain primarily made up by the heavy fraction. The Pt/C catalyst presents an important impact on the depolymerization of lignin based on UV fluorescence.

We have conducted a deconvolution in order to better interpret the UV spectra. Curve deconvolution was carried out using Origin software (Originlab, Northampton, MA, USA) with Gaussian peaks. Peaks were deconvoluted at fixed wavelengths of 306, 350 and 375 nm in line with our discussion. An example of specific deconvolution curve is given in supplementary material.

The deconvolution allows the determination of indicators for assessing lignin depolymerization. We propose the following indexes as:

$$DI = \frac{A_{306}+A_{350}}{A_{306}+A_{350}+A_{375}} \qquad (1)$$

$$MPI = \frac{A_{306}}{A_{306}+A_{350}+A_{375}} \qquad (2)$$

Where:

DI is depolymerization index which describes the relative distribution between depolymerized products (monomers and oligomers at 306 and 350nm respectively) and the total area of the UV spectra;

MPI_{fluo} is a monomer products index, which assess for the relative distribution in monomers;

A_{306} is the area of the deconvoluted peak at 306nm;

A_{350} is the area of the deconvoluted peak at 350nm;

A_{375} is the area of the deconvoluted peak at 375nm.

These indexes assess semi-quantitatively the relative distribution in monomers (peak at 306nm) and depolymerized products (monomers at 306nm and oligomers at 350nm).

A similar approach was proposed by Garcia-Perez on wood bio-oil.[76] It is interesting to note that the Garcia-Perez et al. analysis dealt with a different bio-oil, produced from wood fast pyrolysis and not by lignin liquefaction, but it also exhibited 3 main peaks associated to different size of aromatic clusters (mainly from lignin pyrolysis in the wood, in the case of Garcia-Perez et al.). Deconvolution was also proposed on coal liquids but with a higher number of fitting peaks.[68] Here these 3 peaks have been defined as a sufficient number of different sub-groups of products which are supported by our analysis of individual isolated compounds (monomers, oligomers and lignin).

The evolution of these indexes upon the reaction time is given in Figure 10.

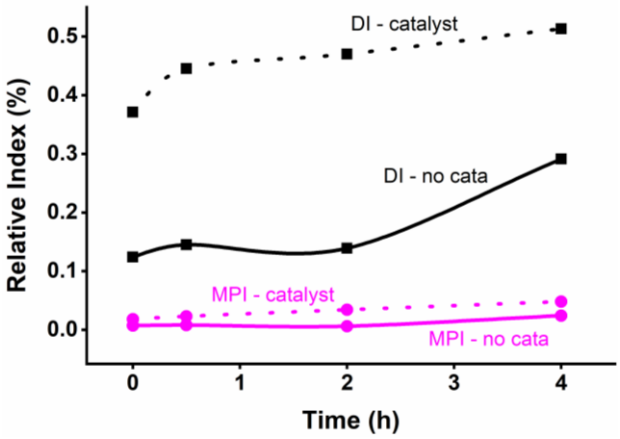

Figure 10 Depolymerization index (DI) and monomeric products index (MPI) obtained by UV fluorescence analysis as a function of liquefaction time (at 250°C), without and with catalyst (Pt/C).

The relative fraction in smaller molecules (DI and MPI) increases with the reaction time. The 2 indexes are higher for the catalytic conditions, most notably for DI. The DI increases much faster (after 0.5hour) and then stays relatively stable for the catalytic conditions. The Pt/C catalyst promotes the formation of oligomers and the conversion of heavy lignin residue. The DI index increases after 2 hours for the uncatalyzed experiment. The MPI index stays relatively small. This analysis reveals that heavy residues are enhanced without catalyst. These soluble heavy residues are probably precursors of solid char. This finding is consistent with the mass of char quantified at the end of the experiment which is much higher for the uncatalyzed experiment (see supplementary material).

These results on UV fluorescence are compared with the other methods in the next section.

4. - Discussion on the complementarity between UV fluorescence and GC/MS, MALDI-TOFMS and GPC analysis

Figure 11 supports the discussion presented in this section.

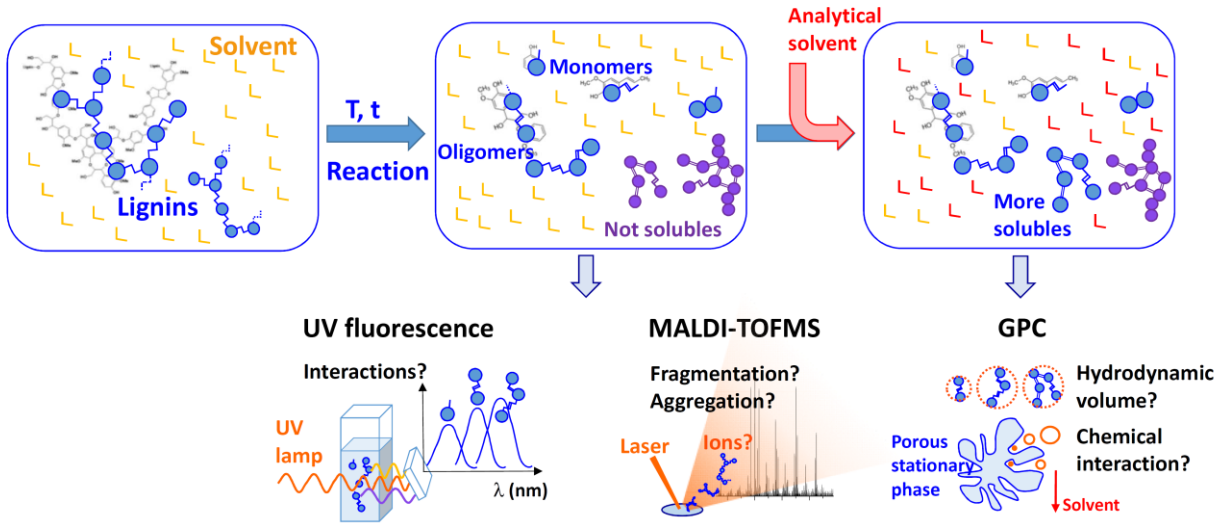

Figure 11 Simplified representation of lignin products in solution and of the analytical methods assessed in this work.

First, lignin is a complex continuum of molecules of various molecular size and chemistry. These macromolecules interact with the solvent (ethanol in our case). Upon liquefaction, they form another continuum of molecules with monomers, oligomers and heavy residues which are partly soluble.

UV fluorescence, MALDI-TOFMS and GC/MS are used directly to analyze this liquid, whereas another solvent (THF) is added for GPC analysis (figure 11). THF may promote the solubility of some big molecules which were in suspension (but not solubilized) in the solution and with a physical dimension smaller than the pores of the filter.

Concerning the average molecular weight of the lignin oil, we have seen differences between GPC and MALDI. This is probably due to calibration issues of the GPC method.[50]

Indeed, GPC separates the molecules based on their hydrodynamic volume in a given solvent (see figure 11). In the case of lignin and its liquefaction products, this volume is different than

the standards used for the molecular weight calibration. [8,50,51,104] Moreover, chemical interactions with the column phase make GPC potentially an inaccurate technique for determining the molecular weight of lignins and products.[49,50,104,105] Valuable efforts have been undertaken to better calibrate GPC, most notably with synthetized oligomers[106] and multi-angle light scattering (MALS) detector.[104] GPC remains as of yet poorly resolved for species smaller than about 1kDa.[49,50] It does not well tailor for the characterization of oligomers. Other HPLC methods must still be looked into for providing a better separation and quantification of oligomers.[58]

Despite the discrepancy between GPC and MALDI, these 2 methods show that the Mw stays relatively stable throughout liquefaction time (figures 3 and 6). This result is also confirmed by the UV fluorescence analysis. Indeed, the peak maxima of the 3 main "families" of products remain at the same wavelength (306, 350 and 375nm) upon reaction time (see figure 9). Therefore, the average molecular weight of soluble conjugated species does not change significantly during liquefaction.

Based on these 3 techniques, lignin seems to produce quickly an oligomeric pool and then the conversion of oligomers to monomers seems to be slow (a limiting process).

Figure 12 compares the depolymerization index as determined by UV fluorescence plotted against the integrated intensity of all ions detected by MALDI (from m/z 0 to 1800, total ion current-TIC).

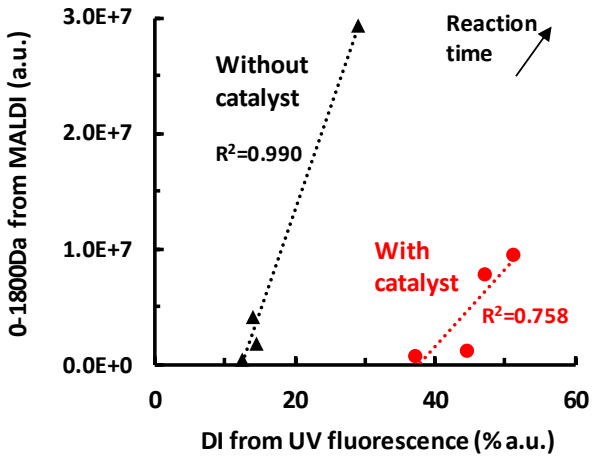

Figure 12 Comparison between the MALDI analysis (integration of all detected ions from m/z 0 to 1800) and the depolymerization index (DI) derived from UV fluorescence for the 8 lignin oils (without and with catalyst, 4 samples upon liquefaction time).

The evolution upon reaction time of the total ion current (TIC) (detected by MALDI, up to m/z 1800) is consistent with the evolution of the depolymerization index (DI) determined by UV fluorescence for the experiments without catalyst (R^2=0.99, see figure 12). The last sampling point (after 4h) produces a very high TIC signal (figure 12) which is not well related to other analyses. The mass spectra presented in figure 4 shows a very broad peaks distribution with a high intensity. UV fluorescence and MALDI are not well correlated (comparatively) for the catalytic experiment (figure 12, R^2=0.76). The point after 0.5h of catalytic liquefaction presents a low TIC which is not related to other reaction times. The TIC displays all species detected by MALDI whereas the DI accounts only for the relative distribution in monomers and oligomers. A part of heavy residues (not accounted for by the DI) may be detected by MALDI.

This discrepancy can be explained by the different fundamentals of each method (see figure 11).

In MALDI-TOF-MS, the analyte is first mixed with a small organic compound (the matrix) and co-crystallized onto a stainless steel sample holder.[107] The irradiation by a short impulse UV laser leads to the desorption and ionization of the analyte [108–110] (see figure 11). The selectivity and the sensitivity of the analysis depends on the matrix and the laser wavelength with respect to the investigated compound. For all these reasons, MALDI results must be interpreted cautiously. Indeed, fragile molecules may be dissociated (mainly by dehydration or decarboxylation) and aggregation process may occur (□-stacking and/or hydrogen bounding)[111]. The ions analyzed by MALDI, in our case on lignin liquids, may be enhanced by the fragmentation of heavier species (as “lignin residue”). Indeed, we observed that MALDI TOFMS of raw lignin generated mainly ion signal in low mass range even though MALDI optimization was performed (laser fluence, matrix/sample ratio). In our operating conditions, ion suppression on the end of the m/z scale might result from poor ionization efficiency of high MW compounds and from the lack of mass resolution. We have checked the high m/z range signals presented in literature. Only unresolved and noisy signals were also detected by previous work on MALDI TOFMS analysis of raw lignin.[112,113] Consequently, common MALDI approaches fail to cover the real mass distribution on the whole broad mass range of lignin and of heavy liquefaction products.[56,57] MALDI or LDI remains an interesting method for oligomer analysis if LDI is combined with high resolution (HR) MS and if careful ionisation conditions are used.[114] (MA)LDI-HRMS can provide the elemental formula of oligomers and even their chemical structure if it is combined with an advanced stochastic modeling approach[57].

The analysis of lighter compounds by MALDI, UV fluorescence and GC/MS is compared in figure 13.

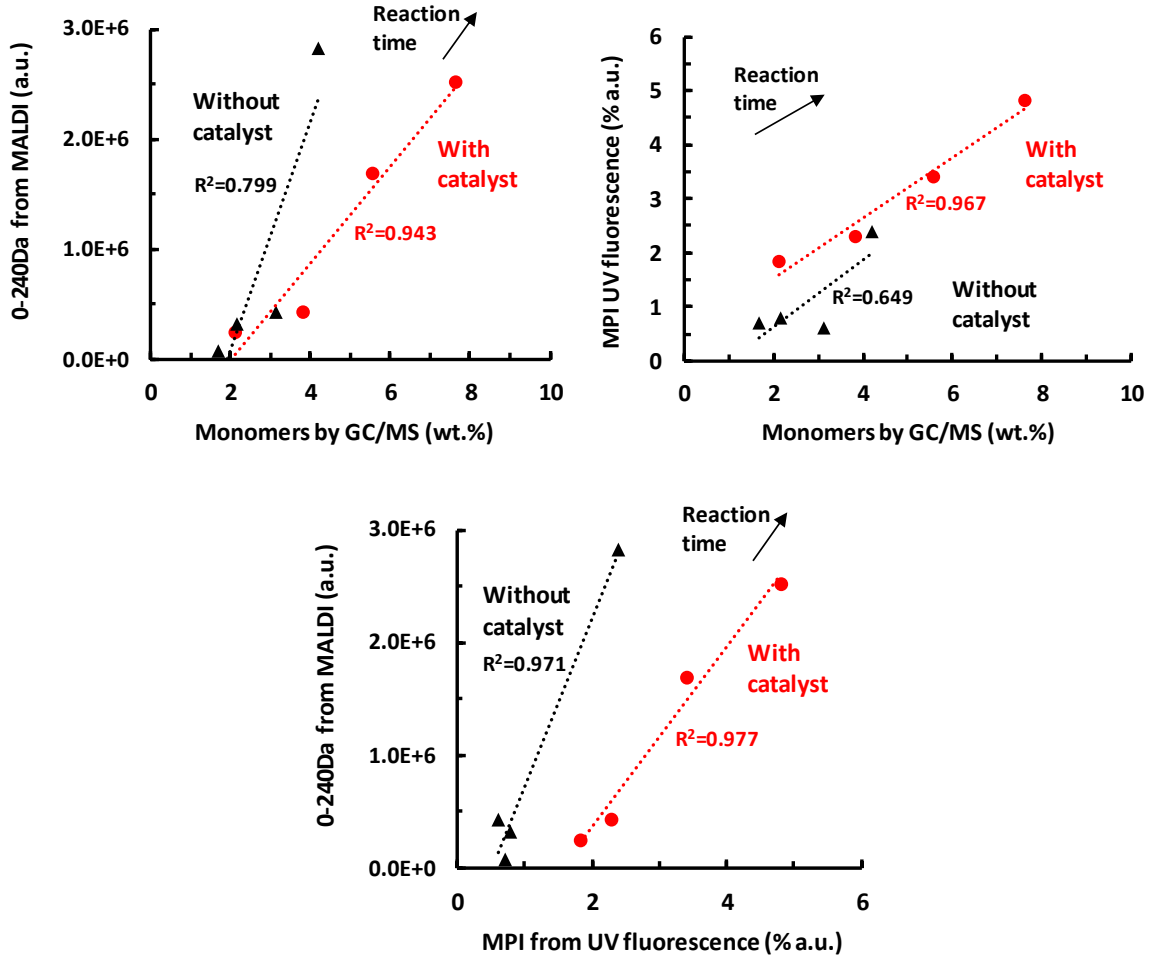

Figure 13 Comparison between low MW species detected by MALDI (m/z 0-240), products quantified by GC/MS (up to 240Da) and the monomers index (MPI) derived from UV fluorescence.

A good correlation is presented in figure 13 between MALDI analysis (m/z from 0 to 240), UV fluorescence (monomer index) and GC/MS, especially for the catalytic liquefaction (R^2 >0.95). The point after 2 hours of uncatalyzed liquefaction is not well related to the others. UV fluorescence is consistent with GC/MS because the major monomers (alkyl phenols) as quantified by GC/MS present a high quantum yield at a fixed emission maximum. Therefore, their signal is well captured by our deconvolution method. GC/MS-FID is the only technique presented in this work which gives a true quantitative mass yield of light products. It is the technique of choice to quantify light species (lower than about 250Da) and to reveal their

molecular structure. Nevertheless, attention must be paid to potential oligomers cracking in the GC injector which may produce monomers and therefore overestimate their yields. This fact has been evidenced on cellulose oil analysis.[115]

MALDI presents some potential pitfalls (as previously explained) but it matches surprisingly well with UV fluorescence.

Fluorescence is the most direct analytical method with less potential side effects. The sample is simply diluted in ethanol. It is not heated (like in GC/MS or in MALDI), not subjected to a high photon flux (like in MALDI) and/or not diluted in another solvent (like for GPC). UV fluorescence is only based on the intrinsic electronic properties of soluble molecules and of the solvent.

Nevertheless, this technique also presents some pitfalls:

1) It requires conjugated molecules without disruption in their conjugation. If the conjugation is disrupted (like in GGGE with □-O-4 linkage), the emission is shifted to lower wavelength and the relative content in small molecules can be overestimated.
2) Big macromolecules with numerous chemical moieties present a broader and less resolved emission peak.
3) The quantum yield ("response factor") is a function of the chemical moieties in molecules. Consequently, UV fluorescence is hardly quantitative if complex liquids with numerous chemical moieties are analyzed without prior separation. This is why "relative distribution" is emphasized in this work.
4) The fluorescence of molecules is impacted by the type of solvent used. Solvents can stabilize the excited state of the fluorophore. This effect becomes larger with increasing solvent polarity, resulting in emission at longer wavelengths.[86]
5) The fluorescence emission of a component may be absorbed by another component (masking or partial masking of one component by others)[116].
6) Intermolecular energy transfer may occur from an excited aromatic molecule to another aromatic molecule[116]. This energy transfer is minimized under our very dilute solutions studied in this work (0.2 absorption at 275nm). Experiments of spiking guaiacol in a naphthol solution demonstrate that no intermolecular energy transfer may occur under our diluted conditions (see supplementary material).
7) Intramolecular energy transfer in a big macromolecule (as oligomers or lignin residues) may also occur from smaller to larger aromatic ring system (in the same

macromolecule). This may result in fluorescence emission at longer wavelength and to an overestimation of big aromatic cluster in the macromolecule[116].

Figure 14 presents a simplified mechanism of lignin solvent liquefaction.

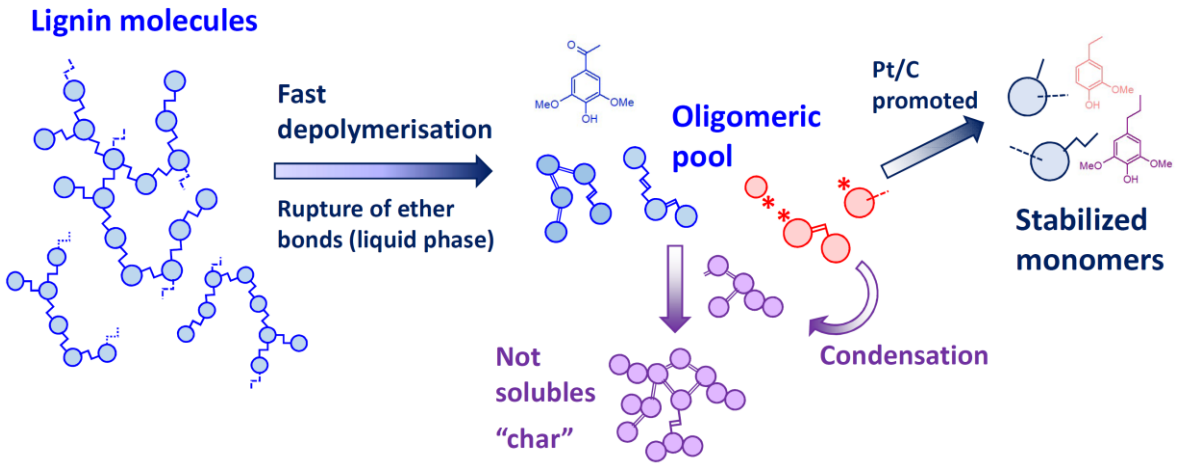

Figure 14 Simplified representation of lignin depolymerization in ethanol based on the complementary methods employed in this work.

This mechanism can be proposed thanks to the complementarity of each method:

1) GPC, MALDI and UV fluorescence show that the average molecular weight of lignin oil stays relatively constant throughout liquefaction reaction time. Therefore, there is a competition between depolymerization of oligomers (production of monomers) and condensation reactions (formation of "secondary" oligomers and char). The conversion of oligomers to monomers seems to be the limiting step.
2) GC/MS gives the evolution of monomers throughout liquefaction time. Alkyl phenols are considerably promoted by the Pt/C catalyst. Pt/C may promote the transfer of H atoms which stabilize the broken bonds and form more stabilized monomers. The early formation of acetosyringone does not depend on the presence of the catalyst. It confirms the fast depolymerization, in the liquid phase, by the rupture of the few □-O-4 bonds present initially in the lignin. This reaction is not promoted by our catalyst.
3) NMR analysis of lignin and oligomers corroborates this finding on the easy conversion of □-O-4 bonds. NMR describes the overall composition of lignin and oligomers and reveals their highly conjugated nature.

4) MALDI and UV fluorescence highlight the relative production of monomers and oligomers throughout liquefaction time.

Other methods may be of interest to get a more complete understanding of lignin liquefaction mechanisms, notably: NMR of insoluble species[117]; direct HRMS combined with lignomics-based approach to reveal the chemical structure of oligomers[57]; LC/MS to quantify oligomers main species; and catalyst characterization.

5. - Conclusions

In this article we have presented the following results:

1) Surrogates of lignin depolymerization products, lignin and isolated oligomers (produced from liquefaction) have been studied in detail by UV fluorescence.
2) Synchronous fluorescence is the more selective mode for discriminating the molecules based on their molecular weight if the conjugation is not disrupted in the molecule (for instance by a β-O-4 bond).
3) NMR characterization has shown that Soda lignin and oligomers are mainly composed of conjugated moieties. Therefore, UV fluorescence is a relevant method to study this complex lignin oil.
4) A depolymerization index has been derived from UV fluorescence.
5) This index allows for a fast and simple analysis (in less than 15min.) of the relative distribution of monomers and oligomers as a function of liquefaction conditions.
6) UV fluorescence is compared to GC/MS, MALDI-TOFMS and GPC characterization of the same liquid samples.
7) These techniques give complementary information.
8) GPC and MALDI results must be interpreted cautiously and need further development on lignin oligomers.
9) UV fluorescence is the most direct analytical method with fewer potential side effects. It is only based on the intrinsic electronic properties of soluble molecules and of the solvent.

Concerning the perspectives of this work, this approach could be extended to other complex liquids presenting conjugated molecules, in other solvents or from other processes, such as biomass pyrolysis oil or hydrothermal liquefaction oils (etc.). We think that UV spectroscopy

has not yet been explored enough for understanding lignin liquids. Many findings can still be instigated based on early studies of fossil fuels, including asphaltenes and coal liquids.

Acknowledgements

This work has been funded by the French National Agency (ANR) through the PhenoLiq project. We thank Sébastien Leclerc (Université de Lorraine) for the NMR analyses which were performed on the "NMR platform of the Jean Barriol Institute", Université de Lorraine.

6. - References

1. Ragauskas, A. J. *et al.* Lignin Valorization: Improving Lignin Processing in the Biorefinery. *Science* **344**, 1246843–1246843 (2014).

2. Zakzeski, J., Bruijnincx, P. C. A., Jongerius, A. L. & Weckhuysen, B. M. The Catalytic Valorization of Lignin for the Production of Renewable Chemicals. *Chemical Reviews* **110**, 3552–3599 (2010).

3. Vermaas, J. V., Dellon, L. D., Broadbelt, L. J., Beckham, G. T. & Crowley, M. F. Automated Transformation of Lignin Topologies into Atomic Structures with LigninBuilder. *ACS Sustainable Chemistry & Engineering* **7**, 3443–3453 (2019).

4. Vanholme, R., De Meester, B., Ralph, J. & Boerjan, W. Lignin biosynthesis and its integration into metabolism. *Curr. Opin. Biotechnol.* **56**, 230–239 (2019).

5. Ralph, J., Lapierre, C. & Boerjan, W. Lignin structure and its engineering. *CURRENT OPINION IN BIOTECHNOLOGY* **56**, 240–249 (2019).

6. Samuel, R., Foston, M., Jiang, N., Allison, L. & Ragauskas, A. J. Structural changes in switchgrass lignin and hemicelluloses during pretreatments by NMR analysis. *Polymer Degradation and Stability* **96**, 2002–2009 (2011).

7. Balakshin, M. Y. & Capanema, E. A. Comprehensive structural analysis of biorefinery lignins with a quantitative 13C NMR approach. *RSC Adv.* **5**, 87187–87199 (2015).

8. Constant, S. *et al.* New insights into the structure and composition of technical lignins: a comparative characterisation study. *Green Chemistry* **18**, 2651–2665 (2016).

9. I. Evstigneyev, E. & M. Shevchenko, S. Structure, chemical reactivity and solubility of lignin: a fresh look. *Wood Science and Technology* **53**, (2018).

10. Bruijnincx, P. C. A., Rinaldi, R. & Weckhuysen, B. M. Unlocking the potential of a sleeping giant: lignins as sustainable raw materials for renewable fuels, chemicals and materials. *Green Chem.* **17**, 4860–4861 (2015).

11. Chen, Z. & Wan, C. Biological valorization strategies for converting lignin into fuels and chemicals. *Renewable and Sustainable Energy Reviews* **73**, 610–621 (2017).

12. Gosselink, R. J. A., de Jong, E., Guran, B. & Abächerli, A. Co-ordination network for lignin—standardisation, production and applications adapted to market requirements (EUROLIGNIN). *Industrial Crops and Products* **20**, 121–129 (2004).

13. Laurichesse, S. & Avérous, L. Chemical modification of lignins: Towards biobased polymers. *Progress in Polymer Science* **39**, (2013).

14. Ten, E. & Vermerris, W. Recent developments in polymers derived from industrial lignin. *Journal of Applied Polymer Science* **132**, (2015).

15. Melati, R. B. *et al.* Key Factors Affecting the Recalcitrance and Conversion Process of Biomass. *Bioenerg. Res.* **12**, 1–20 (2019).

16. Wang, H., Pu, Y., Ragauskas, A. & Yang, B. From lignin to valuable products–strategies, challenges, and prospects. *Bioresource Technology* **271**, 449–461 (2019).

17. Rinaldi, R. *et al.* Paving the Way for Lignin Valorisation: Recent Advances in Bioengineering, Biorefining and Catalysis. *Angewandte Chemie International Edition* **55**, 8164–8215 (2016).

18. Becker, J. & Wittmann, C. A field of dreams: Lignin valorization into chemicals, materials, fuels, and health-care products. *Biotechnol. Adv.* (2019) doi:10.1016/j.biotechadv.2019.02.016.

19. Vriamont, C. E. J. J. *et al.* From Lignin to Chemicals: Hydrogenation of Lignin Models and Mechanistic Insights into Hydrodeoxygenation via Low-Temperature C–O Bond Cleavage. *ACS Catalysis* **9**, 2345–2354 (2019).

20. Yamakawa, C. K., Qin, F. & Mussatto, S. I. Advances and opportunities in biomass conversion technologies and biorefineries for the development of a bio-based economy. *Biomass and Bioenergy* **119**, 54–60 (2018).

21. Liu, X. *et al.* Catalytic depolymerization of organosolv lignin to phenolic monomers and low molecular weight oligomers. *Fuel* **244**, 247–257 (2019).

22. Galkin, M. V. & Samec, J. S. M. Lignin Valorization through Catalytic Lignocellulose Fractionation: A Fundamental Platform for the Future Biorefinery. *ChemSusChem* **9**, 1544–1558 (2016).

23. Yuan, T.-Q., Xu, F. & Sun, R.-C. Role of lignin in a biorefinery: separation characterization and valorization. *Journal of Chemical Technology & Biotechnology* **88**, 346–352 (2013).

24. Schutyser, W. *et al.* Chemicals from lignin: an interplay of lignocellulose fractionation, depolymerisation, and upgrading. *Chemical Society Reviews* **47**, 852–908 (2018).

25. Holladay, J. E., Bozell, J. J., White, J. F. & Johnson, D. Top value-added chemicals from biomass. *DOE Report PNNL* **16983**, (2007).

26. Shabtai, J. S., Zmierczak, W. W. & Chornet, E. Process for conversion of lignin to reformulated, partially oxygenated gasoline. (2001).

27. Faix, O. & Meier, D. Pyrolytic and hydrogenolytic degradation studies on lignocellulosics, pulps and lignins. *Holz als Roh-und Werkstoff* **47**, 67–72 (1989).

28. Chio, C., Sain, M. & Qin, W. Lignin utilization: A review of lignin depolymerization from various aspects. *Renewable and Sustainable Energy Reviews* **107**, 232–249 (2019).

29. Amen-Chen, C., Pakdel, H. & Roy, C. Production of monomeric phenols by thermochemical conversion of biomass: a review. *Bioresource Technology* **79**, 277–299 (2001).

30. Kim, J.-Y., Park, J., Kim, U.-J. & Choi, J. W. Conversion of Lignin to Phenol-Rich Oil Fraction under Supercritical Alcohols in the Presence of Metal Catalysts. *Energy & Fuels* **29**, 5154–5163 (2015).

31. Huang, X., Atay, C., Korányi, T. I., Boot, M. D. & Hensen, E. J. M. Role of Cu–Mg–Al Mixed Oxide Catalysts in Lignin Depolymerization in Supercritical Ethanol. *ACS Catalysis* **5**, 7359–7370 (2015).

32. Huang, X., Korányi, T. I., Boot, M. D. & Hensen, E. J. M. Ethanol as capping agent and formaldehyde scavenger for efficient depolymerization of lignin to aromatics. *Green Chemistry* **17**, 4941–4950 (2015).

33. Huang, X., Korányi, T. I., Boot, M. D. & Hensen, E. J. M. Catalytic Depolymerization of Lignin in Supercritical Ethanol. *ChemSusChem* **7**, 2276–2288 (2014).

34. Huang, X. *et al.* Catalytic Depolymerization of Lignin and Woody Biomass in Supercritical Ethanol: Influence of Reaction Temperature and Feedstock. *ACS Sustainable Chemistry & Engineering* **5**, 10864–10874 (2017).

35. Wildschut, J., Mahfud, F. H., Venderbosch, R. H. & Heeres, H. J. Hydrotreatment of Fast Pyrolysis Oil Using Heterogeneous Noble-Metal Catalysts. *Ind. Eng. Chem. Res.* **48**, 10324–10334 (2009).

36. Terrell, E. *et al.* A Review on Lignin Liquefaction: Advanced Characterization of Structure and Microkinetic Modeling. *Industrial & Engineering Chemistry Research* **59**, 526–555 (2020).

37. Kozliak, E. I. *et al.* Thermal Liquefaction of Lignin to Aromatics: Efficiency, Selectivity, and Product Analysis. *ACS Sustainable Chemistry & Engineering* **4**, 5106–5122 (2016).

38. Gilkey, M. J. & Xu, B. Heterogeneous Catalytic Transfer Hydrogenation as an Effective Pathway in Biomass Upgrading. *ACS Catal.* **6**, 1420–1436 (2016).

39. Yang, J., Zhao, L., Liu, S., Wang, Y. & Dai, L. High-quality bio-oil from one-pot catalytic hydrocracking of kraft lignin over supported noble metal catalysts in isopropanol system. *Bioresource Technology* **212**, 302–310 (2016).

40. Bouxin, F. P. *et al.* Catalytic depolymerisation of isolated lignins to fine chemicals using a Pt/alumina catalyst: part 1—impact of the lignin structure. *Green Chemistry* **17**, 1235–1242 (2015).

41. Shuai, L. *et al.* Formaldehyde stabilization facilitates lignin monomer production during biomass depolymerization. *Science* **354**, 329–333 (2016).

42. Shu, R. *et al.* Efficient and product-controlled depolymerization of lignin oriented by metal chloride cooperated with Pd/C. *Bioresource Technology* **179**, 84–90 (2015).

43. Barta, K. *et al.* Catalytic disassembly of an organosolv lignin via hydrogen transfer from supercritical methanol. *Green Chemistry* **12**, 1640 (2010).

44. Jeong, S., Yang, S. & Kim, D. H. Depolymerization of Protobind lignin to produce monoaromatic compounds over Cu/ZSM-5 catalyst in supercritical ethanol. *Molecular Catalysis* **442**, 140–146 (2017).

45. McClelland, D. J. *et al.* Functionality and molecular weight distribution of red oak lignin before and after pyrolysis and hydrogenation. *Green Chemistry* **19**, 1378–1389 (2017).

46. Mahmood, N., Yuan, Z., Schmidt, J., Tymchyshyn, M. & Xu, C. (Charles). Hydrolytic liquefaction of hydrolysis lignin for the preparation of bio-based rigid polyurethane foam. *Green Chem.* **18**, 2385–2398 (2016).

47. Shrestha, B. *et al.* A Multitechnique Characterization of Lignin Softening and Pyrolysis. *ACS Sustainable Chemistry & Engineering* **5**, 6940–6949 (2017).

48. Barnés, M. C., de Visser, M. M., van Rossum, G., Kersten, S. R. A. & Lange, J.-P. Liquefaction of wood and its model components. *Journal of Analytical and Applied Pyrolysis* **125**, 136–143 (2017).

49. Andrianova, A. A. *et al.* Size exclusion chromatography of lignin: The mechanistic aspects and elimination of undesired secondary interactions. *Journal of Chromatography A* **1534**, 101–110 (2018).

50. Zinovyev, G. *et al.* Getting Closer to Absolute Molar Masses of Technical Lignins. *ChemSusChem* **11**, 3259–3268 (2018).

51. Dong, C., Feng, C., Liu, Q., Shen, D. & Xiao, R. Mechanism on microwave-assisted acidic solvolysis of black-liquor lignin. *Bioresource Technology* **162**, 136–141 (2014).

52. Shao, L., Zhang, Q., You, T., Zhang, X. & Xu, F. Microwave-assisted efficient depolymerization of alkaline lignin in methanol/formic acid media. *Bioresource Technology* **264**, 238–243 (2018).

53. Verziu, M. *et al.* Hydrogenolysis of lignin over Ru-based catalysts: The role of the ruthenium in a lignin fragmentation process. *Molecular Catalysis* **450**, 65–76 (2018).

54. Toledano, A. *et al.* Heterogeneously Catalysed Mild Hydrogenolytic Depolymerisation of Lignin Under Microwave Irradiation with Hydrogen-Donating Solvents. *ChemCatChem* **5**, 977–985 (2013).

55. Andrianova, A. A. *et al.* Electrospray Ionization with High-Resolution Mass Spectrometry as a Tool for Lignomics: Lignin Mass Spectrum Deconvolution. *Journal of The American Society for Mass Spectrometry* **29**, 1044–1059 (2018).

56. Qi, Y. & Volmer, D. A. Chemical diversity of lignin degradation products revealed by matrix-optimized MALDI mass spectrometry. *Analytical and Bioanalytical Chemistry* **411**, 6031–6037 (2019).

57. Terrell, E. *et al.* Contributions to Lignomics: Stochastic Generation of Oligomeric Lignin Structures for Interpretation of MALDI–FT-ICR-MS Results. *ChemSusChem* **n/a**, (2020).

58. Qi, Y. & Volmer, D. A. Rapid mass spectral fingerprinting of complex mixtures of decomposed lignin: Data-processing methods for high-resolution full-scan mass spectra. *Rapid Communications in Mass Spectrometry* **33**, 2–10 (2019).

59. Olcese, R., Carré, V., Aubriet, F. & Dufour, A. Selectivity of Bio-oils Catalytic Hydrotreatment Assessed by Petroleomic and GC*GC/MS-FID Analysis. *Energy & Fuels* **27**, 2135–2145 (2013).

60. Hertzog, J. *et al.* Combination of electrospray ionization, atmospheric pressure photoionization and laser desorption ionization Fourier transform ion cyclotronic resonance mass spectrometry for the investigation of complex mixtures – Application to the petroleomic analysis of bio-oils. *Analytica Chimica Acta* **969**, 26–34 (2017).

61. Aubriet, F. *et al.* Characterization of biomass and biochar by LDI-FTICRMS – Effect of the laser wavelength and biomass material. *J. Am. Soc. Mass Spectrom.* **29**, 1951–1962 (2018).

62. Liu, Q., Li, P., Liu, N. & Shen, D. Lignin depolymerization to aromatic monomers and oligomers in isopropanol assisted by microwave heating. *Polymer Degradation and Stability* **135**, 54–60 (2017).

63. Erdocia, X., Prado, R., Corcuera, M. Á. & Labidi, J. Base catalyzed depolymerization of lignin: Influence of organosolv lignin nature. *Biomass and Bioenergy* **66**, 379–386 (2014).

64. Lee, R. A., Bédard, C., Berberi, V., Beauchet, R. & Lavoie, J.-M. UV–Vis as quantification tool for solubilized lignin following a single-shot steam process. *Bioresource Technology* **144**, 658–663 (2013).

65. *Methods in Lignin Chemistry*. (Springer-Verlag, 1992).

66. Chen, Z., NaderiNasrabadi, M., Staser, J. A. & Harrington, P. B. Application of Generalized Standard Addition Method and Ultraviolet Spectroscopy to Quantify Electrolytic Depolymerization of Lignin. *J. Anal. Test.* **4**, 35–44 (2020).

67. Seca, A. M. L. *et al.* Structural Characterization of the Lignin from the Nodes and Internodes of *Arundo donax* Reed. *Journal of Agricultural and Food Chemistry* **48**, 817–824 (2000).

68. Wang, Z. *et al.* Synchronous fluorimetric characterization of heavy intermediates of coal direct liquefaction. *Fuel* **98**, 67–72 (2012).

69. George, A. *et al.* Fractionation of a coal tar pitch by ultra-filtration, and characterization by size exclusion chromatography, UV-fluorescence and laser desorption-mass spectroscopy. *Fuel* **89**, 2953–2970 (2010).

70. Katoh, T., Yokoyama, S. & Sanada, Y. Analysis of a coal-derived liquid using highpressure liquid chromatography and synchronous fluorescence spectrometry. *Fuel* **59**, 845–850 (1980).

71. Mille, G., Guiliano, M. & Kister, J. Analysis and evolution of coals: UV fluorescence spectroscopy study (demineralized coals-oxidized coals). *Organic geochemistry* **13**, 947–952 (1988).

72. Bayrakceken, S., Gaines, A. F., Keating, P. & Snape, C. E. The fluorescence of suspensions of powdered coals. *Fuel* **84**, 1749–1759 (2005).

73. Badre, S., Carla Goncalves, C., Norinaga, K., Gustavson, G. & Mullins, Oliver. C. Molecular size and weight of asphaltene and asphaltene solubility fractions from coals, crude oils and bitumen. *Fuel* **85**, 1–11 (2006).

74. Goncalves, S., Castillo, J., Fernández, A. & Hung, J. Absorbance and fluorescence spectroscopy on the aggregation behavior of asphaltene–toluene solutions. *Fuel* **83**, 1823–1828 (2004).

75. Lundquist, K., Josefsson, B. & Nyquist, G. Analysis of Lignin Products by Fluorescence Spectroscopy. *Holzforschung* **32**, 27–32 (1978).

76. Garcia-Perez, M. *et al.* Effects of Temperature on the Formation of Lignin-Derived Oligomers during the Fast Pyrolysis of Mallee Woody Biomass. *Energy & Fuels* **22**, 2022–2032 (2008).

77. Pecha, M. B. *et al.* Effect of Pressure on Pyrolysis of Milled Wood Lignin and Acid-Washed Hybrid Poplar Wood. *Industrial & Engineering Chemistry Research* **56**, 9079–9089 (2017).

78. Olmstead, J. A. & Gray, D. G. Fluorescence spectroscopy of cellulose, lignin and mechanical pulps: A review. *Journal of Pulp and Paper Science* **23**, J571–J581 (1997).

79. Delpuech, J. J. *et al.* Characterization of catalytically hydrogenated and pyrolysis coal products. A comparative study of several analytical procedures. *Fuel processing technology* **12**, 205–241 (1986).

80. Zander, M. & Haenel, M. W. Regularities in the fluorescence spectra of coal-tar pitch fractions. *Fuel* **69**, 1206–1207 (1990).

81. Herod, A. A. Limitations of mass spectrometric methods for the characterization of polydisperse materials. *Rapid Communications in Mass Spectrometry* **24**, 2507–2519 (2010).

82. Bayerbach, R., Nguyen, V. D., Schurr, U. & Meier, D. Characterization of the water-insoluble fraction from fast pyrolysis liquids (pyrolytic lignin). *Journal of Analytical and Applied Pyrolysis* **77**, 95–101 (2006).

83. de Saint Laumer, J.-Y., Cicchetti, E., Merle, P., Egger, J. & Chaintreau, A. Quantification in Gas Chromatography: Prediction of Flame Ionization Detector Response Factors from Combustion Enthalpies and Molecular Structures. *Analytical Chemistry* **82**, 6457–6462 (2010).

84. Kim, J.-Y. *et al.* Catalytic depolymerization of lignin macromolecule to alkylated phenols over various metal catalysts in supercritical tert-butanol. *Journal of Analytical and Applied Pyrolysis* **113**, 99–106 (2015).

85. Richel, A., Vanderghem, C., Simon, M., Wathelet, B. & Paquot, M. Evaluation of Matrix-Assisted Laser Desorption/Ionization Mass spectrometry for second-Generation Lignin Analysis. *Analytical Chemistry Insights* **7**, ACI.S10799 (2012).

86. Lakowicz, J. R. *Principles of Fluorescence Spectroscopy*. (Springer US, 2006).

87. Scholze, B., Hanser, C. & Meier, D. Characterization of the water-insoluble fraction from fast pyrolysis liquids (pyrolytic lignin): Part II. GPC, carbonyl goups, and 13C-NMR. *Journal of Analytical and Applied Pyrolysis* **58–59**, 387–400 (2001).

88. Zakzeski, J. & Weckhuysen, B. M. Lignin Solubilization and Aqueous Phase Reforming for the Production of Aromatic Chemicals and Hydrogen. *ChemSusChem* **4**, 369–378 (2011).

89. Zakzeski, J., Jongerius, A. L., Bruijnincx, P. C. A. & Weckhuysen, B. M. Catalytic Lignin Valorization Process for the Production of Aromatic Chemicals and Hydrogen. *ChemSusChem* **5**, 1602–1609 (2012).

90. McDonough, T. J. The chemistry of organosolv delignification. *IPST Technical Paper Series* (1992).

91. Hu, J., Shen, D., Wu, S., Zhang, H. & Xiao, R. Effect of temperature on structure evolution in char from hydrothermal degradation of lignin. *Journal of Analytical and Applied Pyrolysis* **106**, 118–124 (2014).

92. Nakamura, T., Kawamoto, H. & Saka, S. Condensation Reactions of Some Lignin Related Compounds at Relatively Low Pyrolysis Temperature. *Journal of Wood Chemistry and Technology* **27**, 121–133 (2007).

93. Besse, X., Schuurman, Y. & Guilhaume, N. Reactivity of lignin model compounds through hydrogen transfer catalysis in ethanol/water mixtures. *Applied Catalysis B: Environmental* **209**, 265–272 (2017).

94. Li, H. *et al.* Liquefaction of rice straw in sub- and supercritical 1,4-dioxane–water mixture. *Fuel Processing Technology* **90**, 657–663 (2009).

95. Kim, J. Y. *et al.* Effects of various reaction parameters on solvolytical depolymerization of lignin in sub- and supercritical ethanol. *Chemosphere* **93**, 1755–1764 (2013).

96. Taylor, T. A. & Patterson, H. H. Excitation resolved synchronous fluorescence analysis of aromatic compounds and fuel oil. *Analytical Chemistry* **59**, 2180–2187 (1987).

97. Popescu, C.-M., Vasile, C., Popescu, M.-C., Popa, V. I. & Munteanu, B. S. ANALYTICAL METHODS FOR LIGNIN CHARACTERIZATION. II. SPECTROSCOPIC STUDIES. 27.

98. Dean, J. C., Navotnaya, P., Parobek, A. P., Clayton, R. M. & Zwier, T. S. Ultraviolet spectroscopy of fundamental lignin subunits: Guaiacol, 4-methylguaiacol, syringol, and 4-methylsyringol. *The Journal of Chemical Physics* **139**, 144313 (2013).

99. Brouwer, A. M. Standards for photoluminescence quantum yield measurements in solution (IUPAC Technical Report). *Pure and Applied Chemistry* **83**, 2213–2228 (2011).

100. Valeur, B. & Brochon, J.-C. New Trends in Fluorescence Spectroscopy: Applications to Chemical and Life Sciences. (Springer Science & Business Media, 2012).

101. Rouessac, F. & Rouessac, A. Chemical Analysis: Modern Instrumentation Methods and Techniques. (John Wiley & Sons, 2013).

102. Sauer, M., Hofkens, J. & Enderlein, J. Handbook of Fluorescence Spectroscopy and Imaging: From Ensemble to Single Molecules. (John Wiley & Sons, 2010).

103. Pieper, C. M. & Enderlein, J. Fluorescence correlation spectroscopy as a tool for measuring the rotational diffusion of macromolecules. *Chemical Physics Letters* **516**, 1–11 (2011).

104. Sulaeva, I. *et al.* Fast Track to Molar-Mass Distributions of Technical Lignins. *ChemSusChem* **10**, 629–635 (2017).

105. Harman-Ware, A. E. & Ferrell, J. R. Methods and Challenges in the Determination of Molecular Weight Metrics of Bio-oils. *Energy & Fuels* **32**, 8905–8920 (2018).

106. Li, Y. *et al.* Kinetic and mechanistic insights into hydrogenolysis of lignin to monomers in a continuous flow reactor. *Green Chem.* **21**, 3561–3572 (2019).

107. Karas, Michael. & Hillenkamp, Franz. Laser desorption ionization of proteins with molecular masses exceeding 10,000 daltons. *Anal. Chem.* **60**, 2299–2301 (1988).

108. Bocchini, P. *et al.* Matrix-assisted Laser Desorption/Ionization Mass Spectrometry of Natural and Synthetic Lignin. *Rapid Communications in Mass Spectrometry* **10**, 1144–1147 (1996).

109. Zenobi, R. & Knochenmuss, R. Ion formation in MALDI mass spectrometry. *Mass Spectrometry Reviews* **17**, 337–366 (1998).

110. Metzger, J. O. *et al.* Matrix-Assisted Laser Desorption Mass Spectrometry of Lignins**. *Angewandte Chemie International Edition in English* **31**, 762–764 (1992).

111. Aubriet, F. & Carré, V. Chapter 10 - Fourier transform ion cyclotron resonance mass spectrometry and laser: A versatile tool. in *Fundamentals and Applications of Fourier Transform Mass Spectrometry* (eds. Kanawati, B. & Schmitt-Kopplin, P.) 281–322 (Elsevier, 2019). doi:10.1016/B978-0-12-814013-0.00010-7.

112. Jacobs, A. & Dahlman, O. Absolute molar mass of lignins by size exclusion chromatography and MALDI-TOF mass spectroscopy. *Nordic Pulp & Paper Research Journal* **15**, 120–127 (2000).

113. Kosyakov, D. S., Ul'yanovskii, N. V., Sorokina, E. A. & Gorbova, N. S. Optimization of sample preparation conditions in the study of lignin by MALDI mass spectrometry. *J Anal Chem* **69**, 1344–1350 (2014).

114. Qi, Y. *et al.* Assessment of molecular diversity of lignin products by various ionization techniques and high-resolution mass spectrometry. *Science of The Total Environment* **713**, 136573 (2020).

115. Marathe, P. S., Juan, A., Hu, X., Westerhof, R. J. M. & Kersten, S. R. A. Evaluating quantitative determination of levoglucosan and hydroxyacetaldehyde in bio-oils by gas and liquid chromatography. *Journal of Analytical and Applied Pyrolysis* **139**, 233–238 (2019).

116. Kershaw, J. R., Sathe, C., Hayashi, J., Li, C.-Z. & Chiba, T. Fluorescence Spectroscopic Analysis of Tars from the Pyrolysis of a Victorian Brown Coal in a Wire-Mesh Reactor. *Energy & Fuels* **14**, 476–482 (2000).

117. Le Brech, Y. *et al.* Characterization of biomass char formation investigated by advanced solid state NMR. *Carbon* **108**, 165–177 (2016).

7. - Supporting Information

7.1. - References of chemicals

The references of model compounds (Sigma Aldrich) are: phenol (P1037), guaiacol (G5502), syringol (D135550), m-cresol (C85727), p-cresol (C85751), o-cresol (C85700), vanillin (V1104), pyrocatechol (C9510), isoeugenol (I17206), 1-naphthol (N1000), 2-naphthol (185507), naphthalene (84679), guaiacylglycerol-beta-guaiacyl ether (CDS013307). Those model compounds have been chosen because they are representative of the structures of lignin liquefaction products with complementary functionalities. Ethanol (Ethanol absolute anhydrous RS - for HPLC PLUS Gradient grade 1, Carlo Erba 4127012) and tetrahydrofuran (99.8%, for HPLC, unstabilized, ACROS Organics, CAS 109-99-9) were used as solvents for the reaction and for analysis. For MALDI-TOF analysis a DHB matrix was used (2,5-Dihydroxybenzoic acid 99%, CAS 490-79-9).

7.2. - NMR characterization of Soda lignin and oligomers extracted after lignin liquefaction

Oligomers were isolated by acid precipitation (see the method presented hereafter).

The 2D HSQC NMR spectra of lignin and oligomers were acquired on a Bruker Bruker Avance III HD 300 MHz spectrometer equipped with a BBO probe at 50°C using the hsqcetgp pulse program. Matrices of 1024 data points for the 1H-dimension and 256 data points for the 13C-dimension were collected with a relaxation delay of 1.5s and spectral widths from 9.5 to -0.5ppm and from 180 to 0ppm for the 1H and 13C dimensions, respectively. Number of scans was 128. The lignin and oligomers were dissolved in DMSO-d6 after overnight stirring (200 mg/750 μL) and chemical shifts were referenced to the solvent signal (2.50/39.5ppm). The spectra were processed on Topspin 4.0.6 software (LB=10).

HSQC semi-quantification of the main lignin linkages were performed using the correlation peak according to aromatic carbons.[1] S2,6 (104.2/6.7) and G2 (110.2/6.9) have been used as reference and linkages concentration are expressed in Table S1 as a number per 100 aromatic units (S+G). The integral value for each linkage were divided by the integral value for S2,6/2 + integral value for G2.

Table S1. Quantification of ether bonds in Soda lignin by HSQC NMR

		Soda lignin	
	corr. Assig. (ppm, $^{13}C/^{1}H$)	Average %	std
% β-O-4	72.1/4.88	5.6	0.4
% β-β	86/4.69	4.3	0.1
% β-5	87.3/5.53	1.3	0.1

Table S1 shows that ether bonds represent less than 10% of carbons. 90% of aromatic rings are linked together by bonds which are not ether bond, by C-C bonds. This finding is in agreement with literature[2,3] on the same lignin.

Figures S1 to S3 display the HSQC spectra of the pristine Soda lignin and of the 2 oligomers produced after 4h reaction (with and without catalyst). They demonstrate that the signals of ether bonds are no more detected after liquefaction in the oligomers.

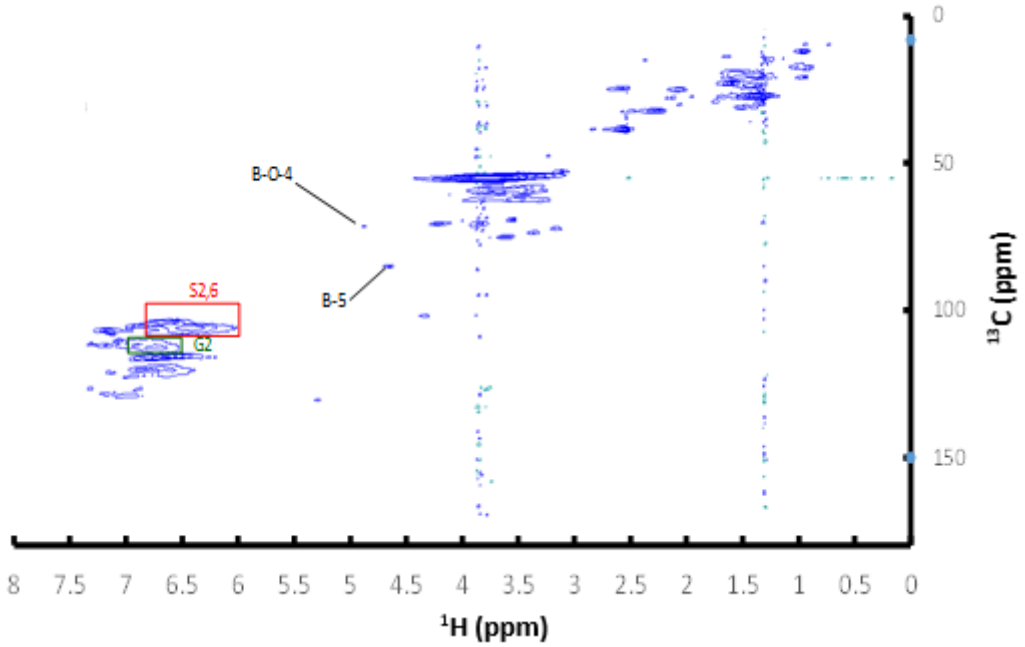

Figure S1.HSQC spectra of Soda Protobind lignin

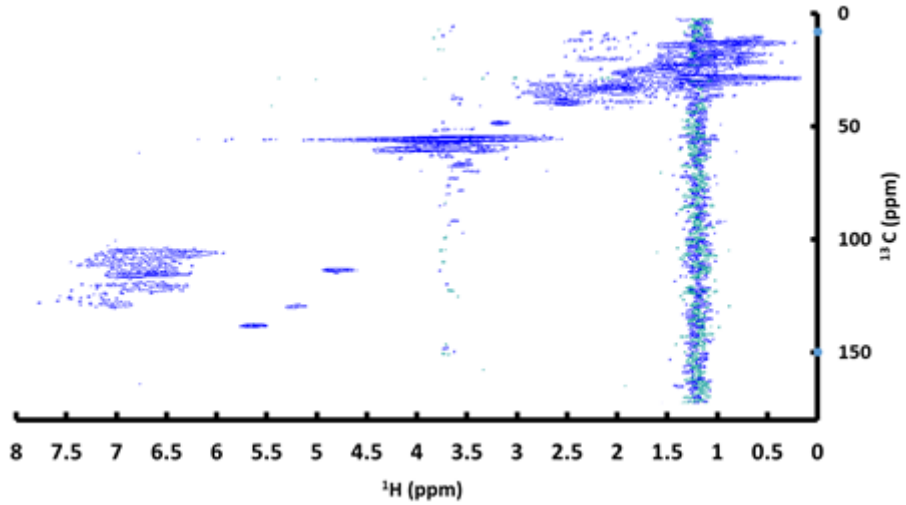

Figure S2. HSQC spectra of precipitated oligomers after reaction (4h, without catalyst)

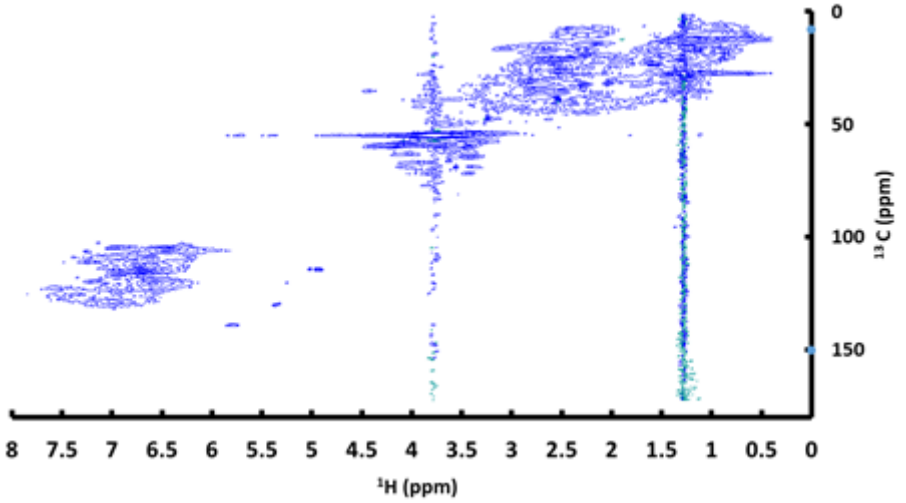

Figure S3. HSQC spectra of precipitated oligomers after reaction (4h, with catalyst)

Lignin and oligomers were also analysed by ^{13}C NMR.

^{13}C NMR spectra were acquired on a Bruker Avance III HD 300 MHz spectrometer (75.46 MHz for ^{13}C) equipped with a BBO probe at 50°C in order to reduce viscosity. An inverse-gated decoupling pulse sequence (zgig pulse program) was used to avoid NOE effects. 10,000 scans were collected with a pulse delay of 12s.

The lignins and oligomers were dissolved in DMSO-d6 after overnight stirring (200 mg/750 µL) and chemical shifts were referenced to the solvent signal (39.5ppm). The spectra were processed on Topspin 4.0.6 software (LB=10).

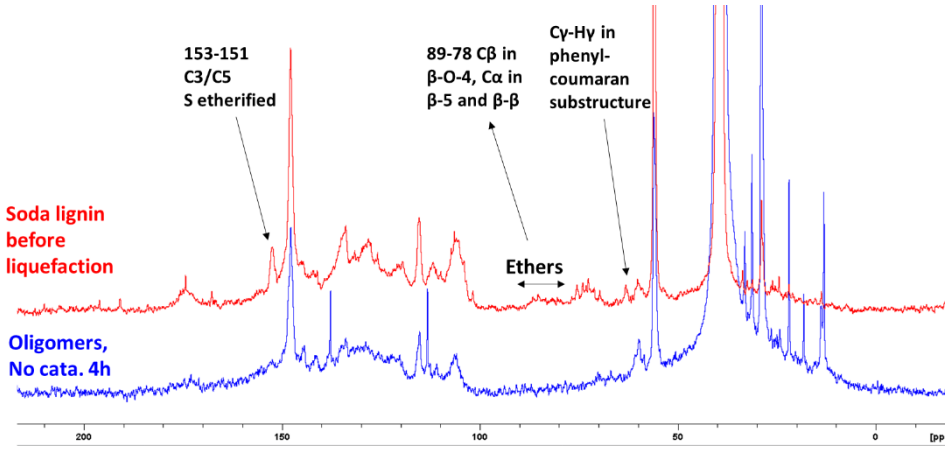

Figure S4. ^{13}C NMR comparison between lignin (before liquefaction) and oligomers (after 4h liquefaction, no catalyst)

Figure S4 clearly shows that characteristic bands of ethers are considerably reduced in oligomers after liquefaction.

7.3. - Autoclave set-up

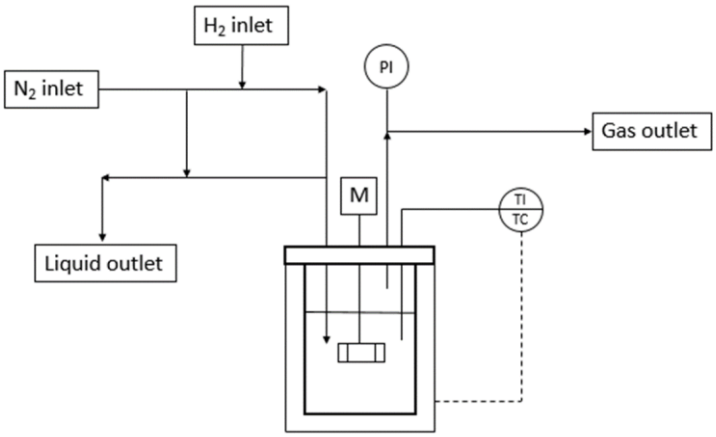

Figure S5. Scheme of the autoclave setup (Parr Instrument, 300mL)

7.4. - Isolation of solid residue and oligomers at the end of liquefaction experiments

Solid residue (not soluble in ethanol) and oligomers (soluble in ethanol) were isolated at the end of the experiments (after 4h at 250°C) on the total products remained after cooling of the autoclave. Briefly, ethanol solution was filtered (11 then 1.2µm). This fraction not soluble in

ethanol is called “solid residue”. The mass of starting catalyst was removed from the measured mass for the catalytic experiment. Therefore, the mass of “solid residue” can also include coke deposit in the catalyst. It was out of the scope of the present work to analyse the carbonaceous solids (char and coke). The filtrate (soluble in ethanol) was then precipitated (by HCl dilute solution and water, by the method proposed by Huang et al. [4]), then filtered (stepwise 11 & 1.2µm). This solid remaining after acid precipitation is called “oligomers”. Results are presented in table S2.

Table S2. Mass yields of char and oligomers for the 2 conditions (after 4h at 250°C)

Catalyst	**Solid residue (%wt based on lignin mass)**	**Oligomers (%wt. lignin)**
none	37.5	44
1% Pt/lig	18	38

Kim et al.[5] has also shown an important effect of Pt/C on char yield, from about 35%wt. (without catalyst) down to about 8 %wt. with Pt/C (under their 20%wt. catalyst/lignin conditions). Our solid residue yield is higher probably due to a longer residence time (associated with a lower liquefaction temperature) which may promote secondary crosslinking reactions.

7.5. - GC/MS6FID analysis

Typical GC/MS chromatogram for two experiments conducted with and without catalyst (4h sampling time) are presented in figure S6.

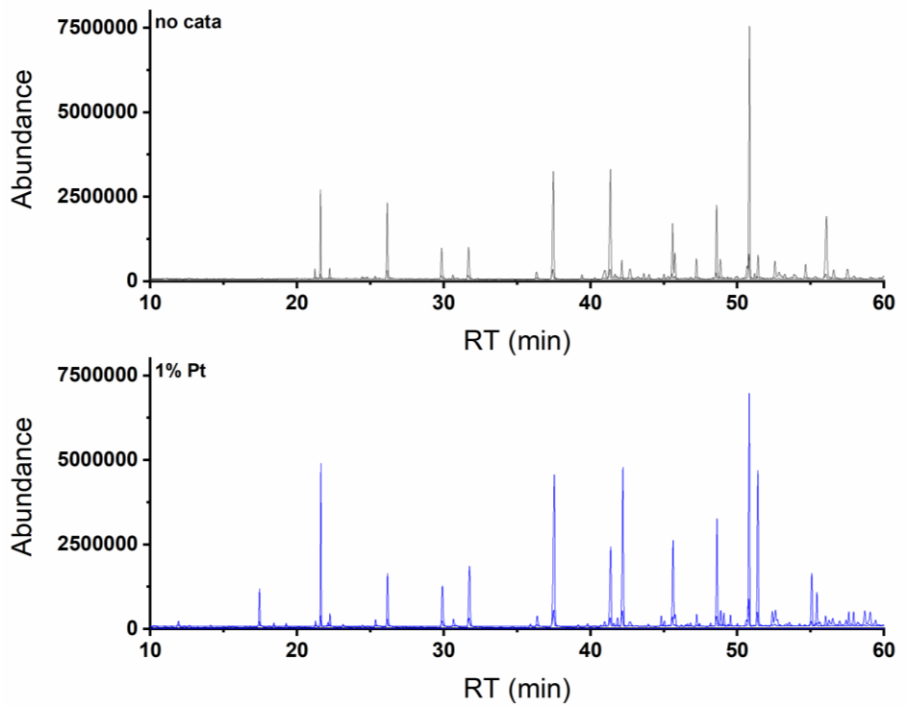

Figure S6. GC/MS chromatograms without catalyst and with catalyst (Pt/C) after 4 hours of isothermal liquefaction (250°C) (internal standard, hexadecane at 50.79min)

The reproducibility of GC/FID quantification is presented in figure S7 and is satisfactory.

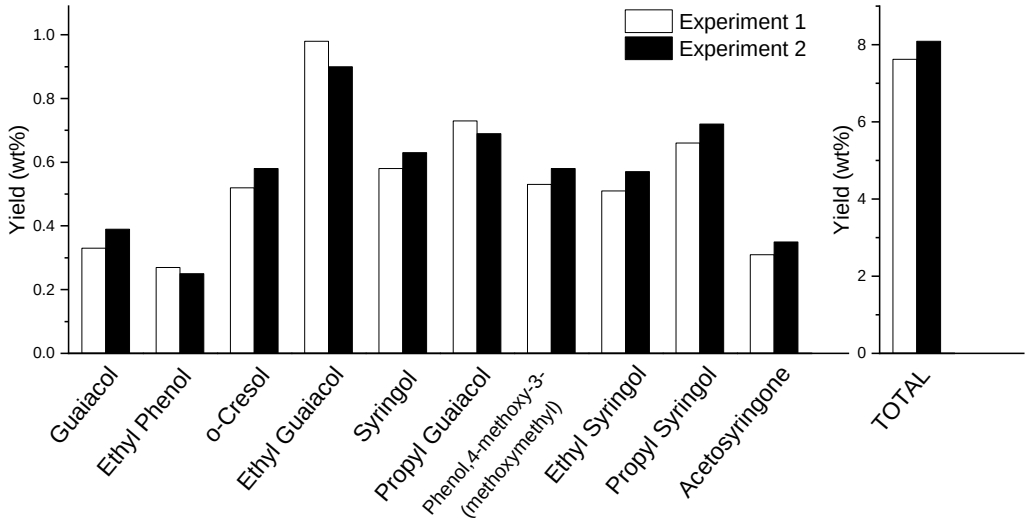

Figure S7. Mass yields of total and main monomeric products of two different experiments performed at same conditions (4 hours sampling time, with 1%wt Pt/lignin)

Monomers with chromatographic retention times and mass yields (based on anhydrous lignin mass) as detected and quantified by GC/MS-FID for the 8 sampling (4 times, without and with catalyst) are presented in Table S3.

Table S3. Retention times and quantification of monomers (wt. % lignin mass basis) by GC/MS-FID for the 8 sampled solutions

n.	RT(min)	Compounds	Formula	MW(g/mol)	Yield (%wt)							
					nocata-0h	nocata-0.5h	nocata-2h	nocata-4h	1%Pt-0h	1%Pt-0.5h	1%Pt-2h	1%Pt-4h
1	6,64	1-Butanol	C4H10O	74	not quant.	not quant.	not quant.	not quant.	not quant.	not quant.	not quant.	0,3
2	7,22	1,4-Dioxin,2,3-dihydro	C4H6O2	86	not quant.	not quant.	not quant.	not quant.	not quant.	not quant.	not quant.	0,48
3	8,47	1,1-diethoxy-Ethane	C6H14O2	118	0,13	0,23	0,34	0,37	1	2,42	4,86	6,41
4	11,91	Butanoic acid, ethyl ester	C6H12O2	116	not quant.	not quant.	not quant.	not quant.	not quant.	not quant.	not quant.	0,1
5	17,42	1,1-diethoxy-Butane	C8H18O2	146	not quant.	not quant.	not quant.	not quant.	not quant.	not quant.	not quant.	0,19
6	18,40	2,4,6-Cyclopentanone,2-ethyl	C7H6O2	122	not quant.	not quant.	not quant.	not quant.	0,05	0,03	0,1	0,03
7	19,24	2-ethyl-Cyclopentanone	C7H12O	112	not quant.	not quant.	not quant.	not quant.	not quant.	not quant.	not quant.	0,03
8	21,24	Phenol	C6H6O	94	-	0,02	0,04	0,06	0,02	0,03	0,05	0,05
9	21,60	1,2-Dimethoxy-4-(1-methoxyethenyl)benzene	C11H14O3	194	-	0,02	0,06	0,15	0,03	0,09	0,22	0,33
10	22,09	2-Methyl-5-hexen-3-ol	C7H14O	114	-	-	0,01	0,03	-	-	-	0,02
11	22,22	2,4,4-Trimethyl-3-(3-oxobutyl)cyclohex-2-enone	C13H20O2	208	-	-	0,01	0,02	-	-	-	0,03
12	25,32	p-Cresol	C7H8O	108	-	-	0,01	0,02	-	0,03	-	0,07
13	26,14	Guaiacol	C7H8O2	124	0,04	0,07	0,18	0,39	0,09	-	-	0,33
14	29,88	4-ethyl-Phenol	C8H10O	122	0,01	0,04	0,1	0,16	-	-	-	0,27
15	30,64	Butanedioic acid, diethyl ester	C8H14O4	174	-	-	-	0,02	-	-	-	0,07
16	31,73	o-Cresol	C7H8O	108	0,01	0,02	0,07	0,2	-	-	-	0,45
17	32,98	vinylphenol	C8H8O	120	0,01	0,02	0,04	-	-	-	-	-
18	35,87	4-propyl-Phenol	C9H12O	136	0,07	0,08	-	0,1	-	-	-	0,03
19	36,33	Pyrocathecol	C7H8O3	140	-	0,01	0,04	0,53	-	-	0,1	0,14
20	37,50	Ethylguaiacol	C9H12O2	152	0,03	0,09	0,29	0,63	-	-	0,91	0,98
21	39,383	vinylguaiacol	C9H10O2	150	0,17	0,21	0,13	-	-	-	-	-
22	41,35	Syringol	C8H10O3	154	0,08	0,13	0,32	-	-	0,3	0,44	0,58
23	42,18	Propylguaiacol	C10H14O2	166	0,02	0,03	0,07	0,07	-	0,43	0,68	0,73
24	42,67	Ethyl β-d-riboside	C7H14O5	178	0,04	0,09	0,12	0,12	-	0,13	0,11	0,11
25	43,59	Vanillin	C8H8O3	152	0,16	0,23	0,1	0,04	-	-	-	-
26	44,79	Acetophenone	C8H8O4	168	-	0,05	0,05	0,03	-	-	-	0,1
27	45,01	4',6'-Dihydroxy-2',3'-dimethylacetophenone	C10H12O3	180	-	0,02	0,03	-	-	-	-	0,04
28	45,60	Methyl Syringol	C9H12O3	168	0,11	0,03	-	0,26	0,2	0,34	0,45	0,53
29	45,74	Iso-eugenol	C8H8O4	168	-	0,19	0,38	0,17	0,17	0,14	0,06	0,1
30	47,20	Acetoguaiacone	C9H10O3	166	0,06	0,08	0,1	0,1	0,08	0,09	0,09	0,08
31	48,15	1-Propanone, 1-(2,4-dimethoxyphenyl)-	C11H14O3	194	-	-	0,01	0,01	-	-	-	0,03
32	48,59	Ethylsyringol	C10H14O3	182	0,03	0,05	0,15	0,29	0,19	0,32	0,44	0,51
33	48,85	Guaiacylacetone	C10H12O3	180	0,02	0,04	0,08	0,1	0,05	0,08	0,1	0,09
34	49,06	5-Sec-butylpyrogallol	C10H14O3	182	-	-	-	0,1	0,02	0,06	0,07	0,07
35	49,51	1-hydroxy-3-(4-hydroxy-3-methoxyphenyl)propan-2-one	C10H12O4	196	0,07	0,06	-	0,03	-	-	0,05	0,06
36	50,61	Ethylvanillate	C10H12O4	196	-	-	-	-	-	-	-	0,06
37	50,79	Hexadecane	C16H34	226	I.S.	I.S.	I.S.	I.S.	I.S.	I.S.	I.S.	I.S.
38	51,38	Propyl syringol	C11H16O3	196	0,01	0,01	0,04	0,09	0,25	0,5	0,65	0,66
39	52,36	Ethyl homovanillate	C11H14O4	210	0,04	0,06	-	-	0,06	0,08	0,09	0,1
40	52,57	Syringaldehyde	C9H10O4	182	0,22	0,05	0,1	0,12	0,12	0,17	0,17	0,18
41	54,62	Methoxyeugenol	C11H14O3	194	0,07	0,1	0,15	0,09	-	0,45	-	-
42	55,05	Acetosyringone	C10H12O4	196	0,45	0,47	0,47	0,43	0,43	0,1	0,39	0,31
43	55,39	Ethyl-β-(4-hydroxy-3-methoxy-phenyl)-propionate	C12H16O4	224	-	-	-	-	-	-	0,14	0,18
44	55,99	Syringyl propan-2-one	C11H14O4	210	-	-	-	-	0,04	0,07	0,06	0,07
45	57,57	3,4,5-Trimethoxyphenylacetic acid	C11H14O5	226	-0,03	-	-	-	-	-	0,08	0,09
46	57,89	Syringyl propan-1-one	C11H14O4	210	-	-	0,06	0,03	0,02	0,05	0,07	0,09
47	58,66	Diphenyl-acetic acid ethyl ester	C16H16O2	240	-	-	0,02	-	0,03	0,05	0,06	0,09

7.6. - GPC analysis

GPC analysis of the liquids sampled upon time on stream (250°C) are presented on Figure S8.

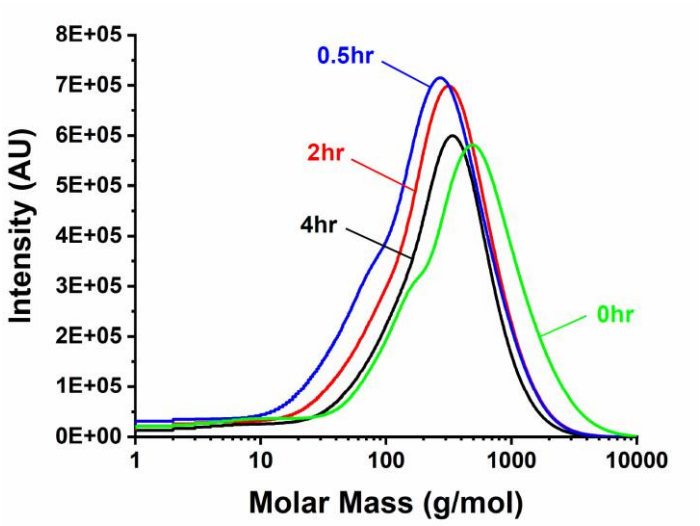

Figure S8. GPC curves of liquefaction products with catalyst at different sampling times

An acetylation method was used only for Soda lignin (not for bio-oils). Soda lignin was dried in an oven overnight. 2 mL of acetic anhydride/pyridine (1:1) mixture were added to 20 mg of Soda lignin. The mixture was kept at room temperature with stirring for 24 hrs. 25 mL of ethanol were added to the reaction mixture and kept for 30 min. Then ethanol was evaporated. This step was repeated until the acetic anhydride and pyridine were evaporated. Acetylated lignin was dissolved in 2 mL of chloroform and this solution was added drop wise into 100 mL magnetically stirred diethyl ether. Precipitated acetylated lignin was collected after centrifugation, then dissolved in 25 mL THF for GPC analysis.

7.7. - MALDI-TOFMS analysis

MALDI-TOF spectra of raw lignin, matrix (DHB) and a mix of DHB and lignin are presented on figure S9.

All detected ions are most probably monocharged species because multicharged ions were only evidence by MALDI in the study of big macromolecules like proteins.

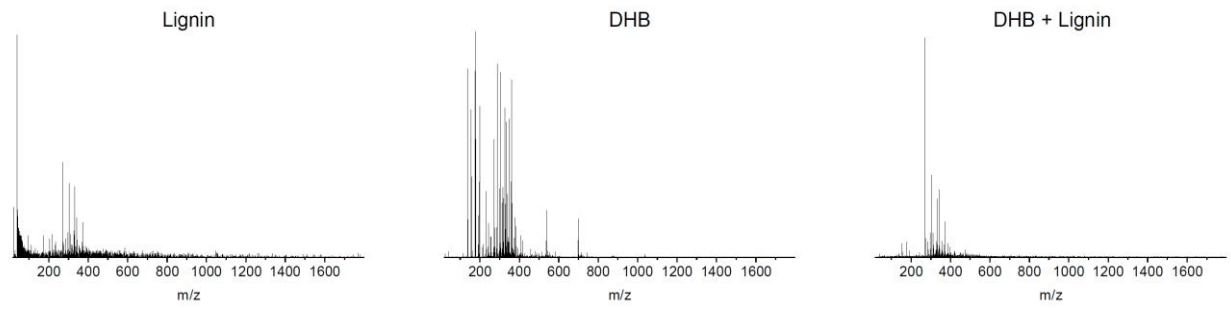

Figure S9. MALDI-TOF spectra of raw lignin, matrix and a mix of the two

7.7.1. - Optimization of MALDI-TOFMS signals

First, different concentrations of lignin derived oils and DHB solution have been tested. Starting from a very diluted sample (around 2.5 mg/mL of lignin), we reached to an optimum at 25 mg/mL of lignin in DHB solution, basically adding the same amount of lignin oil (10g of lignin in 200mL of ethanol, 50mg lignin/mL ethanol) and DHB solution. The more diluted sample gave only a signal from the matrix.

Second, we optimized the power of the laser starting from 51%, which was the minimum power to get a good signal (figure S10). 60% of laser power was found to be a good compromise with a good signal from the sample without having important fragmentation problems due to the laser beam.

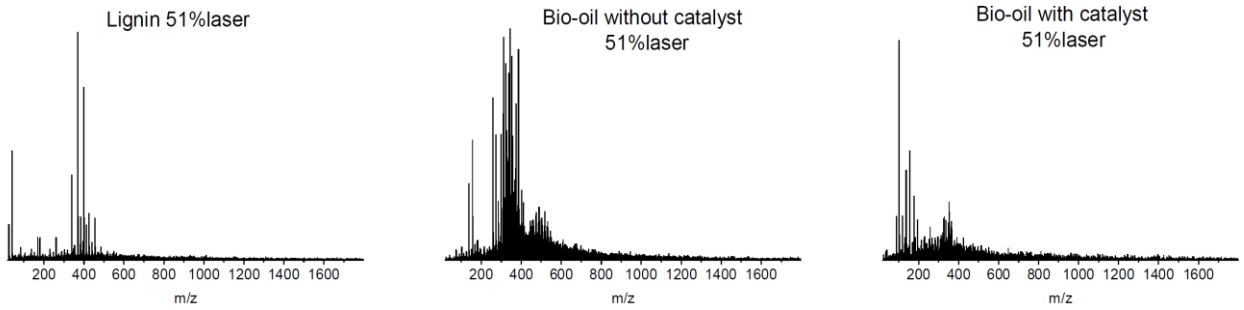

Figure S10. MALDI-TOFMS mass spectra of lignin and bio-oils with 51% of laser power

After the optimization conditions of MALDI-TOFMS analysis, mass spectra were collected on liquefaction samples without and with catalyst for different reaction times (Figure S11).

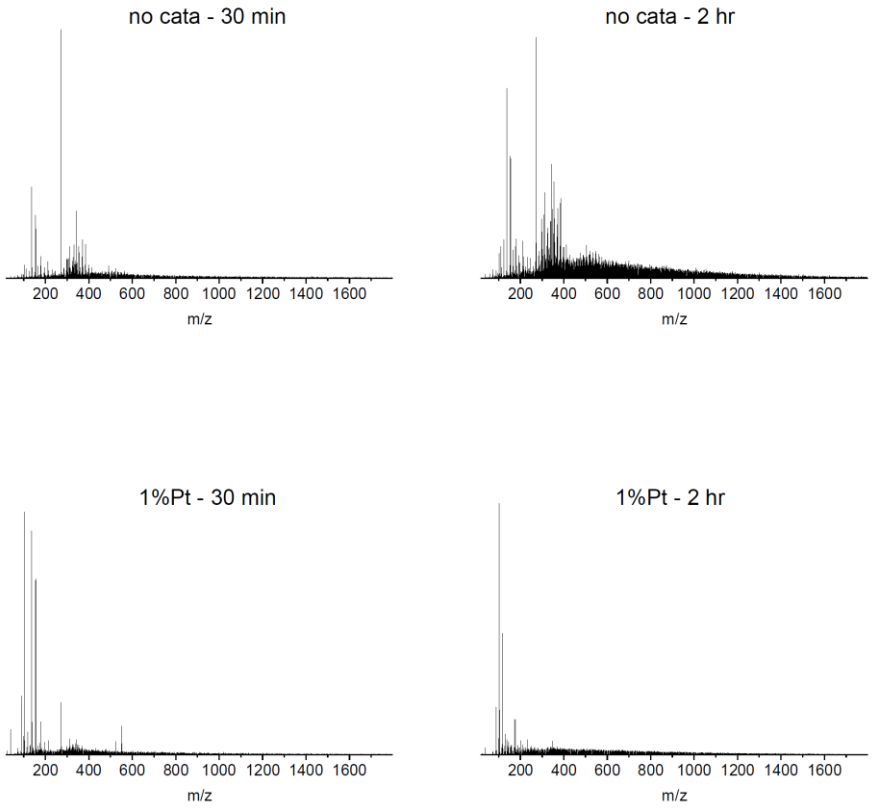

Figure S11. MALDI-TOF mass spectra with and without catalyst at 30 minutes and 2 hours 60% laser power (optimized conditions)

7.8. - UV spectroscopy analysis of model compounds and of lignin liquefaction liquids

First, UV absorption spectra of molecule compounds are displayed in figure S12.

These results have been discussed in the main text.

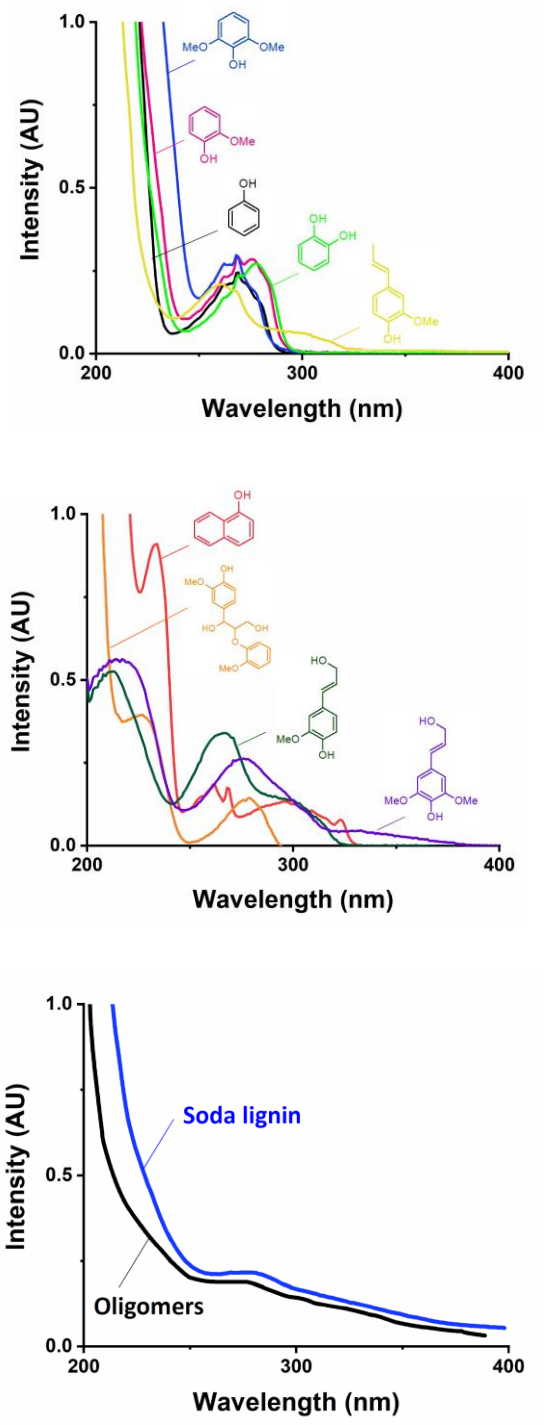

Figure S12. UV absorption spectra of model compounds, lignin and isolated oligomers (also characterized by NMR)

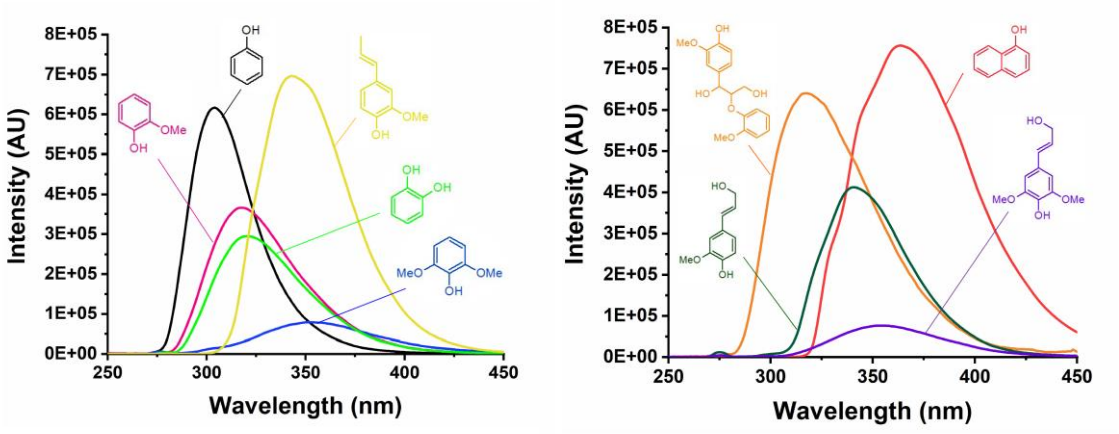

Figure S13. UV fluorescence spectra for model compounds excited at 275 nm. The area of each curve is function of the quantum yield of each compound (as presented in table S4).

Quantum yield increases with the number of C=C double bonds in the molecule and decreases with methoxy groups.

The UV characteristics of model compounds are presented in table S4.

ε [L mol^{-1} cm^{-1}] represents the molecular absorption coefficient of each molecule.

λabs, is the absorption wavelength used for the determination of the molecular absorption coefficient.

λem_{275} is the maximal emission fluorescence wavelength for a fixed excitation at 275nm.

λem_{S20} is the maximal emission fluorescence wavelength for a synchronous excitation with 20nm offset.

"Shift" is the Stokes shift, the difference between λ_{em275} and λ_{abs}.

Fluorescence quantum yield has been determined based on IUPAC method with quinine sulfate as a reference.[6]

Table S4. Main UV absorption and fluorescence characteristics of model compounds (diluted in ethanol)

Model Compound	**Molecular weight (g/mol)**	**Dilution**	**ε (M^{-1} cm^{-1})**	**λabs (nm)**	**λem 275 (nm)**	**λem S20 (nm)**	**Shift (nm)**	**Fluorescence quantum yield**
Phenol	94.11	1-200	1 886	272	304	300	32	0.26
Guaiacol	124.14	1-100000	2 694	275	318	303	43	0.21
Syringol	154.16	1-60	1 029	269	351	330	82	0.06
catechol	110.10	1-200	2 822	278	321	305	41	0.17
eugenol	164.20	1-4000	10 289	260	343	333	113	0.39
vanillin	152.15	1-1000	12 078	278	-	-	-	0.04
naphthol-1	144.17	1-600	6 365	296	362	343	64	0.55
Coniferyl alcohol	180.20	1-600	14 980	267	340	332	73	0.22
Sinapyl alcohol	210.23	1-300	9 683	276	352	325	79	0.05
guaiacylglycerol-β-guaiacyl ether	320.30	1-100	4 235	279	317	304	38	0.44

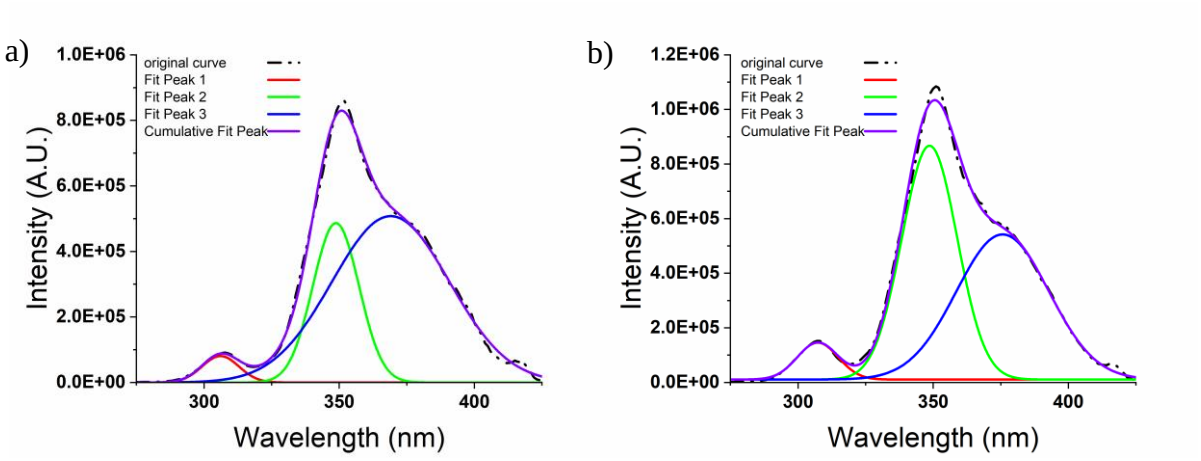

Figure S14. Example of deconvolution on UV fluorescence spectra (20nm offset) with the 3 characteristic peaks (306, 350 and 375nm), a) Pt/C catalytic liquefaction, 2 hours at 250°C, b) Pt/C catalytic liquefaction, 4 hours at 250°C

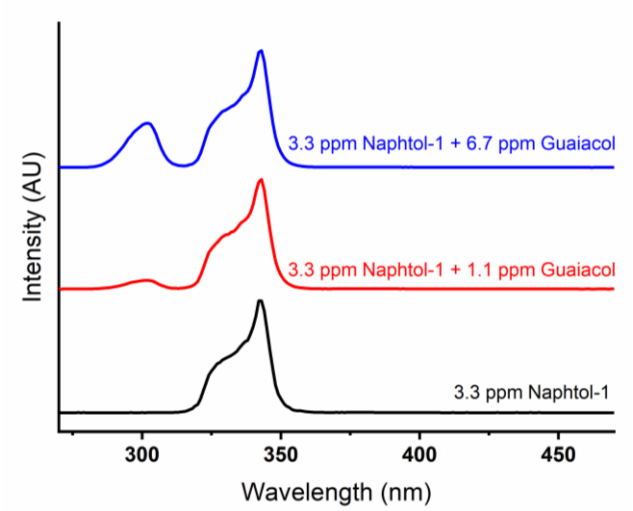

Figure S15. Effect of spiking guaiacol (1.1mg/L and 6.7mg/L of guaiacol in the final solution of ethanol) on the fluorescence spectra of naphthol (at 3.3mg/L in ethanol), 20nm offset.

Figure S15 shows that the spiking of guaiacol does not lead to a modification on the intensity or emission wavelengths on naphthol fluorescence peak because of the high dilution. The dilution in ethanol of naphthol (3.3mg/L) was set to obtain an absorption of 0.2 at 275nm. All fluorescence spectra presented in this work were acquired at such high dilution to get an absorption of 0.2 at 275nm.

7.9. - References cited in supporting information

1. S. Constant, H. L. J. Wienk, A. E. Frissen, P. de Peinder, R. Boelens, D. S. van Es, R. J. H. Grisel, B. M. Weckhuysen, W. J. J. Huijgen, R. J. A. Gosselink, et al., *Green Chemistry* **2016**, *18*, 2651–2665.

2. F. P. Bouxin, A. McVeigh, F. Tran, N. J. Westwood, M. C. Jarvis, S. D. Jackson, *Green Chemistry* **2015**, *17*, 1235–1242.

3. Z. Strassberger, P. Prinsen, F. van der Klis, D. S. van Es, S. Tanase, G. Rothenberg, *Green Chem.* **2014**, *17*, 325–334.

4. X. Huang, T. I. Korányi, M. D. Boot, E. J. M. Hensen, *ChemSusChem* **2014**, *7*, 2276–2288.

5. J.-Y. Kim, J. Park, U.-J. Kim, J. W. Choi, *Energy & Fuels* **2015**, *29*, 5154–5163.

6. A. M. Brouwer, *Pure and Applied Chemistry* **2011**, *83*, 2213–2228.

D. Effect of Technical Lignin Type and Catalyst (Ni/C, Ru/C, Pt/C) on Depolymerization Products in Supercritical Ethanol

To be submitted to Energy&Fuels, 35th years, EB special issue

Erika Bartolomei[a], Yann Le Brech[a], Frédérique Bertaud[b], Roger Gadiou[c], Loïc Vidal[c], Jean-Marc Le Meins[c], Anthony Dufour[a]*

[a] LRGP, CNRS, Université de Lorraine, 1 rue Grandville, 54000 Nancy, France

[b] Centre Technique du Papier, 341 Rue de la Papeterie, 38400 Saint-Martin-d'Hères, France

[c] Institut de Sciences des Materiaux de MulhouseIS2M CNRS UMR7361, 15 rue Jean Starcky, 68057 Mulhouse, France

* corresponding author: anthony.dufour@univ-lorraine.fr

1. - Introduction

In section B of this thesis, we have characterized various technical lignins of different origins (Kraft and Soda) with the partners of this project. These lignins were selected by the CTP as the most representative industrially available lignins. It is of high importance to compare the depolymerization of these available lignins in order to assess the feasibility of lignin depolymerization integrated in the existing pulp industries.

In section C, we have depolymerized one technical lignin (Soda lignin, Protobind) in ethanol with a Pt/C catalyst (ethanol, 250°C, 110 Bar H_2). The scope of this section was to set the analytical procedure in order to better understand the composition of products (monomers, oligomers, solids).

In this section, we use these developed analytical methods, namely 1) NMR and GPC for lignins and 2) UV fluorescence, GC/MS, GPC for the liquids, to compare 3 commercial catalysts (Ni/C, Ru/C, Pt/C) for the Kraft lignin produced by the CTP.

Then, we compare the reactivity of the different technical lignins (3 Kraft lignins and the Soda Protobind lignin) with the Ni/C catalyst.

We have previously highlighted the potential interest of our depolymerization conditions. Indeed, ethanol is a green and low cost solvent. Furthermore, ethanol in its supercritical state presents a good solubilisation of lignins and hydrogen donation behaviours.[1,2]

Table S1 presents an overview of the published work on technical lignins (Kraft or Soda) depolymerization in supercritical alcohols.

Most of the times, severe conditions were tested, namely: several hours of conversion time; temperature higher than 300°C leading to high pressures (higher than 200 Bars) to maintain the solvent at the supercritical state, etc.

These studies have shown the interest of using supercritical ethanol combined with a metal catalyst to produce phenolic species but they did not explore milder conditions of better potential for the industrial deployment of this technology. Indeed, reactor pressures not higher than about 100 Bars may be targeted for reducing the cost of the technology (see Chapter F).

These studies have also shown the potential of catalysts based on metals (Ru, Ni, Pt) deposited on carbonaceous supports. Indeed, carbons like activated carbons are stable supports under the liquefaction conditions and they may be produced by the lignin itself.[3]

Despite the numerous studies on lignin depolymerization, we did not find articles dealing with the effect of the type and structure of technical lignins under supercritical ethanol conditions.

Under other depolymerization conditions, Kraft, Organosolv and Soda lignins were compared by De Wild et al.[4] in a 2 stage process including pyrolysis and the hydrodeoxygenation of the bio-oils. They showed an important impact of the lignin type on the composition of monomers and that a direct hydrotreatment of lignin gives a higher monomers yield than the 2-stage process.

The effect of the type of lignins (hardwood, softwood, Kraft, Soda, Organosolv, etc.) was highlighted by Cabral Almada et al.[5] in a basic solution and without catalyst for oxidative (air)

depolymerization. They have demonstrated a relation between the accessible phenol moieties and inter-unit linkages and the yields of aromatic compounds.

Phongpreecha et al.[6] have related the monomer yields (after hydrogenolysis with Ni/C catalyst) for different alkali lignins as a function of their β-O-4 content. Amiri et al.[7] have completed the approach of Phongpreecha et al. by using a simple ether cleavage model to predict the final depolymerization yields in monomers. Ether linkages were analyzed by an advanced HSQC NMR method. Recently, Xiao et al.[8] have studied the effect of diverse lignins prepared from Eucaplytus with varying β-O-4 contents and phenolic hydroxyl groups on a large range. They clearly show a relation between monomers yields and β-O-4 contents. The Kraft lignin produces less than 5wt. monomers under their conditions (Pd/C, methanol, H2, 180°C, 4h).

Bouxin et al.[9] have prepared uncondensed lignins (by ammonia mild pretreatment) and more condensed ones by Soda and organosolv pulping from the same biomass (poplar). These lignins were depolymerized by Pt/Al_2O_3 under H_2, methanol/water mix, at 300°C during 2h. They have also shown that the content in β-O-4 is a crucial factor for the production of monomers but also that the depolymerization conditions must be tailored in order to reduce the secondary condensation of reactive unstable monomers.

All these studies have mainly used lignins with relatively high ether contents or with a large range of ether contents.

Despite all these extensive studies, to the best of our knowledge, there is still a lack of understanding about the effect of the structure of technical available lignins on their depolymerization under mild depolymerization conditions notably in supercritical ethanol. Indeed, the available technical lignins (Kraft and Soda) present a low content in β-O-4 linkages, so their β-O-4 content may not be their main behaviour controlling their depolymerization.

Furthermore, Pt/C, Ru/C, Ni/C catalysts have been shown of high interest for lignin depolymerization (see Table S1) but these catalysts have not yet been compared for a Kraft lignin under mild supercritical ethanol conditions (250°C, 100 Bar H_2).

Consequently, in this section, we have compared:

1) these 3 catalysts for the depolymerization in supercritical ethanol of the Kraft lignin produced by the CTP;
2) the depolymerization of 3 Kraft lignins and the Soda lignin on the Ni/C catalyst.

2. - Material and Methods

The global methodology of this section is presented in Figure 1.

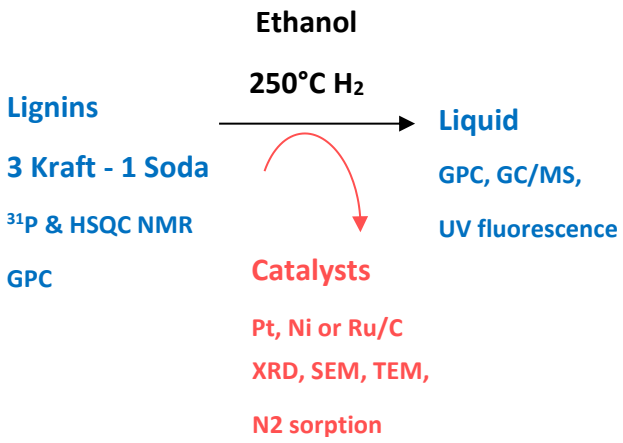

Figure 1 Analytical methods used in this section of the PhD thesis

The scope of this section is to understand the relation between the structure of the technical lignins and their depolymerised products. Therefore, the characterization of lignins by NMR and GPC are recalled and summarized. Then, lignins were converted with the same protocol as in section C: in an autoclave, at 250°C, in supercritical ethanol, 10 bar initial H_2 pressure, with the different catalysts. Catalysts were characterized before and after reaction by microscopy (SEM & TEM), XRD and N_2 sorption. The liquid products were analyzed by UV fluorescence, GPC and GC/MS.

2.1. - Characterization of the technical lignins

Table 1 Code and suppliers of the technical lignins

Name	Lignin type	Biomass	Supplier
K1	Kraft - LignoBoost "BioPiva 1100"	Pine wood	UPM Biochemicals, produced by DOMTAR, USA (Biochoice process)
K2	Kraft	Eucalyptus (leaves)	Fibria, Jacareil-Suzanno, Brazil
K3	Kraft - CTP	Pine wood	Black liquors sampled at the Facture pulp plant (mainly pine wood) and then lignin precipitated by CO_2 for this study by CTP
Soda	Soda lignin - Protobind 1000	Wheat straw	Green Value (USA) produced in India

NMR (^{31}P NMR and HSQC) and GPC methods are detailed in Supporting Information at the end of this chapter.

2.2. - Characterization of catalysts

5%wt.Ru/C and 5%wt.Ni/C were supplied by Ryogen (ref. 0139-CRuA05 and 0158-CNiA05 respectively), 5%wt.Pt/C by Sigma (ref 908010).

The morphology of the catalysts before and after reaction was characterized by Scanning Electron Microscopy (SEM) on a JEOL JSM-6490LV microscope combined with energy dispersive X-ray spectroscopy (EDX) for analysing the global composition of the particles.

Transmission Electron Microscopy (TEM) images and chemical analyses of the samples were obtained with a JEOL ARM200-CFEG microscope operating at 200 kV. The catalyst powders were dispersed into chloroform by ultrasonic treatment and the obtained suspensions were deposited on a gold observation grid covered with a film of amorphous carbon. The EDX analyses and chemical mappings were performed using a JEOL Centurio detector. The particle size distribution of metallic nanoparticles was obtained by analysing the TEM images. 50 to 100 particles were detected and their size was computed from the projected area of each particle (under the ImageJ software).

The textural properties of the catalysts before and after reaction were obtained from adsorption isotherms of N2 at 77K. The experiments were done on a Micromeritics ASAP 2420 device in the relative pressure range 10^{-7} - 1. Prior to the analysis, the samples were outgassed at 300°C

during 12 hr. The CO2 adsorption isotherms at 273K were measured on the same experimental set-up for the pristine catalysts. The surface area of the materials was obtained by applying the BET equation in the relative pressure range 0.01 - 0.05 since most samples exhibited significant amount of micropores. The total pore volume was calculated from the N2 volume adsorbed at a relative pressure of 0.99. The volumes of micropores (pore diameter below 2nm) and of narrow micropores (i.e. ultramicropores with a diameter below 0.7 nm) were obtained by applying the Dubinin-Radushkevich equation on the N2 and CO2 adsorption isotherms, respectively. Pore size distribution was obtained by using the NL-DFT model for slit pores with finite depth.

The structure of the carbon and metal phases in the catalysts was analyzed by X-ray diffraction (XRD) with a Bruker D8 Advance X-ray diffractometer. The detector was a LYNXEYE XE-T 1-D detector in high resolution mode fully opened (2.72°). The wave length used was CuKα1,2. The diffractograms were recorded for 2θ angles between 10° and 130° at a step scan of 0.014° with a step time of 1.80 s. The diffractometer used fixed divergence slits (0.03°). An automatic motorized anti-scatter screen was used for to avoid air-scattering at low angles.

2.3. - Catalytic depolymerization of the technical lignins

The liquefaction method and analysis of liquids were previously presented in details in Chapter C. Briefly, lignin liquefaction was carried out in a 300 mL autoclave. The reactor was loaded with 10 g of lignin, 200 mL of pure ethanol as solvent and Pt/C, Ru/C or Ni/C solid catalyst to reach 1% wt., metal load based on lignin mass (2.0 g of Met/C catalyst, 5% wt. of Met loading, leading to 0.1g of metal for 10g lignin).

An internal standard (100 µl hexadecane) was injected in the autoclave (with 200mL ethanol, lignin and catalyst) before the start of the reaction for a more accurate quantification of monomers present in the sampled solutions by GC/MS-FID. The autoclave was heated by the following temperature program: start temperature = 20°C, heating rate = 5 K min-1, final temperature = 250°C, 4h at 250°C, cooling time of about 35 min to room temperature. In this work, time “0” is defined once the temperature reached 250°C (first sampling). The stirrer was maintained at 400 rpm during the reaction. The liquid was sampled under isothermal condition (at 250°C) by a sampling device including high pressure valves and a fixed sampling volume (of 3 mL). The liquid line was purged 2 times before liquid sampling.

All the liquid samples were analyzed by different analytical techniques without any further manipulation (such as solvent extraction).

The catalysts and solid particles were recovered by filtration the whole remaining solution after 4 hours reaction. Char yield was calculated by subtracting the mass of catalyst.

2.4. - Analysis of liquid products

The as-sampled liquids were analyzed by (see Chapter C for all the details) :

1) GPC-UV (in THF without any acetylation);
2) GC/MS-FID by internal calibration method on an HP-5 column;
3) UV fluorescence with 20nm offset as justified in the previous section.

3. - Results

3.1. - Characterization of lignins

The main chemical compositions for the 4 lignins are presented in Table 2.

Table 2 Main chemical properties of the 4 technical lignins

Chemical properties	Lignin K1	K2	K3	Soda	Method
Mw (Da)	7600	4300	8600	4200	GPC (CTP)
CHO (wt.%) NS	65.5/5.6/21.1 <0.1/2.1	63.6/5.3/26.4 0.1/2.4	71/5.6/21.3 <0.1/2.0	64.6/5.6/25.5 0.5/0.7	CTP
Na (wt.%) K	0.16 0.01	0.17 0.04	0.28 0.15	0.09 0.04	CTP
Ali-OH (150-145ppm) Syringyl OH/ Condensed structure (144-140ppm) Guaiacyl OH / p-hydroxy phenyl OH (140 - 136 ppm) Carboxylic acid (136-132 ppm)	1.66 1.90 2.91 0.58	1.39 3.45 1.38 0.48	1.28 1.21 1.74 0.40	1.32 2.30 1.64 0.90	^{31}P NMR in mmol/g lignin
β-O-4 β-β β-5	7.4 3.6 4.6	10.0 0.8 6.5	4.6 5.4 2.5	5.6 4.2 1.2	HSQC (number of linkages for 100 aromatic rings)

Concerning their molecular weight, K2 and Soda lignins have a lower molecular weight (~4000 Da) than K1 and K3 (7600 and 8600 Da).

K1, K2 and soda lignins present a similar carbon content (65%wt.). The 3 Kraft lignins have the same sulphur content (about 2wt.%) and the Soda lignin a higher N content.

Concerning the main chemical moieties as analyzed by ^{31}P NMR, the K2 lignin presents the highest content in syringyl groups as it is produced from hardwood. K1 lignin has the highest content in guaiacyl groups. The K2 lignin presents the highest content in β-O-4 and β-5 linkages.

3.2. - Characterization of the catalysts

The catalysts were first characterized by SEM-EDX before and after lignin depolymerization (Figure 2).

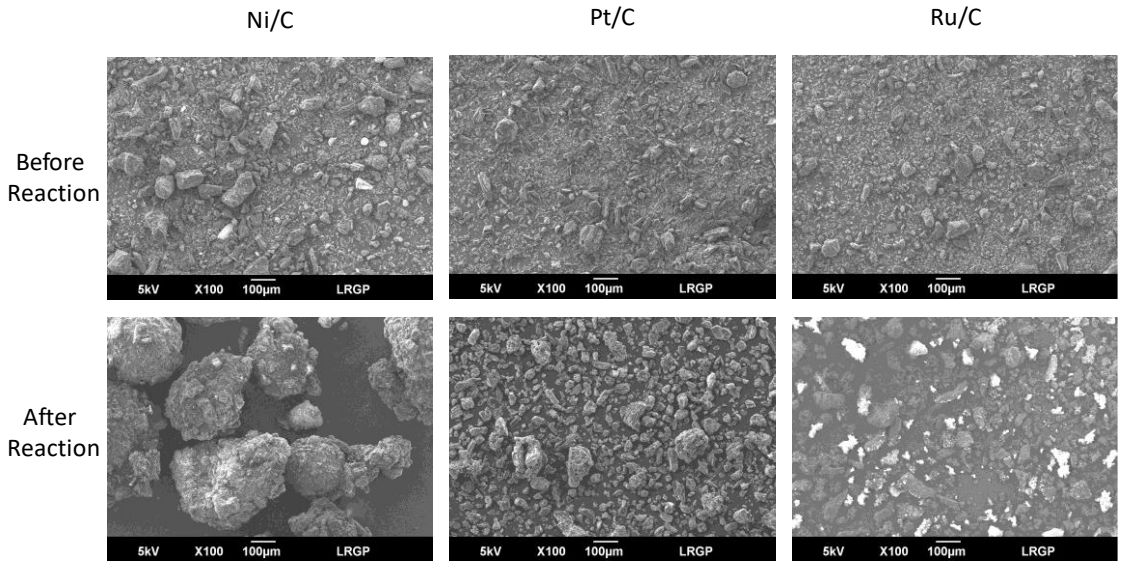

Figure 2 SEM analysis of the catalyst before and after K3 lignin depolymerization

EDX mapping of main elements (C, O, Si, metal, S, etc.) are presented supporting information at the end of the chapter.

First, these commercial catalysts present a wide range of particle sizes between about 10 and 100µm. After reaction, bigger particles are present notably for Ni/C catalyst, highlighting an agglomeration of catalyst particles by lignin-based softened and sticky intermediates.

EDX mapping (in sup. info.) clearly shows a decrease in metal content after reaction on the surface of all catalyst particles (at the µm macro-scale) and a relatively homogeneous

composition of the deposit which is mainly composed of C, O, Na, S. Because our catalysts are composed of carbon as the support of metals, sulphur and sodium are good indicators of the origin of the carbon deposit coming from lignin intermediates (2%wt. of S in K3 lignin, Table 2). Bright particles for Ru/C after reaction are due to contrast analysis issues. We checked by EDX that the composition of the particles was similar (mainly based of C, O and S from lignin deposit).

The ratio of S/metal element may be used as a broad indicator of lignin-based deposit over the catalyst particles. Pt/C and Ru/C present a lower ratio and especially Pt/C is less recovered by lignin-based deposit with still an important fraction of Pt detected by EDX after reaction.

At a smaller scale of observation, TEM highlights the global atomic structure of the carbon support (Figure 3) and the size of the nanoparticles of metals.

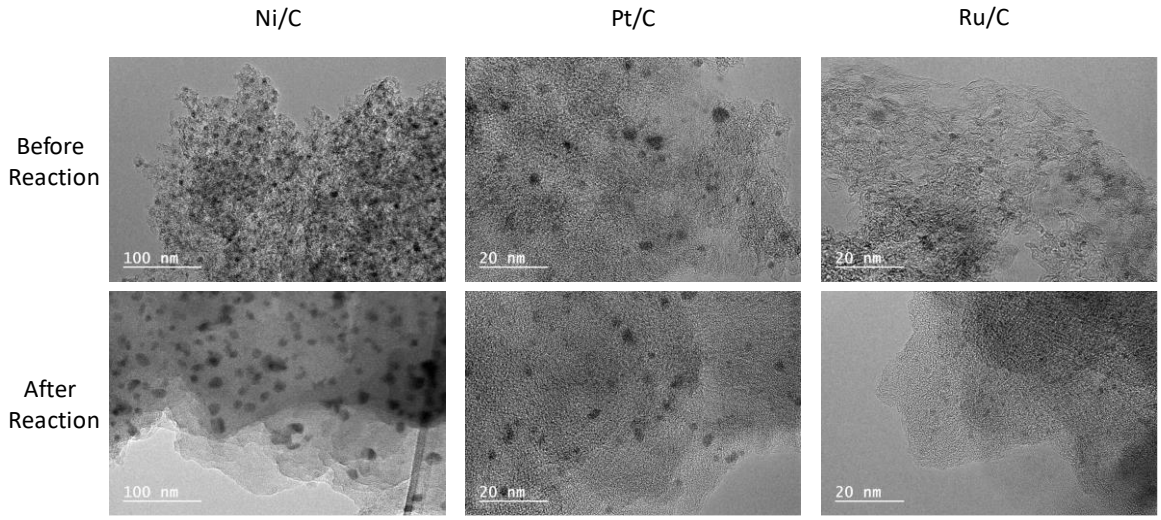

Figure 3 TEM analysis before and after K3 lignin depolymerization

The carbon support is mainly composed of microporous disordered carbons which is typical of activated carbons produced from the pyrolysis of biomass. It was not possible to discriminate by TEM the deposited carbon after reaction vs. the carbon of the support. Further analysis would be needed for instance by advanced NMR method and by XPS to identify the chemistry of the lignin-based carbon deposit.

The particle size of the metal nanoparticles is given in supplementary material. They are of 9.1nm for Ni, 2.6nm for Pt and 2.1nm for Ru before reaction. The metals and notably Pt and Ru are well dispersed in these commercial catalysts.

Metallic nanoparticles dispersed on a carbon support present different mobilities, which depend on the nature of the catalyst and on the temperature.[10] For a given metal, this mobility is correlated with the so-called Tammann temperature, defined as 50% of the fusion temperature.[11] The decrease of the catalytic activity due to the growth of the nanoparticles is strongly related to this mobility. For the three metals tested here, the Tammann temperatures are 863, 1020 and 1291 K for Ni, Pt and Ru, respectively. These values shows that the mobility of nickel nanoparticles is higher than the one of Pt and Ru nanoparticles in carbons. Beside this, a second mechanism based on dissolution-migration-recondensation, known as Ostwald ripening mechanism, can lead to an increase of nanoparticle size, and therefore to a decrease of the activity of the catalyst.[12] When the temperature increases, particle size can increase through the Ostwald ripening mechanism. Nickel catalyst exhibits a larger mean particle size compared to the two other catalysts since the stability of nickel nanoparticles is lower compared to the two other metals.

During the reaction, the dissolution step of Ostwald ripening strongly depends on the different reactions which can take place, and the migration step can occur through the fluid phase (3D mechanism) or on the catalyst surface (2D mechanism).[13] Nickel mean particles size increases from 9.1 to 12.1 nm after reaction, this sintering has been already observed e.g. for ethanol reforming reaction.[12] Due to their higher Tammann temperature, platinum and ruthenium catalysts are less impacted. The values presented in supplementary material shows that no significant increase of nanoparticle size is observed during lignin liquefaction reaction for these two materials.

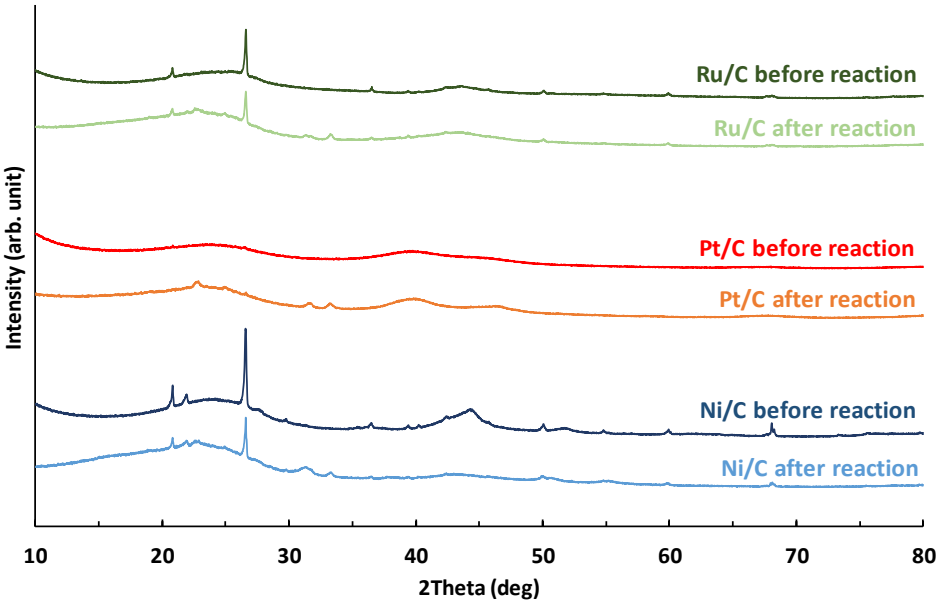

Figure 4 XRD analysis of the catalyst before and after K3 lignin depolymerisation.

XRD diffractograms of pristine and spent catalysts are presented in Figure 4. Metal nanoparticles can be detected with peaks at 44.55 and 51.91° for Ni, 39.76 and 46.24° for Pt, 44.10 and 42.18° for Ru. It was not possible to use Scherrer formula in order to calculate a mean particle diameter of the different supported catalysts since the amount of metal was too low (as show by EDX for Ni catalyst) or the particle size was too small (as shown by TEM analysis for Ru and Pt catalysts). EDX analysis showed that Ru-C and Ni-C catalysts have a significant silicon content, this is confirmed by XRD analysis which shows the presence of silica particles (mains peaks at 20.86, 26.64 and 68.2°). These peaks are somewhat lowered after reaction, showing a partial dissolution of silica. This phenomenon is more important for Ni-C material, in agreement with EDX analysis.

After reaction, several new peaks can be observed and the diffractograms are more difficult to analyze. Some peaks are related to sodium sulfate deposits with mains peaks at 22.54 and 31.19 and 33.11° (PDF 27-0791). This is in agreement with the significant content of sulphur and sodium observed by EDX in the spent catalysts coming from the lignin deposit.

The textural properties of the pristine and spent catalysts are presented in Table 3. The nitrogen adsorption isotherms are given in supporting information. Before reaction, the three catalysts have significantly different surface areas: Pt/C-BR (before reaction) exhibits a high surface area with a relatively large micropore volume (0.52 cm3/g). The mesopore volume estimated from the difference V_p-V_{N2} is also high (0.77 cm3/g). This material is typical of highly activated carbons. The Ru and Ni based catalysts have a lower surface area, with a lower micropore volume and also a lower mesopore volume. It must be noticed that the three catalysts have a very similar volume of ultramicropores which is obtained from CO_2 adsorption isotherm. This is typical of carbon materials with a very low level of organisation. It shows also that the microporous volume of Pt/C-BR material is mainly composed of the so-called super-micropores with a size between 1 and 2 nm.

After reaction, the surface areas and porosities of the catalysts are strongly decreased. In the case of ruthenium and nickel catalysts, the materials are even no more porous. Pt/C-AR keeps a surface area of 103 m2/g, as for the other catalysts, the micropore volume as decreased to a very low, but not null, value and, contrary to the two others, some small mesopores are still observed in the platinum catalyst.

The distribution of pore sizes as determined by NL-DFT is presented in supplementary material. It clearly shows the plugging of the majority of pores with a lower plugging of pores (> 5nm) for Pt/C catalyst. This is in agreement with a lower deposit of lignin-based carbon over Pt/C detected by SEM-EDX.

Table 3 Total pore volume (Vp), BET surface area (SBET), micropore volume (VN_2) and ultramicropore volume (VCO2) for pristine and spent catalysts after K3 lignin depolymerization

	V_p (cm^3/g)	S_{BET} (m^2/g)	V_{N2} (cm^3/g)	V_{CO2} (cm^3/g)
Pt/C-BR (before reaction)	1.29	1541	0.52	0.25
Pt/C-AR (after reaction)	0.17	103	0.04	-
Ru/C-BR	0.68	757	0.30	0.21
Ru/C-AR	0.01	7	0.00	-
Ni/C-BR	0.64	910	0.34	0.24
Ni/C-AR	0.02	16	0.00	-

3.3. - Effect of catalyst (Ni/C, Ru/C, Pt/C) on Kraft lignin liquefaction

Table 4 Yield char, yield monomer (GC/MS) after 4 hours of reaction at 250°C

Type of lignin	K3	K3	K3	K3
Catalyst	no cata	1% Ru	1% Ni	1% Pt
Char (%wt)	46.7	22.5	27.7	15.0
Monomers (%wt)	2.4	4.1	4.7	5.1

Table 4 shows that the char yields are importantly decreased by the 3 catalysts and especially for the Pt/C catalyst. This result is in very good agreement with previous work of Kim et al.[14,15].Pt/C is known as a good catalyst to promote the cleavage of ether bonds but also C-C bonds. It also promotes the transfer of H atoms (from ethanol) to stabilize the broken reactive bonds and therefore to reduce secondary condensation reactions, leading to char (see the previous Chapter C).

The monomer yields as determined by GC/MS is about doubled by the 3 catalysts vs. the uncatalyzed test but these yields (of about 5wt.%) are still low due to the relative mild conditions selected in this work (250°C to get a pressure lower than 110 Bar).

Concerning the average molecular weight of the liquid products soluble in ethanol, the GPC results are presented in supplementary material. Globally, the liquids present a similar molecular weight of about 800 Da for all conditions. This result confirms our proposed mechanism in Chapter C that an “oligomeric pool” exists and here, we show that this pool is present whatever the catalyst used. These 3 catalysts present micropores with important diffusion limitations for the transfer of lignin and oligomers. Lignin and oligomers conversion are likely to occur at liquid state or on the external surface of the catalyst (as highlighted by the deposit over catalysts by SEM analysis). Then, the catalysts rather act for promoting H transfer reactions from ethanol conversion and on monomers stabilisation.

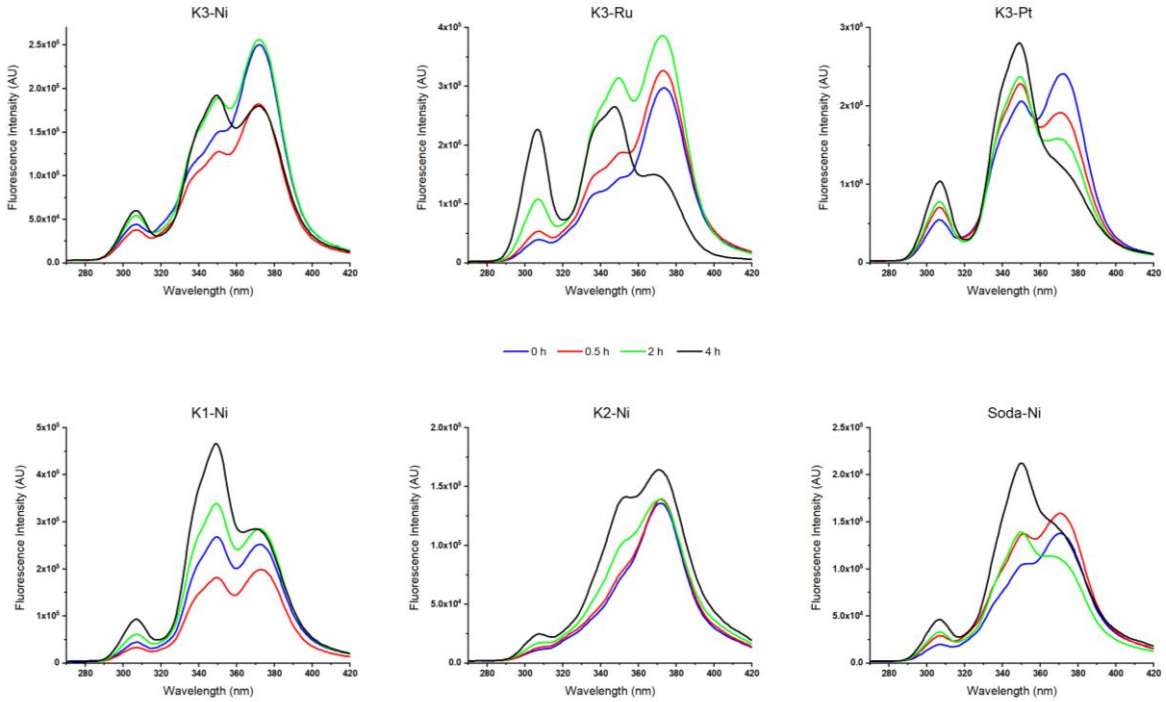

Figure 5 Evolution of the UV fluorescence spectra as a function of time for all studied conditions

UV fluorescence (Figure 5) presents a clear different behaviour of the 3 catalysts upon the time of conversion. We have shown in the previous section that the emission peaks display at 1) 380nm big oligomers soluble in ethanol, 2) 340-350nm smaller oligomers and 3) 305nm monomers.

For all catalysts (as well as for the uncatalysed test), the peak at 380nm is the major one up to the first 30 minutes. Then the peak of oligomers becomes the major one after 2hours time of stream for Pt/C, confirming that this catalyst promotes the depolymerization of the oligomeric soluble pool. Then the monomeric peaks increase as a function of time of stream and it is higher for Pt and Ru/C vs. Ni/C catalyst. Pt/C and Ru/C present a much lower contribution of oligomers vs. Ni/C after 4 hours of reaction which is again consistent with the known higher reactivity of Pt and Ru for hydrogenation and cracking reactions.

Concerning the molecular composition of monomers, Figure 6 shows that Ru and Pt/C form more saturated alkyl phenolic monomers than Ni/C. Ni/C presents a lower catalytic activity to hydrogenate the double bonds on the side chains of the phenolic monomers.

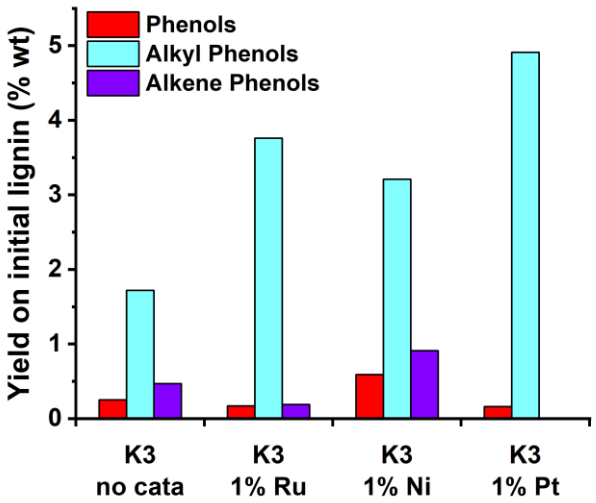

Figure 6 Alkyl, alkene & not substituted phenols yields (wt.%) for the 4 conditions after 4h.

The detailed GC/MS results for the 3 catalysts are presented in supporting information.

Figure 7 presents the mass yields of main monomers after 4 hours of K3 lignin conversion over the 4 conditions.

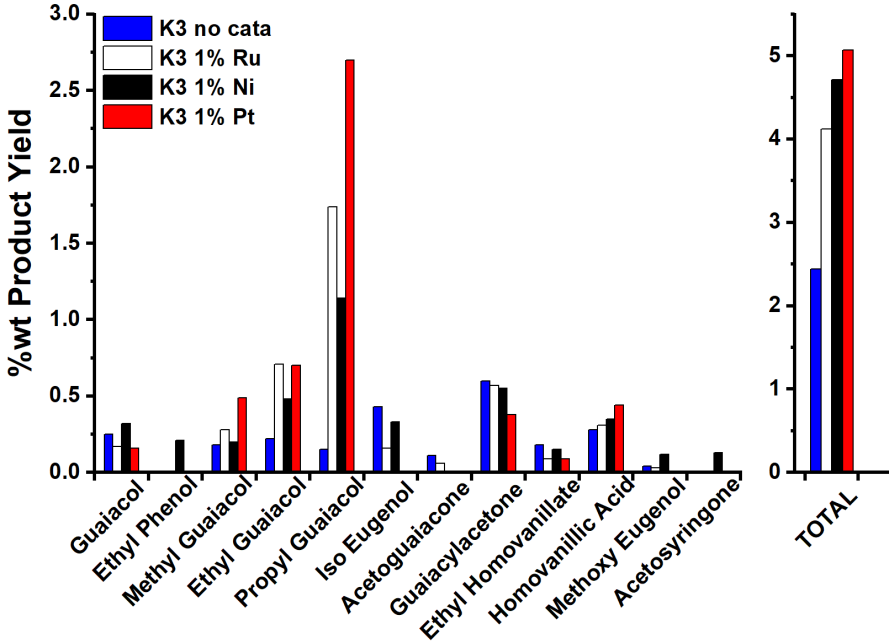

Figure 7 Mass yields of major molecules for 4 conditions after 4hours of K3 lignin depolymerization

It is interesting to notice the Pt and Ru/C catalysts promote the formation of propyl guaiacol by a factor of more than 10 despite their relatively low mass yields (1%wt. of metal vs. the mass of lignin). Ethyl guaiacol is also an important molecule promoted by the 3 catalysts. All the main monomers are based on guaiacyl groups which is consistent with the NMR analysis of the K3 lignin, originated from Pine pulping.

In order to better understand the formation of these molecules, the evolution of the main monomers sampled upon the time of conversion at 250°C is presented in Figure 8.

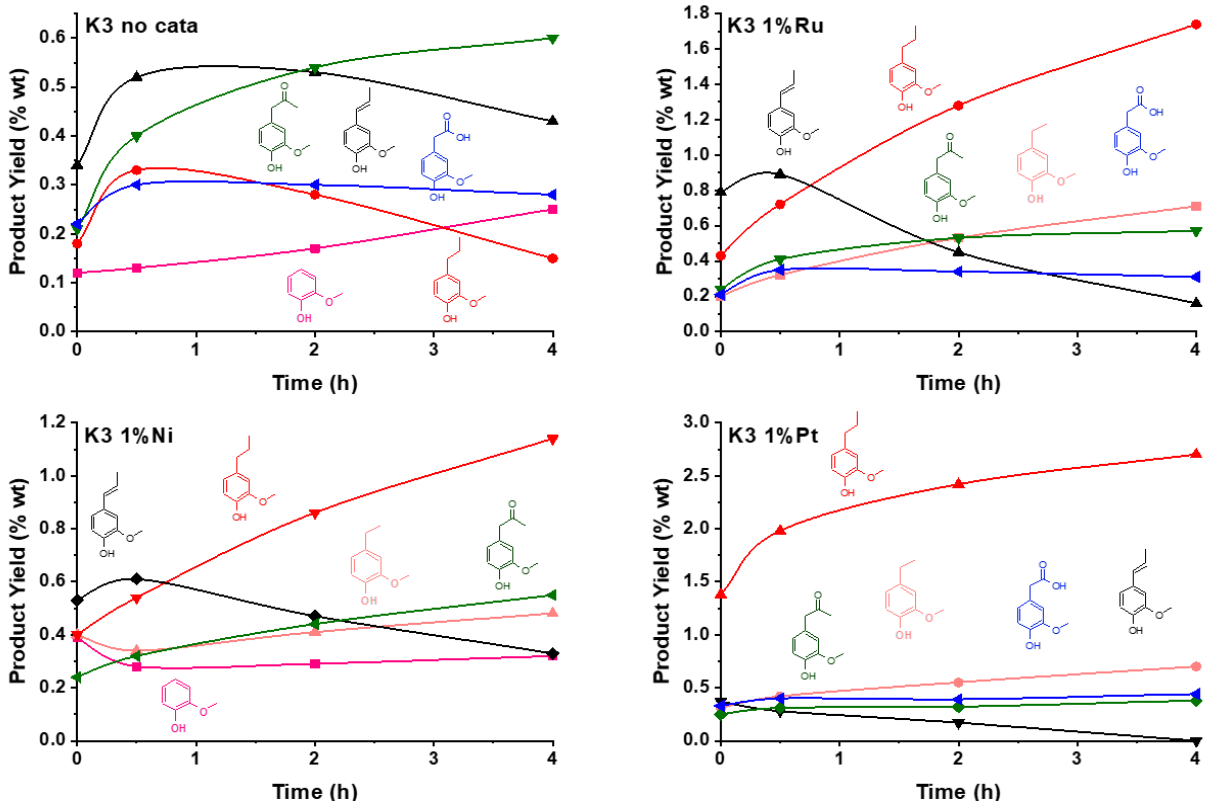

Figure 8 Main monomers as a function of time of stream (lignin K3 conversion at 250°C, ethanol, H_2).

Concerning the uncatalyzed experiment, the methoxyphenols with a ketone or a carboxylic side chain are stable and the major products. As previously discussed in the previous section, these compounds may be formed by the cleavage of β-O-4 linkages through H-transfer hydrogenolysis of an intermediate pentacyclic ether bond.[16]

The Ni and Ru based catalysts present a similar behaviour with progressive increase of propyl-guaiacol upon the time of conversion at the expense of iso-eugenol. Ru/C shows a higher ability to hydrogenate the propenyl chain of isoeugenol than the Ni/C catalyst. Pt/C exhibits a different behaviour with propyl-guaiacol as the major component at the early stage of conversion.

First, we showed that all catalyst particles are recovered by a lignin-based deposit leading to pores plugging and fast deactivation. Therefore, cheap catalysts must be looked for.

For the 3 catalysts, an oligomeric pool is present as highlighted by GPC and UV fluorescence. The depolymerization of this pool is promoted by the catalysts, likely on their external surface (as highlighted by the deposit over catalysts by SEM analysis). The catalysts also act for promoting H transfer reactions to stabilise monomers. They present an important effect on the yield in monomers and notably on propyl-guaiacol by catalysing the hydrogenation of alkene side chains of monomers (like iso-eugenol). But the yield in monomers are still low under our mild conditions whatever the catalyst used.

3.4. - Effect of technical lignin types on their liquefaction with Ni/C

It is important to better understand the effect of the source of the technical lignins on depolymerization products. We have chosen to compares the lignins on Ni/C catalyst as it presents a similar yield in monomers as the other catalysts but with a less precious metal than Pt or Ru.

Table 5 presents the char and monomer yields for the 4 lignins.

Table 5 Yields of char and monomers

Type of lignin	K3	K1	K2	Soda
Catalyst	1% Ni	1% Ni	1% Ni	1% Ni
Char (%wt)	27,7	32,8	10,0	26,1
Monomers (%wt)	4,7	2,2	4,2	4,9

The char yield is 3 times lower (10wt.%) for the K2 lignin. This point may be explained by the combination of different behaviours: a lower molecular weight, higher β-O-4 content and more syringyl unit which are known to be more reactive than guaiacyl one and less prone to condensation reaction and char formation.

UV fluorescence shows a higher contribution of lighter oligomers for K1 and Soda lignins after 4 hours conversion.

The monomer yields cannot be related to the ether content of the lignins (see Table 2) contrary to previous studies on less condensed lignins (with a larger range of β-O-4 content). K1 lignin presents the lowest yield in monomers. Monomers yields cannot even be related to the initial molecular weight of the lignins. Under our conditions of technical lignins mild conversion in supercritical ethanol, we did not succeed to rationalize the effect of lignins structure on monomer or char yields. Under our conditions, lignin conversion may be controlled by other parameters, like mass transfers to catalyst surface, but not by the initial chemical structure. We have checked the good solubility of the 4 lignins in ethanol. Their conversion might also depend on the conformation of lignin and oligomeric pool under liquefaction conditions (at 250°C) and therefore to the local accessibility of chemical bonds to the external surface of catalysts. Further studies are still needed with in-situ analysis to better understand lignin liquid-phase conversion.

Nevertheless, the chemistry of the technical lignins is not well related to char or global monomer yields but it has an important impact on the composition of monomers.

Figure 9 presents the main chemical families of monomers for the 4 lignins. All lignins produce more alkyl phenols than alkene ones with the Ni/C catalyst. K1 produces a very low yield in unsubstituted phenols.

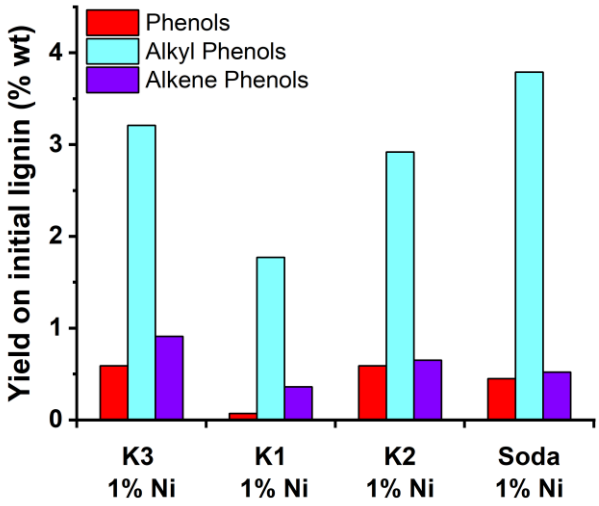

Figure 9 Alkyl, alkene & not substituted phenols yields (wt.%) for the 4 conditions after 4h.

Figure 10 presents the breakdown of major monomers.

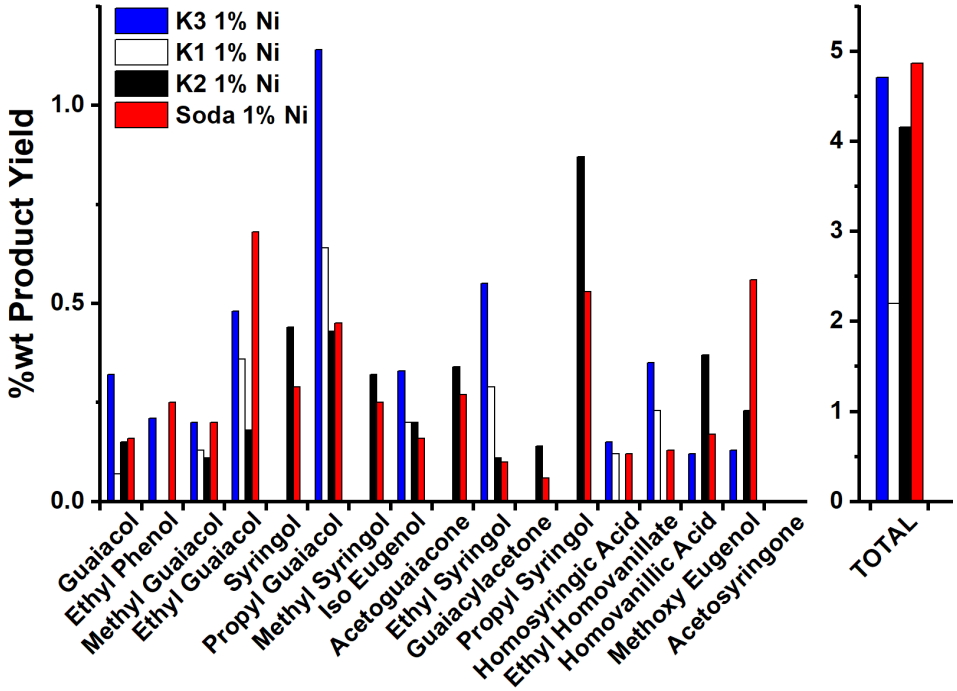

Figure 10 Mass yields of major molecules for the 4 lignins with Ni/C catalyst after 4hours of conversion.

The K2 and Soda lignins form an important yield in propyl-syringol which is in-line with their higher syringyl content as analyzed by NMR. Syringol and propyl syringol are not detected for K3 and K2 lignins whereas ethyl syringol is produced by all lignins. The K3 lignin produces the highest yield in propyl guaiacol. The formation of these products as a function of conversion time is displayed in Figure11.

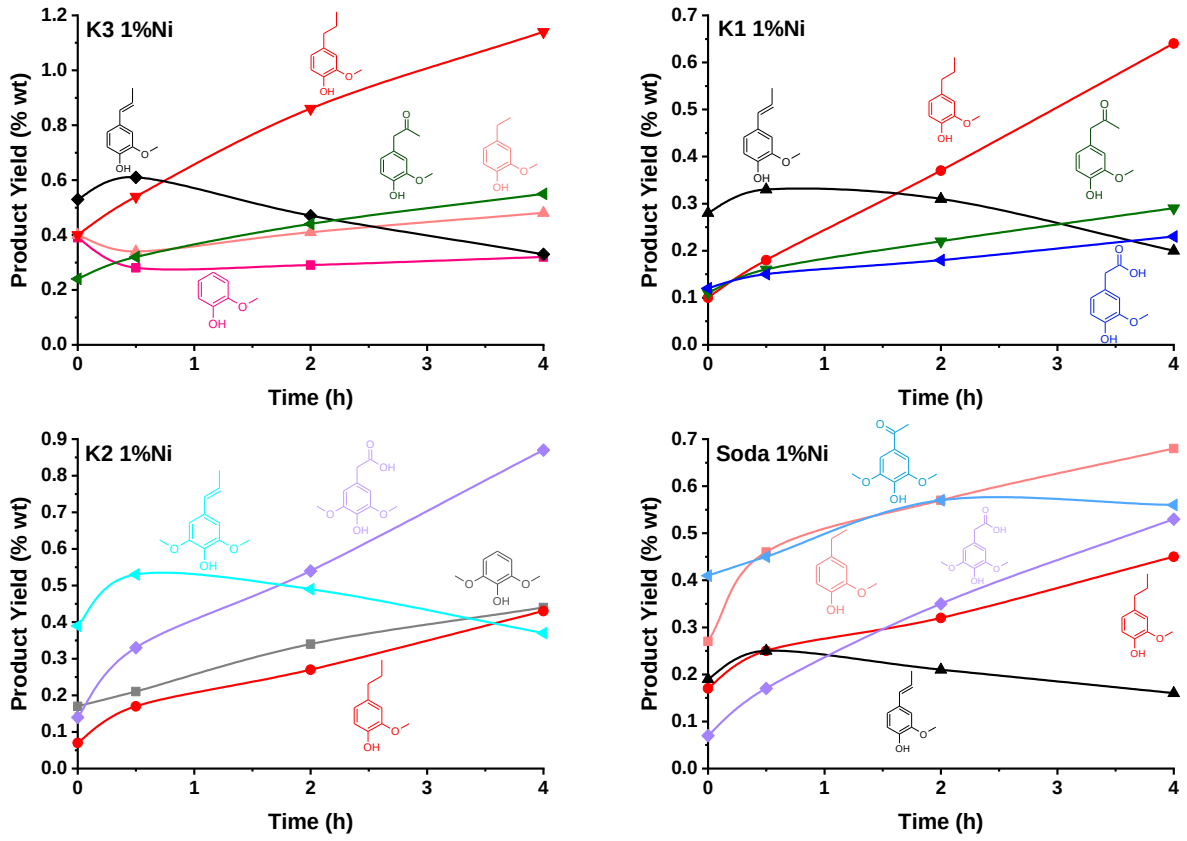

Figure 11 Main monomers as a function of time of stream (different lignins, Ni/C, conversion at 250°C, ethanol, H_2).

For all lignins, alkene phenols are first formed and then hydrogenated. Alkyl guaiacols are progressively formed.

The carboxylic acid side chain in the homosyringic acid is progressively formed for K2 and Soda lignins. The mechanism of formation of this molecule is still unclear.

To summarise, K3 and K1 lignins present similar patterns with a progressive formation of propylguaiacol as a major compounds. These 2 lignins are produced from the same wood (Pine) and they present similar composition (close S/G ratio, etc.). But K1 produces much less monomers than K3. This lower reactivity is not related to the ether bonds present in K1 (slightly higher than in K3).

Soda and K2 lignins exhibit a different behaviour than K3 and K1 producing more syringyl monomers because they present higher S/G ratio (by NMR). Carboxylic acid side chains are progressively produced by these 2 lignins.

4. - Conclusions

The main conclusions of this section are the followings:

1) 3 commercial catalysts (Ni, Ru, Pt/C) were characterized before and after lignin deplymerization.
2) They all present an important plugging of pores with a deposit of a lignin-based carbonaceous deposit over the catalyst particles. Therefore, cheap catalysts and with large pores must be looked for.
3) The 3 catalysts promote significantly the production of monomers and notably of propyl-guaiacol. They promote the hydrogenation of the side chains of phenols. But the monomer yields are still low (<5wt.%) for all catalysts and an oligomeric pool still dominates the composition of the liquids (as analyzed by UV fluorescence).
4) All our technical lignins present a highly condensed nature with a low content in ether bonds. The relation between ether bonds content and monomer yields established by previous studies (on a larger range of ether bond contents) does not perform for these lignins and our conditions.
5) Important differences between lignins are evidenced on the formation profile of some monomers and notably on syringyl/guaiacyl species which are well related to S/G ratio analyzed by NMR. Carboxylic acid side chains are progressively produced by Soda and K2 lignins.
6) The monomers yields are still low for all conditions studied under manageable pressure for industrial reactors under supercritical ethanol conditions (~100 Bars maximum).

Therefore, more efficient low cost catalyst must be looked for or the target for technical lignin depolymerization products may be rather oligomers instead of monomers.

5. - References

1. Yang, J., Zhao, L., Liu, S., Wang, Y. & Dai, L. High-quality bio-oil from one-pot catalytic hydrocracking of kraft lignin over supported noble metal catalysts in isopropanol system. *Bioresour. Technol.* **212**, 302–310 (2016).

2. Huang, X., Korányi, T. I., Boot, M. D. & Hensen, E. J. M. Ethanol as capping agent and formaldehyde scavenger for efficient depolymerization of lignin to aromatics. *Green Chem.* **17**, 4941–4950 (2015).

3. Olcese, R. N., Francois, J., Bettahar, M. M., Petitjean, D. & Dufour, A. Hydrodeoxygenation of Guaiacol, A Surrogate of Lignin Pyrolysis Vapors, Over Iron Based Catalysts: Kinetics and Modeling of the Lignin to Aromatics Integrated Process. *Energy Fuels* **27**, 975–984 (2013).

4. de Wild, P. J., Huijgen, W. J. J., Kloekhorst, A., Chowdari, R. K. & Heeres, H. J. Biobased alkylphenols from lignins via a two-step pyrolysis - Hydrodeoxygenation approach. *Bioresour. Technol.* **229**, 160–168 (2017).

5. Cabral Almada, C. *et al.* Oxidative depolymerization of lignins for producing aromatics: variation of botanical origin and extraction methods. *Biomass Convers. Biorefinery* (2020) doi:10.1007/s13399-020-00897-6.

6. Phongpreecha, T. *et al.* Predicting lignin depolymerization yields from quantifiable properties using fractionated biorefinery lignins. *Green Chem* **19**, 5131–5143 (2017).

7. Amiri, M. T., Bertella, S., Questell-Santiago, Y. M. & Luterbacher, J. S. Establishing lignin structure-upgradeability relationships using quantitative 1H–13C heteronuclear single quantum coherence nuclear magnetic resonance (HSQC-NMR) spectroscopy. *Chem. Sci.* **10**, 8135–8142 (2019).

8. Wang, S. *et al.* Unlocking Structure–Reactivity Relationships for Catalytic Hydrogenolysis of Lignin into Phenolic Monomers. *ChemSusChem* **13**, 4548–4556 (2020).

9. Bouxin, F. P. *et al.* Catalytic depolymerisation of isolated lignins to fine chemicals using a Pt/alumina catalyst: part 1—impact of the lignin structure. *Green Chem.* **17**, 1235–1242 (2015).

10. Devi, T. G. & Kannan, M. P. Nickel Catalyzed Air Gasification of Cellulosic CharsJump in Reactivity. *Energy Fuels* **15**, 583–590 (2001).

11. Baker, R. T. K. The relationship between particle motion on a graphite surface and Tammann temperature. *J. Catal.* **78**, 473–476 (1982).

12. Haasterecht, T. van, Swart, M., Jong, K. P. de & Bitter, J. H. Effect of initial nickel particle size on stability of nickel catalysts for aqueous phase reforming. *J. Energy Chem.* **25**, 289 (2016).

13. Wynblatt, P. & Gjostein, N. A. Supported metal crystallites. *Prog. Solid State Chem.* **9**, 21–58 (1975).

14. Kim, J.-Y. *et al.* Catalytic depolymerization of lignin macromolecule to alkylated phenols over various metal catalysts in supercritical tert-butanol. *J. Anal. Appl. Pyrolysis* **113**, 99–106 (2015).

15. Kim, J.-Y., Park, J., Kim, U.-J. & Choi, J. W. Conversion of Lignin to Phenol-Rich Oil Fraction under Supercritical Alcohols in the Presence of Metal Catalysts. *Energy Fuels* **29**, 5154–5163 (2015).

16. Besse, X., Schuurman, Y. & Guilhaume, N. Reactivity of lignin model compounds through hydrogen transfer catalysis in ethanol/water mixtures. *Appl. Catal. B Environ.* **209**, 265–272 (2017).

17. Jongerius, A. L. *et al.* Stability of Pt/γ-Al $_2$ O $_3$ Catalysts in Lignin and Lignin Model Compound Solutions under Liquid Phase Reforming Reaction Conditions. *ACS Catal.* **3**, 464–473 (2013).

18. Huang, X., Korányi, T. I., Boot, M. D. & Hensen, E. J. M. Catalytic Depolymerization of Lignin in Supercritical Ethanol. *ChemSusChem* **7**, 2276–2288 (2014).

19. Huang, X. *et al.* Catalytic Depolymerization of Lignin and Woody Biomass in Supercritical Ethanol: Influence of Reaction Temperature and Feedstock. *ACS Sustain. Chem. Eng.* **5**, 10864–10874 (2017).

20. Zhou, M. *et al.* Catalytic in Situ Hydrogenolysis of Lignin in Supercritical Ethanol: Effect of Phenol, Catalysts, and Reaction Temperature. *ACS Sustain. Chem. Eng.* **6**, 6867–6875 (2018).

6. - Supporting Information

6.1. - Bibliography

Table S1 Overview of technical lignins (Kraft or Soda) catalytic conversion in alcohols

Reference	Lignin	Catalyst	Solvent	T-P-t	Characterization	Main results
Jongerius, 2013[1]	Organosolv, Kraft & bagasse lignin	Pt/Al_2O_3, then CoMo/Al_2O_3 & Mo_2C/CNF	Ethanol-water	2 stages: 225°C-58Bar, 2h, then 350°C-55Bar H2 - 4h for HDO of oils	GC & GPC	9wt.% monomer
Huang, CSSC2014[2]	Protobind P1000	CuMgAlOx, MgAlOx, PtMgAlOx, NiMgAlOx	EtOH	300°C; 0-8h	GC-MS, HSQC NMR, GPC	monomers 4-23 %wt, char 0-40 %wt
Huang, ACSSus2017[3]	Protobind P1000	Cu20MgAl	EtOH	200-420°C; 4-20h	TGA (char), CHO, GC-MS, GPC, XRD and CO2-TPD(catalyst)	if not supercritical> no monomers; up to 60%wt monomers (not all aromatic) at 380°C+cata
Huang, GreenChem2015[4]	Protobind P1000, Alcell, Kraft	Cu20MgAl	EtOH, MeOH	300-380°C; 4-8h	GC-MS, HSQC NMR, GPC	up to 60%wt monomers (not all aromatic) at 380°C+cata
Zhou, ACSSus2018[5]	Kraft	Ru/C	EtOH +Phenol	230-310°C; 1-10h	CHONS, GPC, BET, XPS, ICP-AES, TGA, XRD, NH3/CO2-TPD	35-40%wt bio-oil

Limarta, JIEC2018	Kraft; Organosolv	Ru/C 10%wt	EtOH	350°C; 4h	GC-MS-FID; GPC; CHONS	88%wt bio-oil; 5%wt monomers
Kim, RSCAdv2017[6]	Soda	Ru/C 5%wt	EtOH	350°C; 40min	GC-MS, HSQC NMR, GPC	62 to 81 %wt lignin oil; 3,4-10 %wt monomers (acetone-fractionated lignin)
Kim, E&F2015[7]	Protobind 1000	Pt/C, Ru/C, Ni/C 5%wt	EtOH	350°C; 40min	GC-MS, HSQC NMR, GPC, CHON	10 %wt monomers for all the catalysts in EtOH, less char with Pt/C
Park, RSCAdv2016[8]	Protobind 1000	Pt/C 5%wt	EtOH	350°C; 40min	cata: FE-SEM, BET, XRD, XPS and HR-TEM. Oil: GC-MS, GPC, CHON	80 %wt lignin-oil
Yang, BioTech2016[9]	Kraft	Pt/C, Ru/C 5%wt	Isopropanol	270–350 °C; 1–5 h	GC-MS, HSQC NMR, GPC, HHV	72-100 %wt bio-oil
Kloekhorst, ACSSus2015[10]	Alcell	Ru/C	EtOH	400°C; 4h	GC-MS, C NMR, GPC	
Xiao et al. 2020[11]	Various lignins from Eucalyptus	Pd/C	MeOH	180°C, 4h	GC-MS, HSQC NMR, GPC	Relations between □-O-4 and phenol OH contents and monomers yields

6.2. - Characterization of lignins

6.2.1. - GPC analysis of lignins

This analysis was conducted by the CTP.

Eluent : DMAc/LiCl (0.5% LiCl in anhydrous DMAc) , 0.5 mL/min

Detector : UV 280 nm

2 columns in series : Waters Styragel 300 Mm x 7.8 mm : 1 [100 – 5 000 Da] and 2 [5 000 – 600 000 Da] ; columns maintained at 60°C,

Injection volume: 20 µL

Standards: Polystyrene 5 g/L in eluent (8 standards between 1 140 to 150 000 g/mol)

Sample preparation: lignin solution at 4 g/L in eluent, 48h of stirring, diluted before filtration (0.22 µm) and injection (d1/25 or d1/50).

Table S2 Molecular weights of the four lignins.

Lignin code	Mn (Da)	Mw (Da)	PD (Mw/Mn)
K1	4600	7600±400	1,65
K2	2950	4300±500	1,46
Soda	2790	4200±100	1,5
K3	4675	8600±500	1,84

6.2.2. - ^{31}P NMR analysis

Lignin samples were dried at 105°C overnight. Approximately 25mg were used for each analysis. Lignin samples were weighed in to a 5ml volumetric flasks. A solvent mixture of pyridine(99.9%)/$CDCl_3$ (1.6/1 v/v) was prepared in a 20ml volumetric flask. We introduced 8ml of pyridine (w.ap: 7.88g for density of 0.978) and 5ml of CDCl3 (7.5g for density of 1.5). This mixture was use for further preparation/dissolution. A solution of chromium (III) acetylacetonate and cyclohexanol were prepared in a solvent mixture of pyridine(99.9%)/$CDCl_3$ (1.6/1 v/v).

Approximately 36mg of Chromium (II) and 40mg of cyclohexanol were weighed into a 10ml volumetric flask and 10ml of Pyridine/$CDCl_3$ mixture was added. This mixture was stirred in order to dissolve the Chromium. Cyclohexanol must be introduce with extremely precaution because any error could change extensively quantification.

400µL of Pyridine/$CDCl_3$ were added to the solid lignin. The solvent mixture was introduced carefully into the 5ml flask and flask was stirred by hands until complete dissolution. 150µL of chromium/cyclohexanol solution was introduced into the 5ml flask. The lignin solution was then mixed. Minutes before the NMR experiments, 50µL of TMDP (2-chloro-4,4,5,5-tetramethyl-1,3,2-dioxaphospholane) was added to the 5ml flask. The flask was shaken (slowly)

by hands for 1-2 minutes. The solution was transferred into a 5mm NMR tube. Each sample was prepared before analysis to avoid chemical evolution during storage.

NMR measurements were performed on a Bruker 300MHz (31P resonance of 121.5MHz). The following acquisition parameters were used: 200 scans, 25s relaxation delay, 62ppm spectral width.

The quantification of OH groups has been done based on the internal standard (cyclohexanol 144.4ppm). The signal assignments were realised as follow (Table S3).

Table S3 Hydroxyl function assignments for 31P NMR

Functions	Integration range (ppm)
Aliphatic OH	150-145
Cyclohexanol	144.6-144.2
Syringyl OH / C5 Condensed structure	144-140
Guaiacyl OH / p-hydroxy phenyl OH (140 - 136 ppm)	140 - 136
Carboxylic acid	136-132

We combined the Syringyl OH moieties with condensed 5-substitued phenolic units in order to prevent the over-estimation of S-units. For some spectra Guaiacyl units was overlapped with free hydroxyl phenyl OH signal. Generally G units are combined with hydroxyl (H units). In other words, the estimation of S/G/H ratio is not possible for these technical lignins by this ^{31}P NMR method.

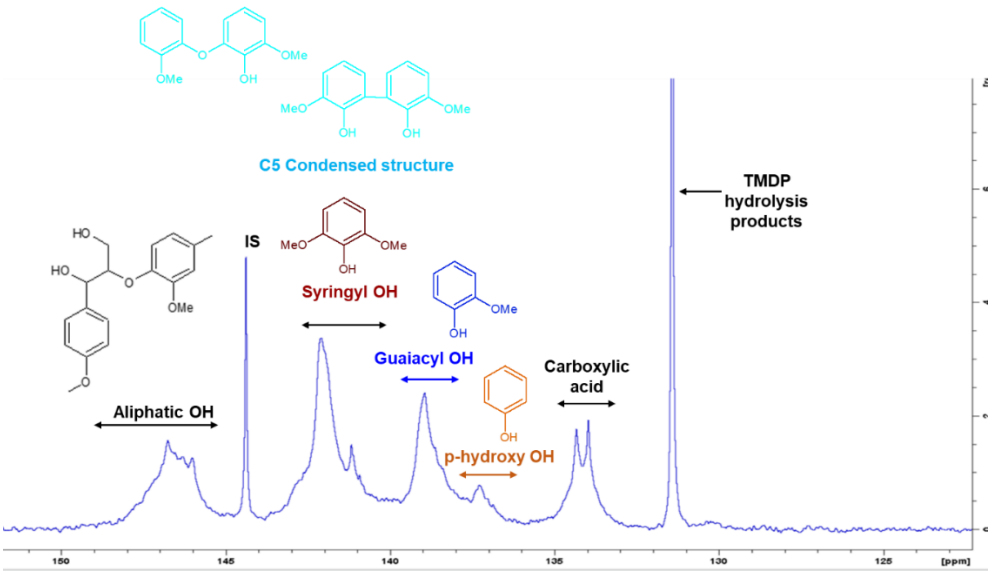

Figure S1 functional group analysis of Soda lignin by quantitative 31P NMR after phosphitylation

Observation: Soda lignin is composed by S/G/H free hydroxyl units. S signal overlapped signal for C5 substitued functions. So we did not attempt the estimation of S units. Peak at 141.15 ppm could be lignins 5-5 condensation.

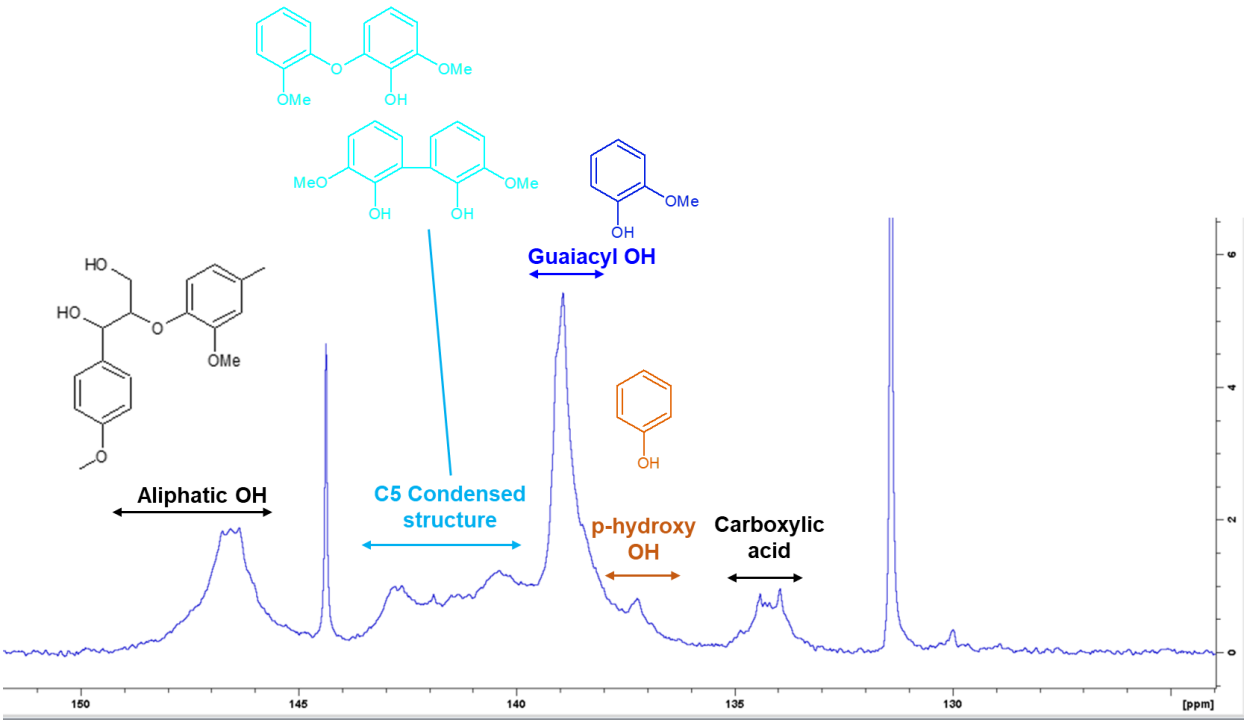

Figure S2 Kraft1 (Southern Pine) 31P NMR

Observation: No S units are detected (normal for Pine lignin).

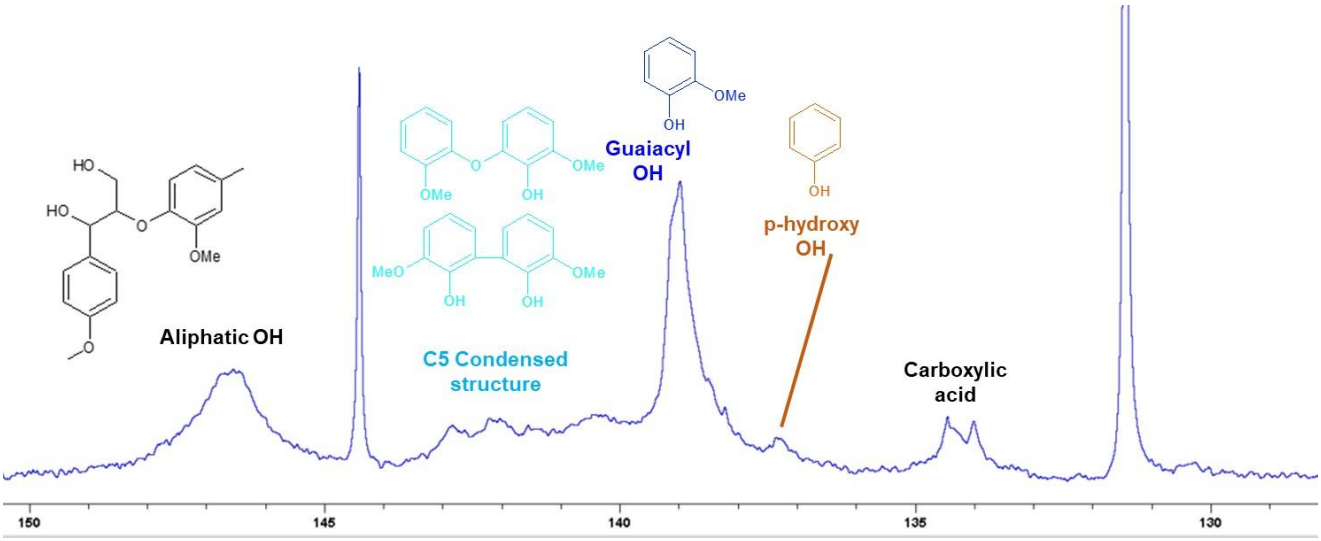

Figure S3 Kraft3 lignin 31P NMR

Observations : G units seems to be the more important units. C5 condensed units are observed and small amount of S units seems to be detected.

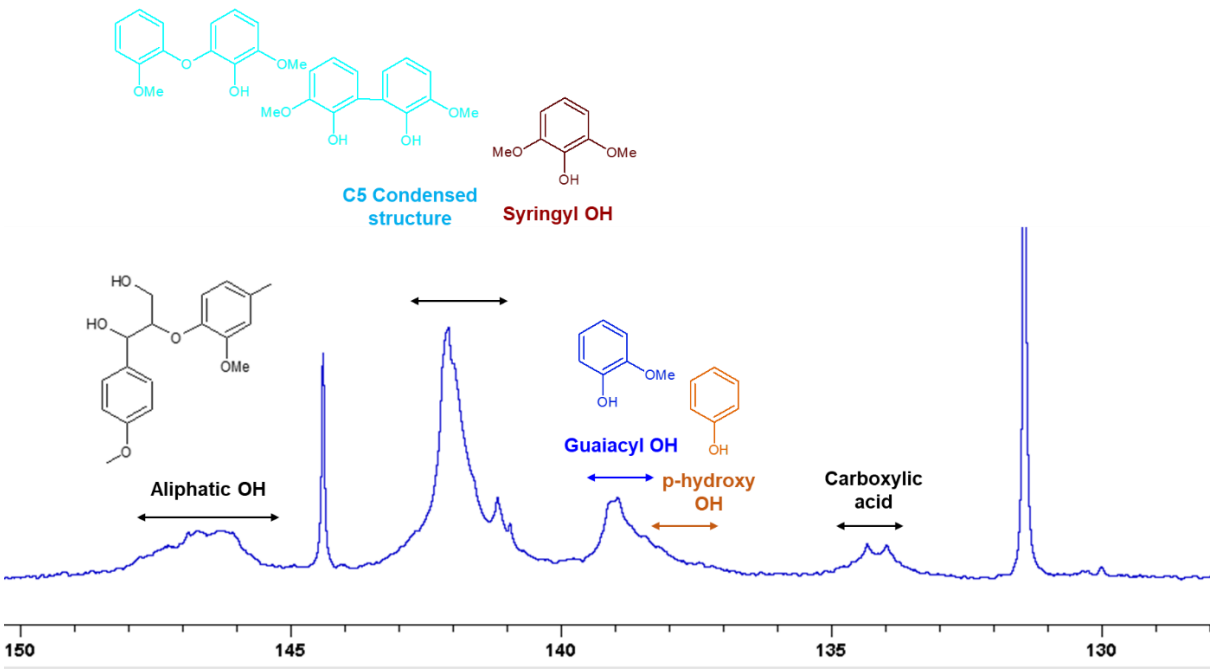

Figure S4 Kraft2 (Eucalyptus) from 31P NMR

Observations: G and H free OH units content is lower than other Kraft. The S free units are the most important unit for this lignin.

6.3. - Results of catalyst characterization

Higher resolution SEM pictures:

Ni/C before **Ni/C after**

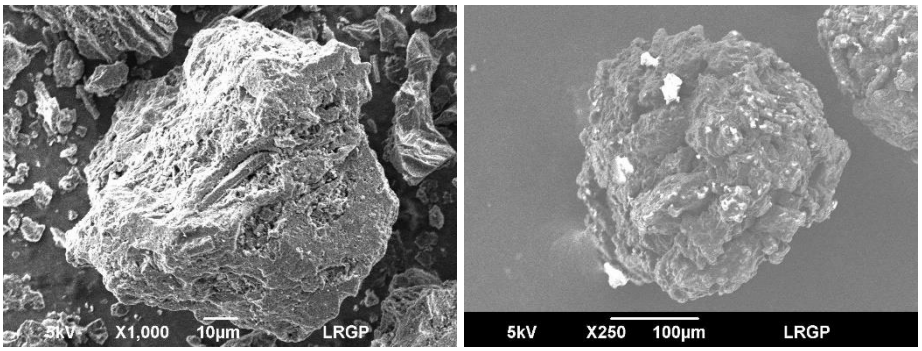

Pt/C before **Pt/C after**

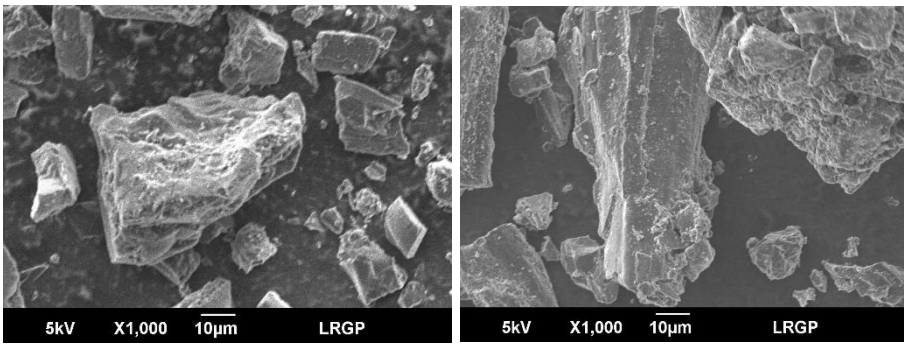

Ru/C **Ru/C after**

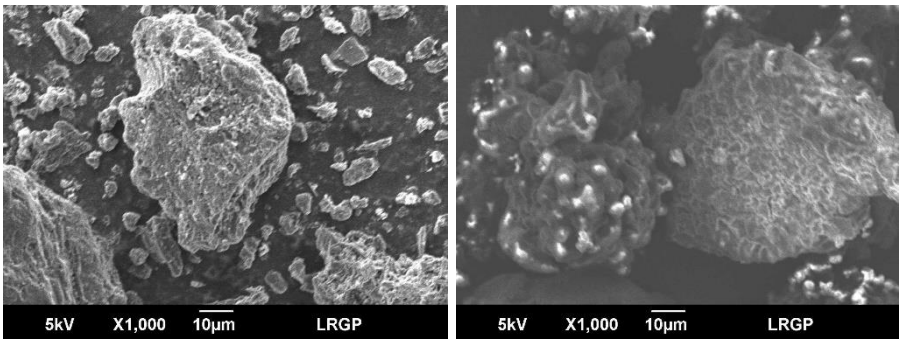

Figure S5 SEM pictures for the three catalysts before and after reaction.

EDX mapping and composition of catalyst particles by SEM before and after reaction.

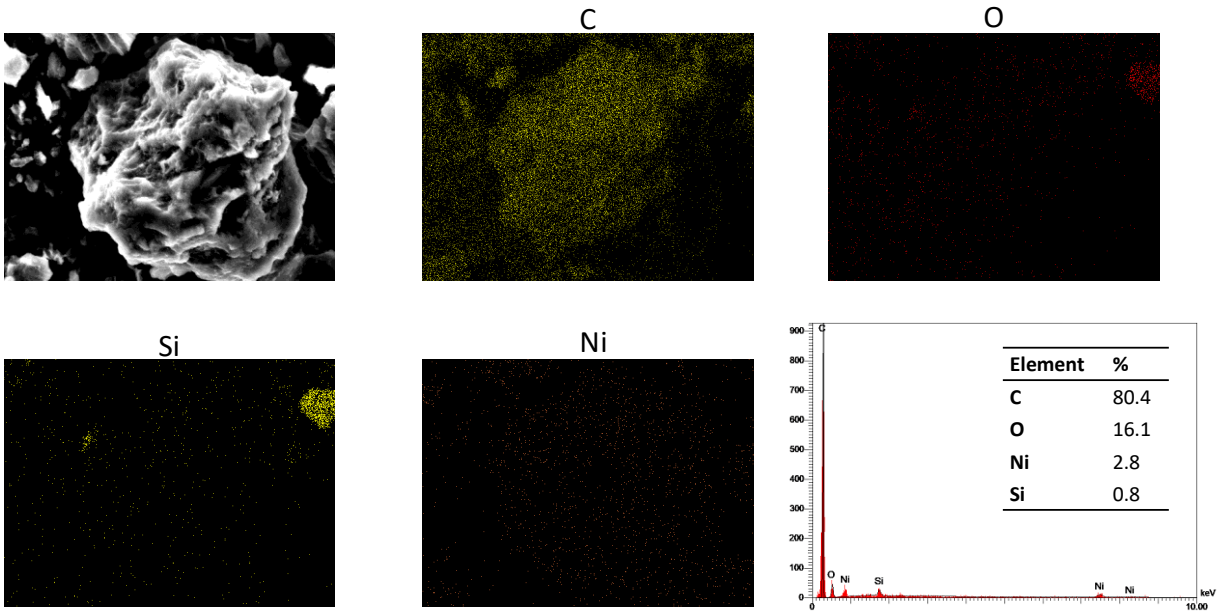

Figure S6 EDX mapping of Ni/C before reaction.

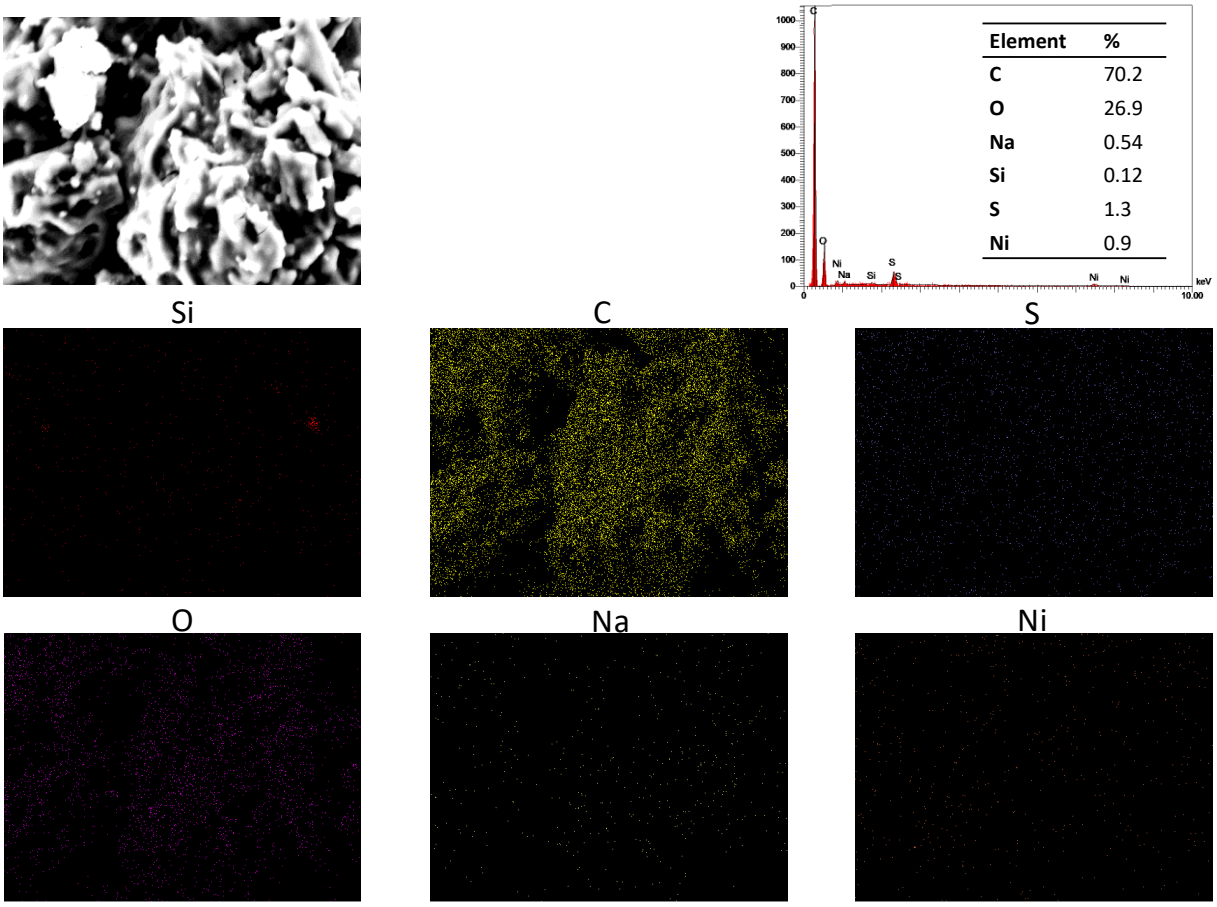

Figure S7 EDX mapping of Ni/C after reaction.

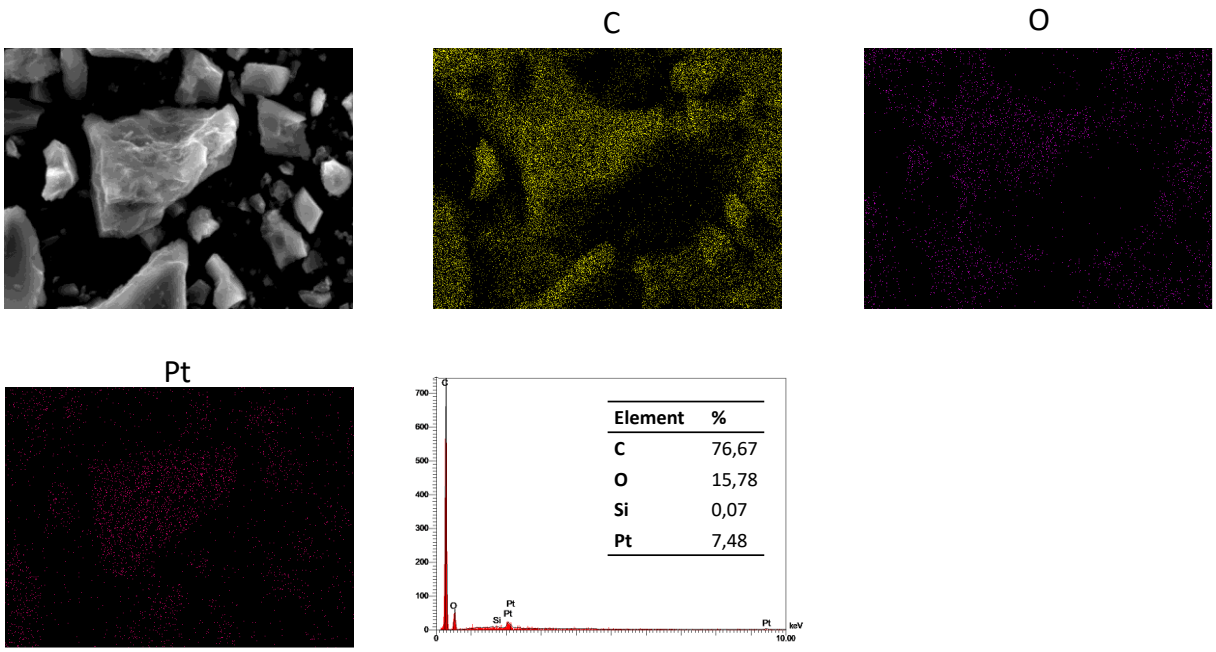

Figure S8 EDX mapping of Pt/C before reaction.

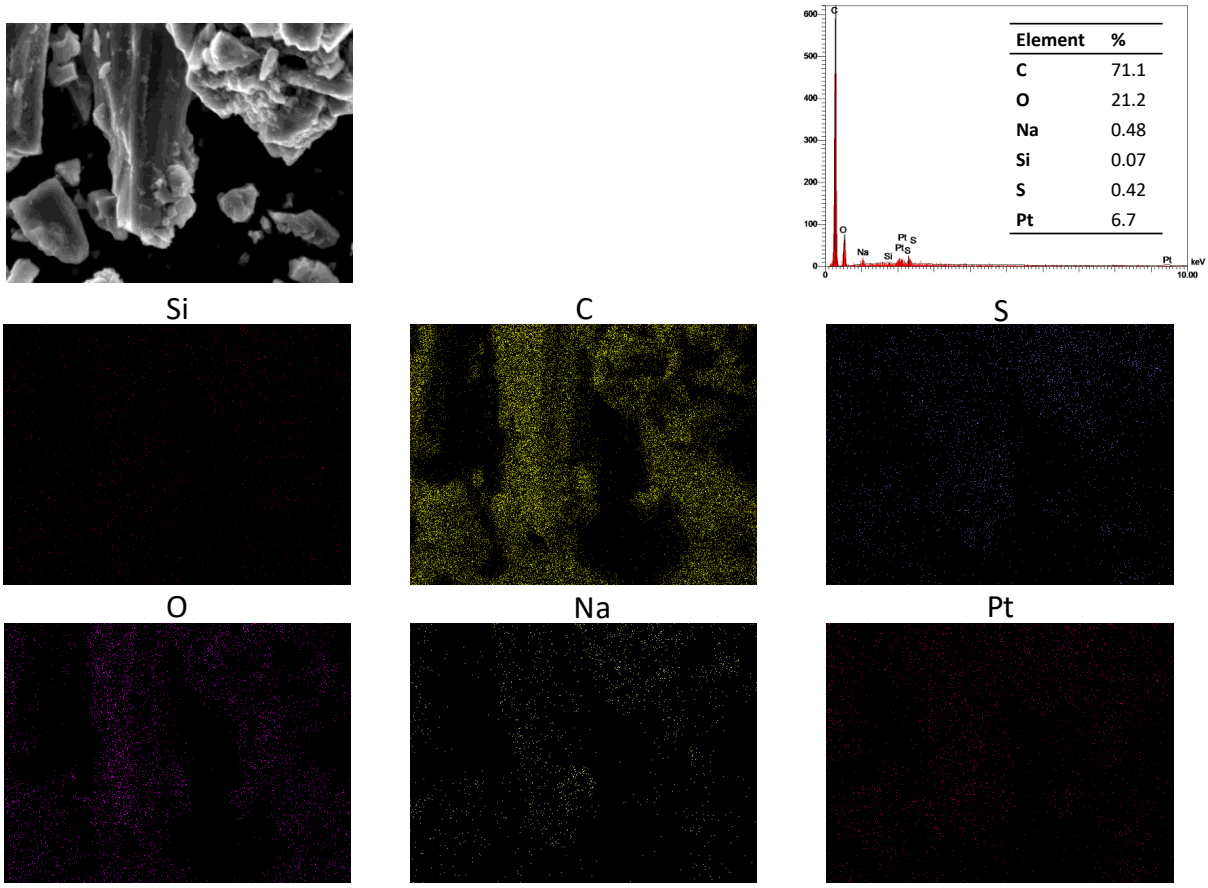

Figure S9 EDX mapping of Pt/C after reaction.

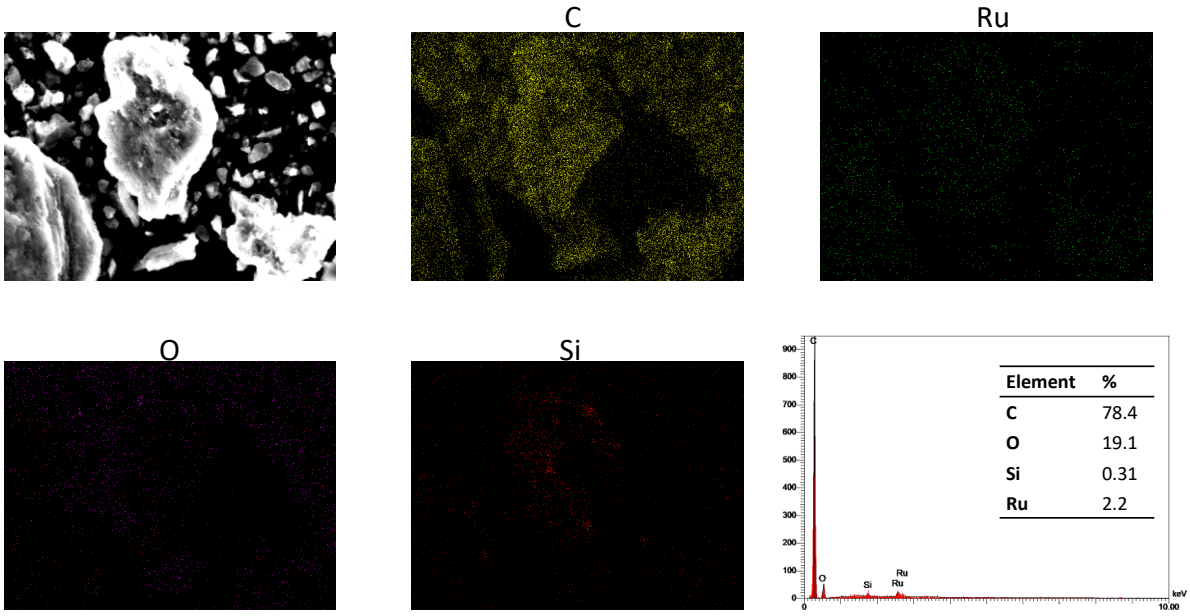

Figure S10 EDX mapping of Ru/C before reaction.

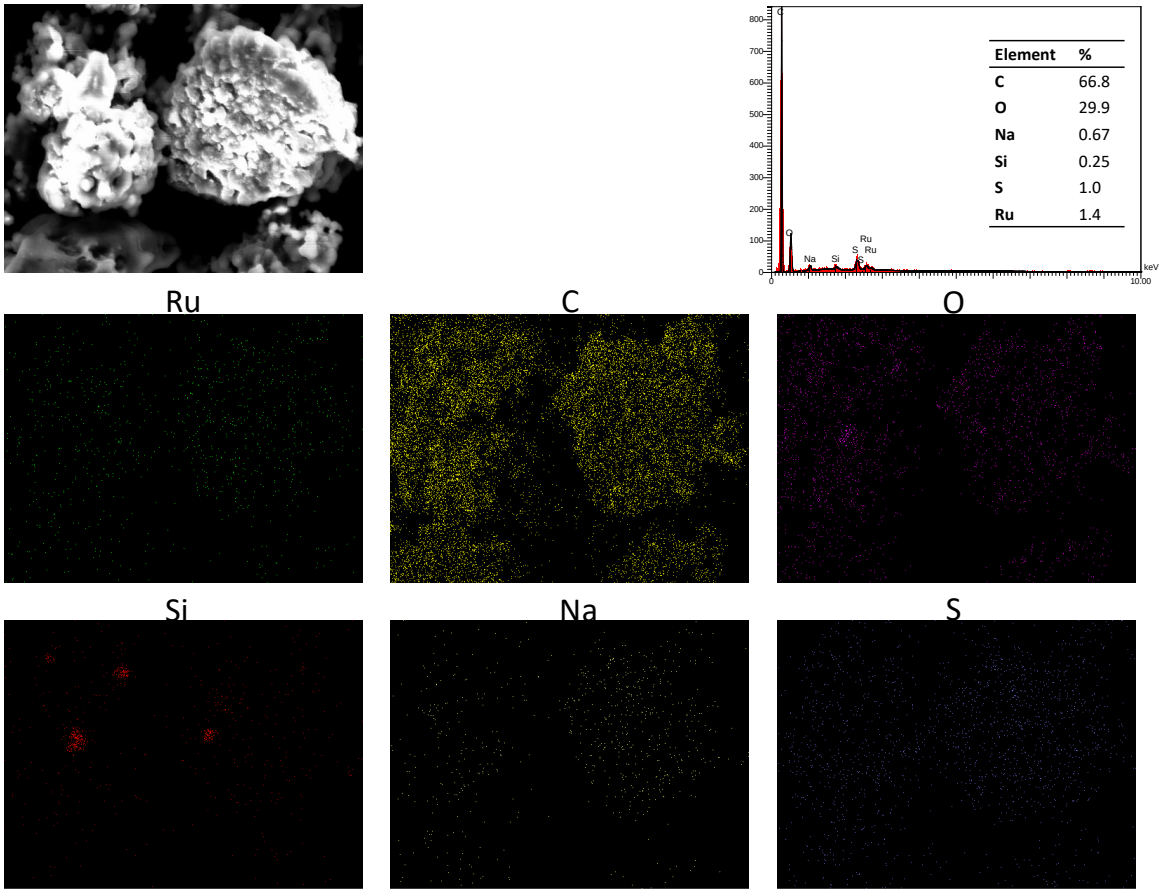

Figure S11 EDX mapping of Ru/C after reaction.

The particle size distribution as analyzed by TEM is presented in Figure S1.

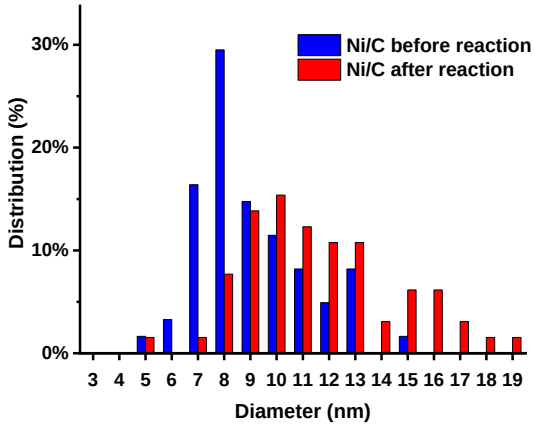

	Before reaction	After reaction
D average (nm)	9.1	12.1
STD	2.05	3.78

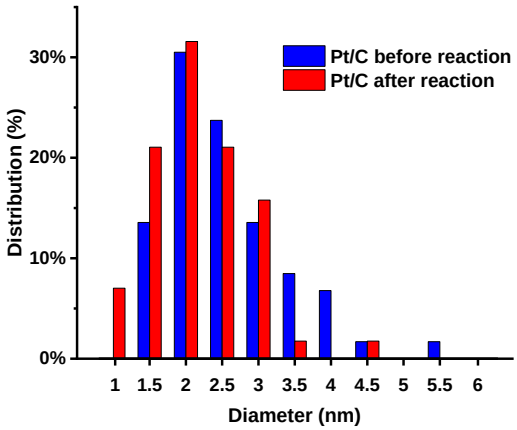

	Before reaction	After reaction
D average (nm)	2.6	2.2
STD	0.84	0.68

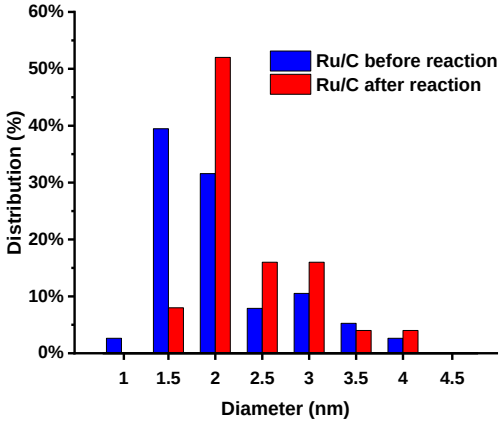

	Before reaction	After reaction
D average (nm)	2.1	2.3
STD	0.65	0.62

Figure S12 Particle size distributions (based on TEM) for the three catalysts before and after reaction.

Sorption of N_2 in the pristine and spent catalysts.

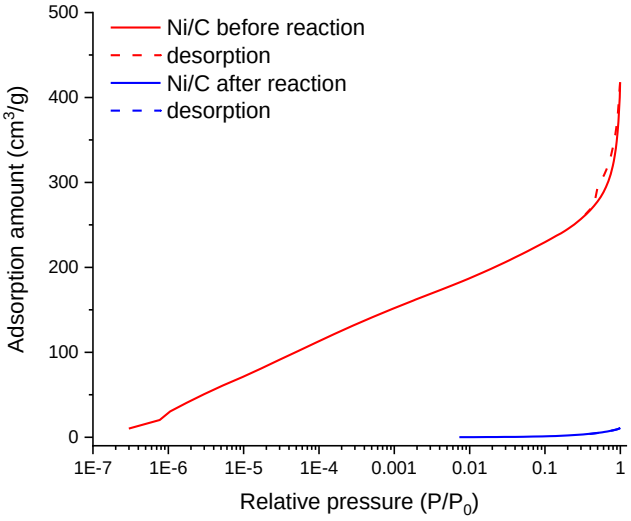

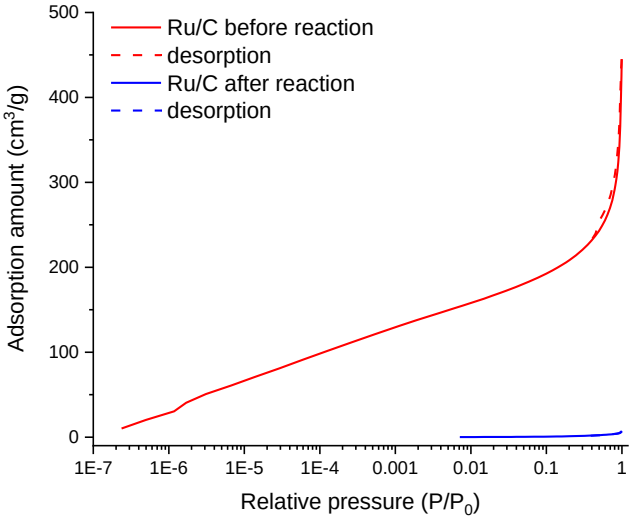

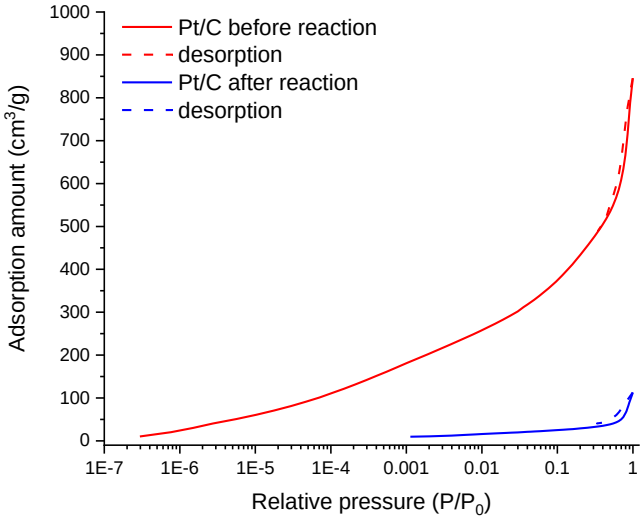

Figure S13 Sorption of N_2 in the pristine and spent catalysts.

Distribution of pores size by NL-DFT:

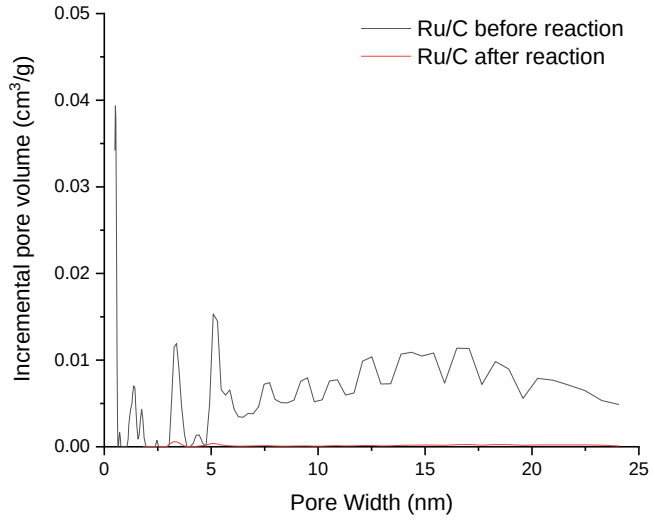

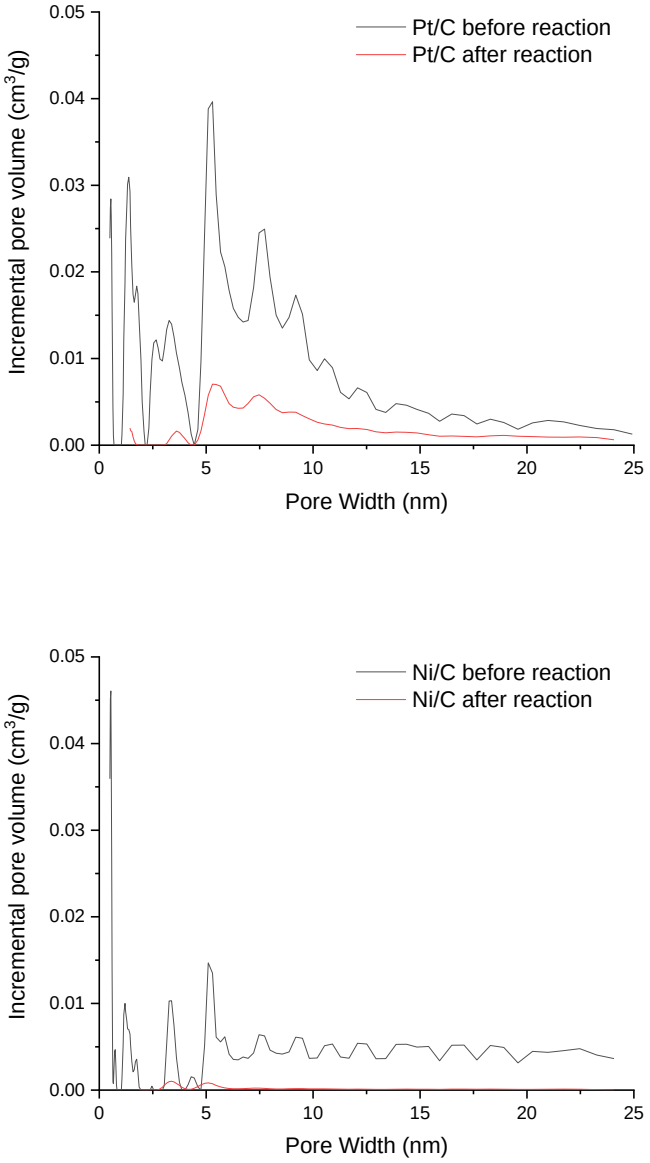

Figure S14 Distribution of pores size by NL-DFT:

6.4. - Analysis of liquids

6.4.1. - Methods

GC-MS analysis The samples were analyzed by an Agilent 7890 gas chromatograph combined to an Agilent 5975C MS (operated by electron impact at 70eV) and an FID placed in parallel to the mass spectrometer. The samples were filtered (0.45 μm glass filters) and no additional dilution was applied. The sample was injected (1 μL) with a split ratio of 10 into an Agilent HP-5MS (5% phenyl 95% methyl siloxane) column. The oven was maintained at 50°C for 10 min; then the temperature was increased with a first ramp of 5°C/min to 120°C, maintained for 10 min and then with a second ramp of 5°C/min to 250°C and maintained for 18 min. By comparison between the mass spectra and the NIST database, more than 40 compounds have been identified. The quantification was achieved by the FID detector based on the de Saint Laumer method as previously described in detail.[12] This method is able to predict the relative response factor of a compound on a FID based on its combustion enthalpy.

GPC-UV analysis The molecular weight distribution of lignin liquefaction products was determined by GPC using a Shimadzu Prominence HPLC system.

The samples, in ethanol from the reaction, were filtered (0.45 μm glass filters) and then diluted in THF (by 1:4 v/v), the same solvent of the mobile phase. 20 μL was injected. The stationary phase was composed of: 1) a Phenomenex Phenogel 5 μm (7.8 x 50 mm) guard column, 2) a Shodex GPC KF-806L 10 μm (8.0 x 300 mm) analytical column and 3) a Phenomenex Phenogel 5 μm 100 Å (7.8 x 300 mm). The samples were separated at 35 ° C with a flow rate of 1 mL/min. The standards used for calibration were polystyrenes. We are aware that polystyrenes and lignin products present different hydrodynamic volumes for a same molecular weight but PS standards were used for sake of comparison with

the available literature on lignin liquefaction. The absorbance of the eluted products is presented at 254 nm (Shimadzu SPD-20A). Data were collected and analyzed with LabSolutions software.

UV spectroscopy UV-visible absorption spectra were recorded on a UV-3600 double beam spectrophotometer (Shimadzu, Marne la Vallée, France). A spectral range from 200 nm to 500 nm and scan speed of 100 nm min-1 were selected with lamp change at 340 nm. The

fluorescence spectra were recorded on a Fluorolog FL3-222 spectrofluorometer (HORIBA Jobin Yvon, Longjumeau, France) equipped with a 450 W Xenon lamp, and a UV-Visible photomultiplier R928 (HAMAMATSU Japan). All spectra were measured in a four-faced quartz cell. Fluorescence spectra were obtained with right angle detector position for both emission and synchronous acquisitions. Emission acquisition was performed with excitation wavelength of 275nm and a slit of 2nm for a spectral range of 280nm to 530nm. Synchronous acquisition was performed with a constant wavelength offset of 20nm in the spectral range from 250nm to 500nm. The 20nm offset has been selected based on previous work.[12] The samples were diluted in ethanol until the absorption wavelength at 275nm was approximately 0.2, in order to avoid self-absorption effects. For this purpose, the solutions sampled from lignin liquefaction (10g of lignin in 200mL ethanol, 50g lignin equivalent/L) were diluted 1000 or 2000 times in ethanol. Therefore, the concentration of analyzed solutions is in the range of 25-50mg lignin equivalent/L ethanol for UV analysis. All the synchronous fluorescence spectra are presented at the same absorbance. The whole procedure (including dilution, scan acquisition and treatment of data) lasts only about 15 minutes.

6.4.2. - Results of liquid analysis

Monomers by GC/MS-FID (wt.% based on internal calibration)

Table S4 Detailed monomers yields from GC-MS/FID.

RT(min)	Compounds	Formula	Mlg/mol)	Kraft3_H2_nocata_EtOH				Kraft3_H2_1%Ru_EtOH				Kraft3_H2_1%Ni_EtOH				Kraft3_H2_1%Pt_EtOH			
				0h	30min	2h	4h	0h	30min	2h	4h	0h	30min	2h	4h	0h	30min	2h	4h
18,28	Anisol	C7H8O	108												0,27				
21,60	1,2-Dimethoxy-4-(1-methoxyethenyl)benzene	C11H14O3	194												0,32				
26,14	Guaiacol	C7H8O2	124	0,12	0,13	0,17	0,25	0,09	0,11	0,12	0,17	0,39	0,28	0,29	0,32	0,13	0,13	0,13	0,16
29,88	4-ethyl-Phenol	C8H10O	122									0,50	0,29	0,22	0,21				
31,73	Methylguaiacol	C8H10O2	138	0,01	0,03	0,09	0,18	0,10	0,14	0,20	0,28	0,17	0,15	0,18	0,20	0,15	0,25	0,35	0,49
37,50	Ethylguaiacol	C9H12O2	152	0,02	0,05	0,11	0,22	0,20	0,32	0,53	0,71	0,40	0,34	0,41	0,48	0,31	0,42	0,55	0,70
41,35	syringol	C8H10O3	154																
41,70	Eugenol	C10H12O2	164									0,10	0,15	0,15	0,14	0,05			
42,18	Propylguaiacol	C10H14O2	166	0,18	0,33	0,28	0,15	0,43	0,72	1,28	1,74	0,40	0,54	0,86	1,14	1,38	1,98	2,42	2,70
42,67	Ethyl β-d-riboside	C7H14O5	178																
43,59	Vanillin	C8H8O3	152																
45,01	4',6'-Dihydroxy-2',3'-dimethylacetophenone	C10H12O3	180																0,11
45,60	methylsyringol	C9H12O3	168																
45,74	Iso-eugenol	C10H12O2	164	0,34	0,52	0,53	0,43	0,79	0,89	0,45	0,16	0,53	0,61	0,47	0,33	0,37	0,28	0,17	
47,20	Acetoguaiacone	C9H10O3	166	0,06	0,09	0,11	0,11	0,05	0,06	0,06	0,06					0,06	0,06		
48,59	ethylsyringol	C10H14O3	182																
48,85	Guaiacyl acetone	C10H12O3	180	0,21	0,40	0,54	0,6	0,24	0,41	0,53	0,57	0,24	0,32	0,44	0,55	0,25	0,31	0,32	0,38
49,06	5-Sec-butylpyrogallol	C11H16O3	196																
51,38	propyl syringol	C11H16O3	196																0,11
51,60	Homosyringic acid	C10H12O5	212																
52,57	Ethyl homovanillate	C11H14O4	210	0,24	0,32	0,26	0,18	0,18	0,23	0,15	0,09	0,15	0,19	0,18	0,15	0,15	0,15		0,09
53,00	Homovanillic acid	C9H10O4	182	0,22	0,30	0,30	0,28	0,21	0,35	0,34	0,31	0,23	0,28	0,3	0,35	0,33	0,4	0,39	0,44
54,04	Ferulic acid	C10H10O4	194													0,15	0,13		
54,82	Methoxyeugenol	C11H14O3	194	0,04	0,05	0,05	0,04	0,06	0,08	0,05	0,03	0,14	0,21	0,18	0,12				
56,06	Acetosyringone	C10H12O4	196									0,13	0,19	0,14	0,13				
		TOTAL (%wt)		1,44	2,22	2,44	2,44	2,35	3,31	3,71	4,12	3,38	3,55	3,82	4,71	3,33	4,11	4,33	5,07

RT(min)	Compounds	Formula	Mlg/mol)	Kraft1_H2_1%Ni_EtOH				Kraft2_H2_1%Ni_EtOH				Soda_H2_1%Ni_EtOH			
				0h	30min	2h	4h	0h	30min	2h	4h	0h	30min	2h	4h
18,28	Anisol	C7H8O	108												
21,60	1,2-Dimethoxy-4-(1-methoxyethenyl)benzene	C11H14O3	194												
26,14	Guaiacol	C7H8O2	124			0,04	0,07	0,08	0,09	0,11	0,15	0,04	0,07	0,12	0,16
29,88	4-ethyl-Phenol	C8H10O	122									0,10	0,20	0,23	0,25
31,73	Methylguaiacol	C8H10O2	138	0,03	0,05	0,08	0,13	0,02	0,05	0,09	0,11	0,07	0,10	0,16	0,20
37,50	Ethylguaiacol	C9H12O2	152	0,09	0,14	0,24	0,36	0,05	0,1	0,14	0,18	0,27	0,46	0,57	0,68
41,35	syringol	C8H10O3	154					0,17	0,21	0,34	0,44	0,07	0,12	0,21	0,29
41,70	Eugenol	C10H12O2	164	0,05	0,07	0,07	0,08		0,05	0,07	0,08	0,03	0,04	0,04	0,04
42,18	Propylguaiacol	C10H14O2	166	0,10	0,18	0,37	0,64	0,07	0,17	0,27	0,43	0,17	0,25	0,32	0,45
42,67	Ethyl β-d-riboside	C7H14O5	178											0,10	0,11
43,59	Vanillin	C8H8O3	152									0,11	0,09	0,05	0,02
45,01	4',6'-Dihydroxy-2',3'-dimethylacetophenone	C10H12O3	180									0,06		0,03	0,04
45,60	methylsyringol	C9H12O3	168					0,07	0,16	0,23	0,32	0,06	0,12	0,20	0,25
45,74	Iso-eugenol	C10H12O2	164	0,28	0,33	0,31	0,20	0,22	0,28	0,27	0,20	0,19	0,25	0,21	0,16
47,20	Acetoguaiacone	C9H10O3	166									0,07	0,09	0,10	0,10
48,59	ethylsyringol	C10H14O3	182									0,07	0,13	0,21	0,27
48,85	Guaiacyl acetone	C10H12O3	180	0,11	0,16	0,22	0,29	0,10	0,18	0,25	0,34	0,07	0,08	0,08	0,10
49,06	5-Sec-butylpyrogallol	C10H14O3	182						0,05	0,08	0,11	0,04			
51,38	propyl syringol	C11H16O3	196						0,05	0,10	0,19			0,03	0,03
51,60	Homosyringic acid	C10H12O5	212					0,08	0,11	0,13	0,14	0,03		0,05	0,06
52,57	Ethyl homovanillate	C11H14O4	210					0,14	0,33	0,54	0,87	0,07	0,17	0,35	0,53
53,00	Homovanillic acid	C9H10O4	182						0,06					0,11	0,12
54,04	Ferulic acid	C10H10O4	194	0,09	0,13	0,18	0,23		0,13					0,13	0,13
54,82	Methoxyeugenol	C11H14O3	194	0,12	0,15	0,12	0,12							0,05	0,04
56,06	Acetosyringone	C10H12O4	196	0,09	0,13	0,12	0,08							0,05	0,04
		TOTAL (%wt)		1,01	1,40	1,84	2,20	1,60	2,85	3,35	4,16	2,07	2,93	4,24	4,87

GPC analysis of liquefaction bio-oils

The samples, in ethanol from the reaction, were filtered (0.45 mm glass filters) and then diluted in THF (by 1:4 v/v), the same solvent of the mobile phase. 20 µL were injected. The stationary phase was composed of:

1) a Phenomenex Phenogel 5 mm (7.8 x 50 mm) guard column,

2) a Shodex GPC KF-806 L 10 mm (8.0 x 300 mm) analytical column

3) a Phenomenex Phenogel 5 mm 100 Å (7.8 x 300 mm).

The samples were separated at 35°C with a flow rate of 1 mL.min^{-}1. The standards used for calibration were polystyrenes.

Table S5 Molecular weights of bio-oils.

	Mn (Da)	Mw (Da)	PD (Mw/Mn)
K3 1% Ru	368	720	1,96
K3 1% Ni	389	826	2,12
K3 1% Pt	409	865	2,11
K1 1% Ni	394	850	2,16
K2 1% Ni	396	829	2,09
Soda1% Ni	380	935	2,46

6.5. - References

1. Jongerius, A. L. *et al.* Stability of Pt/γ-Al $_2$ O $_3$ Catalysts in Lignin and Lignin Model Compound Solutions under Liquid Phase Reforming Reaction Conditions. *ACS Catal.* **3**, 464–473 (2013).

2. Huang, X., Korányi, T. I., Boot, M. D. & Hensen, E. J. M. Catalytic Depolymerization of Lignin in Supercritical Ethanol. *ChemSusChem* **7**, 2276–2288 (2014).

3. Huang, X. *et al.* Catalytic Depolymerization of Lignin and Woody Biomass in Supercritical Ethanol: Influence of Reaction Temperature and Feedstock. *ACS Sustain. Chem. Eng.* **5**, 10864–10874 (2017).

4. Huang, X., Korányi, T. I., Boot, M. D. & Hensen, E. J. M. Ethanol as capping agent and formaldehyde scavenger for efficient depolymerization of lignin to aromatics. *Green Chem.* **17**, 4941–4950 (2015).

5. Zhou, M. *et al.* Catalytic in Situ Hydrogenolysis of Lignin in Supercritical Ethanol: Effect of Phenol, Catalysts, and Reaction Temperature. *ACS Sustain. Chem. Eng.* **6**, 6867–6875 (2018).

6. Kim, J.-Y., Young Park, S., Hoon Lee, J., Choi, I.-G. & Weon Choi, J. Sequential solvent fractionation of lignin for selective production of monoaromatics by Ru catalyzed ethanolysis. *RSC Adv.* **7**, 53117–53125 (2017).

7. Kim, J.-Y., Park, J., Kim, U.-J. & Choi, J. W. Conversion of Lignin to Phenol-Rich Oil Fraction under Supercritical Alcohols in the Presence of Metal Catalysts. *Energy Fuels* **29**, 5154–5163 (2015).

8. Park, J. *et al.* Comparison of degradation features of lignin to phenols over Pt catalysts prepared with various forms of carbon supports. *RSC Adv.* **6**, 16917–16924 (2016).

9. Yang, J., Zhao, L., Liu, S., Wang, Y. & Dai, L. High-quality bio-oil from one-pot catalytic hydrocracking of kraft lignin over supported noble metal catalysts in isopropanol system. *Bioresour. Technol.* **212**, 302–310 (2016).

10. Kloekhorst, A. & Heeres, H. J. Catalytic Hydrotreatment of Alcell Lignin Using Supported Ru, Pd, and Cu Catalysts. *ACS Sustain. Chem. Eng.* **3**, 1905–1914 (2015).

11. Wang, S. *et al.* Unlocking Structure–Reactivity Relationships for Catalytic Hydrogenolysis of Lignin into Phenolic Monomers. *ChemSusChem* **13**, 4548–4556 (2020).

12. Bartolomei, E. et al. Lignin Depolymerization: A Comparison of Methods to Analyze Monomers and Oligomers. ChemSusChem 13, (2020).

E. Selective Catalytic TEMPO-mediated Oxidation of Kraft Lignin to Vanillin

To be submitted to *Industrial Crops and Products*

Erika Bartolomei[a], Antonio Hernández-Mañas[b], Evan Terrell[c], Manuel Garcia-Perez[c], Yann Le Brech[a], Laurent Djakovitch[b]*

[a] LRGP, CNRS, Université de Lorraine, 1 rue Grandville, 54000 Nancy, France

[b] Université de Lyon, Université Claude Bernard Lyon 1, CNRS, IRCELYON, UMR 5256, 2 avenue Albert Einstein, F-69626 Villeurbanne cedex, France

[c] Department of Biological Systems Engineering, Washington State University, Pullman, WA 99164 (USA)

* corresponding author: laurent.djakovitch@ircelyon.univ-lyon1.fr

Abstract

Lignin is a heterogeneous aromatic biopolymer typically generated as a co-product from the pulp and paper and biorefinery industries. Through oxidation processes, lignin methoxyphenylpropane subunits can be converted into monomeric aldehydes (e.g., vanillin, a high-value compound). In this work we studied lignin catalytic oxidation with the addition of TEMPO (2,2,6,6-Tetramethylpiperidine-1-oxyl), an oxygen radical source typically utilized for the oxidation of primary alcohols. In order to mimic industrially relevant conditions, we used precipitated Kraft lignin from pulp industry. We report high vanillin selectivity of up to 80% with maximum yield of 7 wt. % vanillin for Kraft lignin direct air oxidation mediated by TEMPO. Therefore, we assess that TEMPO can effectively promote lignin oxidation and its depolymerization to monomeric aldehydes (vanillin) in combination with safe, stable and environment-friendly oxygen donor (air).

1. - Introduction

Lignin is an aromatic biopolymer resulting from condensation of methoxyphenylpropane monomeric units, accounting for roughly one-third of woody biomass dry weight[1,2]. Therefore, lignin represents the most abundant source of renewable aromatic carbons with great opportunity as a feedstock for high-value added chemicals and materials[1–4]. At present, technical lignin (i.e., lignin that is industrially-derived) is under-utilized and is considered as a byproduct and/or waste from pulp and paper operations and various cellulosic biorefinery concepts[5–7]. In order to work toward a more sustainable circular economy centered on renewable natural resources, the effective valorization of industrially produced technical lignin is necessary.

A large body of work dedicated to research on lignin upgrading is focused at present on advancing high-yield depolymerization strategies for the production of aromatic monomers[7,8]. One monomer of particular interest is vanillin, derived from lignin oxidation to form aldehydes[9,10], because of its direct commercial high added-value. Although the oxidative conversion of lignin model compounds to vanillin has been reported with high yield (greater than ~90%)[11,12], the conversion of real technical lignin to vanillin is significantly lower (less than ~10%)[13] or 20-30% for nitrobenzene oxidation [14,15]. Nitrobenzene oxidation is a frequently employed analytical technique to quantify the monomer composition of a given lignin sample [16]. The reported total monomer yield of lignin oxidation is typically between 10 and 20%[17]. This underscores the fact that the primary challenge in lignin valorization is the depolymerization of the whole material, and not the conversion from representative low molecular weight compounds (i.e., model monomers and dimers) to final monomers[17].

TEMPO (2,2,6,6-tetramethylpiperidine-N-oxyl) has been shown in several studies to be an effective and potentially recyclable oxidation mediator for catalytic lignin conversion to vanillin[18–23]. A summary of some recent relevant research is given in Table S1 (supporting info), regarding a) applications of TEMPO and b) vanillin production from Kraft lignin.

Gharehkhani et al. have extensively reviewed catalytic TEMPO lignin oxidation[13]. In their review, the highest reported vanillin yield is 3.5% from real polymeric (viz., not model compounds) lignin[19]. Rahimi et al reported a 3.5% yield of vanillin and 8.5% yield of syringaldehyde from aspen lignin (from cellulolytic enzyme preparation). This study features a two-step process, in which lignin was first oxidized (with 4-acetamido-TEMPO mediator) and then depolymerized with formic acid[19]. Similarly, Das et al. reported 1.3%, 1.7% and 0.9%

yields of vanillin from poplar, maize and maple lignins, respectively; the authors also reported 3.8%, 2.4% and 0.6% syringaldehyde yields from these lignins[24].

The goal of this work is to further explore Kraft lignin conversion to vanillin through catalytic wet oxidation with TEMPO in alkaline solution (pH=13). Simultaneously, we focused on using air directly as an oxidizer. Additionally, with the aim of contributing to further green and sustainable industrial applications, TEMPO was associated to copper co-catalyst that was shown to be efficient for this purpose[25], to reduce TEMPO loading while maintaining high conversions.

2. - Experimental Section

The Kraft lignin used in this work was provided by the French Technical Centre of Paper (CTP, Grenoble). It has been extracted from marine pine (softwood) by the Lignoboost process[26,27]. All commercial products were purchased from Sigma Aldrich and Alfa Aesar. All solvents were used as supplied without further purification. TiO_2 Aerolyst 7711 was kindly supplied by Evonik (Aerolyst extrudates 1x4mm).

Reactions were catalyzed by a CuO / TiO_2 catalyst (Cu 5 % wt.) synthesized by incipient wetness impregnation, using Cu $(NO_3)_2.5H_2O$ as precursor[28]. CuO/TiO2 was chosen based on currently ongoing research and previously published work[25] that indicates good stability under the oxidative reaction conditions. The TiO_2 extruded support was impregnated by an aqueous solution of the Cu $(NO_3)_2.5H_2O$ precursor with continuous stirring and then dried at 110 °C overnight. Calcination was carried out on dried samples at 550 °C for 5 h (5 °C/min) under air atmosphere. A brief discussion of catalyst XRD analysis is given in the supporting material.

The oxidation of lignin (~0.75g dry mass) was conducted in a Parr® autoclave (0.2L) equipped with a magnetic rotary stirrer (1800rpm) at constant pressure and temperature (20 bar and 150 °C) for 1 hour. Pressure was maintained in the desired reaction atmosphere (i.e., N_2 or air) using a backpressure regulator. Lignin was dissolved in an aqueous NaOH solution at pH 13 (150mL). The pH was chosen to emulate the alkalinity of the black liquor of a Kraft process, which is the most largely used process in pulp and paper mills29. For experiments concerning TEMPO, it was added in approximately stoichiometric ratio compared to lignin (1:1 and 2:1). Lignin molecular weight was calculated based on elemental analysis composition (71% C, 5.6% H, and 21.3% O). After the reaction, the reactor was cooled with an ice bath to 15°C and then pressure was released.

A fractionation process (presented in Supporting Information, Figure S1) was followed to isolate the different product varieties for further analysis. The collected organic phase was analyzed by HPLC and GC-MS/FID to evaluate the mass yield of aromatic monomers. Solid residues were analysed by nuclear magnetic resonance (^{1}H NMR) and qualitatively investigated by FT-IR analysis (in SI). In addition, the molecular weights of the liquid products have been analysed by gel permeation chromatography.

3. - Results

We show TEMPO and/or copper catalyst efficiency in lignin oxidation by aromatic monomers identification and quantification (GC/MS-FID) after reaction. Besides, only vanillin, acetovanillone and vanillic acid have been detected by GC/MS-FID, which is coherent with literature[4]. The GC/MS-FID analysis results from catalytic oxidation experiments are reported in Table 1 (further details are provided in supporting material).

Table 1 Experimental results for catalytic air oxidation of kraft lignin

Exp.	Catalyst (Cu/TiO_2) loading	TEMPO[b]	Gas	Vanillin[d] (wt.%)	Acetovanillone[d] (wt.%)	Vanillic Acid[d] (wt.%)	Tot Phenolic Monomers[d] (wt.%)	Vanillin Selectivity (%)
1	none	0 g	N_2	n.a.	n.a.	n.a.	0.0	0
2	5%Cu/lignin[a]	0 g	N_2	0.5	0.3	0.3	1.1	0
3	none	1.5 g	N_2	1.5	0.6	0.5	2.6	57.7
4	none	0 g	AIR	3.4	0.7	0.5	4.5	75.5
5	5%Cu/lignin[a]	0 g	AIR	5.1	1.2	0.9	7.2	70.8
6	5%Cu/lignin[a]	0.75 g	AIR	5.2	1.2	0.9	7.3	71.2
7	5%Cu/lignin[a, c]	1.5 g	AIR	5.6 5.9	1.1 0.8	0.8 0.5	7.4 7.2	75.7 81.9
8	none	1.5 g	AIR	7.1	0.7	0.8	8.6	82.5

a. 5%Cu/lignin indicates a catalyst loading of 5% Cu relative to lignin mass
b. Stoichiometric amounts of TEMPO are used, such that 1 guaiacyl unit + O_2 = 1 vanillin; 1-TEMPO = 1 oxygen radical; 2-TEMPO = 2 oxygen radical (on a molar basis)
c. Duplicate runs of 5%Cu/lignin + 2-TEMPO were conducted to assess reproducibility
d. All the mass yields (wt.%) are evaluated on dry lignin initial weight

Exp.1, conducted without TEMPO nor copper catalyst and under inert atmosphere, does not yield any detectable monomers. The addition of copper as catalyst (Exp.2) yields over 1 wt.% of monomers; its beneficial effect in lignin oxidation is already well-known[25,30,31]. Conversely, the addition of TEMPO (Exp.3), even under inert gas-phase atmosphere, yields 2.6 wt.% total monomers (with 57.7% selectivity). This highlights that TEMPO, even without any other

oxidant agent, is able to achieve lignin oxidation into vanillin. The mechanism of TEMPO-mediated lignin oxidation is depicted in Figure 1[18,24].

Concerning the reaction under only air atmosphere (Exp.4), the total monomer yield reaches 4.5 wt.%, with 75.6% vanillin selectivity. Under these conditions, Kraft lignin conversion into monomers starts to be significant[32–34]. The combination of oxidative atmosphere and the addition of 5 wt.%Cu (Exp.5) leads to higher amount of monomers (7.2 wt.%), with relatively similar vanillin selectivity (70.8%).

In these conditions, the addition of TEMPO in stoichiometric ratio on lignin 1:1 (Exp.6) and 2:1 (Exp.7) does not show effective evolution in monomers yields and selectivity. TEMPO activity seems to be blocked by copper; indeed, their coupling does not appear suitable for lignin conversion into monomers.

Therefore, the highest overall vanillin (7.1 wt.%) and total monomer yield (8.6 wt.%) occurs with TEMPO and no added CuO/TiO_2 catalyst (Exp.8). This could be explained by the fact that TEMPO adsorption may occur at the surface of the CuO/TiO_2 catalyst, partially affecting TEMPO oxidizing/catalytic capacity.

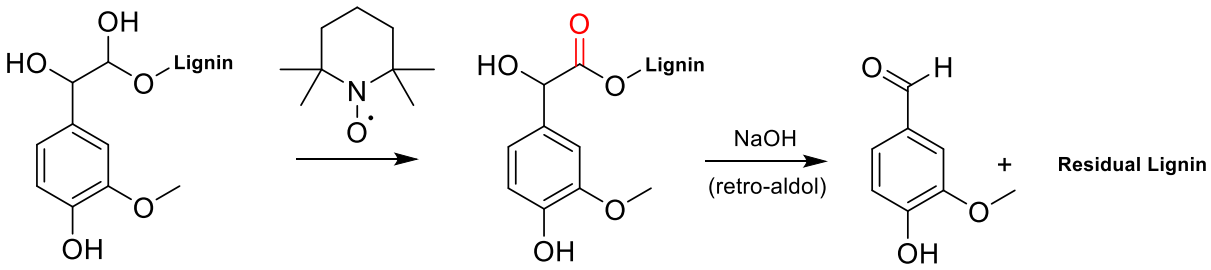

Figure 1 Proposed mechanism of TEMPO-mediated oxidation of lignin[18,24]

4. - Conclusions

In this study, we show that TEMPO can act as a primary radical oxidant mediator in air-depolymerization of Kraft softwood lignin, producing a significant amount of monomers (8.6 wt%) with high vanillin selectivity (82.5%). CuO/TiO_2 also produces a notable monomers yield (7.2 wt%, 70.8% vanillin selectivity). Nevertheless, when the catalyst is used at the same time with TEMPO, the vanillin yields stay similar.

We have achieved high yields of vanillin, with respect to previous studies[21]. In comparison to the literature (as presented in supporting material), our approach presents a high yield of vanillin

by using only air and TEMPO. Furthermore, it is conducted on a recalcitrant, industrial Kraft lignin under basic conditions.

This approach demonstrates one pathway by which value can be extracted from all wood constituents in a biomass-utilizing industry seeking to effectively upgrade/valorize whole lignocellulosic biomass, increasing the economic balance and sustainability of its processing.

Future work will focus on the development of a process in which TEMPO will be sustainably regenerated and recycled for continuous, high-yield vanillin production.

Aknowledgements

This study was supported by University of Lorraine through the funding project DrEAM – Lorraine Université d'Excellence. The authors gratefully acknowledge the National Agency of Research (Phenoliq N° ANR-16-CE06-0007-03) for funding. The authors thank Evonik for the generous gift of Aerolyst catalyst support. IRCELYON scientific and technical services and AXELERA cluster for the chemical and environmental sectors are kindly acknowledged, as well as Dr. Anthony Dufour (CNRS, Nancy, France) for helpful discussion and for the promotion of this project.

5. - References

1. Li, C., Zhao, X., Wang, A., Huber, G. W. & Zhang, T. Catalytic Transformation of Lignin for the Production of Chemicals and Fuels. *Chem. Rev.* **115**, 11559–11624 (2015).

2. Wang, H., Pu, Y., Ragauskas, A. & Yang, B. From lignin to valuable products–strategies, challenges, and prospects. *Bioresource Technology* **271**, 449–461 (2019).

3. Calvo-Flores, F. G. & Dobado, J. A. Lignin as Renewable Raw Material. *ChemSusChem* **3**, 1227–1235 (2010).

4. Mathieu, Y. *et al.* Molecular oxygen lignin depolymerization: An insight within phenolic monomers stability. *ChemSusChem* (2020) doi:10.1002/cssc.202001295.

5. Vishtal, A. G. & Kraslawski, A. Challenges in industrial applications of technical lignins. *BioResources* **6**, 3547–3568 (2011).

6. Bajwa, D. S., Pourhashem, G., Ullah, A. H. & Bajwa, S. G. A concise review of current lignin production, applications, products and their environmental impact. *Industrial Crops and Products* **139**, 111526 (2019).

7. Chio, C., Sain, M. & Qin, W. Lignin utilization: A review of lignin depolymerization from various aspects. *Renewable and Sustainable Energy Reviews* **107**, 232–249 (2019).

8. Zhang, R. *et al.* Facile synthesis of vanillin from fractionated Kraft lignin. *Industrial Crops and Products* **145**, 112095 (2020).

9. Fache, M., Boutevin, B. & Caillol, S. Vanillin Production from Lignin and Its Use as a Renewable Chemical. *ACS Sustainable Chem. Eng.* **4**, 35–46 (2016).

10. Galadima, A. I. *et al.* Biovanillin: production concepts and prevention of side product formation. *Biomass Conversion and Biorefinery* **10**, 589–609 (2020).

11. Lin, J. Y. *et al.* Selective Aerobic Upgrading of Lignin-Derived Compound Using a Recyclable Dual-Functional TPO-Loaded Cu-BTC Catalyst. *Waste and Biomass Valorization* (2020) doi:10.1007/s12649-020-01009-1.

12. Zheng, M.-W., Lin, K.-Y. A. & Lin, C.-H. TEMPO-Functionalized Silica as an Efficient and Recyclable Oxidation Catalyst for Conversion of a Lignin Model Compound to Value-Added Products. *Waste Biomass Valor* (2019) doi:10.1007/s12649-019-00910-8.

13. Gharehkhani, S., Zhang, Y. & Fatehi, P. Lignin-derived platform molecules through TEMPO catalytic oxidation strategies. *Progress in Energy and Combustion Science* **72**, 59–89 (2019).

14. Pew, J. C. Nitrobenzene Oxidation of Lignin Model Compounds, Spruce Wood and Spruce "Native Lignin". *J. Am. Chem. Soc.* **77**, 2831–2833 (1955).

15. Katahira, R. & Nakatsubo, F. Determination of nitrobenzene oxidation products by GC and1H-NMR spectroscopy using 5-iodovanillin as a new internal standard. *J Wood Sci* **47**, 378–382 (2001).

16. Schutyser, W. *et al.* Revisiting alkaline aerobic lignin oxidation. *Green Chem.* **20**, 3828–3844 (2018).

17. Behling, R., Valange, S. & Chatel, G. Heterogeneous catalytic oxidation for lignin valorization into valuable chemicals: what results? What limitations? What trends? *Green Chem.* **18**, 1839–1854 (2016).

18. Rahimi, A., Azarpira, A., Kim, H., Ralph, J. & Stahl, S. S. Chemoselective metal-free aerobic alcohol oxidation in lignin. *J. Am. Chem. Soc.* **135**, 6415–6418 (2013).

19. Rahimi, A., Ulbrich, A., Coon, J. J. & Stahl, S. S. Formic-acid-induced depolymerization of oxidized lignin to aromatics. *Nature* **515**, 249–252 (2014).

20. Patankar, S. C. *et al.* Isolation of phenolic monomers from kraft lignin using a magnetically recyclable TEMPO nanocatalyst. *Green Chem.* **21**, 785–791 (2019).

21. Dabral, S., Hernández, J. G., Kamer, P. C. J. & Bolm, C. Organocatalytic Chemoselective Primary Alcohol Oxidation and Subsequent Cleavage of Lignin Model Compounds and Lignin. *ChemSusChem* **10**, 2707–2713 (2017).

22. Dabral, S., Wotruba, H., Hernández, J. G. & Bolm, C. Mechanochemical Oxidation and Cleavage of Lignin β-O-4 Model Compounds and Lignin. *ACS Sustainable Chem. Eng.* **6**, 3242–3254 (2018).

23. Sun, C., Zheng, L., Xu, W., Dushkin, A. V. & Su, W. Mechanochemical cleavage of lignin models and lignin via oxidation and a subsequent base-catalyzed strategy. *Green Chem.* **22**, 3489–3494 (2020).

24. Das, A. *et al.* Lignin Conversion to Low-Molecular-Weight Aromatics via an Aerobic Oxidation-Hydrolysis Sequence: Comparison of Different Lignin Sources. *ACS Sustainable Chem. Eng.* **6**, 3367–3374 (2018).

25. Sedai, B. *et al.* Aerobic Oxidation of β-1 Lignin Model Compounds with Copper and Oxovanadium Catalysts. *ACS Catal.* **3**, 3111–3122 (2013).

26. Zhu, W., Westman, G. & Theliander, H. Investigation and Characterization of Lignin Precipitation in the LignoBoost Process. *Journal of Wood Chemistry and Technology* **34**, 77–97 (2014).

27. Mattsson, C. *et al.* Using 2D NMR to characterize the structure of the low and high molecular weight fractions of bio-oil obtained from LignoBoostTM kraft lignin depolymerized in subcritical water. *Biomass and Bioenergy* **95**, 364–377 (2016).

28. Boccuzzi, F. *et al.* Preparation, Characterization, and Activity of Cu/TiO2Catalysts. I. Influence of the Preparation Method on the Dispersion of Copper in Cu/TiO2. *Journal of Catalysis* **165**, 129–139 (1997).

29. Dessbesell, L., Paleologou, M., Leitch, M., Pulkki, R. & Xu, C. (Charles). Global lignin supply overview and kraft lignin potential as an alternative for petroleum-based polymers. *Renewable and Sustainable Energy Reviews* **123**, 109768 (2020).

30. Deng, H., Lin, L. & Liu, S. Catalysis of Cu-Doped Co-Based Perovskite-Type Oxide in Wet Oxidation of Lignin To Produce Aromatic Aldehydes. *Energy Fuels* **24**, 4797–4802 (2010).

31. Villar, J. C., Caperos, A. & García-Ochoa, F. Oxidation of hardwood kraft-lignin to phenolic derivatives with oxygen as oxidant. *Wood Science and Technology* **35**, 245–255 (2001).

32. Ansaloni, S., Russo, N. & Pirone, R. Wet Air Oxidation of Industrial Lignin Case Study: Influence of the Dissolution Pretreatment and Perovskite-type Oxides. *Waste Biomass Valor* **9**, 2165–2179 (2018).

33. Borden, M. H. & Alfred, S. C. Method of producing vanillin. (1950).

34. Fargues, C., Mathias, Á. & Rodrigues, A. Kinetics of Vanillin Production from Kraft Lignin Oxidation. *Ind. Eng. Chem. Res.* **35**, 28–36 (1996).

35. Cui, M., Huang, R., Qi, W., Su, R. & He, Z. Synthesis of 2,5-diformylfuran from 5-hydroxymethylfurfural in ethyl acetate using 4-acetamido-TEMPO as a recyclable catalyst. *Catalysis Today* **319**, 121–127 (2019).

36. Vadivelu, M., Sampath, S., Muthu, K., Karthikeyan, K. & Praveen, C. Harnessing the TEMPO-Catalyzed Aerobic Oxidation for Machetti-De Sarlo Reaction toward Sustainable Synthesis of Isoxazole Libraries. *J. Org. Chem.* **84**, 13636–13645 (2019).

37. Zirbes, M. *et al.* High-Temperature Electrolysis of Kraft Lignin for Selective Vanillin Formation. *ACS Sustainable Chem. Eng.* **8**, 7300–7307 (2020).

38. Shrestha, B. *et al.* A Multitechnique Characterization of Lignin Softening and Pyrolysis. *ACS Sustainable Chemistry & Engineering* **5**, 6940–6949 (2017).

39. Faix, O. Classification of Lignins from Different Botanical Origins by FT-IR Spectroscopy. *Holzforschung* (1991) doi:10.1515/hfsg.1991.45.s1.21.

40. Li, H. & McDonald, A. G. Fractionation and characterization of industrial lignins. *Industrial Crops and Products* **62**, 67–76 (2014).

6. - Supporting Information

6.1. - Literature review

Table S1 Summary of recent relevant research for applications of TEMPO in catalytic reaction systems and production of vanillin from model and kraft lignin

Authors	Type of study	Summary
Cui, et al. (2019)[1]	TEMPO	The oxidation of 5-hydroxymethylfurfural to 2,5-diformylfuran (2,5-DFF) is reported with high yield, using 4-acetamido-TEMPO as a catalyst at room temperature and pressure; $Fe(NO_3)_3$ and NaCl are used as co-catalysts. Due to low solubility in the employed solvent (ethyl acetate), catalyst recovery is achieved though centrifugation and recycled effectively for 2,5-DFF synthesis.
Vadivelu, et al. (2019)[2]	TEMPO	The synthesis of isoxazole/isoxazoline derivatives under "sustainable conditions" is reported, with the use of TEMPO catalysis. Polymer-immobilized TEMPO (denoted as "PS-TEMPO") is employed, and is shown to have comparable yield to free TEMPO catalyst application. The PS-TEMPO is commercially available (100-200 mesh, 1mmol/g loading, 1% cross-linked with divinylbenzene; in the cited study, purchased from Sigma-Aldrich)
Lin, et al. (2020)[3]	TEMPO & Vanillin production (from model compound)	The oxidation of vanillyl alcohol to vanillin is reported using a novel Cu/TEMPO-based catalyst. Using a co-precipitation method, TEMPO and Cu species are integrated into a single heterogeneous catalyst *via* the embedding of TEMPO into copper benzene-1,3,5-tricarboxylate MOFs. Octahedral morphology and crystalline MOF structure are retained following TEMPO introduction. The novel heterogeneous catalyst is reported to be recyclable/reusable without significant efficiency loss for vanillyl alcohol oxidation.
Zheng, Lin, Lin (2019)[4]	TEMPO & Vanillin production (from model compound)	The oxidation of vanillyl alcohol to vanillin is reported using a TEMPO-functionalized silica catalyst. Catalyst preparation occurs through the condensation of OH-TEMPO and tetrahedral orthosilicate to insert TEMPO functional groups into silica matrices. This results in composite TEMPO@SiO_2; Cu is also reported as a co-catalyst. The novel heterogeneous catalyst is reported to be sustainable/recyclable with good stability, despite slightly decreasing conversions of vanillyl alcohol over reuse cycles.

Patankar, et al. (2019)[5]	TEMPO & Vanillin production (from kraft lignin)	The oxidative depolymerization of Kraft lignins is reported featuring the use of a magnetically separable TEMPO catalyst. The primary oxidant is NaOCl in combination with NaBr. Catalyst synthesis occurs in four stages (precipitation, condensation, silanization, reductive amination; reported in earlier work from Patankar and Renneckar, 2017). The resulting magnetic heterogeneous catalyst, denoted "Fe@MagTEMPO," is reported to prevent the release of TEMPO and can be reused without any loss of activity. Roughly 20-25%wt monomer yield is reported with ~60% vanillin selectivity from Indulin AT lignin.
Zirbes, et al. (2020)[6]	Vanillin production (from Kraft lignin)	The electrochemical depolymerization of several technical Kraft lignins is reported. Primary oxidative products are vanillin and acetovanillone. The highest reported vanillin yield is nearly 5% from Indulin AT Kraft lignin, with 60% yield relative to vanillin measured from nitrobenzene oxidation.
Zhang, et al. (2020)[7]	Vanillin production (from Kraft lignin)	The two-step catalytic oxidation of fractionated Kraft lignin is reported. Bio-based alcohols (ethanol, 1-propanol, 1-butanol) are used to produce lower molecular weight fractions with improved homogeneity, in comparison to the starting Kraft lignin. $CuSO_4$ catalyst is used with H_2O_2 oxidant. Optimized vanillin yields are reported to be approximately 10%.

6.2. - Fractionation method

A fractionation process was carried out in order to separate the different reaction products and to quantify the aromatic compounds. First, the aqueous solution was filtered to recover the solid catalyst. It was then dried before carrying out analyses.

The reaction solution was then acidified by adding hydrochloric acid (10%wt) until the pH was ~1.0. This produces the precipitation of the non-depolymerized lignin and the biggest oligomers (only soluble at high pH values). The precipitate was separated by centrifugation at 4000 rpm for 20 min, washed with hydrochloric acid (10%) and water before being dried at 60°C for 9 hours under vacuum. It was called "Klason phase".

The liquid fraction recovered from the centrifugation was extracted with dichloromethane (DCM) (200mL), obtaining the main part of the apolar compounds present in the reaction medium, mainly aromatics and oligomers. This organic phase was then concentrated and dried under vacuum at ambient temperature for 30 minutes. Finally it was diluted again in acetonitrile and analysed by GC-FID using naphthalene as standard.

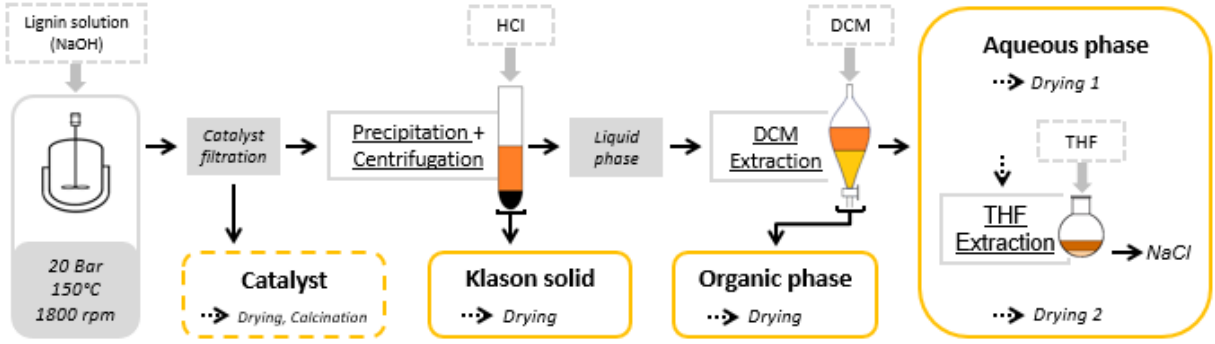

Figure S1: Fractionation method

6.3. - GC-MS/FID

GC analyses were performed on a Shimadzu GC-2010 chromatograph equipped with a FID detector, a AOC-20i+ autosampler and a Phenomenex Zebron ZB-5HT column (cross-linked of 5 % Phenyl – 95 % dimethylpolysiloxane, 30 m x 0.25 mm x 0.25 µm). Nitrogen was used as carrier gas. The mass spectra were obtained on a Shimadzu GC-MS-QP2010S equipped with an AOC-20i+ autosampler and a Sulpelco SLB-5MS column (5% Phenyl - 95 % dimethylpolysiloxane, 30m x 0.25mm x 0.25µm). Helium was used as carrier gas.

An example of chromatograms is given below.

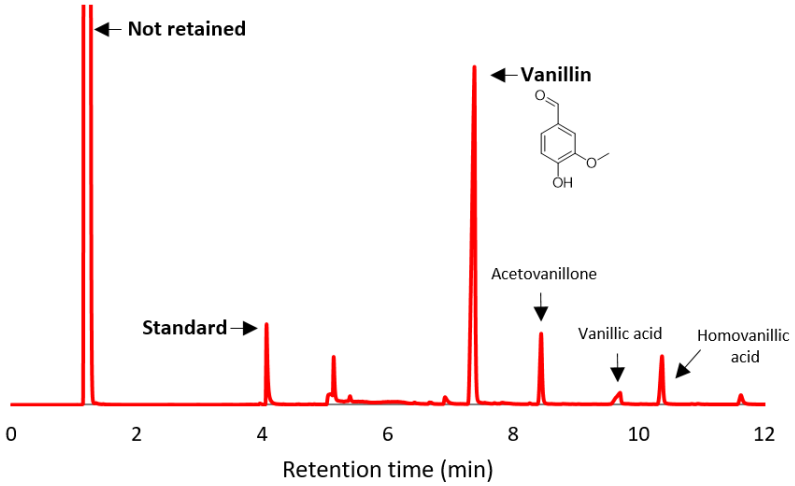

Figure S2: Example of GC-MS/FID chromatogram of one oxidized bio-oil

An external calibration for vanillin was carried out. Its curve is presented below.

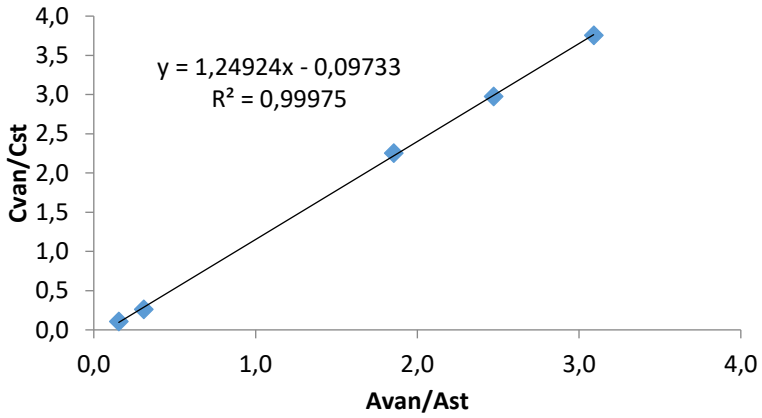

Figure S3: Vanillin calibration curve.

6.4. - FT-IR

In order to better understand the oxidation mechanisms, FTIR was conducted on the solid residues (obtained after fractionation, see supporting material). The FTIR spectra of solid residues of different runs are shown in Figure S4. The unreacted Kraft lignin sample exhibits different spectral characteristics compared to oxidized lignin residues; however, the oxidized samples do not show many appreciable differences for assignable peaks. The peak at 1504 cm-1 (aromatic skeletal vibrations) is more intense in unreacted Kraft lignin, indicating a relative lack of monomeric units and a lower degree of condensation and/or polyaromatic content in oxidized lignin residues.

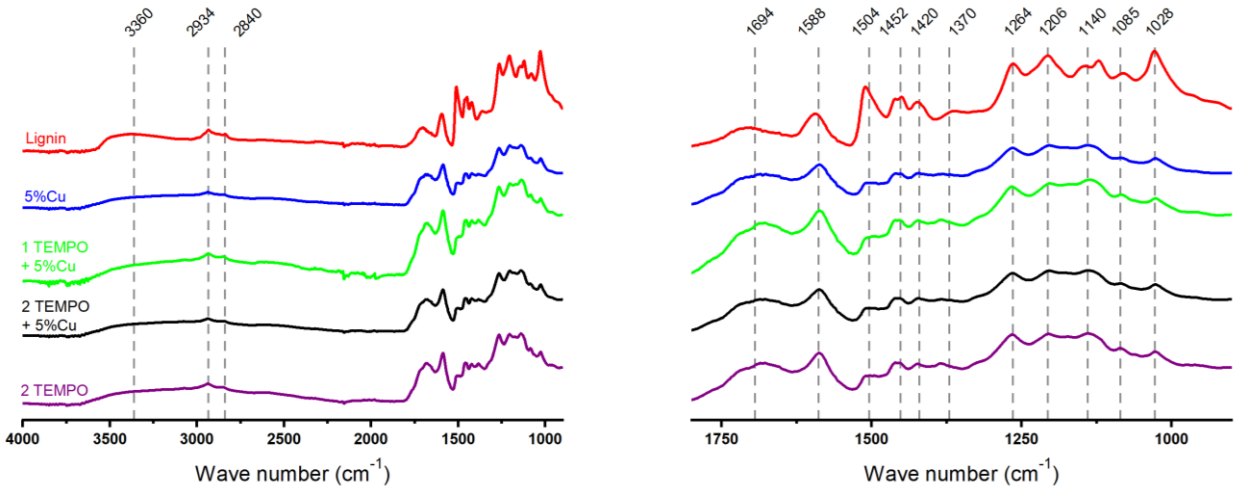

Figure S4: FT-IR spectra of solid residue (precipitated at pH=1) for different reaction conditions.

This is supported by the decrease of the bands at 1264, 1206 and 1028 cm^{-1} associated to C=O stretches. Deformation of C-O in primary alcohols also contributes to the peak at 1028 cm^{-1}. Its relatively large decrease between unreacted Kraft lignin and oxidized residues is consistent with the vanillin production scheme shown in Figure 1 of the main text.

In the following table, a list of peak assignment derived from literature[8-10] is provided. The results in the main text are based on these assignments.

Table S2 Peaks assignment for FT-IR spectra

Wave number (cm^{-1})	**Assignment**
3360	O-H stretch
2934	C-H stretch (aliphatic)
2840	C-H stretch (aliphatic)
1694	C=O stretch (not conjugated)
1650	C=O stretch (conjugated)
1588	Aromatic ring deformation, symmetric
1504	Aromatic ring stretch, asymmetric
1452	C-H deformation, asymmetric
1420	Aromatic ring stretch
1370	C-H aliphatic, O-H phenolic stretches
1329	S unit, G condensate
1264	C=O stretch (G unit)
1206	C-C, C-O, C=O stretches (G unit)
1140	C-H deformation (G unit)
1120	C-O (secondary alcohols), C=O (S unit) stretches
1085	C-O (secondary alcohols), R-O-R (aliphatic) deformations
1028	C-H (G unit), C-O (secondary alcohols), C=O (not conj.) deformations
915	C-H deformation (aromatic, out of plane)
834	C-H deformation (aromatic, out of plane)

6.5. - XRD of catalyst

XRD analysis was conducted on the catalyst (Cu/TiO_2) before and after reaction. As it is possible to see in the following figures, the analysis reports no significant difference between the samples analysed. The green peaks, which represent the CuO, do not change after the oxidation reaction. The only difference is in the Anatase phase (red peaks) for TiO_2: when titania is heated, which is the case during lignin oxidation, the Anatase phase becomes Rutile (blue peaks), a more stable aggregation phase for TiO_2. The addition of TEMPO does not

present an effect on the composition of the catalyst after reaction as shown by XRD (Figures S5-7).

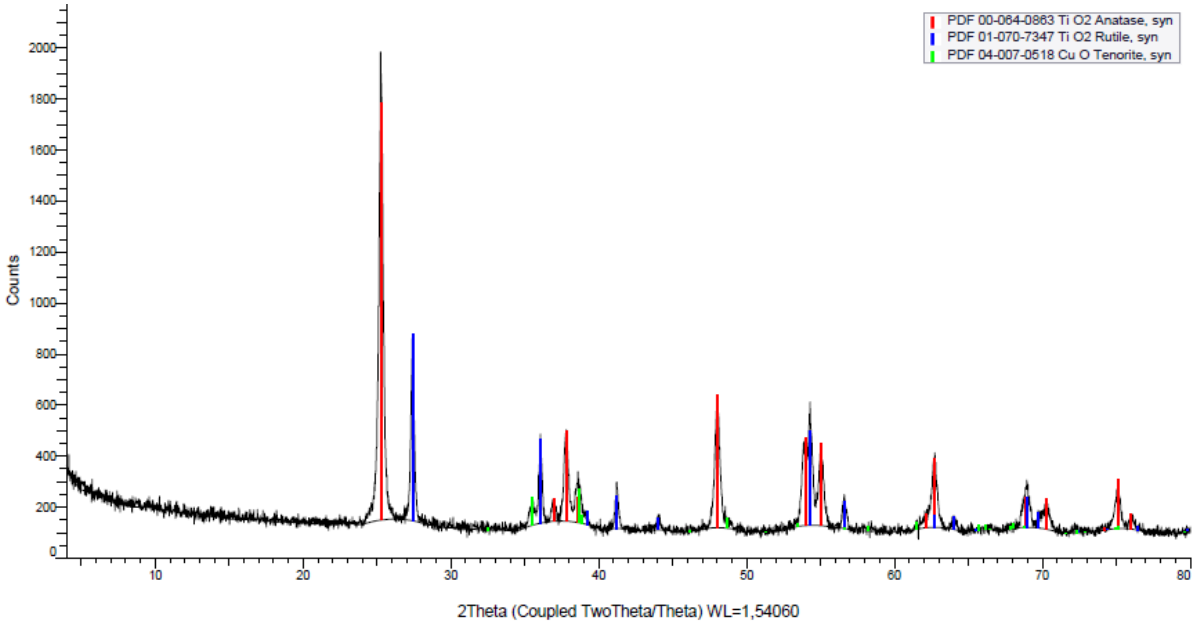

Figure S5: XRD spectrum of CuO/TiO2 catalyst before reaction

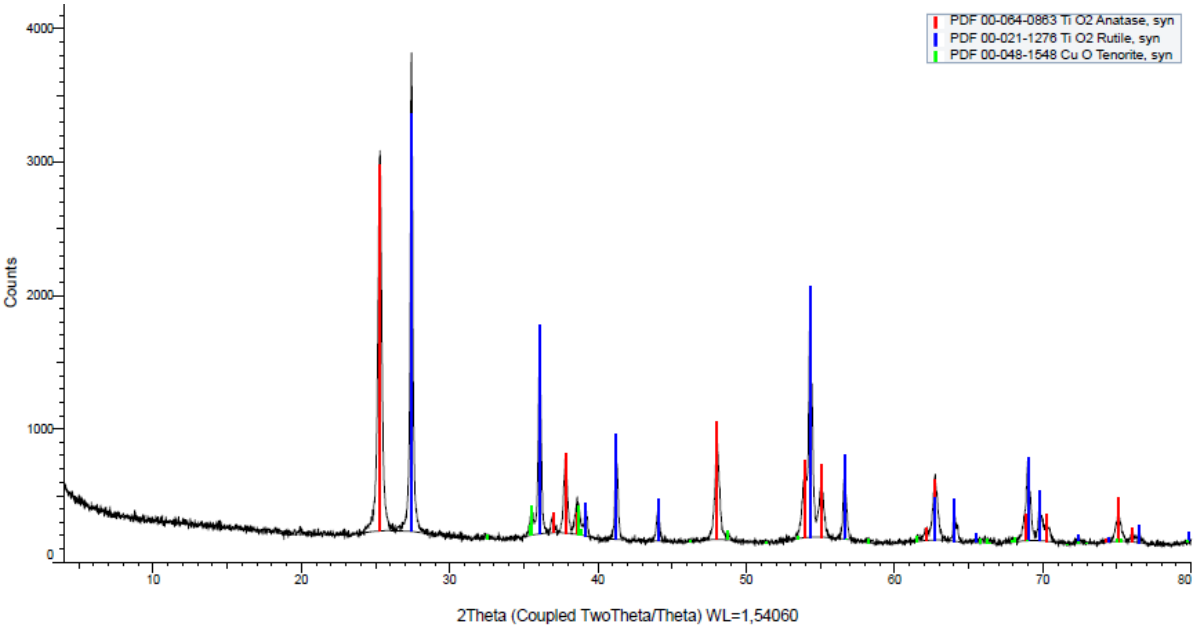

Figure S6: XRD spectrum of CuO/TiO2 after oxidation with only copper-based catalyst

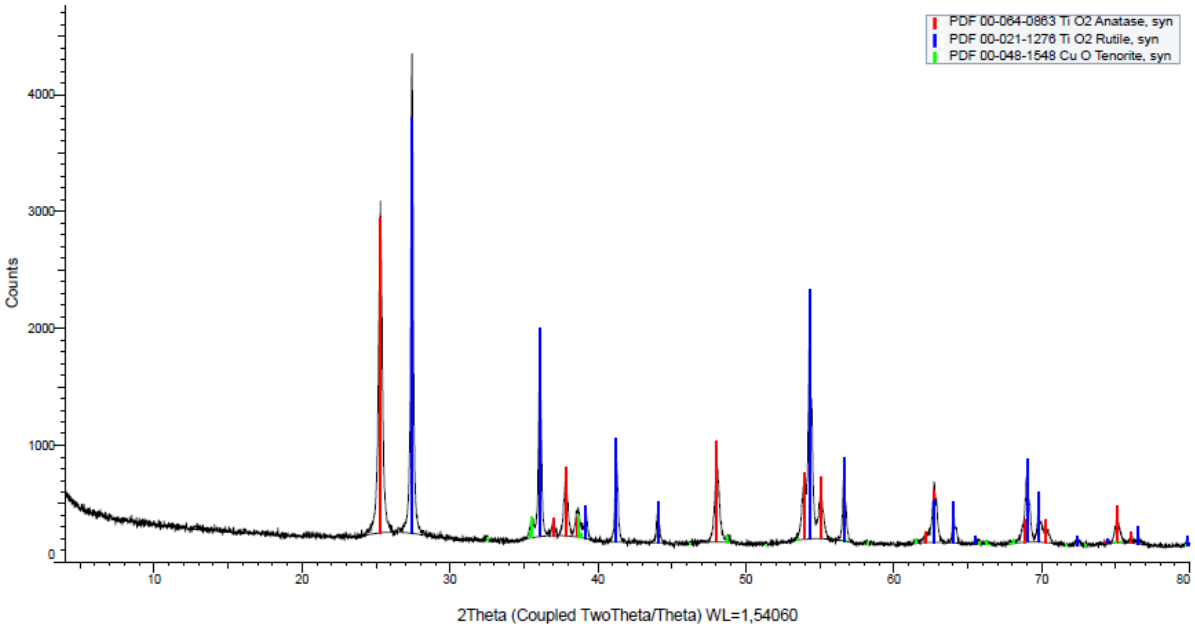

Figure S7: XRD spectrum of CuO/TiO2 after oxidation with 2-TEMPO

6.6. - References cited in the supporting info

1. M. Cui, R. Huang, W. Qi, R. Su, Z. He, *Catalysis Today*. **2019**, *319*, 121–127. DOI: 10.1016/j.cattod.2018.03.054.

2. M. Vadivelu, S. Sampath, K. Muthu, K. Karthikeyan, C. Praveen, *J. Org. Chem.* **2019**, *84* (21), 13636–13645. DOI: 10.1021/acs.joc.9b01896.

3. J. Y. Lin, F. Ghanbari, Y. S. Ok, G. Lisak, K. Y. A. Lin, F. C. Chang, *Waste and Biomass Valorization*. **2020**. DOI: 10.1007/s12649-020-01009-1.

4. M.-W. Zheng, K.-Y. A. Lin, C.-H. Lin, *Waste Biomass Valor*. **2019**. DOI: 10.1007/s12649-019-00910-8.

5. S. C. Patankar, L.-Y. Liu, L. Ji, S. Ayakar, V. Yadav, S. Renneckar, *Green Chem.* **2019**, *21* (4), 785–791. DOI: 10.1039/C8GC03304H.

6. M. Zirbes, L. L. Quadri, M. Breiner, A. Stenglein, A. Bomm, W. Schade, S. R. Waldvogel, *ACS Sustainable Chem. Eng.* **2020**, *8* (19), 7300–7307. DOI: 10.1021/acssuschemeng.0c00162.

7. R. Zhang, R. Maltari, M. Guo, J. Kontro, A. Eronen, T. Repo, *Industrial Crops and Products*. **2020**, *145*, 112095. DOI: 10.1016/j.indcrop.2020.112095.

8. B. Shrestha, Y. le Brech, T. Ghislain, S. Leclerc, V. Carré, F. Aubriet, S. Hoppe, P. Marchal, S. Pontvianne, N. Brosse, et al., *ACS Sustainable Chemistry & Engineering*. **2017**, *5* (8), 6940–6949. DOI: 10.1021/acssuschemeng.7b01130.

9. O. Faix, *Holzforschung*. **1991**. DOI: 10.1515/hfsg.1991.45.s1.21.

10. H. Li, A. G. McDonald, *Industrial Crops and Products*. **2014**, *62*, 67–76. DOI: 10.1016/j.indcrop.2014.08.013.

F. Integrating Lignin Depolymerization in Kraft Mills: experiments, process modelling and techno-economic assessment

To be submitted to ACS Sustainable Chemistry & Engineering

Erika Bartolomei[a], Rémi Demol[a], Felipe Buendia-Kandia[a], Sarah Bena[a], Fédérique Bertaud[b], Yann Le Brech[a], Anthony Dufour[a]*

[a] LRGP, CNRS, Université de Lorraine, 1 rue Grandville, 54000 Nancy, France

[b] CTP, 341 Rue de la Papeterie, 38400 Saint-Martin-d'Hères, France

* corresponding authors: anthony.dufour@univ-lorraine.fr

Abstract

The aim of this study is to investigate the integration of a lignin depolymerization unit in an existent Kraft paper mill (100 ton/h of dry wood) from a techno-economic point of view. The simulation of the whole process has been done on AspenPlus® based on experimental results achieved on black liquor supplied by the mill itself. Four different scenarios have been compared experimentally: one scenario involves the direct liquefaction of black liquor and in the other three ones, lignin is first precipitated and then sent to the liquefaction unit, varying the solvent for liquefaction (alkaline water or ethanol) and the catalyst (Ni-based). The AspenPlus® model integrates the experimental results of liquefaction (mass and atomic balances) as well as experiments on solvent extraction of monomers. Therefore, the whole process from the black liquor to the purified monomers is modelled, based on the mass and energy balances, a techno-economic assessment has been conducted for all the scenarios. The ethanol based liquefaction is able to increase the profitability of the mill. Lignin precipitation followed by liquefaction presents better results than the direct depolymerization of black

liquors. Moreover, significant economic benefit comes from these scenarios compared to using lignin just for heat and power production.

Keywords Techno-economic analysis, Biorefinery, Solvent liquefaction, Kraft mill, Lignin, AspenPlus®

1. - Introduction

More than one century ago, researchers realized the intrinsic potential of biomass as a renewable petroleum substitutes.[1] Currently, it is even more important to reduce oil demand and use carbon neutral resources to mitigate the effects of global warming.[2,3] Among the different kinds of biomass feedstock, lignin from Kraft pulping operation is particularly attractive because of its large availability.[4–6] In paper mills, lignin is separated from wood and it goes in a side liquid stream, called black liquor. It is considered a waste product and burned to recover energy.[7,8] There is still a lack of alternatives for black liquor utilization, even though it can contribute to the new generation of biofuels and/or platform chemicals because of its nature. In fact, lignin is a biopolymer composed of aromatic subunits, mainly p-courmaryl, coniferyl and synapyl alcohols bonded together principally through aryl/diaryl ether, dibenzodioxicin and phenyl-courmaran linkages.[9,10] If lignin has already a complex and recalcitrant structure, black liquor is even more complex since it is composed by a mixture of alkali lignin, sodium salts of sugar oligomers and carboxylic acid, and also some inorganic species, residual reagents of Kraft pulping.[11]

In the original Kraft process, black liquor is burnt in the recovery boiler, but in the last decades, researchers realized that the economic and environmental performance of the mills could be improved. The critical step in the process is the chemical recovery, so to debottleneck the mill a lignin removal from black liquor before the boiler through precipitation has been made.[12,13] Lignin is separated from black liquor decreasing the pH with carbon dioxide and filtering the flocculates. The lignin cake is then washed. The rest of the black liquor stream is sent to the recovery boiler as well. Lignin removal has different effects on the process. Indeed, the physical properties and the heating value of the black liquor change. For instance, the heat recovered from the boiler decreases if the air to mass unit ratio is maintained constant.[13] On the other hand, if the power produced from the combustion of black liquor is maintained constant, the wood feedstock demand increases, with a proportional raise in pulp production. Introducing the lignin precipitation unit in the pulping process involves a rebalance of material and energy.[14]

The lignin separated in this way has to be valorized and upgraded into added-value products. Many studies have been already conducted to find an effective way to depolymerize or deconstruct lignin, such as hydrothermal liquefaction under subcritical/supercritical conditions.[15–21] The scope of this conversion is to obtain a biocrude containing the organic resources of the initial feedstock with higher heating value, high viscosity and lower oxygen content.[22,23]

Lignin hydrothermal conversion requires the extraction process (precipitation, drying and purification) and then a solubilization in a liquid solvent, which can be alkaline water or alcohols. Apparently, those supplementary steps generate an increase of the cost of the feedstock[24], but also a consistent investment to add those units in the pulp process. That is why it is interesting to evaluate a black liquor direct conversion for simplified unit of lignin valorization in the pulp mill. In this way, it would be possible to avoid the steps of drying and purification, saving energy.

Taking in account previous studies on this subject and based on the data we have on a real paper mill, we propose different scenarios for the valorization of the lignin stream to produce green aromatic platform chemicals (see Figure 1). Direct hydrothermal liquefaction of black liquor is compared to lignin precipitation and consequent lignin liquefaction under different conditions.

The scope of this study is to evaluate which scenario would be the most efficient one for the paper mills from the energetic and economic point of views, putting particular attention on platform molecules production, sodium and energy recoveries.

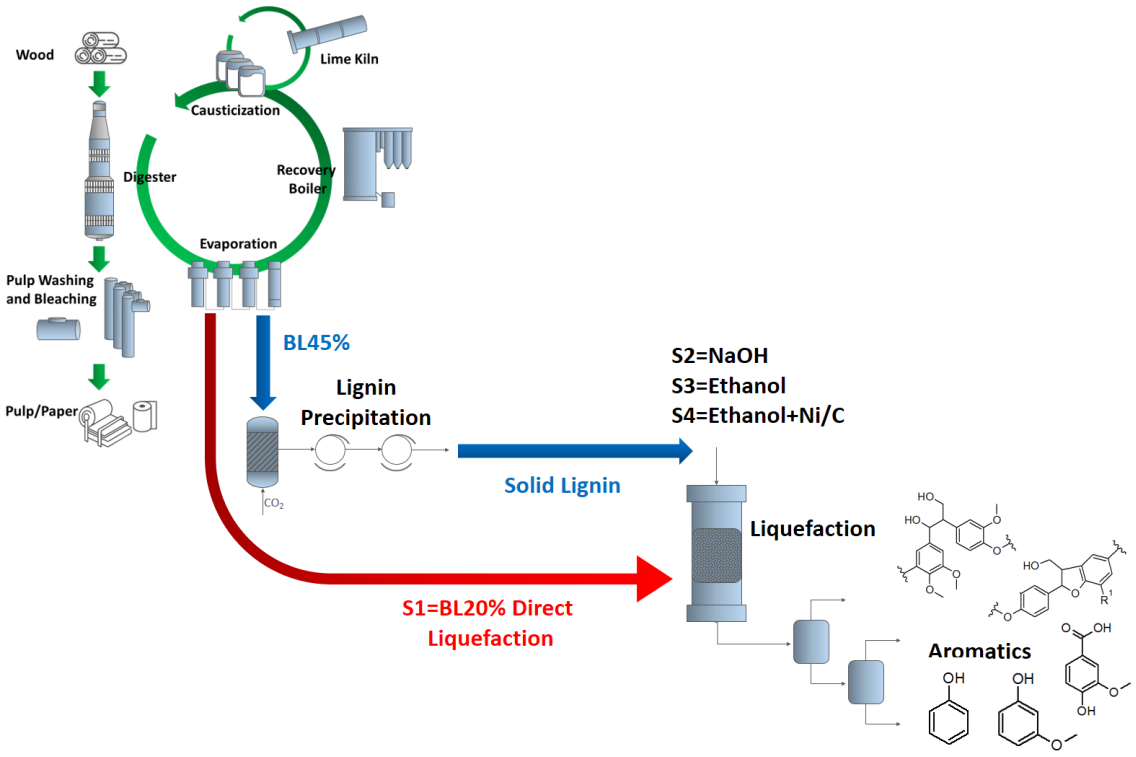

Figure 1 Scheme of the process with all the scenarios.

2. - Methodology

2.1. - Experimental section

Table 1 Experimental conditions.

Scenario	Feed	T °C	t (h)	Gas	Solvent	Catalyst	Monomers (%wt)	Oligomers (%wt)	Char (%wt)	Rest (%wt)
S1	BL20%	300	1	N_2	-	-	0.44	7	77	15.56
S2	Kraft lignin	300	1	N_2	NaOH	-	2.67	14	79	4.33
S3	Kraft lignin	250	4	H_2	EtOH	-	2.44	41	47	9.56
S4	Kraft lignin	250	4	H_2	EtOH	Ni/C	4.71	42	28	25.29

Direct black liquor (BL20%, 20%wt of lignin content) and precipitated Kraft lignin (Kraft lig. according to S2, S3 and S4) liquefactions were performed in a batch reactor (stirred 300mL Parr® autoclave).

S1: Black liquor (BL20%, 20%wt lignin content) tapped from the evaporation unit of a real paper mill is directly converted under nitrogen atmosphere (100bar) for 1 hour at 300°C, without the addition of any solvent or catalyst.

S2: Kraft lignin (previously precipitated from black liquor with 45%wt lignin content, K3 from previous sections) is solubilized in alkaline water (10g/L NaOH) to reach pH ~13 (same as the one of the black liquor). The reaction is conducted at 300°C and 100bar of N_2.

S3: Kraft lignin is solubilized in ethanol and depolymerized for 4 hours under hydrogen atmosphere (100 bar) at 250°C without catalyst.

S4: Kraft lignin is solubilized in ethanol and depolymerized via liquefaction for 4 hours under hydrogen atmosphere (100 bar) at 250°C in presence of 2g of Ni/C (5%wt) from Riogen® (0158-CNiA05-Powder).

Those scenarios have been chosen after previous liquefaction screenings because of their complementarity. The purpose of this study is to compare the integration of a lignin valorization unit in Kraft pulp mills with a techno-economic assessment considering scenarios who differ between each other for solvent, lignin content, use of catalyst, atmosphere and temperature.

In the cases in which the NaOH solution is used, hydrogen did not show any benefit in depolymerization yield and the use of catalyst was not useful because of fast poisoning in these conditions[8]. See section 3.1 for product mass distribution discussion.

After reaction, the bio-oil is firstly filtered (11 µm) to separate the char formed during the reaction and eventually the catalyst. Then the liquid can be directly analyzed by GC-MS/FID if it is ethanol-based, otherwise it requires a liquid/liquid L/L extraction with ethyl acetate. A part of the bio-oil is acidified with HCl until pH~1 to precipitate oligomers, which are separated by centrifugation. Elemental and proximate analysis have been performed on the initial lignin, chars and oligomers formed during liquefaction tests.

Monomers quantification from GC/MS with method in supporting information.

Elemental and proximate analysis for solids with method in supporting information.

2.2. - Description of the AspenPlus® model

The whole existing pulp mill the lignin precipitation and the valorization units have been simulated on AspenPlus® (v8.8). The base capacity of the Kraft mill is 100 ton/h of dry wood (pinewood) and an extraction of 2.2%wt (on the total lignin feed) of lignin has been fixed. This

amount corresponds to the 10%wt of the black liquor (with 22%wt lignin content) taken before the evaporation step. The steam and electricity provided by the boiler must stay constant. As a result, the wood feed of the mill is adjusted accordingly.

2.2.1. - Definition of the solid compounds

LIGNIN, CHAR and OLIGOMERS are defined as non-conventional solids with their proximate and elemental experimental composition (Table S1-S4 in supporting information). For each scenario, atomic balance is closed based on experimental elemental analysis of char and oligomers. Equation 1 is the depolymerisation stoichiometric equation. To ensure elemental mass conservation an additional specie called REST is defined. It represents all the species which were not analysed.

2.2.2. - Liquefaction reactor

The liquefaction reactor is modelled with RSTOIC and Equation 1. The stoichiometric coefficient and the detailed elemental composition of the non-conventional species are gathered in supporting information for each scenario.

Equation 1 Lignin liquefaction equation from experiments used in Aspen Plus.

$$Lignin \rightarrow \gamma_1 \cdot Guaiacol + \gamma_2 \cdot Syringol + \gamma_3 \cdot Phenol + \gamma_4 \cdot Catechol + \gamma_5 \cdot Char + \gamma_6 \cdot Oligomers + \gamma_7 \cdot Rest$$

2.2.3. - Products separation

After the liquefaction unit, the different phases are separated. The gas (N_2 or H_2) is recycled in the liquefaction reactor. The recovery of char and oligomers is assumed to be conducted by ultrafiltration. The liquid phase (bio-oil) is sent to liquid-liquid extraction in the cases S1 and S2 to extract the organic phase from alkaline water into ethyl acetate. Then a distillation unit is used to concentrate the lighter aromatics (monomers such as phenol, guaiacol, catechol, and syringol) and recover the solvent. For the cases S3 and S4 the liquid-liquid extraction is not necessary since the bio-oil is ethanol-based. For ethanol depolymerization, a direct distillation is set up. The recycle of gases and solvents reduces the cost of make-ups.

Not only the liquefaction unit has been simulated based on experimental results, but also the liquid-liquid extraction necessary in S1 and S2. In fact, at laboratory scale, we have quantified the extraction factor for the main monomers (phenol, guaiacol, syringol and catechol) for an

organic extraction using ethyl acetate (see Appendix 2 - Study on the extraction of phenolic compounds from bio-oils). Those parameters have been integrated into the model. The separation of the monomers is achieved by distillation. A shortcut model is firstly use to achieve 95% solvent recovery. The minimal number of stage and the reflux ratio obtained is then used in a RADFRAC model.

2.3. - Techno-economic assessment

Each equipment is sized according to the heat & mass balance. The cost of equipment is estimated from various literature data (more details for equipment cost are given in supporting information) and updated to year 2019 with the chemical engineering price cost index. The total fixed capital investment is estimated with an overall Lang factor of 4.1.[26] More details can be found in supplementary material for equipment costs, products prices and general assumptions.

3. - Results and discussion

The results will be presented in three sections: experimental work, modelling (mass/energy balances), and evaluation of different scenarios based on economic assessments.

3.1. - Experiments on lignin depolymerization

Table 1 reports the yields of the three main products of liquefaction for the four scenarios. For the two cases in alkaline water (S1 and S2), char is the main product (77%wt and 79%wt respectively), while oligomers and monomers are very low. In those two scenarios we find lignin dissolved in a high alkaline water: in S1 is black liquor at 22%wt lignin content, which has generally 10.0 (±0.1) %wt of Na content (from experimental analysis); in S2 the same alkaline condition was used (pH~13) and the necessary NaOH concentration for this purpouse is 10 g/L.

According to S3 and S4 (where ethanol is used as solvent), the char yields are lower. It is wellknown that ethanol can reduce condensation reactions by promoting hydrogen transfer and stabilization of cleaved bonds[27,28]. For this reason, these two scenarios produce less char and higher yields of monomers and especially oligomers (41-42%wt). In S4, the presence of Ni/C as catalyst doubles the monomer yield (as presented in Chapter D) with respect to the equivalent scenario without any catalyst (S3), up to 4.7%wt.

The composition of the solid products (char and oligomers) has been investigated by elemental and proximate analysis (see supporting information). In general volatil matter, fixed carbon and

moisture content are very similar for chars and oligomers from different scenarios. The elemental analysis, indeed, reveals that char from S1 has a different composition compared to the others: it has a lower C content probably due the mineral (Na and K) content present in the residues (higher in black liquor than in precipitated lignin).

The monomer yields for the four scenarios vary between 0.44 and 4.71 %wt (increasing from S1 and S4). The main difference is the selectivity for different phenolic families (see section 5.2 in supporting information). S1 yields almost only catechols, S2 mainly catechols and guaiacols, and S3 and S4 mostly guaiacols.

The results obtained from experimental liquefaction tests and analytical investigation are used in AspenPlus® in order to have the most possibl erealistic scenarios from the simulated integration of lignin valorization chain into a paper mill biorefinery.

3.2. - Modelling

Figure 2 summarizes the key results from simulation based on the experimental data. For each scenario the main streams are reported, relative flow rates, and heat/power needs. To optimize the efficiency of the lignin valorization unit, all the possible heat and streams who could be reintegrated into the plant have been recycled. Except for the S1 (BL20%), where the black liquor 22%wt lignin content is directly sent to liquefaction, in all the scenarios black liquor is tapped from the evaporation unit with a lignin concentration of 45%wt to make lignin precipitation more efficient. Anyway, the share of lignin subtracted and sent to valorization is always the same for all the cases to compare the different valorization pathways.

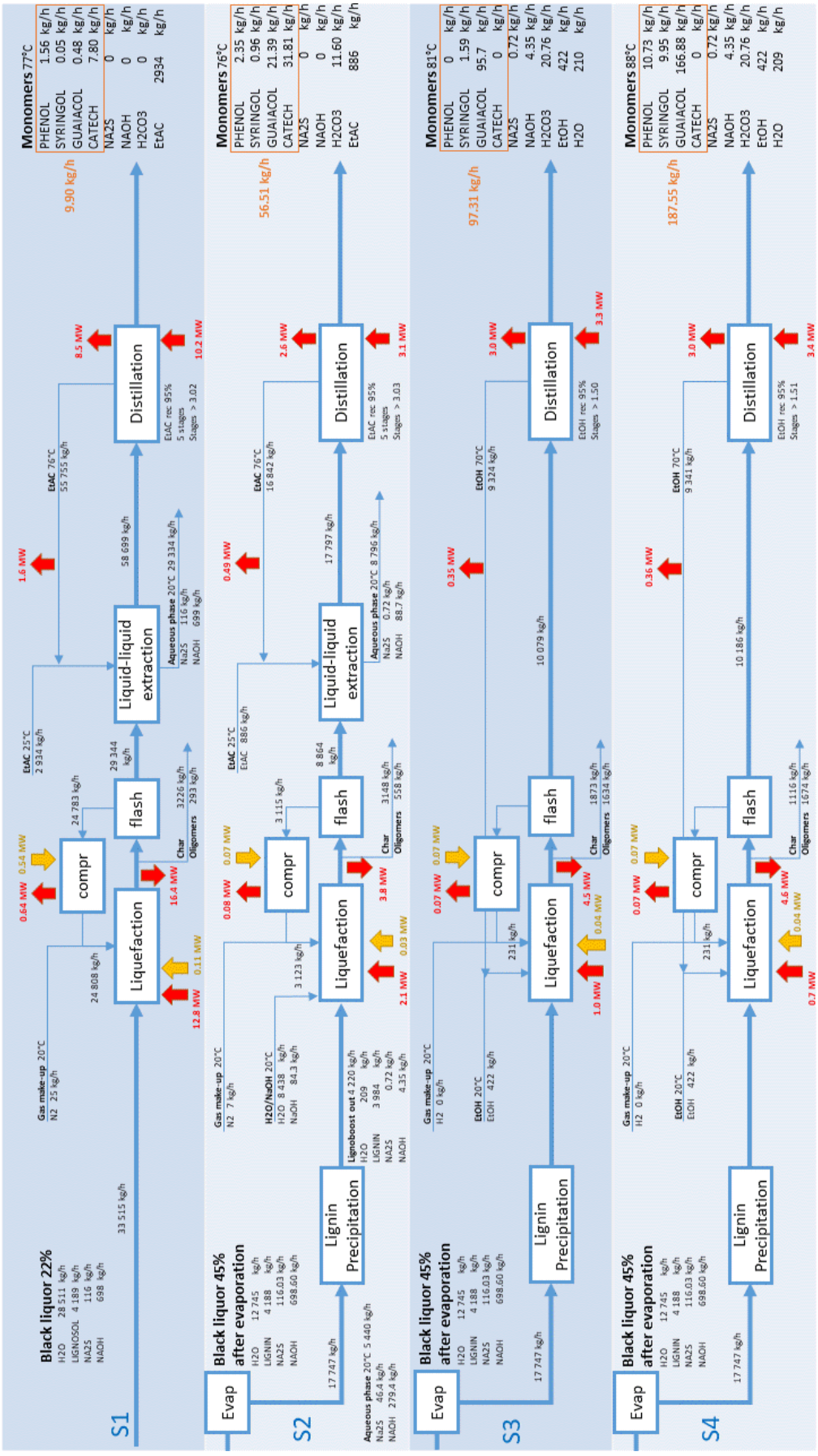

Figure 2 Mass and heat main streams for the four scenarios.

For S1, the mass and heat balances show that the direct liquefaction of black liquor is not convenient. Based on experimental monomers analysis and liquid-liquid extraction factors, the production of monomers is very low compared to the other scenarios, under our experimental conditions studied (with operable pressure of about 100 bar max.). Different reasons can explain this result. The liquor who enters the liquefaction reactor is more diluted than the other cases (22%wt instead of 33%wt lignin content). It does not only make the monomer yield lower but affects also the products separation steps. A larger amount of extraction solvent is required because after liquefaction we find a liquid stream around three times higher than the other cases for L/L extraction. This huge volume of liquid makes distillation much more energy consuming.

In S2, liquefaction occurs again in alkaline water (NaOH), but in this case lignin is CO2 precipitated and dissolved into sodium hydroxide water solution (10g/L). The amount of solvent is fixed as two times the lignin mass for S2, S3 and S4. Since lignin results more concentrated, the ethyl acetate required for extraction is less important. Also distillation requires less energy. In this case the monomer yield is higher than in S1, but both these two first scenarios are affected from the extraction efficiency. In fact, experimental test revealed that ethyl acetate can extract around the 60%wt of the monomers in the bio-oil, so a huge part of them are recirculated into the process.

In the last two scenarios (S3 and S4), the precipitated lignin is solubilized in ethanol for the liquefaction reaction. Moreover, hydrogen is used instead of nitrogen because in experimental tests it revealed an important contribution in lignin depolymerization, while for aqueous-based solvent liquefaction (S1 and S2) it had no impact. For S3 and S4, the liquid-liquid extraction step is not necessary, so the ethanol-based bio-oil is directly sent to distillation. Avoiding monomers extraction helps to recover almost the total amount of them (ethanol recovery is set at 95%). Because of that reason and also because ethanol has a benefic effect in lignin depolymerization, we find a higher amount of monomers at the end of the process. S4 differs from S3 because of the presence of Ni-based catalyst in the liquefaction reactor. Thanks to it, the monomer yield is almost the double.

3.3. - Techno-economic analysis

Following the AspenPlus® simulation, it was possible to make a techno-economic analysis for the four scenarios. Taking in account the mass and heat balances, a detailed assessment for CAPEX, OPEX and revenues for the integrated process are presented in Figures 3-5.

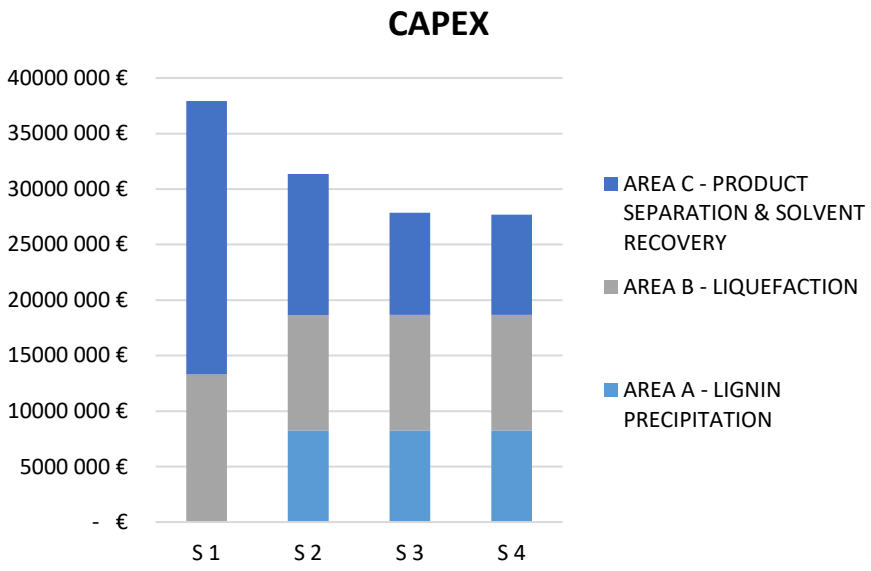

Figure 3 Fixed capital investment required for the fours scenarios and contribution of each sub process area.

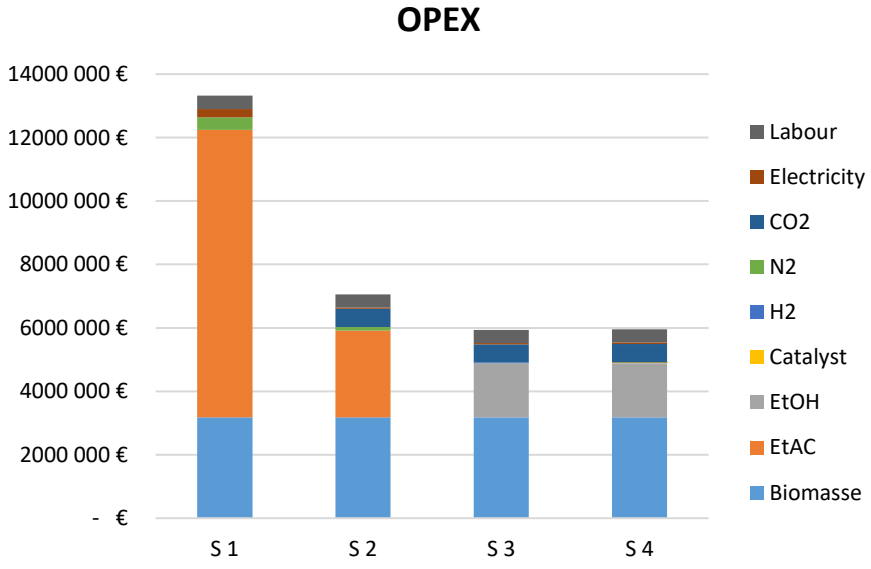

Figure 4 Main operating costs for the four scenarios.

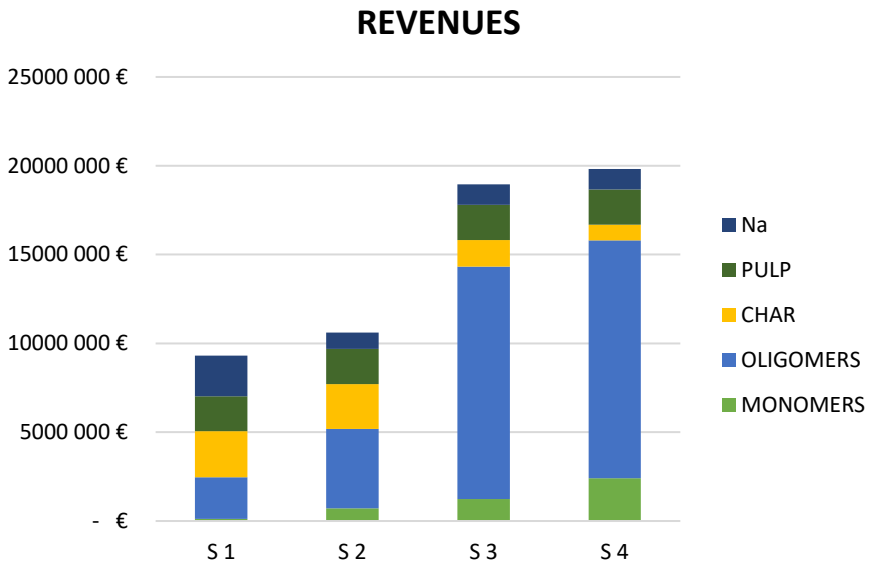

Figure 5 Revenues sources for the four scenarios.

The CAPEX given in Figure 3 is ventilated to the three sub processes integrated to the paper mill: lignin precipitation (area A), liquefaction (area B) and product separation and solvent recovery (area C). It can be noticed that, even if the cost of lignin precipitation unit for S1 is not present, the total CAPEX results higher that the other scenarios. The reason is the higher amount of solvents involved in this scenarios compared to the others. In fact, the product separation and solvent recovery units are more expensive. For the other scenarios the CAPEX are very similar.

Also the OPEX (Figure 4) of S1 is higher than the others because of the huge amount of ethyl acetate necessary for the liquid-liquid extraction. The other scenarios have very similar OPEX.

Figure 5 presents the revenues for the liquefaction products, the sodium recovered that can be recycle into the mill, and the surplus of pulp. In fact, if a part of the black liquor is taken and the power produced in the recovery boiler is set constant, an extra amount of wood has to be processed in the mill. In that way the boiler will stay at the same power with a constant production of steam, which is also converted in electricity for the plant thanks to a turbo-generator. Moreover, this extra amount of wood increases the production of pulp. Char can be sold as fuel or other application, while oligomers and monomers are assumed to be sold as chemicals.

Selling prices are taken from market data, literature and assumption made (see supporting information).

Based on these results, the cash flow is calculated leading to the Net Present Value (NPV) after 20 years for the four scenarios (see Figure 6). This indicator that take into account money value over time is positive when an investment is profitable and negative otherwise.

$$NPV = \sum_{0}^{n} \frac{(R_k - COM_k - d_k) \cdot (1 - t) + d_k}{(1 + i)^k}$$

R_k, COM_k, d_k are the revenue, cost of manufacturing and depreciation at the year k, t in tax rate and i the discounting rate, n the time period

For S1 and S2 we find a negative NPV, while for S3 and S4 it is positive. The investment should be considered interesting only for the two last options.

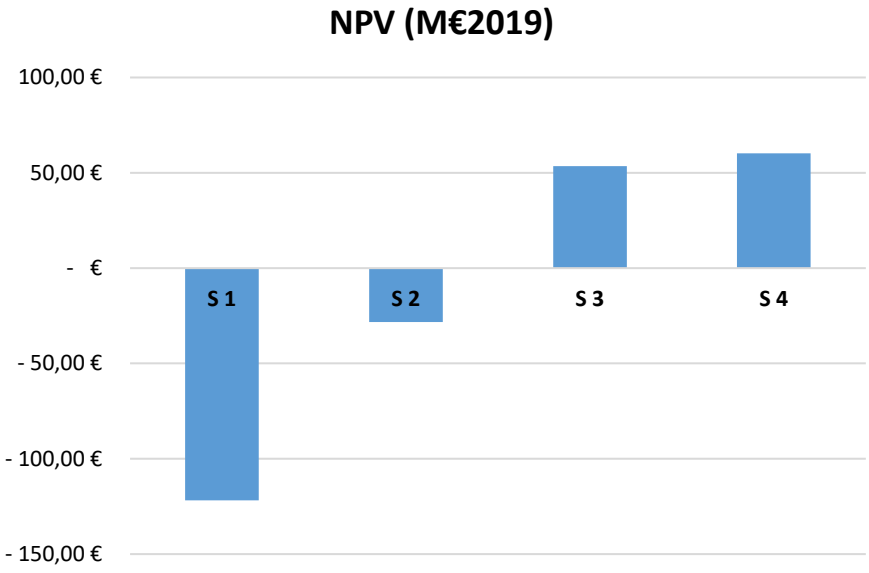

Figure 6 Net Present Value for the four scenarios.

In order to evaluate the added value for the existing mill, the NPV was divided by the total production of pulp (see Figure 7). When this indicator is positive, the impact of this investment is an additional cost for the mill (S1 and S2). On the contrary, when it is negative, the investment provides extra revenues and decrease the production cost of pulp. Choosing S3 or S4 leads to a decrease of pulp production cost around 0.12-0.14 €/kg of pulp.

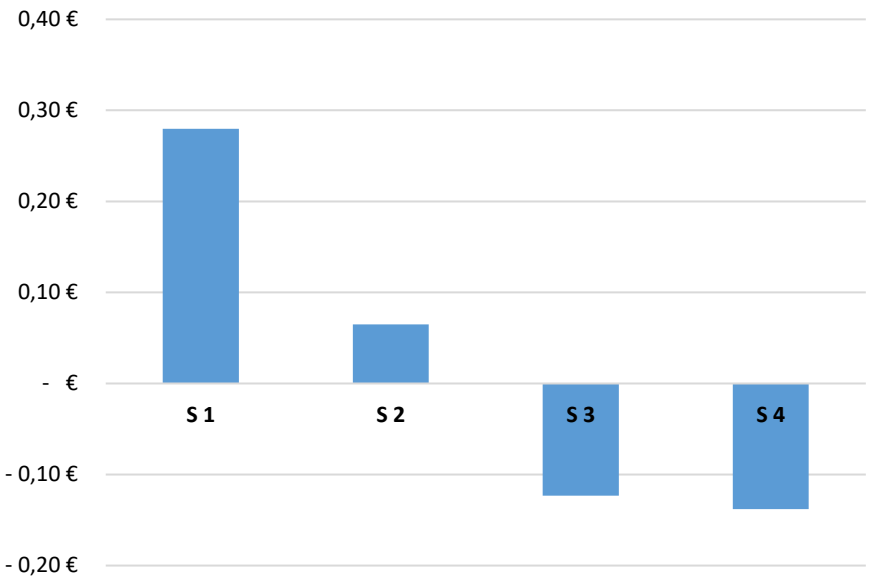

Figure 7 Impact of the investment on pulp production cost [€/kg of pulp] for the four scenarios.

Considering all the economic parameters evaluated, scenarios 3 and 4 are very similar. They both show that the integration of a lignin valorization unit in a paper mill is not only feasible, but also economically convenient, reaching a NPV of approximately 50-60 M€$_{2019}$ after 20 years.

A sensitivity analysis on the reduction pulp production cost is conducted on S3 by varying some costs by ±30% Among the parameters varied, we investigated the impact of the estimation of CAPEX and the prices of the main products and chemicals required. The results are presented in Figure 8.

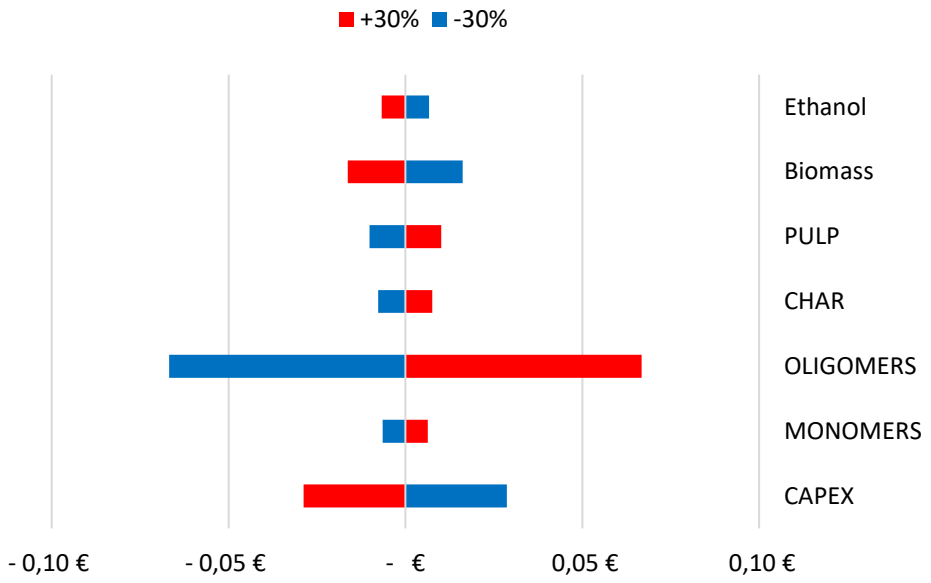

Figure 8 Sensitivity analysis for scenario 3.

The parameter investigated for this sensitivity analysis are the prices for the selling products, feedstock (biomass, ethanol) and CAPEX. It is possible to see that the most critical parameter is the price of oligomers. In fact, oligomers are one of the most abundant product of lignin liquefaction under our relatively mild conditions.

Indeed, it has been previously shown that oligomers (or "depolymerized lignin") can be an interesting targeted products for lignin depolymerization instead of targeting monomers.[32-35]

In conclusion, in this section, we have included our experimental results in a complete Aspen Plus model of the pulp mill. This model has given mass and energy balances. Furthermore a techno-economic analysis has been conducted. Based on our experimental conditions and assumed modeling data, the integration of a lignin depolymerization unit in an existent Kraft pulp mill can be possible and profitable. In particular, between the analyzed different scenarios, the most efficient seems with a precipitation of the lignin followed by ethanol depolymerization to reduce the cost of L/L extraction and purification and to increase monomer yields. With a NPV around 50 M€, this integrated process may be considered viable and profitable. In the next future, we will improve the oligomers and monomers yields with other operating conditions, tailored based on this technical-economical model of the whole biorefinery. The economical part may be precised with industrial partners.

4. - References

1. Hubbard, E. *The Utilisation of Wood-waste*. (Scott, Greenwood & Son, 1915).

2. Brandt, C. C. *et al. 2016 Billion-Ton Report: Advancing Domestic Resources for a Thriving Bioeconomy, Volume 1: Economic Availability of Feedstocks*. https://www.osti.gov/biblio/1435342-billion-ton-report-advancing-domestic-resources-thriving-bioeconomy-volume-economic-availability-feedstocks (2016) doi:10.2172/1435342.

3. Chundawat, S., Beckham, G., Himmel, M. & Dale, B. Deconstruction of Lignocellulosic Biomass to Fuels and Chemicals. *Annual Review of Chemical and Biomolecular Engineering* 2, 121–145 (2011).

4. Maciel, A. V., Job, A. E., Mussel, W. N. & Pasa, V. M. D. Pyrolysis and auto-gasification of black liquor in presence of ZnO: An integrated process for Zn/ZnO nanostructure production and bioenergy generation. *Biomass and Bioenergy* **46**, 538–545 (2012).

5. French, R. & Czernik, S. Catalytic pyrolysis of biomass for biofuels production. *Fuel Processing Technology* **91**, 25–32 (2010).

6. Peng, C., Zhang, G., Yue, J. & Xu, G. Pyrolysis of black liquor for phenols and impact of its inherent alkali. *Fuel Processing Technology* **127**, 149–156 (2014).

7. Saraeian, A. *et al.* Evaluating lignin valorization via pyrolysis and vapor-phase hydrodeoxygenation for production of aromatics and alkenes. *Green Chem.* **22**, 2513–2525 (2020).

8. Funkenbusch, L. T. *et al.* Technoeconomic assessment of hydrothermal liquefaction oil from lignin with catalytic upgrading for renewable fuel and chemical production. *WIREs Energy and Environment* **8**, e319 (2019).

9. del Río, J. C. *et al.* Structural Characterization of the Lignin in the Cortex and Pith of Elephant Grass (*Pennisetum purpureum*) Stems. *Journal of Agricultural and Food Chemistry* **60**, 3619–3634 (2012).

10. Chakar, F. S. & Ragauskas, A. J. Review of current and future softwood kraft lignin process chemistry. *Industrial Crops and Products* **20**, 131–141 (2004).

11. Ragnar, M. *et al.* Pulp. in *Ullmann's Encyclopedia of Industrial Chemistry* 1–92 (American Cancer Society, 2014). doi:10.1002/14356007.a18_545.pub4.

12. Li, T. & Takkellapati, S. The current and emerging sources of technical lignins and their applications. 62 (2019).

13. Vakkilainen, E. & Välimäki, E. *Effect of Lignin Separation to Black Liquor and Recovery Boiler Operation*. (2009). doi:10.13140/2.1.2039.6485.

14. Tomani, P., Axegård, P., Berglin, N., Lovell, A. & Nordgren, D. INTEGRATION OF LIGNIN REMOVAL INTO A KRAFT PULP MILL AND USE OF LIGNIN AS A BIOFUEL. 8.

15. Yong, T. L.-K. & Matsumura, Y. Kinetic Analysis of Lignin Hydrothermal Conversion in Sub- and Supercritical Water. *Ind. Eng. Chem. Res.* **52**, 5626–5639 (2013).

16. Lavoie, J.-M., Baré, W. & Bilodeau, M. Depolymerization of steam-treated lignin for the production of green chemicals. *Bioresource Technology* **102**, 4917–4920 (2011).

17. Beauchet, R., Monteil-Rivera, F. & Lavoie, J. M. Conversion of lignin to aromatic-based chemicals (L-chems) and biofuels (L-fuels). *Bioresource Technology* **121**, 328–334 (2012).

18. Azadi, P., Inderwildi, O. R., Farnood, R. & King, D. A. Liquid fuels, hydrogen and chemicals from lignin: A critical review. *Renewable and Sustainable Energy Reviews* **21**, 506–523 (2013).

19. Roberts, V. M. *et al.* Towards Quantitative Catalytic Lignin Depolymerization. *Chemistry – A European Journal* **17**, 5939–5948 (2011).

20. Fang, Z. *et al.* Reaction chemistry and phase behavior of lignin in high-temperature and supercritical water. *Bioresource Technology* **99**, 3424–3430 (2008).

21. Okuda, T. *et al.* Estimation of aboveground biomass in logged and primary lowland rainforests using 3-D photogrammetric analysis. *Forest Ecology and Management* **203**, 63–75 (2004).

22. Huet, M., Roubaud, A., Chirat, C. & Lachenal, D. Hydrothermal treatment of black liquor for energy and phenolic platform molecules recovery in a pulp mill. *Biomass and Bioenergy* **89**, 105–112 (2016).

23. Chen, J., Liu, C., Wu, S., Liang, J. & Lei, M. Enhancing the quality of bio-oil from catalytic pyrolysis of kraft black liquor lignin. *RSC Adv.* **6**, 107970–107976 (2016).

24. Farag, S. & Chaouki, J. Economics evaluation for on-site pyrolysis of kraft lignin to value-added chemicals. *Bioresource Technology* **175**, 254–261 (2015).

25. Sun, S.-N., Li, H.-Y., Cao, X.-F., Xu, F. & Sun, R.-C. Structural variation of eucalyptus lignin in a combination of hydrothermal and alkali treatments. *Bioresource Technology* **176**, 296–299 (2015).

26. Peters, M. S., Timmerhaus, K. D. & West, R. E. *Plant design and economics for chemical engineers*. (McGraw-Hill, 2003).

27. Yang, J., Zhao, L., Liu, S., Wang, Y. & Dai, L. High-quality bio-oil from one-pot catalytic hydrocracking of kraft lignin over supported noble metal catalysts in isopropanol system. *Bioresource Technology* **212**, 302–310 (2016).

28. Huang, X., Korányi, T. I., Boot, M. D. & Hensen, E. J. M. Ethanol as capping agent and formaldehyde scavenger for efficient depolymerization of lignin to aromatics. *Green Chemistry* **17**, 4941–4950 (2015).

29. de Saint Laumer, J.-Y., Cicchetti, E., Merle, P., Egger, J. & Chaintreau, A. Quantification in Gas Chromatography: Prediction of Flame Ionization Detector Response Factors from Combustion Enthalpies and Molecular Structures. *Analytical Chemistry* **82**, 6457–6462 (2010).

30. Bangalore Ashok, R. P. *et al.* Techno-economic assessment for the large-scale production of colloidal lignin particles. *Green Chem.* **20**, 4911–4919 (2018).

31. Dessbesell, L. *et al.* Bio-based polymers production in a kraft lignin biorefinery: techno-economic assessment. *Biofuels, Bioproducts and Biorefining* **12**, 239–250 (2018).

32. Dessbesell, L., Paleologou, M., Leitch, M., Pulkki, R. & Xu, C. (Charles). Global lignin supply overview and kraft lignin potential as an alternative for petroleum-based polymers. *Renewable and Sustainable Energy Reviews* **123**, 109768 (2020).

33. Xu, C., Arancon, R. A. D., Labidi, J. & Luque, R. Lignin depolymerisation strategies: towards valuable chemicals and fuels. *Chem. Soc. Rev.* **43**, 7485–7500 (2014).

34. Xu, C. C., Dessbesell, L., Zhang, Y. & Yuan, Z. Lignin valorization beyond energy use: has lignin's time finally come? *Biofuels, Bioproducts and Biorefining* **15**, 32–36 (2021).

35. Feghali, E., van de Pas, D. J. & Torr, K. M. Toward Bio-Based Epoxy Thermoset Polymers from Depolymerized Native Lignins Produced at the Pilot Scale. *Biomacromolecules* **21**, 1548–1559 (2020).

5. - Supporting Information

5.1. - Elemental and Proximate analysis of solids

Below are presented the elemental and proximate analysis of Kraft lignin, chars and oligomers from the experimental tests conducted.

Table S1 Proximate analysis of Kraft lignin and chars for different scenarios.

	Moisture (%)	Volatil matter (%)	Total carbon (%)	Ash (%)
Kraft lignin	2,91	63,67	34,15	2,18
Char S1	2,85	67,20	32,80	0,00
Char S2	2,71	39,21	52,24	8,54
Char S3	2,47	53,13	45,93	0,94
Char S4	1,42	40,79	52,38	6,83

Table S2 Elemental analysis of Kraft lignin and chars for different scenarios.

	%C	%H	%N	%S	%O
Kraft lignin	63,32	5,53	0,08	1,81	27,39
Char S1	53,76	3,99	0,02	1,58	21,78
Char S2	72,43	4,82	0,02	0,55	16,99
Char S3	68,83	5,13	0,02	1,16	22,32
Char S4	71,18	3,42	0,03	1,71	16,68

Table S3 Proximate analysis of oligomers for different scenarios.

	Moisture (%)	Volatil matter (%)	Total carbon (%)	Ash (%)
Oligomers S1	1,15	76,46	23,39	0,16
Oligomers S2	2,34	58,97	39,91	1,12
Oligomers S3	10,84	65,00	21,83	13,16
Oligomers S4	n.a.	n.a.	n.a.	n.a.

Table S4 Elemental analysis of oligomers for different scenarios.

	%C	%H	%N	%S	%O
Oligomers S1	56,08	4,67	0,14	5,78	20,47
Oligomers S2	68,42	5,50	0,05	0,73	21,48
Oligomers S3	39,11	5,51	0,02	0,61	27,10
Oligomers S4	70,51	6,31	0,07	1,03	21,66

TGA method:

from 30 to 105°C with 15°C/min heating rate, under N_2;

105°C for 20min, under N_2;

from 105 to 900°C with 15°C/min heating rate, under N_2;

900°C for 20min, under N_2;

900°C for 20min, under AIR.

CHNS analysis is conducted at 1090°C under 1200mbar. The samples are injected with 30mL/min of O_2. For the oxygen analysis, the oven is heated up to 1150°C under 200 mbar of He.

In the table below are presented the atomic balances, for all the solids involved in the liquefaction, for the different scenarios, used for the simulation in AspenPlus®.

Table S5 Atomic balances for each solids and all the scenarios.

	%C	**%H**	**%N**	**%S**	**%O**	**%ASH**
LIGNOSOL	63.13%	5.52%	0.08%	1.80%	27.31%	2.17%
CHAR						
S1	66.27%	4.92%	0.02%	1.94%	26.85%	0.00%
S2	70.08%	4.66%	0.02%	0.53%	16.44%	8.26%
S3	69.95%	5.21%	0.02%	1.18%	22.68%	0.96%
S4	70.21%	3.54%	0.03%	1.68%	17.71%	6.83%
OLIGOMERS						
S1	64.36%	5.36%	0.15%	6.63%	23.50%	0.00%
S2	71.14%	5.72%	0.06%	0.76%	22.33%	0.00%
S3	54.05%	7.62%	0.03%	0.84%	37.45%	0.00%
S4	70.81%	6.34%	0.07%	1.04%	21.75%	0.00%
REST						
S1	46.90%	8.54%	0.32%	-1.01%	31.29%	13.97%
S2	-91.85%	20.21%	1.20%	29.46%	241.62%	-100.56%
S3	67.38%	-2.24%	0.55%	9.42%	6.89%	18.04%
S4	41.65%	6.18%	0.15%	3.54%	47.47%	1.03%

5.2. - GC-MS/FID method and monomers yields

The samples were analyzed by an Agilent 7890 gas chromatograph combined to an Agilent 5975C MS (operated by electron impact at 70 eV) and an FID placed in parallel to the mass spectrometer. The samples were filtered (0.45 mm glass filters) and no additional dilution was applied. The sample was injected (1 mL) with a split ratio of 10 into an Agilent HP-5MS (5% phenyl 95% methyl siloxane) column. The oven was maintained at 50 8C for 10 min; then the temperature was increased with a first ramp of 5°Cmin^{-1} to 120°C, maintained for 10 min and then with a second ramp of 5°Cmin^{-1} to 250°C and maintained for 18 min. By comparison between the mass spectra and the NIST database, more than 40 compounds have been identified. The quantification was achieved by the FID detector based on the de Saint Laumer[29]. This method is able to predict the relative response factor of a compound on an FID based on its combustion enthalpy.

In the table below are presented all the monomers detected in the different bio-oils by GC-MS/FID.

Table S6 Detailed monomers yields from GC-MS/FID analysis.

RT(min)	Compounds	Formula	M(g/mol)	S1	S2	S3	S4
18,28	Anisol	C7H8O	108				0,27
21,31	Phenol	C6H6O	94	0,02	0,10		
21,60	1,2-Dimethoxy-4-(1-methoxyethenyl)benzene	C11H14O3	194				0,32
24,54	o-Crresol	C7H8O	108	0,00	0,01		
25,43	p_Cresol	C7H8O	108	0,00	0,01		
26,14	Guaiacol	C7H8O2	124		0,01	0,25	0,32
28,49	Ethylphenol	C8H10O2	122	0,00	0,01		
28,91	Dimethoxybenzene	C8H10O2	138		0,09		0,21
30,95	4Methoxy-3Methyl-Phenol	C8H10O2	138		0,02		
31,40	2Methoxy-5Methyl-Phenol	C8H10O2	138		0,05		
31,73	Methylguaiacol	C8H10O2	138			0,18	0,2
31,96	Pyrocatechol	C6H6O2	110	0,02	0,93		
34,82	Dimethoxy-toluene	C9H12O2	152		0,80		
36,25	Methylpyrocatechol	C7H8O2	124	0,00	0,01		
37,50	Ethylguaiacol	C9H12O2	152		0,04	0,22	0,48
38,04	Homocatechol	C7H8O2	124	0,01	0,37		
39,27	Dimethylhydroquinone	C8H10O2	138	0,15	0,01		
40,81	Ethylcatechol	C8H10O2	138	0,15	0,03		
41,35	syringol	C8H10O3	154	0,00	0,03		
41,70	Eugenol	C10H12O2	164				0,14

42,18	Propylguaiacol	C10H14O2	166			0,15	1,14
42,67	Ethylcatechol	C8H10O2	138	0,01	0,08		
43,59	Vanillin	C8H8O3	152	0,00	0,02		
44,87	Acetophenone	C8H8O	120	0,06			
45,60	methylsyringol	C9H12O3	168		0,01		
45,74	Iso-eugenol	C10H12O2	164		0,04	0,43	0,33
47,20	Acetoguaiacone	C9H10O3	166	0,01		0,11	
48,22	Dimethylmethoxyphenol	C9H12O2	152	0,01			
48,85	Guaiacylacetone	C10H12O3	180			0,60	0,55
52,57	Ethyl homovanillate	C11H14O4	210			0,18	0,15
53,00	Homovanillic acid	C9H10O4	182			0,28	0,35
54,82	Methoxyeugenol	C11H14O3	194			0,04	0,12
56,06	Acetosyringone	C10H12O4	196				0,13
	TOTAL (%wt)			**0,44**	**2,67**	**2,44**	**4,71**

5.3. - Assumption and prices for the techno-economic assessment

Table S7 Cost information

Assumptions		
Plant life	20	years
Operation hours	8000	hours/year
Taxation rate	30	%
Depreciation	linear	over 15 years
Discounting rate	7	%
Working capital	10	% of FCI
Operating supplies	1	% of FCI
Laboratory cost	20	% of labor cost
Insurance cost	3	% of FCI
Administrative cost	20	% of labor cost
Initial funding	50	% on loan at 1.5%
Equity	50	%

Chemicals, Feedstock, Products prices		
Monomers	1,6	€/kg
Oligomers	1	€/kg
Char	0,1	€/kg
Pulp	1	€/kg
Na	0,35	€/kg
Biomass	0,04	€/kg
EtAC	0,386	€/kg
EtOH	0,389	€/kg

Catalyst	10	€/kg
H2	2	€/kg
N2	2	€/kg
CO2	0,09	€/kg
Electricity	50	€/MWh
Employees	15	

Those prices have been set after an internal market study and compared with literature.[30,31]

In S4, a Ni-based catalyst is used for the liquefaction reaction. Its price comes from the market (10 €/kg) and its lifetime is fixed at 1000 hours.

G. Catalytic Hydrotreatment of Lignin in a Trickle Bed Reactor

Article in development

Erika Bartolomei[a], Jean-François Potha[a], Gabriel Wild[a], Yann Le Brech[a], Anthony Dufour[a]*

[a] LRGP, CNRS, Université de Lorraine, 1 rue Grandville, 54000 Nancy, France

* Corresponding author : anthony.dufour@univ-lorraine.fr

1. - Introduction

In this chapter, it will be presented a semi-continuous reactor for catalytic lignin hydrotreatment, from the theoretical design to the preliminary experimental results. The aim of this work is to find and create an intermediate reactor, which can link batch lab-scale experiments and industrial needs.

Trickle bed reactor is suitable for lignin catalytic depolymerization because it is a three-phase reactor who can stand high temperature and pressures, and it can be very flexible in terms of heat and mass transfers. Moreover, this kind of technology is up-scalable for industry.

A large screening of lignin types, catalyst, solvents and atmosphere has been done in order to identify the most suitable conditions to perform an industrially interesting catalytic lignin liquefaction. Part of those results has been presented in previous chapters.

Softwood Kraft lignin is solubilized in alkaline water (NaOH at pH=12) to mimic black liquor of pulp mills. The reaction is performed under reductive atmosphere, using H_2, and in presence of Ni/SiC pellets as catalyst. Temperature and pressure reached for the preliminary study are respectively 250°C and 75 bar. The depolymerisation of lignin was assessed by monomers' analysis by HPLC and GC-MS/FID.

This study is of significant importance for the further deployment of lignin conversion in the industrial catalytic reactors.

2. - Theoretical reactor design

2.1. - Hydrodynamics

To design the trickle bed reactor, the rest of the set-up and decide all the reaction parameters, many criteria have been evaluated and practical considerations have been taken in account.

The minimum hydrogen flowrate has been evaluated stoichiometrically with respect to the lignin content in the liquid and then multiplied by 100 to ensure an excess of hydrogen for the reaction.

The maximum liquid flowrate is set at 50 g/h and the chosen lignin content is 2% (mass fraction). So the maximum lignin flowrate is 1 g/h. Consequently, the maximum hydrogen flowrate is 0.46 L/min. Previous studies demonstrated that the most appropriate regime for lignin depolymerization is a co-current downflow one.[1–6] Such flowrates allow us to have superficial gas and liquid velocities which assure a trickle flow.

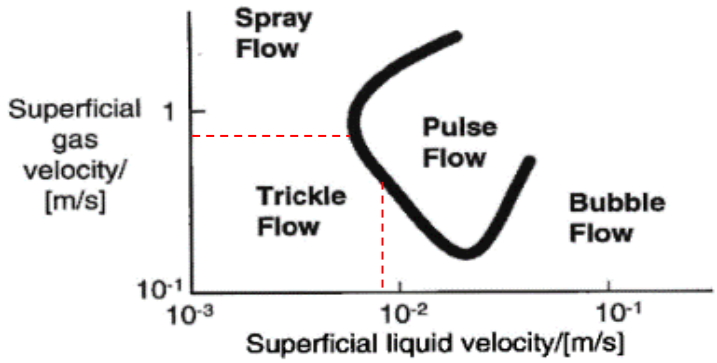

Figure 1 Co-current downflow regimes.[7]

Trickle flow regime checking: the following criteria have to be simultaneously validated:

$$\frac{\rho_L \dot{v}_L \psi}{\phi} \leq \left(\frac{\rho_G \dot{v}_G}{\lambda}\right)^{-0.25} \text{ and } 0.01 \leq \frac{\rho_G \dot{v}_G}{\lambda} \leq 1$$

With:

$$\psi = \frac{\sigma_{ref}}{\sigma}\left(\frac{\mu_L}{\mu_{L-ref}}\left(\frac{\rho_{L-ref}}{\rho_L}\right)^2\right)^{1/3}$$

$$\lambda = \sqrt{\frac{\rho_G}{\rho_{G-ref}} \frac{\rho_L}{\rho_{L-ref}}}$$

$$\phi = 4.76 + 0.5 \frac{\rho_G}{\rho_{G-ref}}$$

$\rho_{G-ref} = 1.2$ kg.m^{-3}, $\rho_{L-ref} = 1000$ kg.m^{-3}, $\sigma_{ref} = 0.074$ N.m^{-1}, $\mu_{L-ref} = 0.001$ Pa.s

The calculation of the wetting efficiency criterion[8] is important to determine if the catalyst is correctly wetted.

$$f_w = 1.104 \left(\frac{\rho_L \dot{v}_L d_p}{\mu_L \varepsilon_S}\right)^{1/3} \left(\frac{|\Delta P_{LG}/Z\rho_L g| + 1}{Ga_L}\right)^{1/9}$$

$$Ga_L = \frac{\rho_L^2 g d_p^3 (1-\varepsilon_S)^3}{\mu_L^2 \varepsilon_S^3}$$

If the calculation leads to value of f_w higher than 1, then $f_w = 1$.

2.2. - Pre-sizing

The reactor has been designed considering catalyst's dimensions. The pellets are about 5mm long and their diameter is 2mm, so their characteristic length (L=V/S) is about 0.4mm. According to empiric rules which can be applied to trickle bed, it is necessary to have an internal diameter 15 times the catalyst characteristic length, so at least 7.5mm. The length of the reactor has to be at least 5 time its internal diameter, but according the literature of trickle bed for slow reaction as lignin depolymerization, it is better to increase that ratio. So, a standard reactor of 13.1mm internal diameter (external diameter 3/4 inches) and 305mm long has been chosen for our study.

2.3. - Pressure drops

A preliminary evaluation of the pressure drops attended in the reactor has been conducted. In the following Table are presented all the dimensionless numbers and diphasic pressure drops expressions used for the calculation and their values.

Table 1 Correlations for diphasic pressure drops.[8]

Name	Formula	Value
Weber number (We_L)	$We_L = \frac{\rho_L v_L^2 d_P}{\sigma}$	7.5 10^{-07}
Reynolds (Re_L)	$Re_L = \frac{\rho_L v_L d_P}{\mu_L}$	3.6 10^{-04}
X_G	$X_G = \frac{m_G}{m_L}\sqrt{\frac{\rho_L}{\rho_G}}$	0.63
κ	$\kappa = X_G(Re_L\, We_L)^{0.25}$	0.0025
Gas-Liq friction factor (f_{LGG})	$f_{LGG} = \frac{1}{\kappa^{1.5}}\left(31.3 + \frac{17.3}{\sqrt{\kappa}}\right)$	2.9 10^{06}
d_h	$d_h = d_P\left(\frac{16(1-\varepsilon_S)^3}{9\pi\varepsilon_S^2}\right)^{0.33}$	1.9 10^{-04} m
External saturation (β_L)	$\beta_L = 1 - 10^{-\Gamma}$	0.83
Γ	$\Gamma = 1.22 We_L^{0.15}\, Re_L^{-0.2}\, X_G^{-0.15}$	0.77
Pressure drop (ΔP)	$\Delta P = \frac{f_{LGG}\, 2\, \rho_G\, v_G^2}{d_h}$	425330 Pa/m 4.25 bar/m

The attended value for pressure drops has been measured and confirmed by experimental tests in the reactor.

2.4. - Set-up development

In Figure 2 is presented a scheme of the whole set-up necessary for the lignin liquefaction in trickle bed. The liquid is pumped by a HPLC pump in a semi-closed circuit which assure a constant liquid flowrate at the right pressure thanks to a system of Swagelok manual backflows. The flow is measured by a Coriolis mass meter. Hydrogen flowrate is controled by a Brooks gas regulator. Both feedstock lines have check valves. Before the trickle bed reactor, the two

lines converge together and there are a valve for purge and a safety valve to avoid pressure higher than 200 bar (because of material limitations).

The trickle bed is filled with a catalytic bed (Ni/SiC pellets) and glass beads (d = 3 mm) to avoid misdistribution of gas and liquid. At reactor exit there is a condenser, cooled by an ice bath. It allows the collection of all the liquid. Exit pressure is maintained at the desired value thanks to a Kammer valve (a system used generally in oil-refining plants). Gas are sent to the vent or collected for analysis (by micro-GC). All along the system, many pressure and temperature probes are placed to monitor those parameters in the critical points. In particular, a triple points thermocouple is placed the catalytic bed. It mesures the temperature at the top of the reactor, in the middle and at the end at the same time.

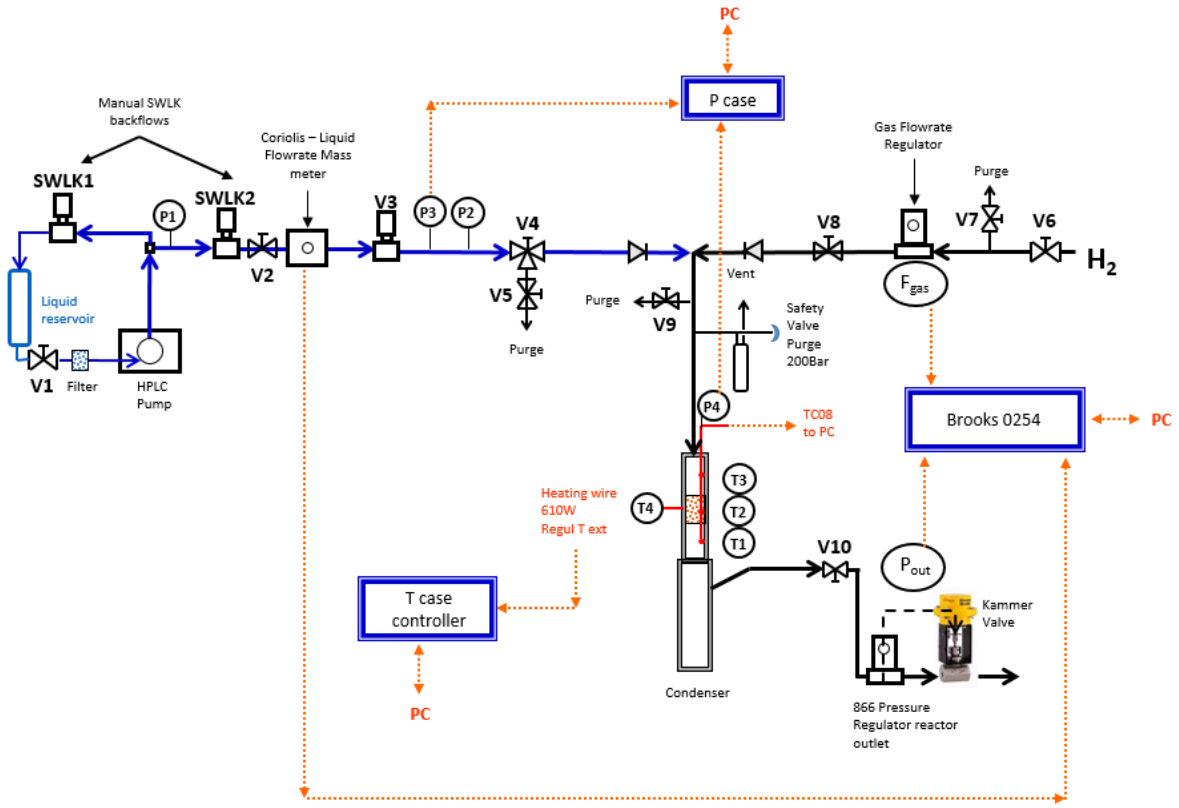

Figure 2 Set-up scheme.

2.5. - Mass transfer

From our previous studies on batch reactors, we evaluated the kinetic of lignin depolymerization reaction. The diffusion of lignin into the catalyst has been measured by NMR and the porosity and tortuosity of the catalyst are respectively equal to 0.5 and 3 (from suppliers). Thank to those data we can evaluate the diffusivity of lignin in to the catalysts pores. The results are given in Table 2 below.

Table 2 Kinetics and diffusivity parameters.

Kinetics	Order	first order
	k.φ (min^{-1})	$9{,}18\ 10^{-4}$
	k.φ (s^{-1})	$1{,}53\ 10^{-5}$
Diffusivity	D_{lignin} (m^2/s)	$1{,}00\ 10^{-10}$
	d_{pore} (m)	$2{,}00\ 10^{-9}$
	$D_{Knudsen}$ (m^2/s)	$1{,}78\ 10^{-7}$
	D (m^2/s)	$9{,}99\ 10^{-11}$
	D_{eff} (m^2/s)	$1{,}67\ 10^{-11}$

From the velocities used for this preliminary study and the apparent kinetic from batch experiments, we want to evaluate internal and external mass transfer limitations. In the following table are resumed the main parameter calculated and taken in account (Table 3).

Table 3 Internal and external mass transfer criteria for lignin.[8,9]

Internal Mass Transfer	Thiele modulus, Φ	0,48
	Catalyst efficiency, η	0,88
	Weisz-Prater criterion, $N_{W\text{-}P}$	0,23
External Mass Transfer	k_D (m/s)	$1{,}00\ 10^{-5}$
	r_{liq} (mol/s/m3)	$6{,}65\ 10^{-7}$
	Mears criterion	$7{,}65\ 10^{-4}$

According to those calculated parameters, the external mass transfer limitations are negligible. The internal mass transfer correlations show that the regime is intermediate implying that mass transfer limitations will decrease the catalyst efficiency to 0.88.

No particular thermic effects have been observed, probably because the high dilution of the liquid phase.

3. - Preliminary experimental results

3.1. - Catalyst

Three different kinds of SiC supports have been chosen: two cylindrical extrudates with different porosity (one mesoporous and one macroporous) and mesoporous trilobes extrudates (see Figure 3).



Figure 3 Cylindrical pellets and trilobes of SiC.

The catalysts have been prepared by incipient wet impregnation using hexa-hydrate nitrate of nickel. SiC has been charged with 5%wt of nickel on the support mass. Calcination under 150 mL/min air flow has been performed at 350°C (heating rate of 5°C/min) for 2 hours. The catalyst has to be reduced before its actual utilization during the reaction, so it is reduced under a H_2 flow (200mL/min) at 400°C (heating rate of 5°C/min) for 1 hour.

Below are presented some preliminary XRD analysis on the SiC support and the Ni/SiC catalyst before and after reaction. It can be noticed that Ni has been well impregnated on the support and its XRD not impacted after the reaction, meaning that it is not poisoned or deactivated.

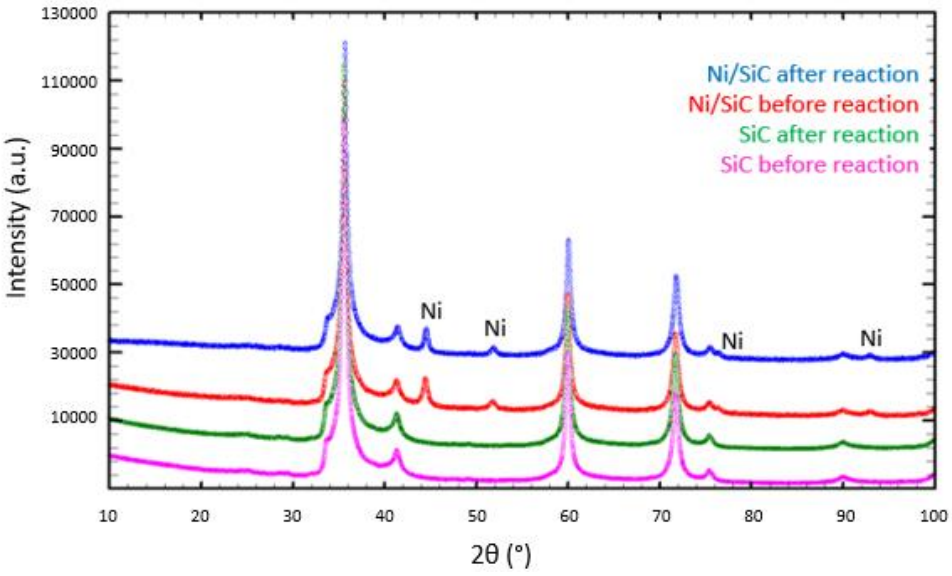

Figure 4 XRD of SiC and Ni/SiC before and after reaction.

3.2. - Bio-oils analysis

Some preliminary tests have been conducted at 250°C, under H_2 atmosphere (75 bar) in presence of raw SiC or Ni-impregnated SiC (5%Ni on SiC mass as described before). After 30 minutes of reaction, the bio-oils have been collected in the condenser and then analysed. In the following table are presented the HPLC results of the direct analysis of the bio-oil and the GC-MS/FID of the DCM extracted bio-oil. It is possible to notice that the organic liquid/liquid extraction cannot allow a correct analysis of the bio-oil, in fact the most part of the monomers are not well extracted from the aqueous phase into the organic one.

Table 4 Bio-oils analysis by HPLC and GC-MS/FID.

Compound	**Non-catalytic - 250°C**		**Catalytic (5% Ni/SiC) - 250°C**	
(%wt)	**HPLC**	**GC-MS**	**HPLC**	**GC-MS**
Phenol	0,02		0,03	
Guaiacol	0,53		0,52	
Methylguaiacol	0,03		0,10	
Ethylguaiacol	0,23		0,53	0,18
Propylguaiacol			0,12	0,05
Vanillin	0,46		0,36	
Eugenol	0,03		0,03	
Vanillic acid	0,30		0,24	
Syringic acid	0,02		0,02	
Syrinaldehyde	0,01		0,01	
Acetosyringone	0,03		0,03	
Acetovanillone	0,31		0,35	
TOTAL	**1,96**	**0**	**2,33**	**0,23**

Furthermore, those results show that the Ni catalyst has a low impact for the production of monomers under those conditions (250°C and 75 bar of H_2). Results are consistent with recent diffusion analysis confirming that mass transfer of lignin in pores of catalyst is very slow (confirmed by Weisz modulus determination). Apparent kinetic is mainly controlled by internal mass transfer.

Considering all these factors, we believe that macroporous supports or trilobes shape could promotethe mass transfer of lignin intermediates of lignin intermediates to catalytic active sites. Also temperature and pressure conditions could be increased.

More experiments are planned to evaluate the effect of hydrodynamics, varying liquid and gas velocities. SiC macroporous pellets and trilobes will be compared to investigate if the shape of the catalyst support can help interfacial effects. Since the mass transfer of lignin in the catalyst seems to be limited, a third catalyst support will be tested to see if macro-porosity in SiC can avoid this problem.

Nomenclature

ρ = density (kg/m^3)

μ = dynamic viscosity (Pa.s)

σ = surface tension (N/m)

ε_s = solid retention (dimensionless)

φ = bulk density (g/m^3)

Φ = Thiele modulus

k = velocity constant ($m^3/(g.min)$)

v = superficial velocity (m/s)

m = specific mass flowrate ($kg/m^2/s$)

d = diameter (m)

D = diffusivity (m^2/s)

4. - References

1. Moulijn, J. A., Makkee, M. & Berger, R. J. Catalyst testing in multiphase micro-packed-bed reactors; criterion for radial mass transport. *Catalysis Today* **259**, 354–359 (2016).

2. Mederos, F. S., Ancheyta, J. & Chen, J. Review on criteria to ensure ideal behaviors in trickle-bed reactors. *Applied Catalysis A: General* **355**, 1–19 (2009).

3. Mapiour, M., Sundaramurthy, V., Dalai, A. K. & Adjaye, J. Effects of the operating variables on hydrotreating of heavy gas oil: Experimental, modeling, and kinetic studies. *Fuel* **89**, 2536–2543 (2010).

4. Dietz, A., Julcour, C., Wilhelm, A. M. & Delmas, H. Selective hydrogenation in trickle-bed reactor: experimental and modelling including partial wetting. *Catalysis Today* **79–80**, 293–305 (2003).

5. Olarte, M. V. *et al.* Stabilization of Softwood-Derived Pyrolysis Oils for Continuous Bio-oil Hydroprocessing. *Topics in Catalysis* **59**, 55–64 (2016).

6. Bej, S. K., Dalai, A. K. & Maity, S. K. Effect of diluent size on the performance of a micro-scale fixed bed multiphase reactor in up flow and down flow modes of operation. *Catalysis Today* **64**, 333–345 (2001).

7. Sie, S. T. & Krishna, R. Process Development and Scale Up: III. Scale-up and scale-down of trickle bed processes. *Reviews in Chemical Engineering* **14**, (1998).

8. Al-Dahhan, M. H. & Duduković, M. P. Catalyst wetting efficiency in trickle-bed reactors at high pressure. *Chem. Eng. Sci.* **50**, 2377–2389 (1995).

9. Iliuta, I., Ortiz-Arroyo, A., Larachi, F., Grandjean, B. P. A. & Wild, G. Hydrodynamics and mass transfer in trickle-bed reactors: an overview. *Chem. Eng. Sci.* **54**, 5329–5337 (1999).

10. Wild, G., Midoux, N., Laurent, A. & Larachi, F. Effet de la pression sur la transition ruisselant-pulsé dans les réacteurs catalytiques à lit fixe arrosé. *Can. J. Chem. Eng.* **71**, 319–321 (1993).

H. Conclusions and Perspectives

In this work many different aspects of lignin valorization have been presented. The interesting novelty of this work is the multidisciplinary approaches applied to lignin: if on one side the aim is to optimize and make more sustainable pulp and paper industries from an economical and environmental point of view, on the other detailed laboratory analytical measurements have been performed to deeply understand the possible mechanisms involved in lignin depolymerization.

To evaluate lignin structure and consider the possible depolymerization pathways, all the lignins involved in this project have been deeply and extensively characterized. In Chapter B are presented the main analytical results obtained from lignin and black liquors analysis. They show characteristic features depending on the biomass source and the extraction method. Thank to this analytical study it was possible to quantify and understand better the results of lignin depolymerization achieved via liquefaction.

Along with the most traditional methods to analyze lignin and lignin-derived products, a peculiar method has been developed and optimize for lignin-derived bio-oils: UV-fluorescence spectroscopy (Chapter C). This method has been used in the past for coal and asphaltenes analysis, also for pyrolytic lignin sometimes, but here we use this method for the first time for lignin depolymerization tracking and screening. We demonstrate that this fast and inexpensive method can overcome many limitations we can find with more traditional methods, such as fragmentation of the product, column/mobile phase interaction and so on.

In Chapter D a large screening of technical lignin liquefaction (under reductive conditions) is given to highlight the effects of the catalyst and the kind of lignin used for the reaction. After a bibliographical study, three different carbon-supported catalyst have been chosen because of their efficiency in lignin conversion and their possible different mechanisms on lignin depolymerization. Pt/C, Ni/C and Ru/C have been compared under the same condition for the depolymerization of four different technical lignins. Only technical lignin were chosen for the entire project because our aim is to provide a realistic approach on lignin valorization for pulp and paper industries. For that reason three commercial/technical Kraft lignins (the most spread pulping process worldwide) from different biomasses and one Soda lignin (the second extraction method in pulp industries) have been tested in this screening. From the results of this study we concluded that the three catalyst have a similar effect on the total monomers yield,

but they show different selectivity. To compare the 4 four lignins we chose Ni/C because it was the catalyst who yielded more phenols and alkyl phenols compared to the others. The lignin screening show that the selectivity depends from the biomass source of course, but more than that from the solubility and thermal stability of the lignin in the reaction conditions.

A study on oxidative TEMPO-mediated lignin depolymerization is given in Chapter E. This work is the result of a fruitful collaboration between our laboratory (LRGP, Nancy), IRCELyon in Lyon and the Biological System Engineering Department at Washington State University. After previous optimization of oxidative lignin liquefaction, an experimental study has been conducted using TEMPO (acronyms of (2,2,6,6-Tetramethylpiperidin-1-yl)oxyl) as oxygen-donor, also in presence of CuO/TiO_2 to investigate their interaction and possible coupling. This study shows that TEMPO is very effective for lignin depolymerization, even more if not coupled with any other catalyst. Up to 7,2%wt of vanillin has been produced from a technical Kraft lignin in oxidative mild conditions. This result is very promising for vanillin market because to our knowledge there are not other studies on real lignin who yielded such a significant amount.

The scope of the chapter F is to evaluate and compare the feasibility of the integration of the lignin valorization unit in already existent pulp mills. This work compares different scenarios for lignin valorization: direct black liquor liquefaction, lignin precipitation and solubilization in alkaline water or ethanol, and also the use of a Ni-based catalyst are investigated and compared. Experimental tests have been performed both on direct black liquors and precipitated Kraft lignin (from the same black liquor at the *Centre Technique du Papier* in Grenoble, partner of this project). Based on experimental data, mass and heat balanced have been evaluated on AspenPlus® and used for a complete techno-economic assessment. From this study, the integration of a lignin liquefaction unit in an existent paper mill is viable and profitable. In particular, it shows that lignin precipitation and solubilization in ethanol for liquefaction is the favorable pathway to follow.

In the last chapter (Chapter G), a preliminary study on a trickle bed reactor is presented. The aim of this work is to link batch lab-scale experiments to industrial needs Theoretical study for the design of a trickle bed reactor are given, along with some preliminary experimental results.

In conclusion, this work provides new insights on lignin valorization from analytical and depolymerization points of view. A method to fast and easily analyze lignin products has been

assessed. UV-fluorescence allows the analysis of lignin-derived monomers, but also of the heavier fractions which are generally challenging to investigate.

Concerning lignin depolymerization, low amounts of monomers have been achieved under the conditions tested during this work, a marginal improvement could be reached varying the conditions. So far, oligomers are not considered valuable products of lignin liquefaction because of their difficult understanding. Indeed, a valorization of this fraction should be considered (for example for epoxy resins, bio-bitumen and so on). Furthermore, even if the depolymerization results are not so high, from the techno-economic study conducted it is clear that the integration of a lignin liquefaction unit in existent Kraft mills is a very interesting way to move forward to a biorefinery optimization of paper industries.

I. Appendices

This part of the manuscript includes papers related to the thesis subject, the research work has been conducted in some cases in collaboration with international partners and/or with the help of interns who worked under my supervision.

1. - Article in development: Catalytic depolymerization of lignins with Ru/C: effect of lignin structure and H_2

Tina Ročnik[a,b], Erika Bartolomei[b], Anthony Dufour[b], Philippe Arnoux[b], Edita Jasiukaityte-Grojzdek[a], Miha Grilc[a], Blaž, Likozar[a], Yann Le Brech[b] *

[a] Department of Catalysis and Chemical Reaction Engineering, National Institute of Chemistry, 1000 Ljubljana, Slovenia

[b] LRGP, CNRS, Université de Lorraine, 1 rue Grandville, 54000 Nancy, France

* Corresponding author : anthony.dufour@univ-lorraine.fr

1.1. - Introduction

One of the main goals of the last decades is to be able to forget fossil fuel resources and produce green and sustainable energy. One part of the challenge is to design processes to get fuels and chemicals from renewable resources. Lignin, which is one of the main component of lignocellulosic biomass, is described as a crucial biomaterial resource to design green process to get bio-derived value-added fuels, chemicals and materials. Lignocellulosic biomass (wood, herbaceous,…) is a complex network of macromolecules (cellulose, hemicelluloses, lignin). Its production is estimated to 300 billions/tons annual. Lignin is a structural material to add strength and rigidity to cell walls and constitutes between 15 wt% and 40 wt% of the dry matter of woody plants. Therefore, lignin is a one of the most abundant renewable material on earth. Pulp and paper industries are the main industrial source of lignin. Indeed, their lignin's production is estimated to 50-70 millions tons annually[1]. Despites the abundant number of research focusing on lignin conversion into high-value products, currently, most of the lignin

produced from paper industries is burned to generate electricity and heat. Therefore, its valorisation is one of the most promising ways for the substitution of fossil resources to produce aromatic compounds. Indeed, lignin is an interesting starting material for the synthesis of aromatics and intermediates which are important in petrochemical industry. However, technical lignins from pulp industries present condensed structures making there dissolution in liquid and depolymerisation difficults. Different methodologies have been applied to convert lignin to high value compounds, indeed process intend to depolymerize lignin to get aromatics monomers (Pyrolysis, Gazeification, Liquefaction). The mechanisms of lignin[2] solubilisation/dissolution have been studied in order to design catalysis for their conversion. In the native biomass, lignin consists of a tridimensional aromatic polymer composed of phenylpropenyl units (coumaryl, coniferyl and syringyl alcohols), which are randomly connected through carbon–carbon and carbon–oxygen (ether) bonds[2,3]. Seven main linkages between theses phenylprenyl units have been identified: five include ether linkages (β-O-4, α-O-4, ββ, 4-O-5, β5) and two include only carbon-carbon linkage (β-1 and 5-5). Therefore, ether linkages abundance is relatively high[4] (between 50 and 85% number of linkages) and the repartition between different linkages is function of the species (softwood, hardwood, grass, energy crops). During biorefinery process as pulping process, ethers linkages are more likely to be cleaved[5] . Especially for woody biomass which are used in paper industries process. Indeed the β-O-4 and α-O-4 linkages which are abundant in woody biomass are largely cleaved[5] leading to the formation of carbon-carbon linkages by condensation reactions[6,7] whereas natural carbon-carbon linkages are mostly preserved[6]. Accordingly to these structural modifications, lignin structure identity is dramatically changed. Indeed technical lignins are described as highly condensed aromatic structures where the low β–ether bonds needs to be considered into lignin valorisation strategies.

Technical lignins are produced by four main process : sulfite process (acid catalyzed), kraft process (alkaline and sulfide), Soda process (alkaline) and Organosolv (ethanol-water extraction). Kraft and Soda processes are the most important process for pulp production respectively for chemical pulping from wood and non woody biomass[8] (bagasse, wheat straw,…). They conduct to the production of huge amount of lignin. Strong sodium hydroxyde condition contributes to relatively high pH which contributes to lead the ether bonds cleavage. Hydrosulfide anions (Kraft) may react with lignin to ensure depolymerisation[9]. The lignin recovery from Kraft process is achieved by acidic precipitation. Indeed, LignoBoost and

LignoForce processes are the two main commercial technologies for precipitating lignin from spent liquors[10].

In order to develop an effective technology that converts lignin to fuel or marketable chemicals, one challenge is to depolymerize technical lignin to intermediate phenolics monomers which can be used as platform molecules for several applications[1]. The various method can be divided in four categories: reductive, oxidative, base/acid catalyzed and solvolytic/thermal depolymerisation[11]. Reductive depolymerisation in presence of supported metal catalyst and molecular hydrogen (H_2) is one of the approaches widely studied[12]). Noble metal still attract interest due to their high performance in the reductive conversion (hydrogenolysis) of lignin[2,13], especially to their effectiveness in cleaving ether bonds[12,14]. Alcohols solvent (Methanol and Ethanol) are used because of their capacity to solubilize lignin products and also for their H-donor abilities[15]. Many Noble catalysts have been used to convert lignin to monomeric products. Many studies focus on model compounds, technical lignin or soft extracted lignin. Ruthenium based catalyst have been studied for the conversion of technical lignin.Many conditions were studied (solvent, atmosphere, pressure, time, catalyst support, loading amount). Commercial Ru/C is often good for conversion and/or selectivity.

Reaction mechanisms of Ru/C catalyzed lignin hydrogenolysis have been extensively studied on model compounds (dimeric, trimeric, polymeric) but catalytic conversion involving technical lignin is still rare. Ru/C is described as an accelerator of the C-O bond cleavage in the B-O-4 moeity and avoid the recondensation reaction[16] (etherification of Cg-OH) even at mild conditions[17].

Many parameters can influence the conversion efficiently of technical lignin (solvent, temperature, time, catalyst,….). In this paper, we offer to study the influence of a reductive atmosphere (H_2) under mild condition (250°C, 100 bars) in supercritical Ethanol on two technical lignins (Kraft and Soda).

1.2. - Materials and Methods

1.2.1. - Materials: lignins and chemicals

- Lignins: soda (Protobind 1000 wheat straw) and Kraft (CTP).
- Catalyst: ruthenium on carbon (5%wt loading).
- Solvent: ethanol.

- Internal standard: hexadecene and 1-tetradecene: for calculation of monomers yield.
- Gas: nitrogen and hydrogen.

1.2.2. - Experiment set up:

- Experimental process:
    - weighted lignin and catalyst, added ethanol and internal standard
    - fixed the autoclave and safety cover to the standing part then started mixing at 1000 rpm
    - purge nitrogen through the reactor three times and test for the leak at starting pressure 10 bar
    - purge hydrogen through the reactor three times and test for the leaks at starting pressure 10 bar
    - started slowly heating with the oven cover over reactor
    - starting pressure was 10 bar +- 0,2 bar at room temperature, heat to 250 degrees. The highest pressure was around 115 bar
    - first sample was taken when temperature hit the set maximum (250 C) as time 0h.
    - samples were taken each 30 minutes till the 4 hours of experiment
    - remove the oven and cooling down with airflow machine
    - remove the gas through the safety system
    - took off the autoclave
    - filtrated the char 1 after the reaction -> contains the catalyst, not dissolved lignin and carbon residue
    - added another internal standard
    - the acidification: to filtrated bio-oil added water and HCl acid, mixed for 30 mins [5]
    - filtrated twice and got oligomers
    - cleaned autoclave and mixing parts of standing part

1.2.3. - Analytical methods

GC-MS: detection of monomers

The samples were analyzed by an Agilent 7890 gas chromatograph combined to an Agilent 5975C MS (operated by electron impact at 70eV) and an FID placed in parallel to the mass spectrometer. The samples were filtered (0.45 µm glass filters) and no additional dilution was applied. The sample was injected (1 µL) with a split ratio of 10 into an Agilent HP-5MS (5% phenyl 95% methyl siloxane) column. The oven was maintained at 50°C for 10 min; then the temperature was increased with a first ramp of 5°C/min to 120°C, maintained for 10 min and then with a second ramp of 5°C/min to 250°C and maintained for 18 min. By comparison between the mass spectra and the NIST database, more than 40 compounds have been identified. The quantification was achieved by the FID detector based on the de Saint Laumer75 method as previously described in details. This method is able to predict the relative response factor on a FID based on its combustion enthalpy.

UV fluorescence: degree of depolymerisation

UV-visible absorption spectra were recorded on a UV-3600 double beam spectrophotometer (Shimadzu). A spectral range from 200 nm to 500 nm and scan speed of 100 nm min-1 were selected with lamp change at 340 nm. The fluorescence spectra were recorded on a Fluorolog FL3-222 spectrofluorometer (HORIBA Jobin Yvon, Longjumeau, France) equipped with a 450 W Xenon lamp, and a UV-Visible photomultiplier R928 (HAMAMATSU Japan). All spectra were measured in a four-faced quartz cell. Fluorescence spectra were obtained with right angle detector position for both emission and synchronous acquisitions. Emission acquisition was performed with excitation wavelength of 275nm, slit of 2nm for a spectral range of 280nm to 530nm. Synchronous acquisition was performed with a constant wavelength offset of 20nm in the spectral range from 250 nm to 500 nm. 20nm offset has been selected based on previous work.

The samples were diluted in ethanol until the absorption wavelength at 275 nm was approximately 0.2, in order to avoid self-absorption effects62. For this purpose, the solutions sampled from lignin liquefaction (10g of lignin in 200mL ethanol, 50g lignin equivalent/L) were diluted 1000 or 2000 times in ethanol. Therefore the concentration of analyzed solutions is in the range of 25-50 mg lignin equivalent/L ethanol for UV analysis.

All the synchronous fluorescence spectra are presented with lamp and photomultiplier corrections at the same absorbance.

The whole procedure (including dilution, scan acquisition and treatment of data) lasts only about 15minutes.

Elemental analysis: CHN content

The oxygen weight percentages of the precipited oligomers were determined using an elemental analyser ThermoFisher Flash EA111. Carbon, hydrogen, nitrogen were detected as gaseous products (carbon dioxide, water vapour, nitrogen, sulphur dioxide) after combustion at 1000°C under inert atmosphere (helium).

The Carbon, hydrogen, nitrogen, sulfur percentages of the precipited oligomers were determined using an elemental analyser ThermoFisher Flash EA111.

1.3. - Results and Discussion

1.3.1. - Mass balance: Yield of Lignin Depolymerization Products

The mass balance according to the recovered products (char, oligomers, monomers) after reactions under the different conditions is shown in Figure 1 (at the end of the liquefaction after 4h at 250°C). These products are recovered following a procedure described in Section (X.X). Results are presented for both lignin (Soda and Kraft).

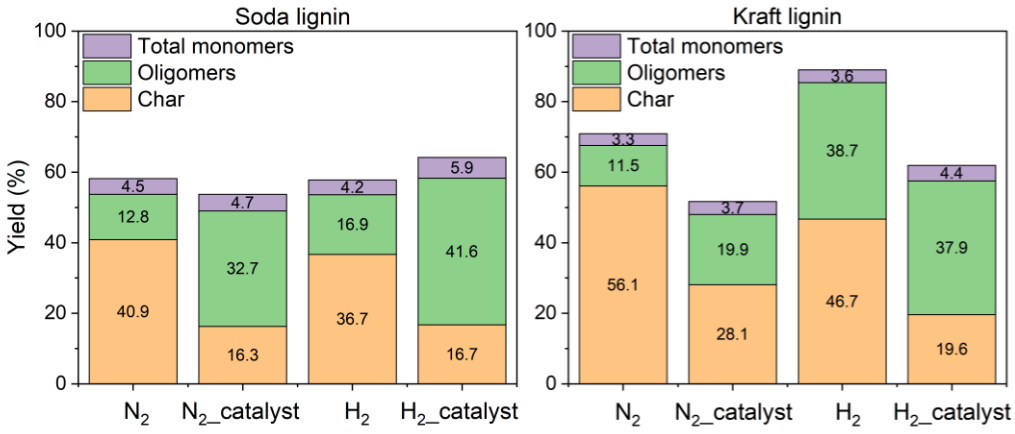

Figure 1 Yield of the products at the different reaction conditions

Regarding mass balances, only recovered and quantifiable products are presented. Char consists of recovered solid after reaction by filtration. It includes catalyst when used for reaction. Oligomers are recovered after acidification, precipitation and filtration[18]. Monomers where quantified by GC-MS/FID. Gases were not analyzed as gas production is relatively low in these conditions[1,18,19]. The missing part may be dedicated to non precipitated oligomers which are not analyzed by GC. For both lignin, experiments under inert atmosphere and without catalyst show the formation of high amount of char. Indeed, char yields are about 40.9%wt for soda and 56.1%wt for kraft lignin. These results are in agreement with char yields given by different studies presenting close[18-20] reaction conditions. The char-forming reactions occur due to the recondensation[18] of the oligomers that consequently give a rise to the insoluble, high molecular weight structures such as residual solids. Indeed, during the solvolysis of lignin, the primary decomposition products of phenolic oligomers and monomers were reported to be highly reactive[15,16]. Furthermore, ether-bonds between lignin units breaks leading to the formation of very reactive free phenolic hydroxyl groups[20] (though radical or charged species) and unsaturated side chains which are both involves into condensation[7,20] reactions. Consequently, the depolymerisation process is followed by a condensation process leading to a more condensed structure, described as a char like structure with fused aromatic rings[20,21].

Addition of reductive atmosphere during experiments, for both lignins, conducted to a reduction of the amount of char. Indeed, recovered char decrease from 40.9 to 36.7% for Soda lignin and 56.1 to 46.7% for Kraft lignin. No significant change in the amount of quantified monomers

was observed. However, a significant evolution in the yields of oligomers recovered is observed.

The catalyst addition (without H_2) for reaction induces a significant reduction concerning the char formation compared to experiments under inert atmosphere without catalyst (for soda 40.9 to 16.3% and kraft lignin 56.1 to 28.1%). This observation could be explain by the action of catalyst on solubilized lignin in supercritical ethanol. In fact, solubilized lignin and oligomers from depolymerization/solvolysis reactions may occur reaction with catalyst leading to soluble compounds/molecules. Catalyst may also quench the recombination reaction. This can be correlated to the increase, for both lignin, of oligomers fragments. 32.7%wt vs 12.8%wt for soda and 19.9%wt vs 11.5%wt for kraft lignin.

1.3.2. - Elemental Analysis

Elemental analysis (CHN) have been performed on precipitated oligomers after reaction and a Van Krevelen diagrams are provided to describe atomic ratios between carbon, oxygen and hydrogen for each reaction conditions (Figure 2).

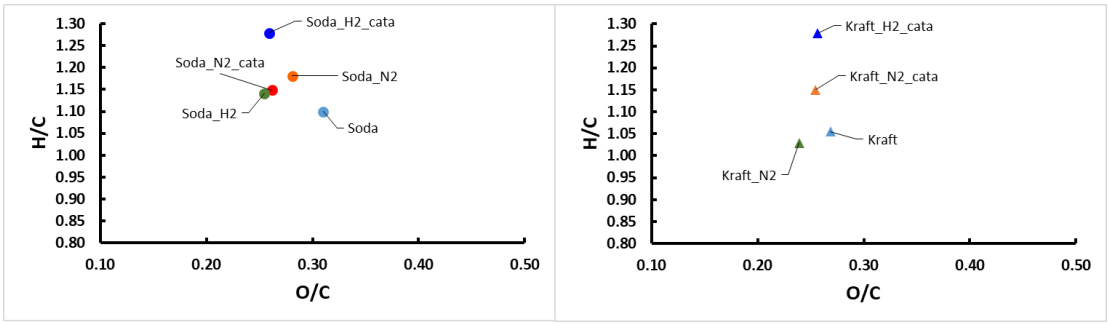

Figure 2 Van Krevelen diagram for precipitated oligomers

Concerning Soda lignin, the atomic ratio are consistent with literature[18]. O/C ratio decrease is observed for each conditions whereas H/C ratio increase. This could provide evidence that under ethanol supercritical conditions, lignin is subjected to hydrogenolysis and hydrogenation. This can be explain by the hydrogenolysis of C-O bonds and hydrogenation of unsaturated propyl chains during lignin depolymerization. Furthermore, carbon content also could increase simultaneously due to the carbon-carbon recondensation of products from depolymerization.

1.3.3. - NMR Analysis

In order to understand lignin depolymerisation and conversion reactions, we first use NMR 1H to investigate the structural change. Figure 3 and 4 shows ^{1}H and ^{13}C NMR Soda lignin structure and its precipitated oligomers obtained in different conditions.

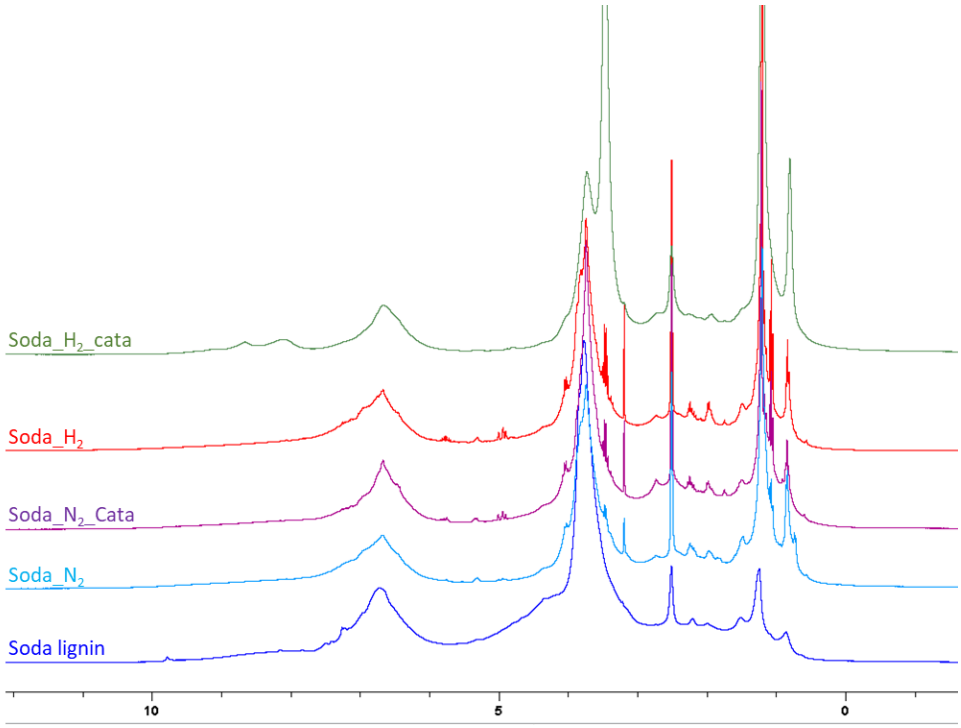

Figure 3 ^{1}H NMR spectrum of Soda lignin and its precipitated oligomers obtained after reaction

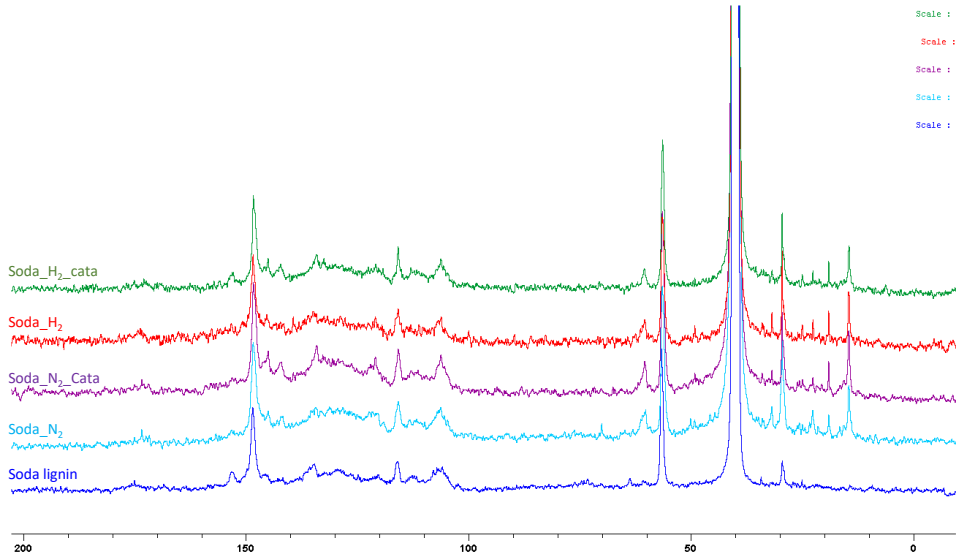

Figure 4 ^{13}C NMR spectrum of Soda lignin and its precipitated oligomers obtained after reaction

1.3.4. - FTIR results

The best performing experiments (H_2 and H_2_catalyst) were selected for the FTIR analysis. The assignment of lignin FTIR spectra was reported by several authors and allows the identification of characteristic bands for hydroxyl groups (O-H stretching at 3400 cm^{-1}), C-H stretching in methoxyl and methylene groups (at 2930 and 2850 cm^{-1}, respectively) and aromatic ring vibrations (at 1600, 1510 and 1455 cm^{-1}).[22-24] All characteristic lignin bands were identified for both starting lignins. In addition, a typical band corresponding to the G-units (guaiacyl ring with C-O stretching) at 1265 cm^{-1} was observed for kraft lignin[23] shown in Figure 5B, while only minor absorption band was detected in spectrum of soda lignin in Figure 5A. Another intensive characteristic absorption bands for G-units in lignin are at 1140 and 1033 cm^{-1} [22] and strongly recognized in Figure 5B as well. The presence of the absorption band at 1335 cm^{-1} corresponding to the syringyl ring breathing with C-O stretching[25,26] in spectrum of soda lignin has an strong effect on shifting the typical transmission maximum of G-units at 1140 cm^{-1} to 1125 cm^{-1}.[22] Therefore, the intensive absorption band at 1125 cm^{-1} clearly indicates an existence of the GS-type of lignin (lignin bearing guaiacyl and syringyl moieties) displayed in Figure 5A.

The FTIR spectra of the oligomeric fragments obtained after the catalytic and non-catalytic hydrotreatment exhibit all characteristic signals for the starting lignin. The spectra of the oligomeric fragments shown in Figure 5A and B look very much alike and at the same time very similar to the spectrum of the initial lignin thus showing the absence of the severe structural changes in the biopolymer structure.[24] Beside the spectra resemblance, the reduced intensity of all absorption bands draws a conclusion about an effective lignin depolymerization.

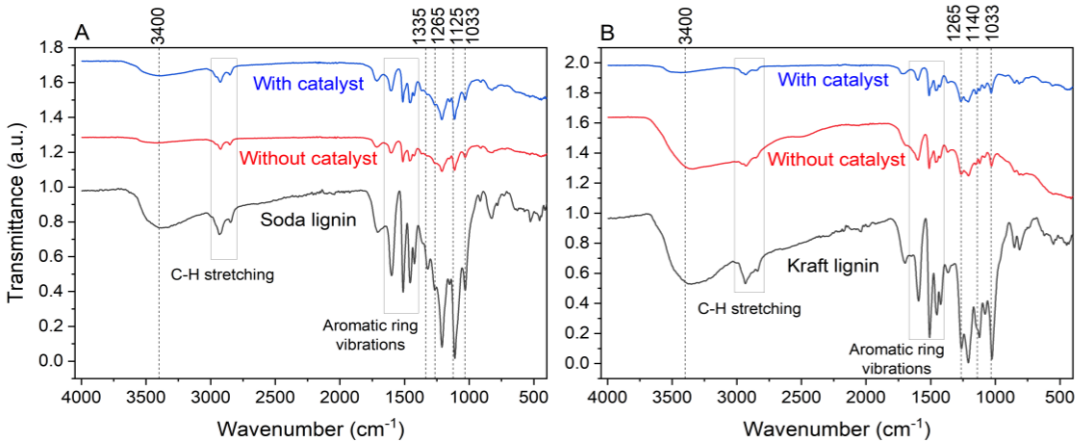

Figure 5 FTIR spectra of soda lignin, kraft lignin and oligomeric fragments produced after the catalytic and non-catalytic hydrogenation.

1.3.5. - GPC method

Table 1: GPC molecular weight of bio-oil and in THF-soluble oligomer fragments.

		Mw	
		Oil	Oligomer fragments
Soda	N2	692	979
	N2_Ru	764	1049
	H2	673	980
	H2_Ru	770	1032
	H2_Ru_2	767	1078
Kraft	N2	688	1031
	N2_Ru	676	1024
	H2	653	1123
	H2_Ru	720	1078

1.3.6. - UV-Vis synchronous fluorescence spectroscopy

UV-Vis synchronous fluorescence spectroscopy is a relatively new method for further characterization of depolymerization. The method focuses primarily on the change in the structure of lignin during the reaction, but does not determine the exact size or which oligomers and monomers are present. Three peaks are observed on the emission spectra, the first at 306 nm represents monomers, at 350 nm - oligomers and at 375 nm - polymers.

Figure 6 shows synchronous fluorescence spectra of diluted samples during the depolymerization reaction for the soda lignin experiment with Ru/C and hydrogen. For the sample taken at the beginning 0 h, the highest peak is at 375 nm, which decreases with the reaction time, while the peaks at 350 and 306 nm increase. In the sample taken after 4 hours, peaks representing the monomers and oligomers have a very high intensity, which means that the initial polymeric structure of lignin has changed. The peak intensity at 375 nm is slightly

increased after half an hour of the reaction, due to the detection of not solubilized lignin emission in the bio-oil which dissolves after the prolonged depolymerization time.

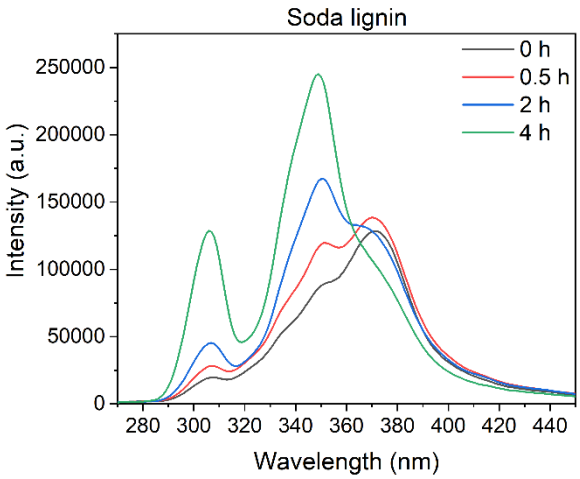

Figure 6 UV-Vis synchronous fluorescence spectra of soda lignin samples withdrawn at different time intervals of catalytic hydrogenation (H_2_catalyst).

The described method was used to compare the efficiency of all the experiments and to evaluate the effect of the reaction conditions on the extent of lignin depolymerization. For this purpose, only spectra of the final samples after 4 hours of the reaction are shown in Figure 7. In case of soda lignin catalytic depolymerization intensive absorption peaks representing monomeric and oligomeric part of the sample were observed. Additionally, intensity of the corresponding peaks increase when the depolymerization takes place under the hydrogen atmosphere. Spectra of the samples at the end of the non-catalytic soda lignin depolymerization under the both atmospheres displayed analogous profiles. Only the intensity of the peak at 305 nm corresponding to the monomeric part of the sample remained not changed suggesting that in both cases a comparable lignin depolymerization was achieved.

Without the catalyst used after 4 hours of depolymerization process in different atmosphere, the peak at 375 nm, representing polymers, was still at the high intensity, which did not decrease or at least converted into oligomers, in order to summarize that the polymeric structure of lignin changed.

UV-Vis synchronous fluorescence spectra (UV-Vis SF) of kraft lignin final samples are shown in Figure 7B. The high intensity peak at 375 nm of samples after the catalytic depolymerization under the N_2 atmosphere (N_2_catalyst) and non-catalytic depolymerization under the H_2

atmosphere (H_2) implies lignin to become highly soluble after the four-hour treatment. However, particular reaction conditions were not sufficient to initiate lignin depolymerization. Interestingly, in case of kraft lignin, UV-Vis SF spectra show the additional peak at 335 nm which could possibly correspond to the smaller oligomeric fragments, for instance trimers or tetramers. The effective lignin conversion into the smaller fragments is evidenced with the highly intensive peaks at 306 nm and 350 nm and accordingly reduced intensity of the 'polymeric' peak obtained after the catalytic depolymerization under the H_2 atmosphere (H_2_catalyst).

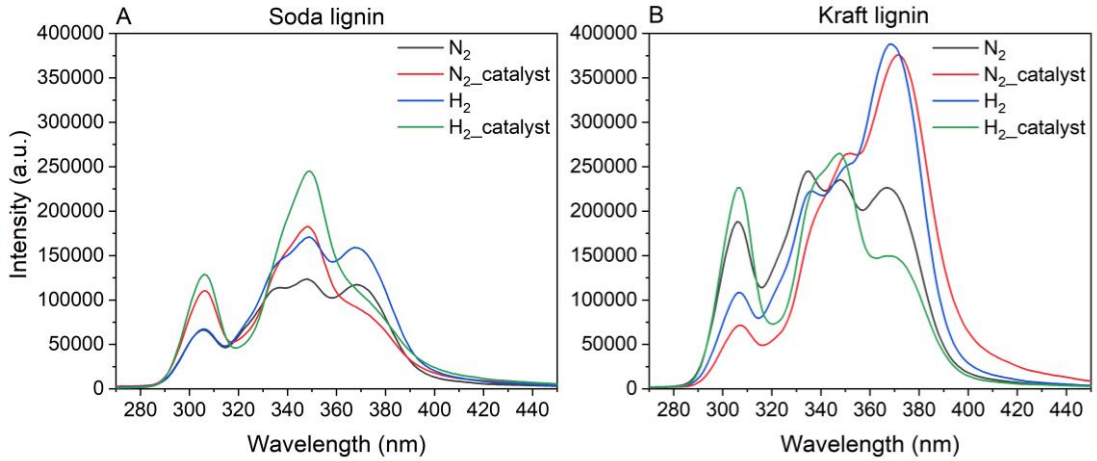

Figure 7 UV-Vis synchronous fluorescence spectra after 4h at different reaction conditions.

Lignin depolymerization index (DI) at different process conditions is calculated after deconvolution of the UV-Vis measurements and results are summarized in Table 2.

Table 2: Lignin depolymerization index (DI) based on from UV-Vis measurements at the different reaction conditions.

		N_2	N_2_catalyst	H_2	H_2_catalyst
Soda	Monomers	0,10	0,16	0,08	0,28
	Monomers and oligomers	0,72	0,76	0,68	0,71
Kraft	Monomers	0,26	0,05	0,17	0,30
	Monomers and oligomers	0,50	0,34	0,42	0,75

1.3.7. - GC-MS analysis

Samples taken every 30 min from the reaction mixture were analyzed using GC-MS. The yield of monomers was calculated using a hexadecane as an internal standard. The total monomer yield detected by GC-MS is shown in Figure 8, while the yield of the most relevant monomers indicating efficiency of the lignin depolymerization is displayed in Figure 8. The highest amount of monomers produced after the catalytic kraft lignin depolymerization made 4.2 % and in case of soda lignin - 3.8 %, while the total amount displayed in Figure 8 was 4.4 % and 5.9 %, respectively. Comparison of the obtained results demonstrates a significant effect of catalyst on the extent of the soda lignin depolymerization. Similarly, as shown in Figure 8, the yield of the most relevant monomers increased after the addition of the catalyst, while the other 1 % was gained by substituting nitrogen atmosphere with hydrogen. The continuous increase of the monomer concentration was observed even during the non-catalytic depolymerization, however the concentration at the end of the treatment made approximately 50 % of monomers generated after catalytic depolymerization. As it is evident from the Figure 8B, the higher monomer amounts (up to 4 %) from the kraft lignin are obtained only after catalytic depolymerization under the hydrogen atmosphere, while just up to 2.5 % of monomers are produced at the other tested reaction conditions. Schutyser *et al.*[11] described that the β-O-4 content in lignin is one of the crucial factors determining susceptibility of lignin to depolymerization. If during the depolymerization only ether bonds are cleaved, the maximum monomer yield roughly equals the square of the fraction of cleavable inter-unit ether bonds.[11] In general the monomer yield increases in the following order *softwoods* < *herbaceous crops* < *hardwoods*, which correlate with their respective β-O-4 content. Technical lignins like softwood kraft lignin and soda Protobind 1000 have low β-O-4 bond contents, even below 10 %[11] which partially justifies the highest yield of the most relevant monomers (up to 4.5 %) obtained in the current work. Nevertheless, the depolymerization of lignin could be affected by impurities from the biomass feedstock, chemicals used during biomass processing or from external source.[11]

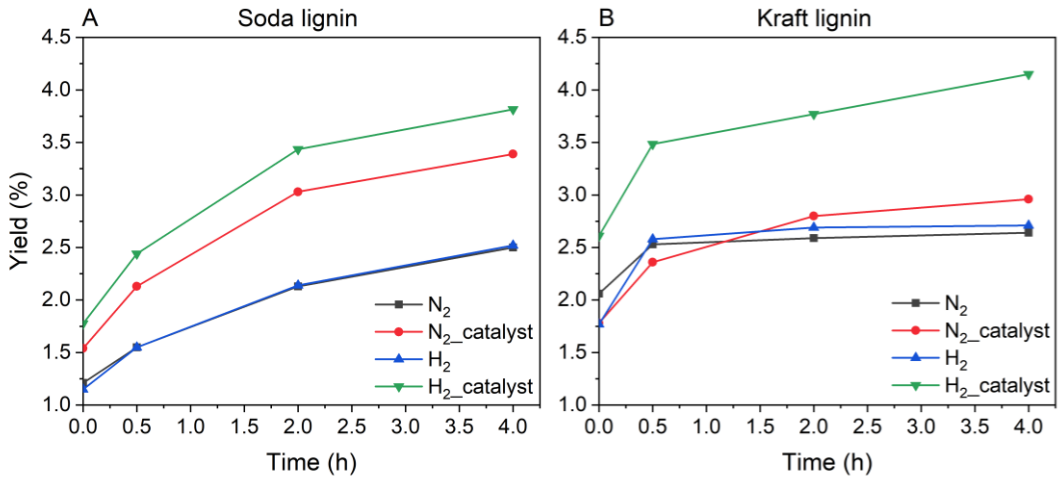

Figure 8 The yield of the most relevant monomers with time under the different reaction conditions.

Figure 9 shows the yield of six aromatic monomers obtained from soda lignin wih the reaction time. Here, guaiacol, methyl-, ethyl- and propylguaiacol were originating from the G-units, while syringol and acetosyringone from the S-units in soda lignin. The highest yields of ethyl- and propylguaiacol were acquired at the end of the treatment and made 0.8 % and 0.65 %, respectively. In general, the most effective soda lignin depolymerization was achieved using catalyst under the hydrogen atmosphere, however the highest yields of guaiacol and syringol were attained after the non-catalytic treatment resulting 0.3 % and 0.5 %, correspondingly.

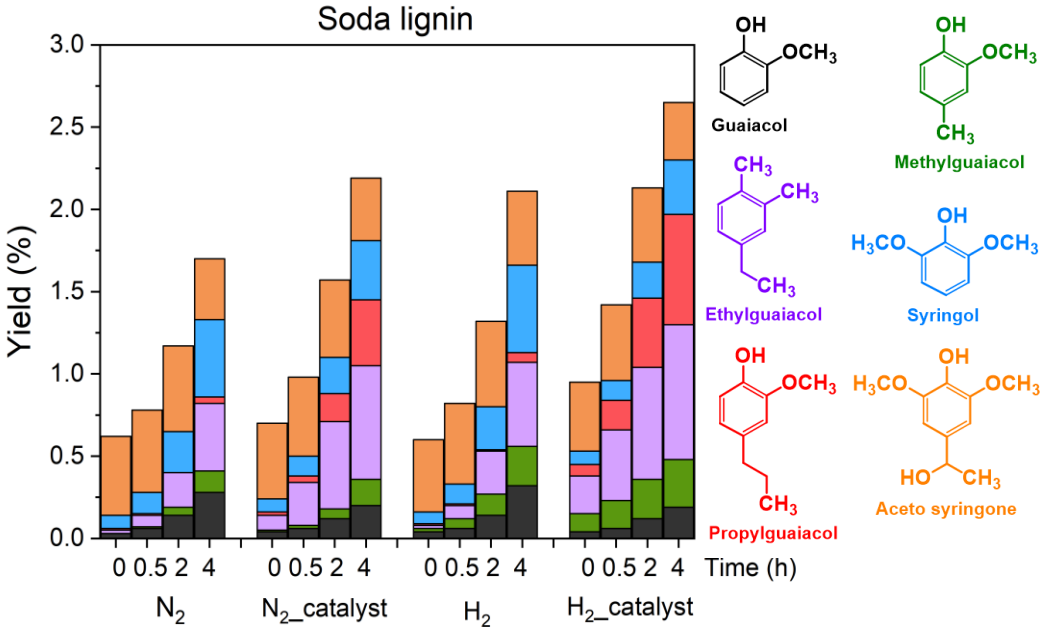

Figure 9 The yield of monomers obtained after soda lignin depolymerisation as a function of time.

The predominance of the G-units in the kraft lignin structure accordingly determines the emergence of the guaiacol alcohols shown in Figure 10. Hence, the highest yield and the most pronounced increase of propylguaiacol up to 1.8 % was achieved using catalyst under the hydrogen atmosphere, while lower but still noteworthy yield of ethylguaiacol made up to 0.8 %. As it is evident from the Figure 10, only the minor change of the guaiacol and methylguaiacol amount has been detected within the 4-hour reaction under the different conditions.

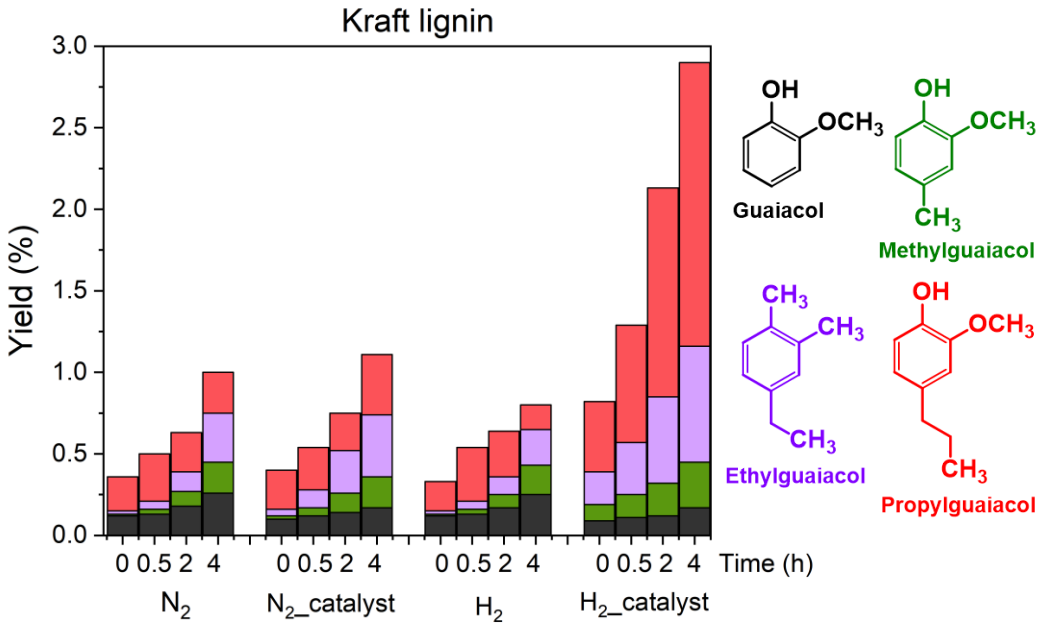

Figure 10 The yield of monomers obtained after kraft lignin depolymerization as a function of time.

1.4. - References

1. J.-Y. Kim, J. Park, U.-J. Kim, et J. W. Choi, « Conversion of Lignin to Phenol-Rich Oil Fraction under Supercritical Alcohols in the Presence of Metal Catalysts », *Energy Fuels*, vol. 29, nº 8, p. 5154-5163, août 2015, doi: 10.1021/acs.energyfuels.5b01055.

2. R. Rinaldi, *Catalytic Hydrogenation for Biomass Valorization*. Royal Society of Chemistry, 2014.

3. J. Zakzeski, P. C. A. Bruijnincx, A. L. Jongerius, et B. M. Weckhuysen, « The Catalytic Valorization of Lignin for the Production of Renewable Chemicals », *Chem. Rev.*, vol. 110, nº 6, p. 3552-3599, juin 2010, doi: 10.1021/cr900354u.

4. C.-H. Zhou, X. Xia, C.-X. Lin, D.-S. Tong, et J. Beltramini, « Catalytic conversion of lignocellulosic biomass to fine chemicals and fuels », *Chem. Soc. Rev.*, vol. 40, nº 11, p. 5588-5617, oct. 2011, doi: 10.1039/C1CS15124J.

5. R. B. Santos, P. Hart, H. Jameel, et H. Chang, « Wood Based Lignin Reactions Important to the Biorefinery and Pulp and Paper Industries », *BioResources*, vol. 8, nº 1, Art. nº 1, janv. 2013.

6. R. Rinaldi *et al.*, « Paving the Way for Lignin Valorisation: Recent Advances in Bioengineering, Biorefining and Catalysis », *Angew. Chem. Int. Ed.*, vol. 55, nº 29, p. 8164-8215, juill. 2016, doi: 10.1002/anie.201510351.

7. T. J. McDonough, « The chemistry of organosolv delignification », oct. 1992, Consulté le: juin 08, 2021. [En ligne]. Disponible sur: https://smartech.gatech.edu/handle/1853/2069

8. W. O. S. Doherty, P. Mousavioun, et C. M. Fellows, « Value-adding to cellulosic ethanol: Lignin polymers », *Industrial Crops and Products*, vol. 33, nº 2, p. 259-276, mars 2011, doi: 10.1016/j.indcrop.2010.10.022.

9. F. S. Chakar et A. J. Ragauskas, « Review of current and future softwood kraft lignin process chemistry », *Industrial Crops and Products*, vol. 20, nº 2, p. 131-141, sept. 2004, doi: 10.1016/j.indcrop.2004.04.016.

10. L. Dessbesell, M. Paleologou, M. Leitch, R. Pulkki, et C. (Charles) Xu, « Global lignin supply overview and kraft lignin potential as an alternative for petroleum-based polymers », *Renewable and Sustainable Energy Reviews*, vol. 123, p. 109768, mai 2020, doi: 10.1016/j.rser.2020.109768.

11. W. Schutyser, T. Renders, S. Van Den Bosch, S. F. Koelewijn, G. T. Beckham, et B. F. Sels, « Chemicals from lignin: An interplay of lignocellulose fractionation, depolymerisation, and upgrading », *Chemical Society Reviews*, vol. 47, n° 3, p. 852-908, 2018, doi: 10.1039/c7cs00566k.

12. S. O. Limarta, J.-M. Ha, Y.-K. Park, H. Lee, D. J. Suh, et J. Jae, « Efficient depolymerization of lignin in supercritical ethanol by a combination of metal and base catalysts », *Journal of Industrial and Engineering Chemistry*, vol. 57, p. 45-54, janv. 2018, doi: 10.1016/j.jiec.2017.08.006.

13. I. Hita, P. J. Deuss, G. Bonura, F. Frusteri, et H. J. Heeres, « Biobased chemicals from the catalytic depolymerization of Kraft lignin using supported noble metal-based catalysts », *Fuel Processing Technology*, vol. 179, p. 143-153, oct. 2018, doi: 10.1016/j.fuproc.2018.06.018.

14. M. A. Hossain, T. K. Phung, M. S. Rahaman, S. Tulaphol, J. B. Jasinski, et N. Sathitsuksanoh, « Catalytic cleavage of the β-O-4 aryl ether bonds of lignin model compounds by Ru/C catalyst », *Applied Catalysis A: General*, vol. 582, p. 117100, juill. 2019, doi: 10.1016/j.apcata.2019.05.034.

15. I. Kristianto, S. O. Limarta, H. Lee, J.-M. Ha, D. J. Suh, et J. Jae, « Effective depolymerization of concentrated acid hydrolysis lignin using a carbon-supported ruthenium catalyst in ethanol/formic acid media », *Bioresource Technology*, vol. 234, p. 424-431, juin 2017, doi: 10.1016/j.biortech.2017.03.070.

16. H. Li et G. Song, « Ru-Catalyzed Hydrogenolysis of Lignin: Base-Dependent Tunability of Monomeric Phenols and Mechanistic Study », *ACS Catal.*, vol. 9, n° 5, p. 4054-4064, mai 2019, doi: 10.1021/acscatal.9b00556.

17. L. Cao *et al.*, « Hydrothermal liquefaction of agricultural and forestry wastes: state-of-the-art review and future prospects », *Bioresource Technology*, doi: 10.1016/j.biortech.2017.08.196.

18. X. Huang, C. Atay, T. I. Korányi, M. D. Boot, et E. J. M. Hensen, « Role of Cu–Mg–Al Mixed Oxide Catalysts in Lignin Depolymerization in Supercritical Ethanol », *ACS Catal.*, vol. 5, n° 12, p. 7359-7370, déc. 2015, doi: 10.1021/acscatal.5b02230.

19. S. Cheng, L. Wei, J. Julson, P. R. Kharel, Y. Cao, et Z. Gu, « Catalytic liquefaction of pine sawdust for biofuel development on bifunctional Zn/HZSM-5 catalyst in supercritical ethanol », *Journal of Analytical and Applied Pyrolysis*, doi: 10.1016/j.jaap.2017.06.001.

20. E. I. Kozliak *et al.*, « Thermal Liquefaction of Lignin to Aromatics: Efficiency, Selectivity, and Product Analysis », *ACS Sustainable Chem. Eng.*, vol. 4, nº 10, p. 5106-5122, oct. 2016, doi: 10.1021/acssuschemeng.6b01046.

21. J. Hu, D. Shen, S. Wu, H. Zhang, et R. Xiao, « Effect of temperature on structure evolution in char from hydrothermal degradation of lignin », *Journal of Analytical and Applied Pyrolysis*, vol. 106, p. 118-124, mars 2014, doi: 10.1016/j.jaap.2014.01.008.

22. O. Faix, « Classification of Lignins from Different Botanical Origins by FT-IR Spectroscopy », *Holzforschung*, vol. 45, nº s1, p. 21-28, 1991, doi: 10.1515/hfsg.1991.45.s1.21.

23. H. Li et A. G. McDonald, « Fractionation and characterization of industrial lignins », *Industrial Crops and Products*, vol. 62, p. 67-76, 2014, doi: 10.1016/j.indcrop.2014.08.013.

24. K. Gabov, R. J. A. Gosselink, A. I. Smeds, et P. Fardim, « Characterization of lignin extracted from birch wood by a modified hydrotropic process », *Journal of Agricultural and Food Chemistry*, vol. 62, nº 44, p. 10759-10767, 2014, doi: 10.1021/jf5037728.

25. G. Guo, S. Li, L. Wang, S. Ren, et G. Fang, « Separation and characterization of lignin from bio-ethanol production residue », *Bioresource Technology*, vol. 135, p. 738-741, 2013, doi: 10.1016/j.biortech.2012.10.041.

26. B. Joffres *et al.*, « Catalytic hydroconversion of a wheat straw soda lignin: Characterization of the products and the lignin residue », *Applied Catalysis B: Environmental*, vol. 145, p. 167-176, 2014, doi: 10.1016/j.apcatb.2013.01.039.

2. - Article in development: Study on the extraction of phenolic compounds from bio-oils

Siqin Li[a,b], Erika Bartolomei[b], Haiping Yang[a], Anthony Dufour[b]*

[a] China-EU Institute for Clean and Renewable Energy, Huazhong University of Science and Technology, 430074 Wuhan, China
[b] LRGP, CNRS, Université de Lorraine, 1 rue Grandville, 54000 Nancy, France

* Corresponding author : anthony.dufour@univ-lorraine.fr

Keywords: Liquid-liquid extraction, Phenols, Ethyl acetate, Bio-oil, Lignin

Abstract

Lignin as a very promising energy source, but the complexity of lignin depolymerization solution hinders its application. Liquid-liquid extraction is a commonly used separate phenols from the mixed solutions. In this thesis, ethyl acetate (EA) and dichloromethane ((DCM) were used to explore the factors affecting extraction efficiency and optimal extraction conditions. The extraction experiments with EA and DCM were performed on the lignin model compounds first and then applied on the pyrolysis wood tar and gasification tar of alkaline lignin. It was found that EA has better extraction performance for phenols. The addition of model compounds can improve its extraction efficiency and the enhancement effects of guaiacol and eugenol are the most significant. The composition of wood tar is very complex, dominated by phenolic substances, and EA has better extraction performance for phenols. The alkali lignin gasification tar extracted by EA also contains some ketones and alcohols. Increasing the extraction time can improve the extraction effect of EA.

2.1. - Introduction

Lignin is the main component of lignocellulosic biomass, which accounts for 15% ~ 30% of their dried weight and ~40% energy of lignocellulosic biomass.[1] The total amount of lignin is pretty huge, which is over 300 billion tons in the biosphere and keeps increasing by 20 billion

tons every year. Lignin is produced worldwide in amounts close to 70 million tones, and as the major component of black liquor, nearly 40 ~ 60 million tons of waste lignin is generated per year from the pulp and paper industry.[1,2] It is estimated by 2030, this number will increase by 225 million tonnes per year since Renewable Fuel Standard (RFS) program has mandated the production of 60 billion gallons of biofuel, and lignin is the main byproduct of biofuel production. Lignin is composed of three phenylpropane groups, which are connected by different ether bonds or C-C bonds.[3] The difference in side chain structure has a significant impact on the pyrolysis behavior of lignin.[4] Due to the different thermal stability of each functional group in lignin, the pyrolysis temperature range of lignin is wide, and the main weight loss range is 360 - 400℃. The presence of some aromatic ring substances will cause more char residues after lignin pyrolysis.[5,6]

Despite the production of lignin is huge and it has a promising perspective, however, only less than 2% of the 1.5 - 1.8 million tons of industrial lignin waste are used as an additive in building materials worldwide annually.[7] And for the pulp and paper industry, the lignin wastes are chiefly used as a burning fuel and only less than 5% is used for other purposes.[2] This inefficient way of lignin using is not only a waste of resources, but also causes serious environmental problems.[8] The resource utilization of lignin has become an urgent problem to be solved.

Phenol is one of the main products after lignin depolymerization. Thus, obtaining phenol from lignin provides a new pathway of clean manufacture out of a renewable feedstock.[9] Since 2010, the annual output of phenol has maintained an annual growth rate of 1.8%, but it still cannot meet the rapid growth consumption demand.[10] Because phenol is one of the most important aromatic chemicals utilized in industry[11], mainly used as synthesis polymer precursors, food additives, fine chemicals, phenolic resins as well as pharmaceuticals and herbicides.[12] Today, nearly 95% of the world's phenol production is based on the "cumene process", which is the most important industrial process for the simultaneous production of phenol and acetone from benzene and propylene.[13] The entire process is very complicated[14] and consumes a lot of fossil fuels, causing many environmental problems.[15] This process is also accompanied by disadvantages such as high risk factor, high investment cost, and large output of acetone, which greatly reduces its technical and economic feasibility.[16] Although lignin is a promising source to produce phenols, the decomposed lignin is most often a complex mixture compounds hindering its direct use as chemical materials.[17] Besides, some researches point out that the presence of phenolic compounds in the deplolymerized lignin will cause several operational problems such as fouling, corrosion and catalytic deactivation.[18] Therefore, if a method can be

found to separate phenol form lignin effectively, it will bring huge economic and environmental benefits to society.

Regarding the subject of separation and purification of lignin depolymerization solution, researchers have also conducted many relevant studies and proposed some tailor-made methods like membrane separation[19], preparative chromatography[20], distillation[21], column separation, and the most commonly used method liquid-liquid extraction (LLE)[22]. Overall, LLE is easier to perform with simple devices and operating under mild conditions[23]. Ru et al.[24] pointed out that the performances of methanol, ethyl acetate and acetone just had a slight difference; Cesari et al.[23] stated that the ionic liquid [Choline][NTf2] was a good solvent for the recovery of phenolic compounds; Ljudmila and Alma[22] declared that methyl isobutyl ketone was found to be more selective organic solvent in comparison to acetates. Feng and Meier[25] also tried to use supercritical carbon dioxide to extract valuable chemicals and pyrolysis liquids, and reported that pressures had a higher impact on the yield of extracts rather than on their chemical composition.

Therefore, the objective of the present work is to find an extracting agent with higher selectivity to phenols. Five main lignin depolymerization model compounds were dissolved together or individually in a certain proportion of sodium hydroxide solution (pH=9) to simplify and simulate the real solution state of lignin after hydrothermal reaction. The recovery yields of phenol separated from these different mixed solutions were compared to know the extraction performance of ethyl acetate and dichloromethane, and the effect of different monomers on the extraction and separation of phenol was also investigated. The results of this study will provide some fundamental support and theoretical guidance for the efficient valorization of lignin and the effective separation of phenol to help achieve the goal of green phenol production faster.

2.2. - Materials and methods

2.2.1. - Materials

Guaiacol (C7H8O2, liquid, Rionlon Co., Ltd.), catechol (C6H6O2, solid), syringol (C8H10O3, solid), vanillin (C8H8O3, solid) and eugenol (C10H12O2, liquid) are all analytical reagents and used as model compounds of lignin depolymerization solution because they are the main monomers after the lignin decomposition. Phenol (C6H6O, solid) was used as the target product to be extracted from the mixture. Take an appropriate amount of sodium hydroxide solid, and prepare a sodium hydroxide solution with a pH of about 9 with distilled water as the base liquid

for dissolving the above-mentioned model compound. Ethyl acetate (C4H8O2, EA, Rionlon Co., Ltd.) and dichloromethane (CH2Cl2, DCM, Rionlon Co., Ltd.) were used as extracting agents to obtain the phenol products from the solutions above. 1-Tetradecene (C14H28, Rionlon Co., Ltd.) was used as the internal standard to calculate the recovery yield of phenol and the other organic compounds from the GC-MS specturm. The following Table 1 is a summary of the structural and molecular formulas of all reagents mentionsed above. These reagents are dissolved in the prepared sodium hydroxide solution together or individually according to the experimental needs.

Table 1 The structural and molecular formulas of all reagents used The summary of the structural and molecular formulas of all reagents.

The summary of the structural and molecular formulas of all reagents				
Name	Guaiacol	Catechol	Syringol	Vanillin
Molecular formula	$C_7H_8O_2$	$C_6H_6O_2$	$C_8H_{10}O_3$	$C_8H_8O_3$
Structural formula	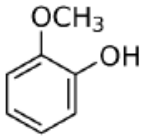	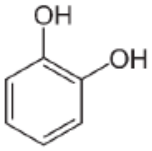	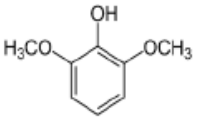	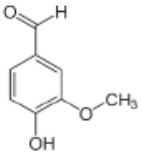
Name	Eugenol	Phenol	Ethyl acetate	Dichloromethane
Molecular formula	$C_{10}H_{12}O_2$	C_6H_6O	$C_4H_8O_2$	CH_2Cl_2
Structural formula	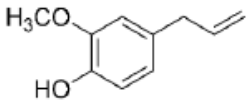	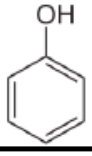	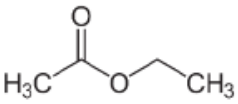	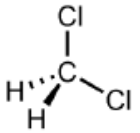

2.2.2. - Experimental methods and contents

Figure 1 describes the operation steps of liquid-liquid extraction and separation of phenolic products from the model compound solutions. Take an appropriate amount of the mixed solution with or without model compounds and put it in a sample bottle with magnets, add the same amount of ethyl acetate or dichloromethane, and put the sample bottle a multi-station magnetic stirring cell under 25°C at the stirring speed of 500 rpm. Magnetic stirring is carried out for 24 hours in the stirring tank to ensure sufficient extraction. After the stirring, remove the sample bottle and place it at room temperature for 24 hours to ensure complete separation of the inorganic aqueous phase and the organic extraction phase. Take all the organic phase solution out, add a certain amount of internal standard substance (1-tetradecene) to prepare the samples for GC/MS testing and analysis. Since temperature is one of the main factors affecting the extraction effect, during the stirring process, keep the liquid level in the pool always higher than the liquid level in the sample bottle to ensure the stability of the temperature during the

extraction process. And pay attention to placing the bottles in the center of the magnetic stirring to prevent the displacement or tipping caused by vibration.

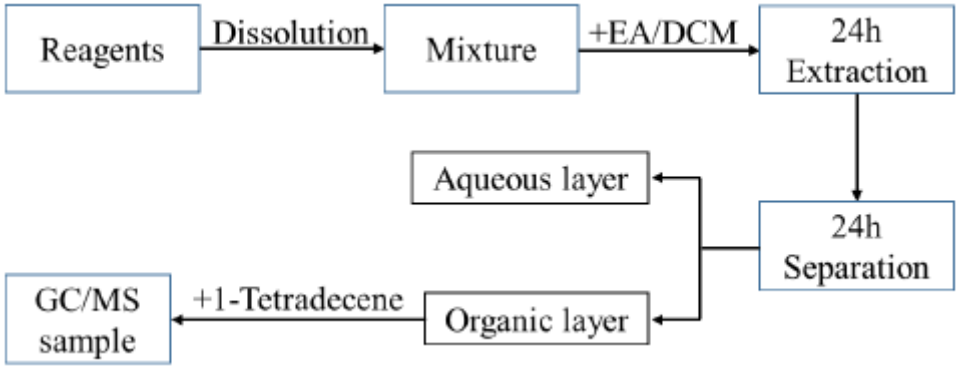

Figure 1 Scheme process of extracting phenols experiment

The experiment contains two variables: the extractant type and the composition of base solution. By comparing the extraction performance of ethyl acetate and dichloromethane, explore a more efficient method of separating phenols; add only phenol to the prepared alkaline sodium hydroxide solution with a pH of 9 for a blank experiment; then add guaiacol, catechol, eugenol, vanillin, and eugenol together or separately to study the effect of each monomer compound on extraction

performance. The volume of the extractant and the base fluid are both 10 mL, and all experiments are carried out at least twice under the same conditions to ensure the reliability of the experimental results.

2.2.3. - Product analysis method

The compositon analysis of the product after extraction was performed with an Agilent 7890A Gas Chromatography coupled to an Agilent 5975C MS analyzer. The samples (1μL) were injected by an Agilent 7683B auto-sampler with a split ratio of 20. First, the sample was sent to an Agilent HP-5MS (30 m × 250 μm × 0.25 μm) column. The exit of the HP-5MS column was connected either

to an Agilent DB-Wax123 (30 m × 320 μm × 0.25 μm) column which connected with a flame ionization detector (FID) or simultaneously to a FID and a mass spectroscopy (MS). The temperature programming was as follows: the oven was firstly maintained at 323 K for 5 minutes and then heated up to 523 K at a heating rate of 5 K/min, and the final temperature was held for 15 minutes[23].

The quantification of the phenolic compounds as well as other model compounds was performed using FID results. By comparing the peak area of the obtained component with the peak area of the internal standard substance 1-Tetradecene, the content of phenol and the model compound in the extracted fraction can be obtained. The yield of these substances can be calculated by the following equation (3):

$$\eta = \frac{m_f - m_i}{m_i} * 100\% \quad (3)$$

where, m_i is the initial mass that contained in each sample before the extraction, m_f is the final mass contained the extracted fraction.

2.3. - Results and Discussions

2.3.1. - Separation characteristics of phenol components in model compounds

By comparing the content of each substance before and after extraction, the recovery yields of phenol and organics were calculated, and the results were summarized in the Figure 2 below. It can be seen from the Figure 2 (a) that the extraction efficiency of EA to phenol was always higher than that of DCM with or without model compounds. It showed that EA had a better selectivity to phenol, and this may be affected by the polarity of the molecules[23]. The polarity of EA is higher than that of DCM, and phenol is also a polar molecule. Therefore, according to the rule of the likes dissolve each other, the solubility of phenol in EA is higher. At the same time, it can be seen that the presence of model compounds can increase the extraction efficiency of EA to phenol, and the enhancement effects of guaiacol and eugenol are the most significant. This may be related to their different acidity.

The organics recovery yield means the sum of the recovery yields of all five model compounds and phenol. As shown in Figure 2 (b), the recovery yield of EA was also higher than that of DCM, except in the presence of syringol. It can also be seen that in the presence of catechol, the recovery yield of both EA and DCM was much lower than other cases. Because the peak of catechol is missing in the GC-MS spectrum of the oil phase after extraction in this case, its organic recovery yield was about half that without the presence of model compounds. This phenomenon was in accordance with its solubility in water, followed by vanillin. Higher water solubility is more likely the result of the polarity and ability to form hydrogen bond due to the presence of two hydroxyl groups (OH) groups on the aromatic ring for catechol and presence of hydroxyl and aldehyde groups in vanillin structure, beside the methoxy group[22]. In many biomass pyrolysis and gasification studies, most of the oil products are collected and tested with

DCM. According to the results in this research, EA had a higher extraction efficiency for phenolic substances. If EA is used to collect the bio-oil products, the organic components may be collected more fully, and the bio-oil yield can be calculated more accurately.

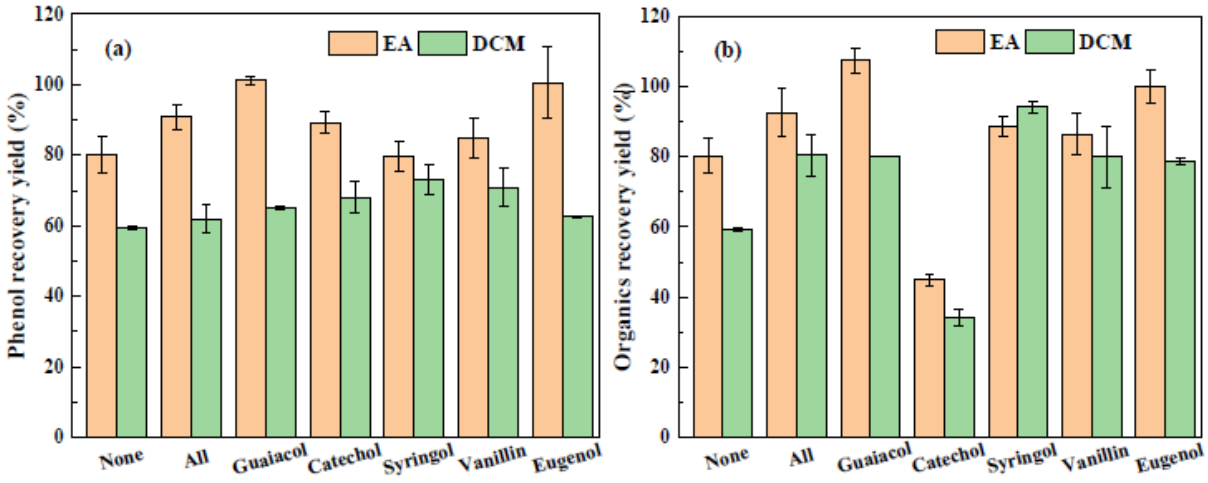

Figure 2 The recovery yields of batch experiments
(a) Phenol recovery yield; (b) Organics recovery yield of batch experiments

2.4. - Conclusions

The extraction performance of ethyl acetate and dichloromethane to phenolic products were compared with GC/MS spectra on the lignin depolymerization model compounds. It was found that ethyl acetate has better extraction performance for phenols. Moreover, adding model compounds can improve its extraction efficiency and the enhancement effects of guaiacol and eugenol are the most significant. The phenolic content of wood tar is very high. Increasing the extraction time can improve the extraction performance of ethyl acetate to phenol to a certain extent, and can reduce the impurity content in phenol after extraction.

2.5. - References

1. Fernandez-Rodriguez J, Erdocia X, Sanchez C, Gonzalez Alriols M, Labidi J. Lignin depolymerization for phenolic monomers production by sustainable processes. J Energy Chem. 2017;26(4):622-31.

2. Kleinert M, Barth T. Phenols from Lignin. Chemical Engineering Technology. 2008;5(31):736-45.

3. Collard F, Blin J. A review on pyrolysis of biomass constituents: Mechanisms and composition of the products obtained from the conversion of cellulose, hemicelluloses and lignin. Renew Sust Energ Rev. 2014;38:594-608.

4. Neutelings G. Lignin variability in plant cell walls: Contribution of new models. Plant Sci. 2011;181(4):379-86.

5. Lv G, Wu S. Analytical pyrolysis studies of corn stalk and its three main components by TG-MS and Py-GC/MS. J Anal Appl Pyrol. 2012;97:11-8.

6. Shen DK, Gu S, Luo KH, Wang SR, Fang MX. The pyrolytic degradation of wood-derived lignin from pulping process. Bioresource Technol. 2010;101(15):6136-46.

7. Gadhave RV, Mahanwar PA, Gadekar PT. Lignin-Polyurethane Based Biodegradable Foam. Open Journal of Polymer Chemistry. 2018;08(01):1-10.

8. Cao L, Yu IKM, Liu Y, Ruan X, Tsang DCW, Hunt AJ, et al. Lignin valorization for the production of renewable chemicals: State-of-the-art review and future prospects. Bioresource Technol. 2018;269:465-75.

9. Omoriyekomwan JE, Tahmasebi A, Yu J. Production of phenol-rich bio-oil during catalytic fixed-bed and microwave pyrolysis of palm kernel shell. Bioresource Technol. 2016;207:188-96.

10. Zhang Y, Lei H, Yang Z, Duan D, Villota E, Ruan R. From glucose-based carbohydrates to phenol-rich bio-oils integrated with syngas production via catalytic pyrolysis over an activated carbon catalyst. Green Chem. 2018;20(14):3346-58.

11. Jung KB, Lee J, Ha J, Lee H, Suh DJ, Jun C, et al. Effective hydrodeoxygenation of lignin-derived phenols using bimetallic RuRe catalysts: Effect of carbon supports. Catal Today. 2018;303:191-9.

12. Kim J. Production, separation and applications of phenolic-rich bio-oil – A review. Bioresource Technol. 2015;178:90-8.

13. Zakoshansky VM. The cumene process for phenol-acetone production. Petrol Chem+. 2007;47(4):273-84.

14. Mancuso A, Sacco O, Sannino D, Venditto V, Vaiano V. One-Step Catalytic or Photocatalytic Oxidation of Benzene to Phenol: Possible Alternative Routes for Phenol Synthesis? Catalysts. 2020;10(12):1424.

15. Schmidt RJ. Industrial catalytic processes—phenol production. Applied Catalysis A: General. 2005;280(1):89-103.

16. Molinari R, Poerio T. Remarks on studies for direct production of phenol in conventional and membrane reactors. Asia-Pac J Chem Eng. 2010;5(1):191-206.

17. Zhang J, Lombardo L, Gözaydın G, Dyson PJ, Yan N. Single-step conversion of lignin monomers to phenol: Bridging the gap between lignin and high-value chemicals. Chinese J Catal. 2018;39(9):1445-52.

18. Anis S, Zainal ZA. Tar reduction in biomass producer gas via mechanical, catalytic and thermal methods: A review. Renew Sust Energ Rev. 2011;15(5):2355-77.

19. Teella A, Huber GW, Ford DM. Separation of acetic acid from the aqueous fraction of fast pyrolysis bio-oils using nanofiltration and reverse osmosis membranes. J Membrane Sci. 2011;378(1-2):495-502.

20. Wang Z, Lin W, Song W, Du L, Li Z, Yao J. Component fractionation of wood-tar by column chromatography with the packing material of silica gel. Chinese Science Bulletin. 2011;56(14):1434-41.

21. Li J, Ding D, Xu L, Guo Q, Fu Y. The breakdown of reticent biomass to soluble components and their conversion to levulinic acid as a fuel precursor. Rsc Adv. 2014;4(29):14985.

22. Fele Žilnik L, Jazbinšek A. Recovery of renewable phenolic fraction from pyrolysis oil. Sep Purif Technol. 2012;86:157-70.

23. Cesari L, Canabady-Rochelle L, Mutelet F. Separation of phenols from lignin pyrolysis oil using ionic liquid. Sep Purif Technol. 2019;209:528-34.

24. Lu R, Sheng G, Hu Y, Zheng P, Jiang H, Tang Y, et al. Fractional characterization of a bio-oil derived from rice husk. Biomass and Bioenergy. 2011;35(1):671-8.

25. Feng Y, Meier D. Extraction of value-added chemicals from pyrolysis liquids with supercritical carbon dioxide. J Anal Appl Pyrol. 2015;113:174-85.

26. Channiwala SA, Parikh PP. A unified correlation for estimating HHV of solid, liquid and gaseous fuels. Fuel. 2002;81:1051-63.

3. - Article in development: Oxidation and Reduction for Kraft Lignin Depolymerization: Comparison and Coupling

Erika Bartolomei[a], Antonio Hernandez Manas[b], Yann Le Brech[a], Laurent Djakovitch[b], Anthony Dufour[a]*

[a] LRGP, CNRS, Université de Lorraine, 1 rue Grandville, 54000 Nancy, France

[b] IRCELyon, CNRS, Université Claude Bernard Lyon1, 2 avenue Albert Einstein, 69626 Villeurbanne, France

* Corresponding author : anthony.dufour@univ-lorraine.fr

3.1. - Development

From our previous works on lignin liquefaction, both under oxidative and reductive conditions, we decided to compare lignin liquefaction under different atmospheres (oxygen and hydrogen) and eventually their combined action on lignin.

In this work we used softwood Kraft lignin in alkaline water (NaOH) first in oxidative atmosphere (O_2) with CuO/TiO_2 as catalyst, secondly in reductive atmosphere (H_2) with and without Ni/C as catalyst, and in the end both these conditions in series.

Table 1 Experiments list.

N	Feed	T °C	t (h)	Gas	Solvent	Catalyst	Name
1	Kraft lignin (K3)	150	1	AIR	NaOH	CuO/TiO2	OXBO
2	Kraft lignin (K3)	300	1	H_2	NaOH	Ni/C	OXBO_H2
3	Oxidized bio-oil (from 1)	300	1	H_2	NaOH	-	OXBO_H2_Ni
4	Oxidized bio-oil (from 1)	300	1	H_2	NaOH	Ni/C	K3_H2_NaOH_Ni

Preliminary results are presented below.

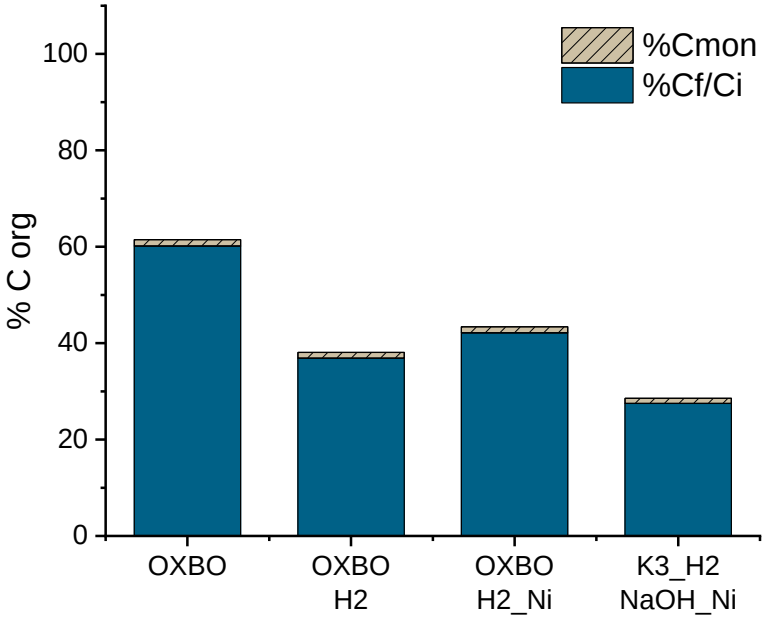

Figure 1 Organic carbon content in the liquid phase.

Figure 1 represents the organic carbon content of the bio-oil after liquefaction. A part of the organic carbon is lost in char/lignin residue and gas, but the most part stays in the liquid phase. In the figure we can see that the 35-60% of the initial carbon rests in the liquid products, but only few of that is representative of monomers (from GC-MS/FID analysis), in grey. After reduction in general there is less %C org in the liquid phase because more char is produced and more gas (because higher temperature than for oxidation only).

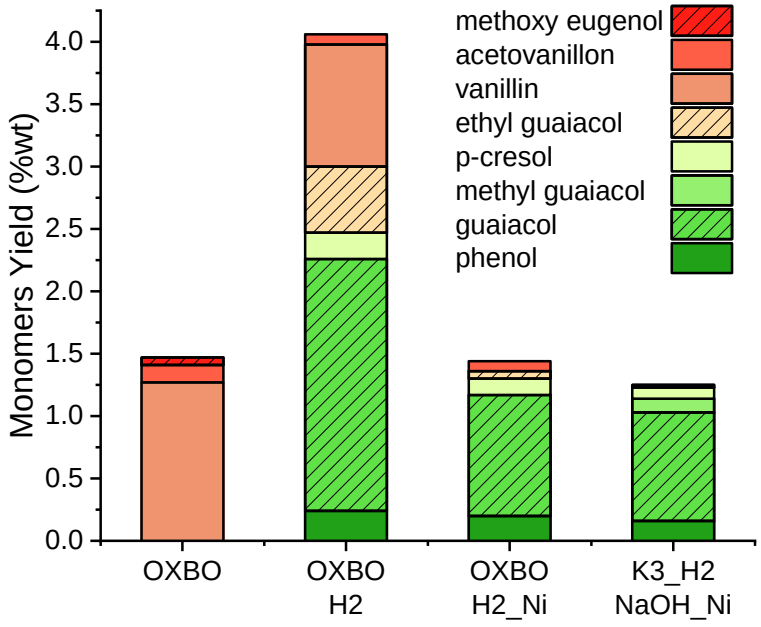

Figure 2 Monomers yields from GC-MS/FID.

In Figure 2 the results of GC-MS/FID analysis on just filtrated bio-oil from oxidation and DCM extracted bio-oil from reduction. In fact, being in aqueous phase, the bio-oil after reduction needs to be extracted in an organic solvent to be analysed.

The main difference between lignin oxidation and reduction are the families of products. From oxidation we get mainly vanillin and few similar molecules, while from reduction we produce phenol and mostly guaiacols. Ones we use Ni/C as catalyst during reduction, vanillin disappears, guaiacol is the main product (high selectivity). By coupling oxidation and reduction, we double the monomers yield, and both vanillin and guaiacols coexist.. Few quantities of pure phenol are also detected.

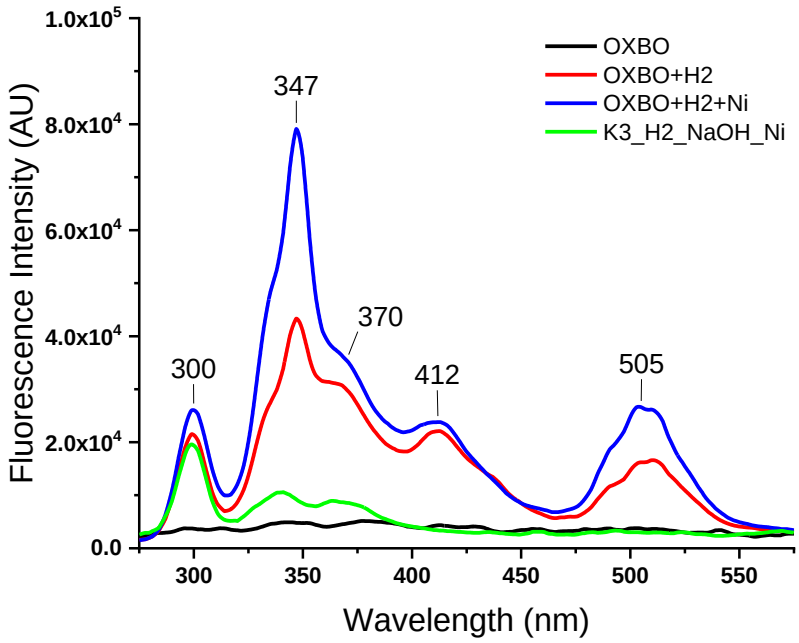

Figure 3 Synchronous (20nm offset) UV fluorescence spectra of the four conditions.

OXBO (only oxidized bio-oil) does not show peaks because aldehydes functionalities do not emit fluorescence (no conjugation).[1]

Kraft lignin direct reduction (green curve) has three characteristic peaks of lignin liquefaction products. The first one at 300nm is representative of small molecules, such as phenolic monomers, then increasing the conjugation in the molecule (e.g., more aromatic rings) we can found peaks at higher wavelength: oligomers at 350nm and heavy fraction of products at 375nm.[1]

The combination of lignin oxidation and reduction show more peaks at higher wavelengths, 412 and 505 respectively. It is a sign that coupling oxidation and reduction yields not only

monomers and dimers, but it can produce also bigger molecules, which stay in solution (in the bio oil).

Summarizing we can say that oxidation and reduction yield different kind of monomers: mostly vanillin for oxidation and guaiacol for reduction. Their coupling can yield a higher weight percentage of monomers and more oligomers (even more importantly).

We think that the combination of those two liquefaction condition is really effective in lignin depolymerization. Moreover, we can affirm that green solvents, cheap catalyst and mild conditions can have the same effect of harsh and expensive reactions if well combined.

3.2. - References

1. Bartolomei, E. *et al.* Lignin Depolymerization: A Comparison of Methods to Analyze Monomers and Oligomers. *ChemSusChem* **13**, (2020).

3.3. - Supporting Information

- GC-MS/FID results

		Kraft air Cu	OXBO H2	OXBO H2 Ni	Kraft H2 NaOH Ni
TOTAL	**(% wt)**	**1,47**	**4,06**	**1,44**	**1,25**
phenol	yield (% wt)		0,24	0,2	0,16
	selectivity (%)		5,91	13,89	12,80
guaiacol	yield (% wt)		2,02	0,97	0,87
	selectivity (%)		49,75	67,36	69,60
methyl guaiacol	yield (% wt)				0,11
	selectivity (%)				8,8
p-cresol	yield (% wt)		0,21	0,13	0,09
	selectivity (%)		5,17	9,03	7,20
ethyl guaiacol	yield (% wt)		0,53	0,06	0,02
	selectivity (%)		13,05	4,17	1,60
vanillin	yield (% wt)	1,27	0,98		
	selectivity (%)	86,39	24,14		
acetovanillon	yield (% wt)	0,14	0,08	0,08	
	selectivity (%)	9,52	1,97	5,56	
methoxy eugenol	yield (% wt)	0,06			
	selectivity (%)	4,08			

- Catalyst XRD on Cu/TiO2 from Lyon
- Synchronous UV fluorescence of Kraft lignin dissolved in alkaline water

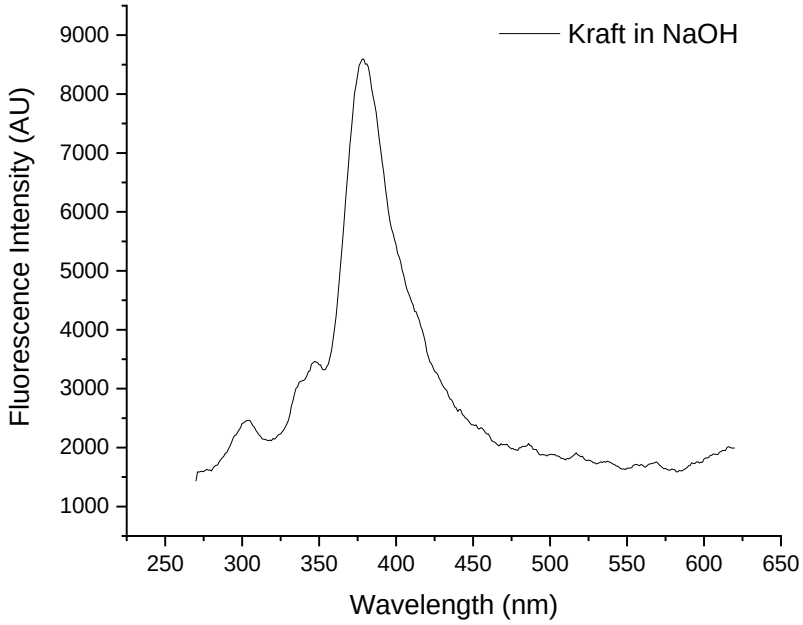

- Deconvolution: OXBO_H2
  OXBO_H2_Ni
  K3_H2_NaOH_Ni

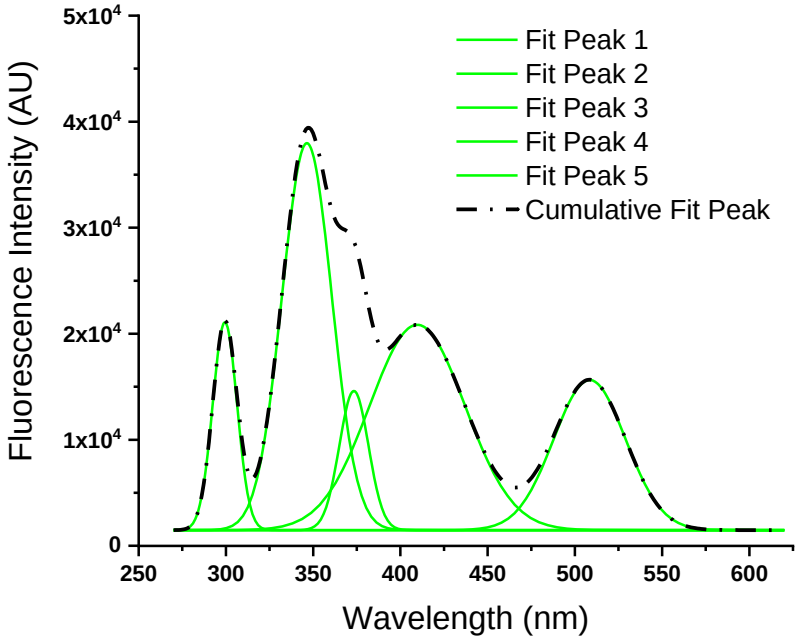

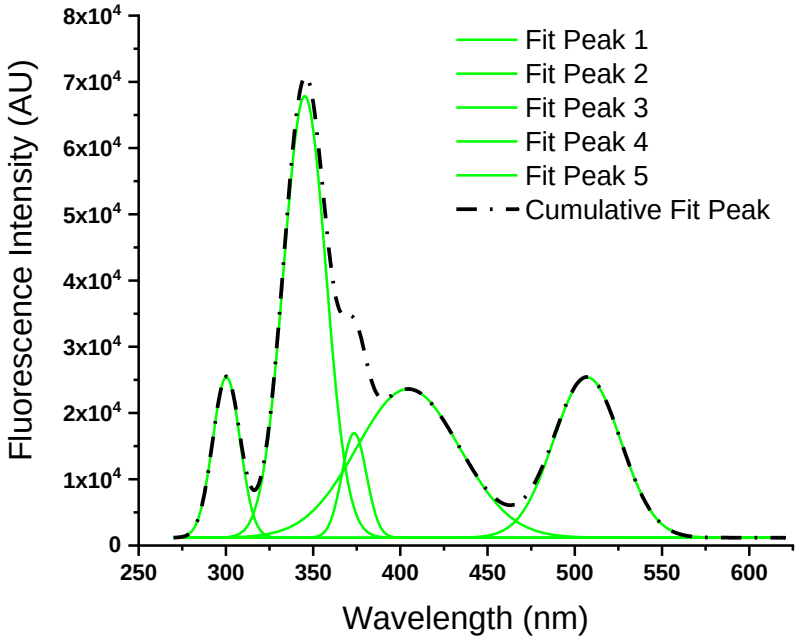
Fit Peak 1
Fit Peak 2
Fit Peak 3
Fit Peak 4
Fit Peak 5
Cumulative Fit Peak
Fluorescence Intensity (AU)
Wavelength (nm)
8x10^4
7x10^4
6x10^4
5x10^4
4x10^4
3x10^4
2x10^4
1x10^4
0
250
300
350
400
450
500
550
600

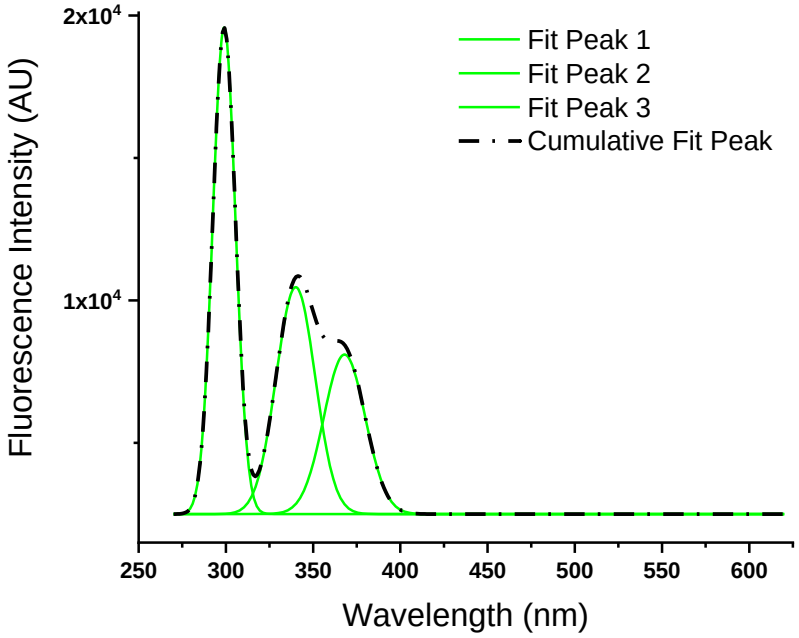
Fit Peak 1
Fit Peak 2
Fit Peak 3
Cumulative Fit Peak
Fluorescence Intensity (AU)
Wavelength (nm)
2x10^4
1x10^4
250
300
350
400
450
500
550
600

J. Résumé

1. - Introduction

Au cours des dernières décennies, la demande mondiale d'énergie a augmenté considérablement et elle est destinée à augmenter encore davantage en raison de l'augmentation combinée de la population mondiale et du développement des pays émergents. Les combustibles fossiles, comme le charbon, le pétrole et le gaz naturel, représentent plus de 80% du mix énergétique mondial.[1] L'exploitation de ces ressources non renouvelables entraîne le réchauffement climatique. Les préoccupations croissantes concernant le changement climatique et les effets environnementaux et économiques liés à l'utilisation des ressources fossiles favorisent le développement de la recherche sur les ressources renouvelables et durables.[2] Parmi ces alternatives, la décarbonisation de la production de carburants et de produits chimiques grâce à une utilisation efficace de la biomasse lignocellulosique est l'une des voies les plusétudiées.[3,4] Parmi les principaux composants de la biomasse, la lignine est sous valorisée et récalcitrante en raison de sa structure chimique complexe: il s'agit d'un biopolymère constitué d'unités aromatiques (principalement alcools p-coumaryl, coniféryl et sinapyle) liés par des liaisons différentes (α-O-4, β-O-4, 4-O-5 et CC entre autres).[5,6] Malgré de nombreuses recherches sur ce sujet, son fort potentiel pour la production de biocarburants et / ou de molécules plateformes (comme les aromatiques) est encore insuffisamment exploité.

Sur cette base, l'objectif de cette thèse est de valoriser la lignine pour produire des composés aromatiques verts pour des bioraffineries plus durables. En particulier, nous nous intéressons à la valorisation du flux de lignine dans les usines de pâtes et papiers. Dans ce contexte spécifique, notre objectif est d'intégrer, dans les industries papetières déjà existantes, une unité de valorisation de la lignine, produisant des produits chimiques aromatiques verts par liquéfaction.

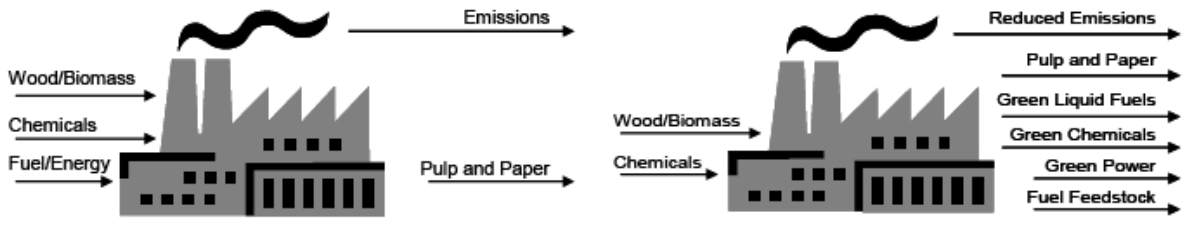

Figure 1 Changement de scénario souhaité pour les usines de pâtes et papiers.[7]

Cette recherche est financée par l'ANR (Agence Nationale de la Recherche). Dans ce projet national, différents laboratoires sont impliqués: Laboratoire Réaction et Génie de Procédé à Nancy pour son expertise en génie chimique et plates-formes analytiques, Centre Technique du Papier à Grenoble pour sa connaissance des procédés de pâte, IRCE Lyon et LGPC à Lyon pour une meilleur compréhension des mécanismes catalytiques. De plus, ce travail est le fruit de collaborations très complémentaires, incluant d'autres partenaires internationaux: Washington State University (USA) et National Institute of Chemistry à Ljubljana (Slovénie).

Dans les chapitres suivants, les résultats les plus pertinents de cette étude seront présentés.

Tout d'abord, une revue de la littérature est donnée au chapitre 1 pour comprendre ce qu'est la lignine, dans quel contexte nous nous situons et quelles sont actuellement les technologies de valorisation de la lignine. Un accent particulier est mis sur les usines de pâtes et papiers en tant que bioraffineries qui produisent de la cellulose et séparent la lignine.

Dans le chapitre 2, une caractérisation détaillée des lignines techniques et des liqueurs noires industrielles utilisées dans ce travail est présentée. Avant de convertir la lignine ou les liqueurs noires, il est fondamental de comprendre autant que possible la structure, les caractéristiques, les comportements thermiques et les compositions des matières premières.

Dans le chapitre suivant, le chapitre 3, est présenté un travail déjà publié dans *ChemSusChem* (7 septembre 2020; 13 (17): 4633-4648) intitulé «Dépolymérisation de la lignine: une comparaison de méthodes pour analyser les monomères et les oligomères». Le but de cette étude est de trouver un moyen rapide et efficace d'analyser les produits de liquéfaction de la lignine. Nous avons comparé différentes techniques analytiques pour mettre en évidence quelles pourraient être les limites et les avantages de chacune.

Le chapitre 4 contient l'article soumis à *Energy & Fuels* sur « l'effet du type de lignine technique et du catalyseur (Ni / C, Ru / C, Pt / C) sur les produits de dépolymérisation dans l'éthanol supercritique». Dans cet article sont mis en évidence les différences de rendements et de produits de liquéfaction de la lignine, les différents catalyseurs et types de lignine.

Le chapitre 5 est consacré à notre collaboration entre la France et les États-Unis d'Amérique sur l'oxydation de la lignine utilisant le TEMPO comme catalyseur. Ce travail a été soumis en tant qu'article complet à la revue *Industrial Crops and Product*.

Pour conclure la section des résultats, le chapitre 6 présente et compare différents scénarios possibles dans les usines de pâtes à papier pour inclure une unité de valorisation de la lignine. Une analyse technico-économique est également fournie.

Une conclusion générale est ensuite donnée pour résumer toutes ces études et proposer des perspectives.

En annexes sont présentés de nombreux matériels, méthodologies et travaux complémentaires liés au sujet de cette thèse et menés entre-temps.

2. - Revue de la littérature: caractéristiques et perspectives de la lignine

Comme évoqué précédemment, la biomasse peut être l'une des solutions pour éviter la surexploitation des énergies fossiles, notamment en raison de sa disponibilité dans le monde. Dans ce chapitre, un aperçu de la biomasse et plus de détails sur la lignine a été donné. Une attention particulière a été accordée aux lignines techniques, car ce sont des déchets / coproduits déjà existants dans les industries papetières. La méthode d'extraction de la lignine impacte ses caractéristiques, sa structure et les applications possibles. L'une des plus abondantes au monde est la lignine Kraft, coproduit de l'industrie papetière qui utilise largement le processus de délignification Kraft pour séparer la pâte de cellulose afin de fabriquer du papier à partir du bois. Cette lignine Kraft est aujourd'hui principalement brûlée dans la papeterie elle-même pour générer de la vapeur pour l'usine (et de l’électricité), mais cette ressource pourrait être mieux valorisée pour produire des molécules intéressantes de grande valeur (pour les biocarburants et les biomatériaux). La composition de la lignine, riche en phénols, en fait une bio-ressource précieuse qui mérite d'être exploitée au maximum et pas seulement brûlée.

De nombreuses voies de conversion existent déjà pour la lignine, mais il y a encore beaucoup de recherche dans ce domaine. Dans ce chapitre, tous les procédés de conversion thermochimique ont été décrits et un accent particulier a été mis sur la liquéfaction de la lignine, car c'est le procédé le plus prometteur pour produire des molécules aromatiques vertes à partir de la lignine. Sur ce sujet, des centaines d'études peuvent être trouvées dans la littérature, mais en fait beaucoup de ces recherches ont été menées sur des composés modèles et juste à l'échelle du laboratoire de nos jours. Il est donc évident que les recherches sur la valorisation de la lignine en général ne sont toujours pas complètes et qu'une plus grande attention devrait être accordée aux lignines techniques et commerciales, puis à des essais aux échelles pilote et industrielle.

3. - Caractérisation multi-analytique des lignines techniques et des liqueurs noires

Cette étude a pour objectif d'analyser et de comprendre en profondeur la composition, la structure et les caractéristiques des lignines techniques. Des techniques analytiques complémentaires ont été utilisées pour cette portée.

En résumé, de la caractérisation de 4 lignines commerciales (2 kraft, 1 soda, 1 organosolv) nous avons déduit les résultats suivants. Les lignines industrielles ont été commercialisées sous forme sèche (siccité ~ 94-96%), seule la lignine de résineux Kraft (BioPivaTM 1000) a été vendue brute sans séchage supplémentaire avec une teneur en eau résiduelle de 35% mas., comme indiqué par le fournisseur. Ils étaient relativement purs avec une teneur en lignine (KL + ASL) variant de 87% à 96%, des minéraux (cendres) de 1% à 2%mas. et des sucres résiduels de 2% à 5%. La lignine organosolv était la plus contaminée avec un taux de sucre résiduel de 5%, un taux de protéines allant jusqu'à près de 11% (données du fournisseur), résultant en 2,2%mas. d'azote (N).

Les contaminants minéraux des lignines Kraft étaient principalement le carbonate de sodium (0,2% de Na), tandis que la lignine Soda et la lignine organosolv étaient plutôt riches en silice compte tenu de la matière première utilisée (paille de blé).

Les teneurs en groupement –aromatiques-OH allaient de 2,0 mmol / g à 3,0 mmol / g par dosage potentiométrique, tandis que la RMN 31P montrait un niveau plus élevé (de 1,4 à 4,8 mmol / g), avec des teneurs phénoliques les plus élevées pour les lignines Kraft.

Les analyses HSQC-RMN ont montré des liens β-O-4 légèrement plus élevés dans la lignine d'Eucalyptus Kraft, que dans la lignine Kraft de résineux et même plus élevés que dans la lignine Soda.

Les analyses TG / DSC ont montré que les lignines présentaient des stabilités chimiques différentes en fonction de la température. En effet, les lignines Organosolv, Kraft et Soda de résineux ont commencé à perdre de la masse en premier (environ 175 ° C) alors que la lignine d'Eucalyptus Kraft a commencé à 200 ° C. La lignine Organosolv présentait également la plage la plus large de volatilisation de température (150 ° C - 500 ° C), tandis que la lignine Soda et Kraft d'eucalyptus avaient des plages de température de volatilisation similaires (225 ° C - 450

° C). Par conséquent, la lignine d'Eucalyptus Kraft serait légèrement plus thermostable que les autres.

Concernant leur masse moléculaire (MM), les analyses GPC ont montré que la lignine Kraft de résineux présentait la MM la plus élevée. Le Mw de lignine Kraft de résineux était d'environ 2900 g/mol avec un DP de 16 en utilisant une méthode SEC avec le THF comme solvant et de 6270 g/mol et un DP de 2,8 en utilisant SEC-THF après acétylation de la lignine. La lignine organosolv analysée par SEC-THF après acétylation conduit à un Mw de 4000 g/mol. La lignine d'eucalyptus Kraft et la lignine de soude ont présenté des profils MM similaires avec Mw de 3600 par THF après acétylation et de 1500 par SEC-THF.

Outre les lignines commerciales, certaines liqueurs noires avec différentes concentrations en matière organique ont été prélevées par le Centre technique du papier, sur une unité industrielle partenaire (Smurfit Kappa).

Sur les caractéristiques des liqueurs noires, nous pouvons affirmer ce qui suit. La qualité du BL à 45% était plutôt stable et contenait ~ 75% de matière organique avec les réactifs de cuisson résiduels restants (alcalins résiduels et composés sulfureux). La composition organique a été en partie identifiée avec ~ 33% de lignine, ~ 1% de sucres et ~ 0,5-1% d'extraits de bois. D'autres petits composés organiques, comme les acides hydroxylés dérivent des glucides, représentaient environ 8% avec principalement de l'acide acétique, de l'acide formique, de l'acide lactique et de l'acide glycolique. Les caractéristiques physico-chimiques du 20% BL étaient plus variables. Des analyses par GPC et TG / DSC ont été effectuées et ont montré que les deux BL présentaient des profils de distribution de masse moléculaire similaires, et que pour les deux échantillons, la volatilisation commence autour de 175 ° C jusqu'à 900 ° C. Deux phases principales ont été détectées. D'abord une dégradation importante entre 175 ° C et 700 ° C (ce qui est cohérent avec l'analyse TGA des lignines précipitées). Le rendement en charbon était d'environ 65% en poids à 700 ° C (pour les deux échantillons). Puis une seconde volatilisation a lieu entre 700 et 900°C. A 900 ° C, le rendement en charbon est d'environ 25% en poids (pour les deux échantillons).

La préparation de lignine a conduit à un rendement en lignine similaire de l'ordre de 22%, contenant une faible quantité d'impuretés, avec ~ 2,3% de sucres résiduels (principalement galactose, xylose et arabinose), et 2% de minéraux (principalement du sulfate de sodium et du carbonate de sodium). Le sodium (Na) et le potassium (K) résiduels étaient respectivement de 0,3% et 0,15%. La pureté était alors de 93%. La teneur finale en soufre est de 2% en poids, ce

qui est dû au soufre organique lié à la lignine en tant que groupe thiol. Toutes ces caractéristiques étaient alors très similaires à celles de la lignine kraft commerciale de résineux.

La poudre de lignine est constituée de fines particules d'environ 16 µm de diamètre moyen, avec une distribution étroite autour de ce diamètre. Ces tailles de particules étaient légèrement supérieures à celles des particules de lignine du commerce (~ 9,5 µm).

La taille polymérique et la distribution de la lignine, analysées par GPC, étaient très similaires aux lignines commerciales précédemment étudiées. Néanmoins, cette lignine préparée a montré un Mw le plus élevé, par rapport aux 4 échantillons commerciaux. La lignine préparée contenait des groupes phénol réactifs significatifs (c'est-à-dire 2,9 mmol / g) et seulement une faible quantité de groupes carboxyle (1,1 mmol / g). Les profils TGA présentent une volatilisation entre 175 ° C à 700 ° C et une vitesse maximale de volatilisation à 370 ° C.

Tous ces résultats étaient nécessaires pour comprendre les caractéristiques et le comportement de la lignine, à la fois si elle est commerciale et si elle provient d'une liqueur noire industrielle. En fait, en connaissant mieux la matière première, il sera plus facile de comprendre les mécanismes pour la convertir par des procédés thermochimiques en produits de grande valeur.

4. - Dépolymérisation de la lignine: une comparaison des méthodes d'analyse des monomères et des oligomers

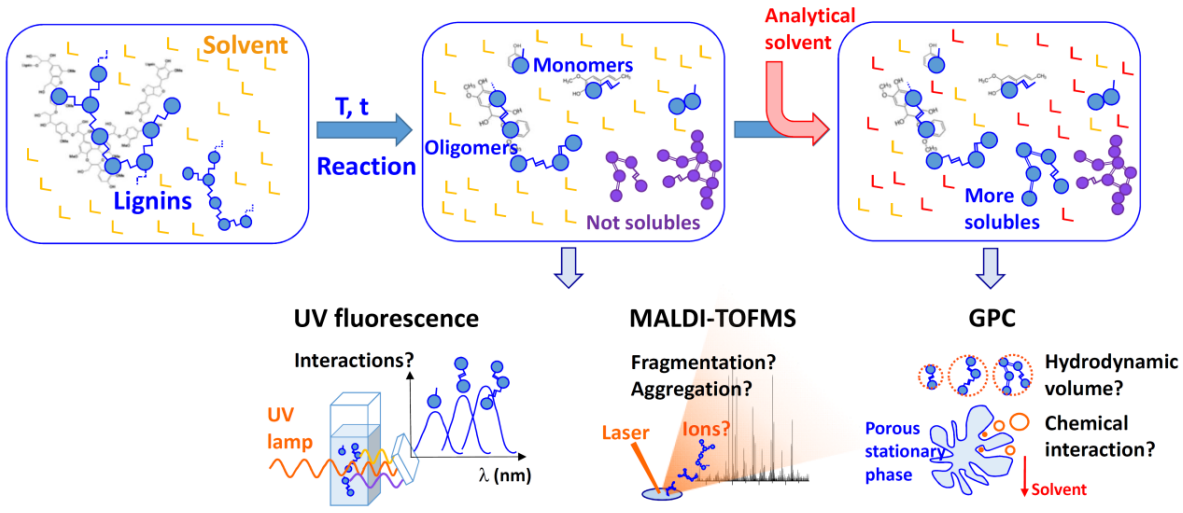

Figure 2. Représentation simplifiée des produits de liquéfaction de lignines et leur méthode d'analyses étudiées dans ce travail.

Premièrement, la lignine est un continuum complexe de molécules de différentes tailles moléculaires et de différentes compositions chimiques. Ces macromolécules interagissent avec le solvant (l'éthanol dans notre cas). Lors de la liquéfaction, ils forment un autre continuum de molécules avec des monomères, des oligomères et des résidus lourds qui sont partiellement solubles.

La fluorescence UV, le MALDI-TOFMS et la GC / MS ont été utilisées directement pour analyser ce liquide, tandis qu'un autre solvant (THF) est ajouté pour l'analyse GPC. Le THF peut favoriser la solubilité de certaines grosses molécules qui étaient en suspension (mais non solubilisées) dans la solution et avec une dimension physique plus petite que les pores du filtre.

Concernant le poids moléculaire moyen de l'huile de lignine, nous avons vu des différences entre GPC et MALDI. Cela est probablement dû à des problèmes d'étalonnage de la méthode GPC et d'interactions durant laser/lignine/matrice dans le MALDI. En effet, la GPC sépare les molécules en fonction de leur volume hydrodynamique dans un solvant donné. Dans le cas de la lignine et de ses produits de liquéfaction, ce volume est différent des standards utilisés pour l'étalonnage du poids moléculaire. [8,50,51,104] De plus, les interactions chimiques avec la phase de la colonne font de la GPC une technique potentiellement inexacte pour déterminer le poids moléculaire des lignines et des produits.[49,50,104,105] La GPC reste encore mal résolu pour les espèces inférieures à environ 1 kDa.[49,50] Il n'est pas bien adapté à la caractérisation des oligomères. D'autres méthodes HPLC doivent encore être étudiées pour fournir une meilleure séparation et quantification des oligomères.[58]

Malgré l'écart entre GPC et MALDI, ces 2 méthodes montrent que le Mw reste relativement stable tout au long du temps de liquéfaction. Ce résultat est également confirmé par l'analyse de fluorescence UV. Une étude détaillée sur des molécules modèles et sur les produits de liquéfaction réels a permis d'identifier 3 pics principaux sur les produits en fonction de la taille des molécules (si elles sont conjuguées). Les maxima des pics des 3 principales familles de produits restent à la même longueur d'onde (306, 350 et 375 nm) lors du temps de réaction. Par conséquent, le poids moléculaire moyen des espèces conjuguées solubles ne change pas de manière significative pendant la liquéfaction.

Sur la base de ces 3 techniques, la lignine semble produire rapidement un pool oligomérique puis la conversion des oligomères en monomères semble lente (processus limitant).

La fluorescence est la méthode analytique la plus directe avec moins d'effets secondaires potentiels. L'échantillon est simplement dilué dans de l'éthanol. Il n'est pas chauffé (comme en

GC / MS ou en MALDI), pas soumis à un flux de photons élevé (comme en MALDI) et / ou non dilué dans un autre solvant (comme pour la GPC). La fluorescence UV est uniquement basée sur les propriétés électroniques intrinsèques des molécules solubles et du solvant.

Néanmoins, cette technique présente également quelques écueils:

1) elle nécessite des molécules conjuguées sans interruption de leur conjugaison. Si la conjugaison est interrompue (comme par une liaison β-O-4), l'émission est décalée vers une longueur d'onde inférieure et le contenu relatif en petites molécules peut être surestimé.

2) Les grosses macromolécules avec de nombreuses fractions chimiques présentent un pic d'émission plus large et moins résolu.

3) Le rendement quantique (facteur de réponse) est fonction des groupements chimiques des molécules. Par conséquent, la fluorescence UV n'est guère quantitative si des liquides complexes avec de nombreux groupements chimiques sont analysés sans séparation préalable. C'est pourquoi nous avons parlé dans ce travail d'une « distribution relative » entre monomères, oligomères et partie plus lourdes.

4) La fluorescence des molécules est impactée par le type de solvant utilisé. Les solvants peuvent stabiliser l'état excité du fluorophore. Cet effet devient plus important avec l'augmentation de la polarité du solvant, ce qui entraîne une émission à des longueurs d'onde plus longues.[86]

5) L'émission de fluorescence d'un composant peut être absorbée par un autre composant (masquage ou masquage partiel d'un composant par d'autres) [116].

6) Un transfert d'énergie intermoléculaire peut se produire d'une molécule aromatique excitée vers une autre molécule aromatique[116]. Ce transfert d'énergie est minimisé dans nos solutions très diluées étudiées dans ce travail (absorption de 0,2 à 275 nm). Des expériences de dopage de gaïacol dans une solution de naphtol ont démontré qu'aucun transfert d'énergie intermoléculaire ne peut se produire dans nos conditions diluées.

7) Le transfert d'énergie intramoléculaire dans une grande macromolécule (sous forme d'oligomères ou de résidus de lignine) peut également se produire d'un système cyclique aromatique plus petit à plus grand (dans la même macromolécule). Cela peut entraîner une émission de fluorescence à une longueur d'onde plus longue et une surestimation de la grande grappe aromatique dans la macromolécule[116].

5. - Effet du type de lignine technique et du catalyseur (Ni/C, Ru/C, Pt/C) sur les produits de dépolymérisation dans l'éthanol supercritique

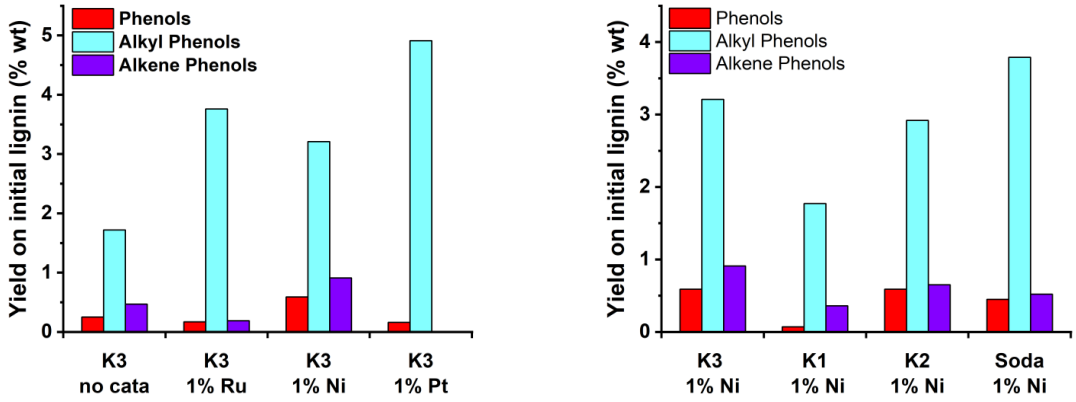

Figure 3 Rendements massiques pour les familles de monomères, après la liquéfaction des différentes lignines avec différents catalyseurs.

Dans ce chapitre, nous avons étudié l'effet de différents catalyseurs (Ni, Ru et Pt sur carbon) sur une lignine Kraft et l'effet du type de lignine pour le catalyseur Ni/carbon. On remarque que les rendements en monomères restent faibles pour les différentes conditions. Le Ni/C favorise la formation d'alkene-phénols et de phénols non substitués. Nous avons ensuite procédé à des tests de liquéfaction avec Ni/C sur toutes les lignines. Dans ce cas, la lignine Soda produit une plus grande fraction massique en alkyl phenols que les lignines Kraft.

6. - Oxydation catalytique sélective à médiation TEMPO de la lignine Kraft en vanilline

Dans cette étude, nous montrons que le TEMPO peut agir comme médiateur d'oxydation radicalaire dans la dépolymérisation à l'air de la lignine de résineux Kraft, produisant une quantité significative de monomères (8,6% en poids) avec une sélectivité élevée en vanilline (82,5%). CuO/TiO2 produit également un rendement notable en monomères (7,2% en poids, 70,8% de sélectivité à la vanilline). Néanmoins, lorsque le catalyseur est utilisé en même temps que TEMPO, les rendements en vanilline restent similaires.

Nous avons obtenu des rendements élevés en vanilline, par rapport aux études de la littérature. Par rapport à la littérature, notre approche présente un rendement élevé en vanilline en utilisant uniquement de l'air et le TEMPO. De plus, il est conduit sur une lignine Kraft industrielle récalcitrante dans des conditions basiques.

Les travaux futurs se concentreront sur le développement d'un procédé dans lequel le TEMPO sera régénéré et recyclé de manière durable pour une production continue de vanilline à haut rendement.

7. - Intégration de la dépolymérisation de la lignine dans les usines de pâte kraft: expériences, modélisation des procédés et évaluation technico-économique

Prenant en compte des études antérieures sur ce sujet et sur la base de la liqueur noire et des données d'une véritable papeterie en partenariat avec le Centre Technique du Papier, nous proposons des scénarii pour la valorisation du flux de lignine pour produire des composés aromatiques verts dans une unité Kraft existante. La liquéfaction hydrothermale directe de la liqueur noire est comparée à la précipitation de la lignine LignoBoost® suivie de sa liquéfaction.

Le but de cette étude est d'évaluer quel scénario serait le plus intéressant du point de vue énergétique, du bilan matière et économique pour les papeteries, en accordant une attention particulière à la production de molécules plates-formes, à la valorisation du sodium et de l'énergie.

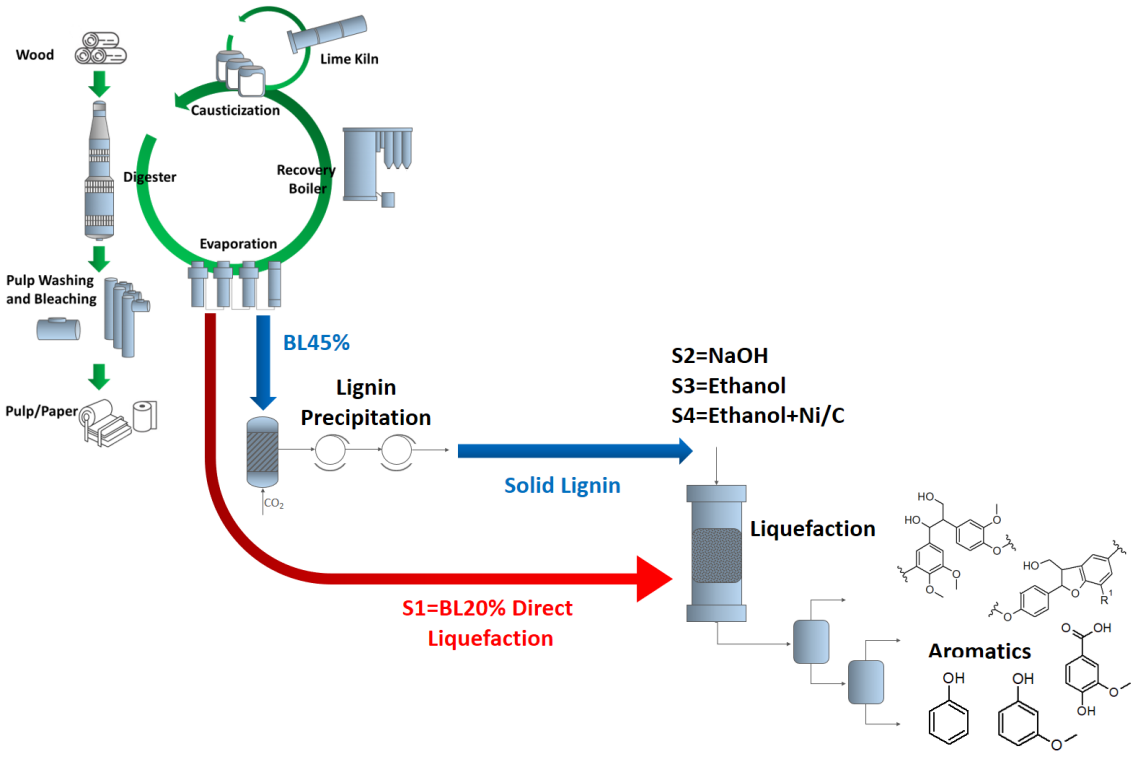

Figure 4 Scheme of the process with all the scenarios.

8. - Conclusions

Dans cette thèse, des aspects différents de la valorisation de la lignine ont été étudiés. La nouveauté de ce travail réside dans les approches multidisciplinaires appliquées à la lignine: d'un côté, l'objectif est de rendre les industries de la pâte à papier plus efficaces par une intégration de la dépolymérisation de la lignine, de l'autre des mesures analytiques de laboratoire détaillées ont été réalisées pour comprendre les mécanismes possibles impliqués dans la dépolymérisation de la lignine.

Biorefinery:
lignin liquefaction to produce green aromatic chemicals

It is necessary and emergent to reduce our dependence to fossil resource and to mitigate climate change. In this context, biomass becomes a strategic renewable resource, for the production of green energy, chemicals and high value materials. Lignocellulosic biomass is the most abundant non-edible feedstock for the synthesis of carbonaceous fuels or chemicals. One important fraction of lignocellulosic biomass is lignin, which is a highly heterogeneous aromatic macromolecule that resists bio-degradation to a much greater extent than cellulosic components. The pulp and paper industry is the largest producers of extracted lignin. Lignin is primarily treated as a by-product and it is valorized for heat and power production. However, this lignin has great potential for value-added development that can capitalize on the unique aromatic features of lignin to potentially replace certain types of petroleum-derived products. In this thesis, industrially available lignins were first characterized. The research focus is to depolymerize these lignins to monomers or oligomers of potential interest for biomaterials synthesis. Both reductive (under H_2) and oxidative (O_2) liquefaction atmospheres are presented. Among the most significant challenges with lignin liquefaction research is the effective characterization of the resulting liquid phase products. In order to address this issue, a novel analytical technique utilizing UV-fluorescence spectroscopy is introduced for rapid screening of lignin liquefaction products. This technique is assessed in conjunction with other analytical methods, which are compared and contrasted. Different catalysts, solvents (ethanol, NaOH) and conditions have been studied. A global process analysis including some technical-economical assessment gives the main process unit to improve for a better valorisation of lignins on a real case pulp & paper mill.

Bioraffinerie:
production de composés aromatiques verts par liquéfaction de lignine

Il est important de réduire notre dépendance aux ressources fossiles et le réchauffement climatique. Dans ce contexte, la biomasse est une ressource renouvelable stratégique pour la production d'énergie, de composés chimiques et de matériaux. La biomasse lignocellulosique est la biomasse non alimentaire la plus abondante. La lignine représente une fraction importante de cette biomasse. C'est une macromolécule avec des motifs variés principalement constitués de noyaux aromatiques. L'industrie de production de la pâte à papier produit une importante quantité de lignine qui est principalement valorisée par combustion pour produire de la chaleur et de l'électricité. Mais des composés à plus haute valeur ajoutée pourraient être produits à partir de la lignine comme notamment des composés aromatiques (phénols, etc.). Durant cette thèse, nous avons tout d'abord caractérisé des lignines techniques disponibles au niveau industriel. Puis, l'objectif est de dépolymériser ces lignines en monomères (phénols) ou oligomères en vue de produire des polymères à haute-valeur ajoutée. Nous avons étudié une dépolymérisation en milieu liquide ("liquéfaction") en présence d'hydrogène ou d'oxygène. La liquéfaction produit une large gamme de composés qui est difficile à analyser. Nous avons proposé la fluorescence UV comme une technique rapide et simple pour analyser les liquides. Cette méthode d'analyse a été comparée à d'autres techniques comme la GPC ou le MALDI-TOFMS. Différents catalyseurs, solvants (eau/NaOH ou éthanol), conditions (températures) ont été testés. Les rendements en monomères restent faibles pour toutes ces conditions du fait du caractère très réticulé de ces lignines industrielles. Une modélisation globale du procédé est proposée pour évaluer les procédés de liquéfaction intégrés dans une unité Kraft de production de pâte à papier industrielle.